Durham E-Theses

The use of catchment-scale riparian intervention measures in downstream flood hazard mitigation

BYERS, EDWARD,ERIC

How to cite:

BYERS, EDWARD,ERIC (2011) *The use of catchment-scale riparian intervention measures in downstream flood hazard mitigation*, Durham theses, Durham University. Available at Durham E-Theses Online: http://etheses.dur.ac.uk/3307/

Use policy

The use of catchment-scale riparian intervention measures in downstream flood hazard mitigation

Edward Byers

Abstract

In recent years there has been debate over increasing flood risk in Britain, whilst the perception of increased flood risk is becoming more prevalent. This comes at a time when funding for flood defence construction and maintenance is thought to be insufficient, but public spending is facing contraction.

This study explores the potential of diffuse, small-scale interventions placed throughout the Uck catchment to reduce the flood peak downstream at Uckfield. Catchment Riparian Intervention Measures (CRIMs) in this study take the form of woody debris dams and riparian vegetation, designed to reduce flow conveyance, and attenuate flow through local flooding. Few studies have investigated the catchment-scale effects of spatially diffuse flood risk reduction measures due in part to the large computational requirement of modelling numerous spatial arrangements of potentially a wide variety of intervention measures.

The reduced complexity hydrological model Overflow was therefore chosen for this study. In contrast to more complex models, Overflow allows the spatial arrangement of flood risk reduction measures to be investigated rapidly, and with ease.

First, the performance of Overflow is evaluated by carrying out sensitivity and uncertainty analyses. It was found that the presence of a number of homogenous parameters, namely roughness parameters, do not prevent useful results from being obtained. However, other parameters are more important to model output. This led to the partial calibration of Overflow to improve the temporal representation of catchment hydrological response throughout the simulated storm event. Following this, Overflow simulated to a good degree the hydrograph observed downstream of Uckfield during the October 2000 flood event.

Second, the effect of the spatial arrangement of CRIMs placed throughout the Uck catchment was explored. The location of a CRIM in the catchment had an important influence on its effectiveness as a risk reduction measure, conditioned to a small degree by local channel and floodplain properties. In a number of reaches, the placement of a CRIM increased downstream peak flow, due primarily to modification of the relative flood wave timing. When several CRIMs were added to reaches throughout the catchment, interaction effects became important. The effect of a CRIM when others were placed throughout the catchment could not be predicted by its effect in isolation. An intervention strategy is developed. Overall, by placing CRIMs in 52 reaches throughout the Uck catchment, simulated peak flow at Uckfield was reduced by 12.5 cumecs, from an initial peak of 124.7 cumecs.

The use of catchment-scale riparian intervention measures in downstream flood hazard mitigation

Edward Byers

Master of Science by Research

Department of Geography

Durham University

January 2011

Table of Contents

List of Figures

Chapter Seven

Chapter Eight

List of Tables

Chapter Eight

Chapter Nine

List of Abbreviations

A definition or explanation for each abbreviation or symbol is also provided in the text. The page numbers below indicate the page on which the abbreviation or symbol is first used.

For a number of abbreviations units are not applicable. This is denoted by (n/a).

Symbol	Meaning	Units	Page Number
Defra	Department for the Environment Food and Rural Affairs	n/a	1
CFMPs	Catchment Flood Management Plans	n/a	1
MIR	Minimum Information Requirement (Models)	n/a	3
CRIMs	Catchment Riparian Intervention Measures	n/a	5
LWD	Large Woody Debris	n/a	9
Cumecs	Cubic Metres per Second	m^3s^{-1}	15
t_{cell}	Cell passage times	hours or seconds	20
l	Distance of travel	m	20
v	Velocity	ms^{-1}	20
S	Slope	dimensionless	20
n	Manning's Roughness Coefficient	dimensionless	20
Q	Discharge	m^3s^{-1}	20
w	Width	m	20
d	Depth	m	22
EA	Environment Agency	n/a	25
CEH	Centre for Ecology and Hydrology	n/a	25
OAT	One at a time (sampling)	n/a	33
Pi	Original parameter value	Variable, dependent on parameter	37
Pmax	Maximum parameter value	Variable, dependent on parameter	37
Pmin	Minimum parameter value	Variable,	37

Symbol	Meaning	Units	Page Number
		dependent on parameter	
NSME	Nash Sutcliffe Model Efficiency	Dimensionless	38
Q_o^t	Observed flow rate at time, t	m^3s^{-1}	38
Q_m^t	Simulated flow rate at tine, t	m^3s^{-1}	38
$\bar{Q}_o$	Mean observed flow rate	m^3s^{-1}	38
t	Time	Hours or seconds	38
PEP	Percentage error in peak flow	%	38
q_{ps}	Simulated peak flow rate	m^3s^{-1}	39
q_{po}	Observed peak flow rate	m^3s^{-1}	39
MAE	Mean Absolute Error	Variable	39
n	Number of measures	n/a	39
RMSE	Root Mean Squared Error	Variable	39
R	Hydraulic radius	m	57
GLUE	Generalised Likelihood Uncertainty Estimation	n/a	62
PDFs	Probability distribution functions	n/a	64
FP	Floodplain	n/a	132

Declaration of Copyright

I confirm that no part of the material presented in this thesis has previously been submitted by me or any other person for a degree in this or any other university. In all cases, where it is relevant, material from the work of others has been acknowledged.

The copyright of this thesis rests with the author. No quotation from it should be published without prior written consent and information derived from it should be acknowledged.

<div align="center">

Edward Byers

Department of Geography

University of Durham

January 2011

</div>

Acknowledgements

I would like to thank my supervisors Professor Stuart Lane and Dr Rich Hardy for their support and advice throughout my study, with special thanks to Stuart, who worked closely with me on my thesis. I would also like to thank Dr Nick Odoni for his hard work developing Overflow, and his regular assistance which allowed me to use the model effectively. Special thanks to Emma, and my family, for their constant support throughout my masters and everything else I do. Finally many thanks to members of the Geography Department and John, Claire and Caroline.

Chapter One   Introduction

A context for this study is provided, followed by a consideration of the potential for diffuse intervention measures to reduce downstream flood peaks. The study aims are discussed in Section 1.2. Finally the study structure is described in 1.3.

1.1   Study context

1.1.2   Flooding in the UK - A brief context

In recent years, a number of severe floods have resulted in the perception of increasing flood risk in Britain (Brown and Damery 2002; Posthumus et al. 2008; Nisbet and Thomas 2006). Although there is debate over the extent to which there are trends in flooding (Robson 2002; Lane 2002; Lane 2008a), particularly due to the relatively short length of many flood records (Hannaford and Marsh 2008), the effects of flooding experienced, for example in 2000 and 2007, have been very real and wide ranging. This comes at a time when funding for flood defence construction and maintenance is thought to be insufficient (SCA in Brown and Damery 2002; Ball 2008), but public spending is facing contraction.

'Making space for water' (Defra 2005) is a Government document published in 2005. It was the UK Governments' first response to a consultation exercise with stakeholders in 2004. It was designed to set the new flood management agenda for the following 20 years and beyond (Defra 2005). The scheme proposes a more holistic, "whole catchment" (Nisbet and Thomas 2006) approach to flood management, encouraging adaptability to future climate change (Posthumus et al. 2008). Central to Defra (2005), and now made explicit in the draft Flood and Water Management Act (2010), there is a shift in emphasis from building flood defences to wider flood risk management (Ball 2008). One element of this management is deployment of flood mitigation measures further upstream so as to reduce downstream flood risk.

Ganouslis (2003) made the distinction between catchment-scale planning and local or small-scale design of protection measures. Catchment-scale planning involves adoption of a large number of measures, adopted across the wider landscape. In the UK Catchment Flood Management Plans (CFMPs) have been developed for many catchments which experience flood risk (Evans et al. 2002) and these include consideration of alternative, upstream mitigation measures associated with the wider catchment.

1.1.2   Diffuse, local-scale flooding and flood peak attenuation

'Making space for water' (Defra 2005) clearly highlights the use of rural catchments for flood mitigation. Werritty (2006) discussed a potential shift away from the existing flood management paradigm which prioritises large-scale structural flood defences, particularly in downstream areas. There is some support for other measures, for instance using the rainfall-runoff model CLASSIC and 1-D hydro-dynamic model iSIS, Acreman et al. (2003) illustrated that reconnection of the river channel and its floodplain can result in attenuation of flood peaks, through increased inundation of the floodplain.

Liu et al. (2004) stated that retention of flood water in "non-critical areas" has the potential for reducing flooding in more populated areas downstream. Local storage of flood waters on the floodplain, as a result of small-scale interventions, can have the effect of slowing the downstream progression of the flood wave (Nisbet and Thomas 2008). Downstream peak flow of the flood event is subsequently decreased. Lane (2007: 312) stated that "river conveyance is generally greater (per unit width) than floodplain conveyance". Therefore by reducing conveyance in the main channel, there is an increased chance of overbank flow (Acreman et al. 2003), with the likely result that more water will be stored or slowed on the floodplain (Lane 2007).

1.1.3   The motivation for diffuse intervention measures and potential conflict

Reconnecting rivers and floodplains is not suitable close to areas of heavy development on the floodplain, where flood risk is likely to increase as a result of removal of embankments and levees. Indeed, Ganoulis (2003) clearly differentiated measures suited to the downstream floodplain area and upstream catchment area. The area at risk of flooding is often much smaller than the catchment area upstream. Due to the large catchment area upstream of the flood risk area, there is a great potential for diffuse, local-scale measures to encourage flooding upstream in order to reduce flooding downstream.

The need for diffuse flood interventions may cause conflict with stakeholders and land owners, especially if areas of their land are to be temporarily flooded (Posthumus et al. 2008; Lane 2008b). This is especially the case if such practices are designed to reduce flood risk many kilometres downstream of their own land. Thus, it is important that the processes occurring are well understood (Nisbet and Thomas 2008). The basic concept and motivation for diffuse flood mitigation measures have been discussed. A particular focus will now be made towards the form of possible intervention measures.

1.1.4   The role of intervention measures

One option for reducing downstream flood risk is to encourage overbank flows in upstream areas. Increased flow of water on floodplains can be achieved through intervention measures

which increase channel roughness. Interventions such as debris dams, reduced channel maintenance, changes in channel morphology and removal of embankments may deliver these effects. Crucially, increasing roughness decreases in-channel velocity, increasing the likelihood of overbank flow thus reconnecting the channel with its floodplain (Acreman et al. 2003; Hooijer et al. 2004).Once overbank flows occur, increased roughness along the floodplain can potentially slow flows further. To this effect, recent research has been carried out on the potential of increased vegetation in the riparian zones for flood attenuation (Archer 1989; Thomas and Nisbet 2004; Thomas and Nisbet 2007) and flood peak delay (Ghavasieh et al. 2006). Nisbet and Thomas (2006) identify woodland located on the floodplain, as opposed to other areas of the catchment, as having the greatest potential for flood reduction. By increasing roughness, vegetation can slow conveyance of flood waters further (Lane 2007). Thomas and Nisbet (2007) demonstrate the following effects of increasing roughness by planting of woodland:

- increased water storage;

- increased water level;

- decreased flow velocity; and

- delayed downstream progression of flood peak wave.

Importantly, Wharton and Gilvear (2006) suggest that such river restoration can potentially decrease downstream flood risk, whilst stating that this potential has as of yet not been extensively demonstrated. Indeed a key challenge to hydrological modelling lies in transferring local-scale modelling of impacts such as those described above, to the catchment-scale (Odoni and Lane, in prep). Soulsby et al. (2006) identify a recent shift towards upscaling of hydrological measurements to the mesoscale to provide more relevant data. However, even with improved data sets, there is likely to be a very large computational requirement associated with exploring several forms of intervention in a large number of channel reaches (Odoni and Lane, in prep), which is problematic for complex models.

Odoni and Lane (2010) stated that complex physically-based models may be difficult to set up and require a long time to run simulations. They conclude therefore that such models are not suitable for use in assessing the optimal spatial arrangement of numerous diffuse intervention measures. It is proposed by Odoni and Lane (2010) and Odoni and Lane (in prep.) that reduced complexity hydrological models are needed for such studies. Such models differ to more-physically based models through simplifying a number of model components (Odoni and Lane (2010), for example applying spatially or temporally homogenous processes or catchment characteristics. Reduced complexity models, sometimes referred to as minimum information requirement (MIR) models, must however still contain model parameters that "retain physical significance" (Quinn et al. 2008). As with all models, the success of such MIR

models lies in practicality with regards to the scope of the model application, and by maintaining an appreciation of the specific model uncertainty (Odoni and Lane 2010).

Through reduced complexity, intervention measures can be simulated more easily with reduced set-up and run time. Such simplifications allow more extensive investigation of multiple different intervention options.

1.2 Project Aims

This study aims to utilise a reduced complexity hydrological model, Overflow, to explore the effects of small-scale flood intervention measures on downstream flood magnitude at Uckfield. Prior to this, Overflow itself will be explored through sensitivity and uncertainty analysis in order to provide an indication of the performance of the model, and thus the uncertainty associated with its output. Hydrograph data from the 2000 flood will be used to analyse the performance of the model and the effectiveness of the intervention measures.

1. **To evaluate the performance of a suitable reduced complexity model for assessing the impacts of small scale riparian woodland interventions**

In order to evaluate the model Overflow a sensitivity analysis and uncertainty analysis will be carried out. The sensitivity analysis will allow an analysis of the influence of key selected model parameters on model output. The uncertainty analysis allows an understanding of parameter interactions and explores the concept of model equifinality and uncertainty.

2. **To develop an intervention strategy with the aim to reduce downstream flood risk, taking into account feasibility**

Once evaluated, Overflow will be applied to develop an intervention strategy that optimises the placement of woody debris dams and riparian vegetation throughout the Uck catchment in order to produce the optimal results in terms of downstream flood mitigation at Uckfield.

Overflow has a number of features which motivated its choice for the study. The model uses simplified physics to allow flood interventions to be modelled both quickly and with ease. This is essential due to the large number of potential sites for interventions and different forms of intervention measures. The model therefore allows the effect of the spatial arrangement of diffuse intervention measures, which increase local channel and floodplain roughness, to be investigated. At the local scale such interventions are likely to reduce flow velocity and increase the likelihood of overbank flow. However at the catchment scale, flood wave timing is likely to become more important.

4

3. To provide a discussion, throughout the study, of uncertainty associated with methods and results

Another key aim of the study is to convey uncertainty to stakeholders and other groups with a vested interest in the research. This is achieved through two main channels. First the uncertainty associated with primarily the model parameters and the results gained are presented and discussed. Second, a research blog will allow the communication of results and uncertainty to local groups in Uckfield.

1.3   Thesis structure

Chapter 2 provides an account of previous studies of the impact of channel and floodplain alteration on flood peaks. Chapter 3 subsequently provides a description of the study site, followed in Chapter 4 by a description of the hydrological model Overflow, which will be applied to the study.

Following a summary of the features of Overflow, Chapters 5, 6 present an exploration of the model parameters. A sensitivity analysis is carried out in Chapter 5, whereby selected parameters are varied one-at-a-time with variation in model output recorded. In Chapter 6 an Uncertainty Analysis is carried out, varying all selected parameters in combination, with the use of a random sampling method. Following exploration of the model parameters, Chapter 7 describes calibration of the rain rate time map parameter to improve goodness-of-fit of model simulations with observed data.

In Chapter 8 the effect of Catchment Riparian Intervention Measures (CRIMs) on downstream peak flow are investigated. The effects of CRIMs in isolation and in combination are identified. An Uncertainty Analysis is carried out in Chapter 9, looking specifically at the roughness values used to simulate the CRIMs throughout the catchment.

Chapter 10 provides a synthesis of the study and draws final conclusions.

Chapter Two   Previous studies of the effects of channel and floodplain alteration on flood peaks

In the following chapter a number of studies will be discussed, wherein the impact of changes in channel and floodplain hydraulic roughness have been investigated. The analysis shows that a number of factors are likely to condition the impact of small-scale flood intervention measures so informing the methodology and kind of model used later in the thesis.

2.1   Modelling studies of channel and floodplain alteration on flood peaks

Early research by Wolff and Burges (1994) employed a 1-D flow routing model to investigate the effect of several channel and floodplain properties along an 80km hypothetical river. The magnitude of reduction in peak discharge along the affected reach was related to the effective storage of the reach in question, influenced by geometry and hydraulic roughness. Both wave celerity and peak discharge were reduced as a result of increased roughness. Woltermade and Potter (1994) similarly found that valley width, stream slope and channel-floodplain-terrace morphology, in addition to hydraulic roughness, influenced peak discharge. Nisbet and Thomas (2008) found that floodplain topography was an importance influence on the floodplain width-flood wave timing delay relationship. The influence of different geomorphic factors on discharge is found to vary with flood magnitude (Woltermade and Potter 1994).

Thomas and Nisbet (2004) found that for an experimental 2.2km reach, where the riparian zone was covered in woodland, flood storage was increased by 71% and flood peak delayed by 140 minutes for a 1 in 100 year flood event (Thomas and Nisbet 2004; Thomas and Nisbet 2007). The key overall effect identified is the slowing of the flood peak, as opposed to a peak flow reduction along the reach. This response was also found in Nisbet and Thomas (2008). It was found that the presence of riparian woodland resulted in a "lower but longer duration" flood downstream (Thomas and Nisbet 2007: 114).

Ghavasieh et al. (2006) carried out at study of the effects of roughened strips up to 2km long on the floodplain along a 20km channel reach. A Manning roughness coefficient of 0.2 was assigned to represent vegetation on the floodplain. Velocity was reduced in the roughened zones, and temporary storage increased. Depending on channel configuration, flood peak attenuation and delay compared to a 'natural state' ranged from 0.3% to 2.1% and 2.4% to 5.6% respectively. As with Wolff and Burgess (1994) and Woltermade and Potter (1994), Ghavasieh et al. (2006) also found that the results were affected by channel properties including slope. Importantly attenuation was seen to decrease rapidly downstream over a distance of up to 30km, whilst peak delay increased downstream. This suggests that, as with

Thomas and Nisbet (2004), the main effect of roughened strips is to delay the flood peak. If indeed a delay in peak timing is the primary effect of roughening of the channel and floodplain, this suggests the necessity for consideration of effects over the entire catchment. There is a need for further work at the catchment scale to provide evidence of the effects of various channel and floodplain interventions throughout the catchment on peak discharge and timing many kilometres downstream. This will be discussed further in 2.2.

Anderson et al. (2006) employed a similar modelling technique to Woltermade and Potter (1994) to analyse the effect of increased riparian vegetation on the flood hydrograph. The results were found to be similar. Wave celerity and peak discharge decreased along the modelled reach as a result of increased roughness due to vegetation. The reduction in wave celerity due to vegetation conditions is concluded to lead to a slowing of catchment response times and subsequently a decrease in peak discharge. However, importantly this study only models the effects along a 50km reach. It therefore does not explore the effects of the spatial distribution of different reach characteristics throughout a catchment, or the interactions of different tributaries, on outlet discharge.

The specific location of variation in reach conditions is addressed to a degree by Liu et al. (2004). Liu et al. (2004) modelled the effect of river rehabilitation, involving primarily increasing floodplain and channel vegetation throughout the headwater streams of the Steinsel sub-basin of the Alzette ($408km^2$). Using the WetSpa distributed hydrological model it was found that the key effect of river rehabilitation was a reduction in velocity in the affected channels. Whilst velocity was not altered in the main channel, the decrease in wave celerity upstream extended the travel time of the flood wave. Importantly, reductions of ~10% in the peak discharge at the outlet of the sub-basin were also found. The study offers a larger-scale analysis of the effects of upstream flood control measures and suggests the potential for such measures.

Woltermade and Potter (1994: 1940) found that some watersheds "translate hydrographs rapidly downstream, while other watersheds store and attenuate discharges much like a reservoir". This suggests that a different flood response may be observed in different sub-catchments. Similarly to Anderson et al. (2006), this indicates the importance of looking at how the spatial distribution of *similar* reach interventions affects the flood response downstream, particularly in modifying sub-catchment flood wave timing. Indeed the relative timing of flood waves from sub-catchments can be very important in relation to peak discharge downstream (see Section 2.5).

2.2   Spatial distribution of flood control measures

Sulaiman et al. (2010) and Saghafian and Khosroshani (2005), using the unit flood response technique identify the contribution of sub-watersheds towards the catchment outlet flood hydrograph. This allows the ranking of watersheds in terms of flood discharge, thus allowing prioritisation of sub-catchments for implementation of flood measures (Roughani et al. 2007). Pattison et al. (2008) highlighted the importance of understanding the flood wave signal of sub-catchments, using a different approach to Saghafian and Khosroshani (2005) in identifying sub-catchments of high and low flood index. Through correlation and principal components analysis, Pattison et al. (2008) largely explained the observed increase in flood magnitude in the River Eden catchment in recent decades by an increase in the flood magnitude of one sub-catchment.

The studies suggest an emphasis on the importance of the spatial distribution of flood control measures implemented throughout the catchment and that the location of a flood mitigation measure is an important control on its effect (Nisbet and Thomas 2006). The issue lies not only in where water storage can be maximised (Roughani et al. 2007 or Saghafian and Khosroshani 2005) but whether such a measure will actually have a positive effect. This will now be further discussed.

2.3   Flood peak timing

Linstead and Gurnell (1999) stated that large woody debris in headwater rivers could have benefits in desynchronising flood peaks from headwater and downstream channels. Similarly Thomas and Nisbet (2007) and Nisbet and Thomas (2008) stated that the impact of floodplain woodland may be limited to a delaying of the flood wave and thus emphasised the importance of careful site selection for intervention to avoid synchronising of the flood waves from several tributaries. Turner-Gillespie et al. (2003), employing a distributed hydrologic and 2-D hydrodynamic model in their study of a ~10km reach in the USA, found that increasing the delay in flood wave delivery in tributaries feeding into the reach increased flood peaks at the downstream gauge. This potential behaviour in relation to upstream flood risk reduction measures is suggested by numerous others; (Brooks et al. 1991; Hooijer et al. 2004; Roughani et al. 2007; Nisbet and Thomas 2008). Pattison et al. (2008) stated that whilst flood magnitude from tributaries is the primary factor, relative timing of sub-catchment peak flows has an important influence on downstream flooding. This was found to be especially the case for larger catchments.

In relation to the impact of land use on flooding, Parrott et al. (2009) and Hurkmans et al. (2009) have presented similar findings. Parrott et al. (2009) stated that whilst land use can have an impact on surface runoff and flood propagation at the local scale, there is greater uncertainty as to the downstream propagation of these effects. Whilst the effect of land use on flood generation and magnitude is seen to decrease in relative importance in larger catchments and for more extreme floods (Parrott et al. 2009), the relative timing of the flood peak from sub-catchments can become an important factor (Pattison et al. 2008). Hurkmans et al. (2009: 14) found "an effective combination of different land use covers in different parts of the basin could be able to significantly alter the magnitude of low flows and/or timing of flood peaks at the basin outlet." This suggests the potential of land use management to reduce the downstream flood peak by reducing the likelihood that the flood peaks from sub-catchments arrive downstream concurrently.

However, at least in relation to woodland, Nisbet and Thomas (2006) hypothesise that the delay in the progression of the flood wave due to *riparian* woodland has the greatest potential for downstream flood mitigation.

2.4 Uncertainty

It has been shown that local-scale diffuse interventions can impact on downstream flooding. Whilst it is apparent that the location of such measures may have an important impact on their effectiveness, it is clear that further work must be carried out at the catchment-scale for different rainfall and flood events. Importantly, there is also great uncertainty regarding the effectiveness of interventions under different conditions.

Anderson et al. (2006) found that the presence of riparian vegetation on the flood peak is likely to have the greatest effect for smaller floods of lower return period as vegetation roughness is less important for high discharge floods. Woltermade and Potter (1994) stated that moderate magnitude floods of a return period of ~5-50 years have the greatest potential for attenuation. For the largest events, increased storage is less likely to have a significant impact in relation to the large volume of water in the catchment. Similarly Saghafian and Khosroshani (2005) and Roughani et al. (2007) found that the contributions of sub-catchments to the outlet peak tend to "converge with an increase in storm duration" (Saghafian and Khosroshani 2005: 274). Additionally Linstead and Gurnell (1999: ii) stated that "the contrast in Manning's n between channels with and without LWD [large woody debris] accumulations converges with increasing discharge." Such findings are similar to those found in literature relating to the significance of land use in relation to flood response during different precipitation events (Bronstert et al. 2002; Niehoff et al. 2002; Chang & Franczyk 2008). These

studies suggest that a catchment specific analysis of the range of storm event over which flood control measures are effective is required, though it is apparent that their effectiveness is likely to decrease for the most extreme rainfall events.

The work presented by Ghavasieh et al. (2006) questions the propagation of attenuation effects on peak flow many kilometres downstream of floodplain roughened strips. It suggests that further work is needed looking at the catchment-scale effects of attenuation measures as discussed in many studies (Wolff and Burgess1994; Woltermade and Potter 1994; Anderson et al. 2006; Thomas and Nisbet 2007). However, as stated by a number of authors (Ghavasieh et al. 2006; Thomas and Nisbet 2007), the significant impact may potentially be on flood peak timing.

Finally it is important to note work by Järvelä (2003) which shows the complexity of the effects of different vegetation types and flow depth on flow velocities. Factors such as these lead to great uncertainty in understanding processes of conveyance (Lane 2007), which present a challenge for future quantification of flow attenuation. The more detailed modelling of vegetation effects such as those presented in numerous works by Järvelä are far beyond the capabilities of modelling studies by, for example Woltermade and Potter (1994), Liu et al. (2004) and Odoni and Lane (2010).

2.5   Conclusion

The previous sections presented the key findings of a number of studies regarding the flood response to changes in channel and floodplain characteristics. Among other factors, increasing channel and floodplain roughness is seen to have an impact on flood flows, at least at the reach scale. However there is a clear need for improved 'spatial exploration' (Odoni and Lane 2010) of these effects at the catchment-wide scale. It has been shown that the spatial distribution of flood control measures may have an important impact on the effectiveness of such measures (Saghafian and Khosroshani 2005 and Roughani et al. 2007), particularly in relation to relative timing of the flood peak from sub-catchments (Pattison et al. 2008, Turner-Gillespie et al. 2003). A number of studies show a significant delay in the flood wave. This could greatly affect timing relationships over the whole catchment scale (Acreman et al. 2003).

Most studies focus on the reach scale effects of interventions, as opposed to the catchment-scale effects such as sub-catchment flood wave interaction, deemed essential in any approach towards addressing downstream flood risk. The catchment-wide effects of planting of woodland have been addressed more closely by Thomas and Nisbet in a number of studies and Liu et al. (2004). However Thomas and Nisbet (2007: 124) state that further work is needed in analysing the hydrographs of tributaries to identify areas throughout a catchment

which would have the most beneficial impact "in terms of desynchronising sub-catchment contributions and therefore the size of the main flood peak."

In Chapter 1 the context of flooding in the UK and the increasing awareness of the potential for small-scale diffuse flood intervention measures is presented. In this chapter, a number of studies are described, which aim to identify the effects of channel and floodplain alteration. In Chapter 3 the study site is described.

Chapter Three   Study area description

This chapter first introduces the context of the study through a brief description of the Knowledge Controversies project (Section 3.1). The characteristics of the Uck catchment are then described (3.2), as is the October 2000 flood, an exceptional event in the flood record at Uckfield (3.3).

3.1   Project context

The catchment was chosen to further develop work previously carried out involving the Uckfield Flood Research Group, and development of the Overflow model in Durham University. The Uckfield Flood Research Group was formed as part of the Understanding Environmental Knowledge Controversies project. The project aims to improve public involvement in scientific research, focused particularly on flood risk. This is achieved by involving non-scientists throughout the research process. The Uckfield Flood Research Group consisted of members of the public, Environment Agency and researchers. Several meetings were held in 2008 and 2009. This study follows the meeting in December 2009 where initial findings from Overflow were presented to the Group as well as local stakeholders. The study aims to develop an intervention strategy for the Uck catchment, with the uncertainty associated with a modelling study clearly presented. A blog was set up detailing the progress of the study, which was available for public viewing. The blog represented a new format on which members of the Uckfield Flood Competency Group could follow and understand the modelling process.

3.2   Site description

3.2.1   Overview

The River Uck catchment covers an area of 104 km^2, and is a major sub-catchment of the River Ouse, Sussex, which the River Uck joins upstream of the village of Isfield (Figure 3.1). The Uck sub-catchment is largely rural, with land use primarily pasture. There are large areas of woodland, with many upstream floodplains containing areas of woodland. The River Uck flows through the town of Uckfield, which in 2004 had a population of 13,200 (Geographical Association 2010). The town of Uckfield experiences regular flooding, the most severe event in recent times occurring on the 12th October 2000. An average rainfall of 761.3mm/year between 1961 and 1990 was estimated (Environment Agency 2008).
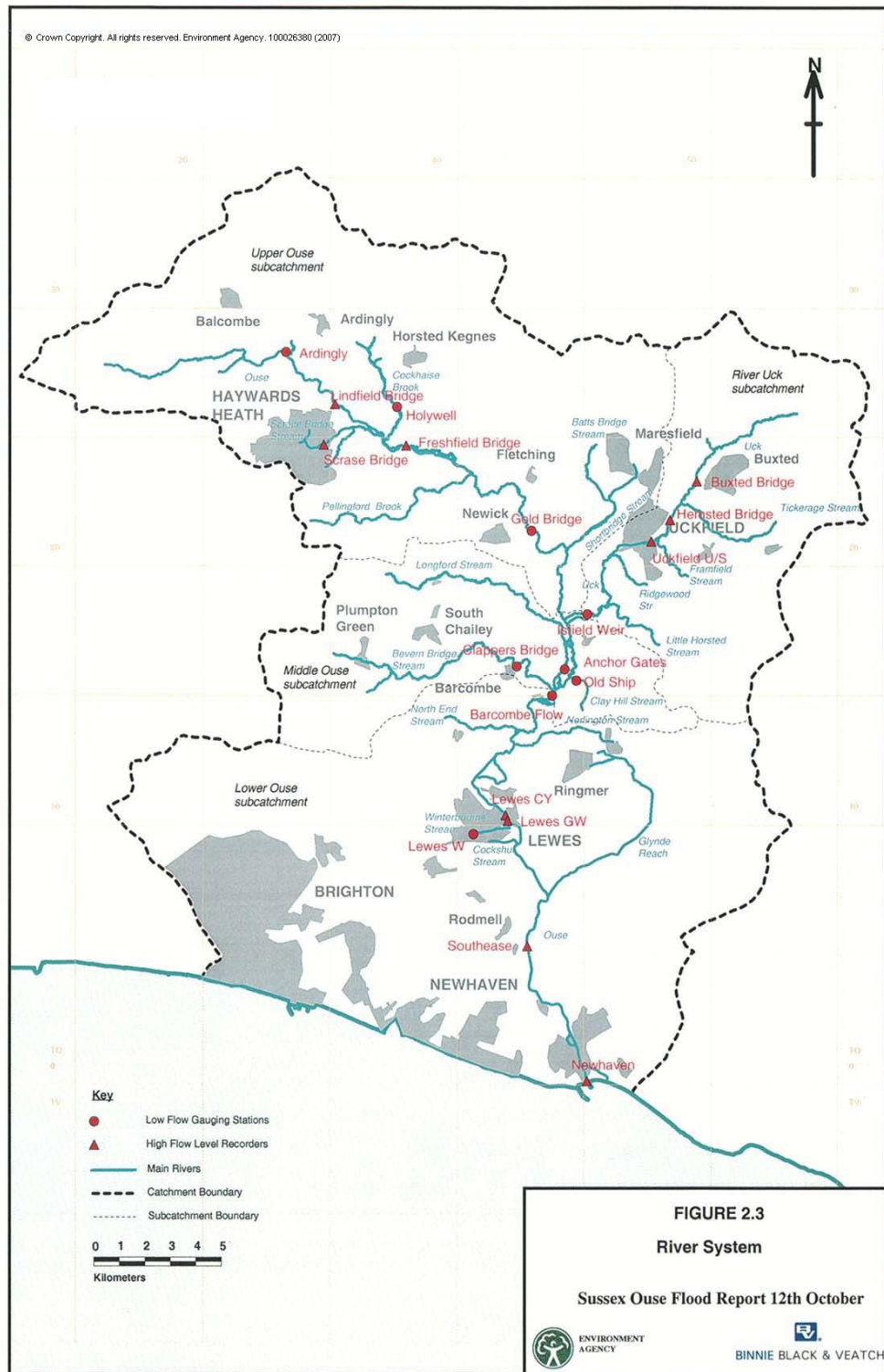
Figure 3.1. (Source: Environment Agency 2001). The location of the Uck sub-catchment of the River Ouse. The Uck is located in the north-east of the Ouse catchment.

3.2.2   Geology

The Uck catchment geology is dominated by mudstone and sandstone. However throughout areas of the catchment the soil is clayey, highlighted by the presence of a large number of pools.

3.2.3 Topography

The Uck catchment has a relatively steep topography, causing run-off often to be rapid (Environment Agency 2008). The main tributaries of the Uck, upstream of Uckfield are Tickeridge Stream and Framfield Stream. Other smaller tributaries of note are High Hurstwood Stream and Lephams Bridge Stream. 234 separate reaches have been identified throughout the Uck catchment, approximately 200 upstream of Uckfield. These reaches are of varied size and characteristics. Channels throughout the Uck catchment are often steep and incised. The effect of these characteristics is a catchment with a flashy response, with a lag of approximately 8 hours between peak rainfall and peak flow identified (Environment Agency 2008). Importantly, as recognized in the 2000 flood report (Environment Agency 2001), the tributaries draining into the Uck upstream of Uckfield are of similar length and the catchment roughly circular. This characteristic means that peak flows from the tributaries often arrive at Uckfield concurrently.

3.2.4 Uckfield floodplain

Historically, the majority of Uckfield was located on relatively high ground, with the centre of Uckfield to the north of the river and the 'New Town' to the south (Environment Agency 2001). However, rapid growth of Uckfield in the last 40 years has led to sections of Uckfield town centre being located within the floodplain. The High Street itself is built on a narrow section of the Uck floodplain and contains commercial and residential properties (Environment Agency 2001). Significantly, located on the floodplain downstream of the High Street bridge, is the Bellbrook Industrial Estate. The latter development has left very little undeveloped floodplain at Uckfield (Geographical Association 2010). In approximately 1986 the River Uck was diverted southwards and straightened to flow under the Brookside access bridge (Environmental Agency 2001).

3.3 2000 flood event

In 2000, England suffered widespread flooding. Uckfield, as well as Lewes downstream, experienced some of the largest flooding in its history (Figures 3.3 and 3.4). The flood event in Uckfield occurred as a result of heavy rainfall in the days preceding the 12th October. The rainfall in a 16 hour period of the 11th/12th October in the Uck catchment was estimated to be a 1 in 150 year event, with an average of 100mm over the catchment (Environment Agency 2001). The resultant flood event reached a peak in the town between 9am and 10am on the 12th October. Water 1.9 metres deep flowed through the town centre of Uckfield. The channel

capacity at Uckfield is estimated at 50-60 cumecs (m^3s^{-1}), whilst the peak flow during the 2000 flood event was estimated at 113m^3s^{-1}. Downstream at the Isfield gauge a peak flow of 132m^3s^{-1} was recorded (Geographical Association 2010). The return period of these flow events is estimated at least 1 in 150 years. Over 80% of the properties damaged during the period were non-residential, the majority businesses. Of the £18.6 million of flood damage in Uckfield, £17.1 million was attributed to businesses (Environment Agency 2001). The extent of the flood waters and the buildings affected are shown in Figure 3.5.
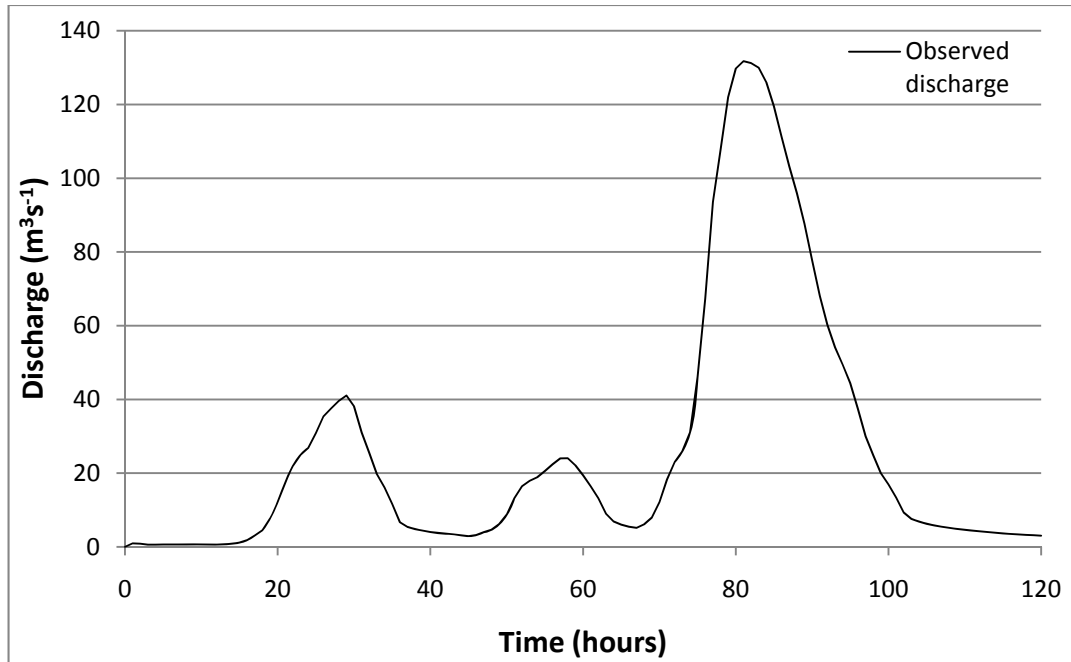
Figure 3.2 Observed discharge recorded at Isfield gauging station during the 2000 flood. 0 hours equates to 00.00 hours on 9th October 2001.

Figure 3.3. (BBC, 2009) Flooding in Uckfield, October 2000

Figure 3.4. (BBC, 2009) Flooding in Uckfield, October 2000
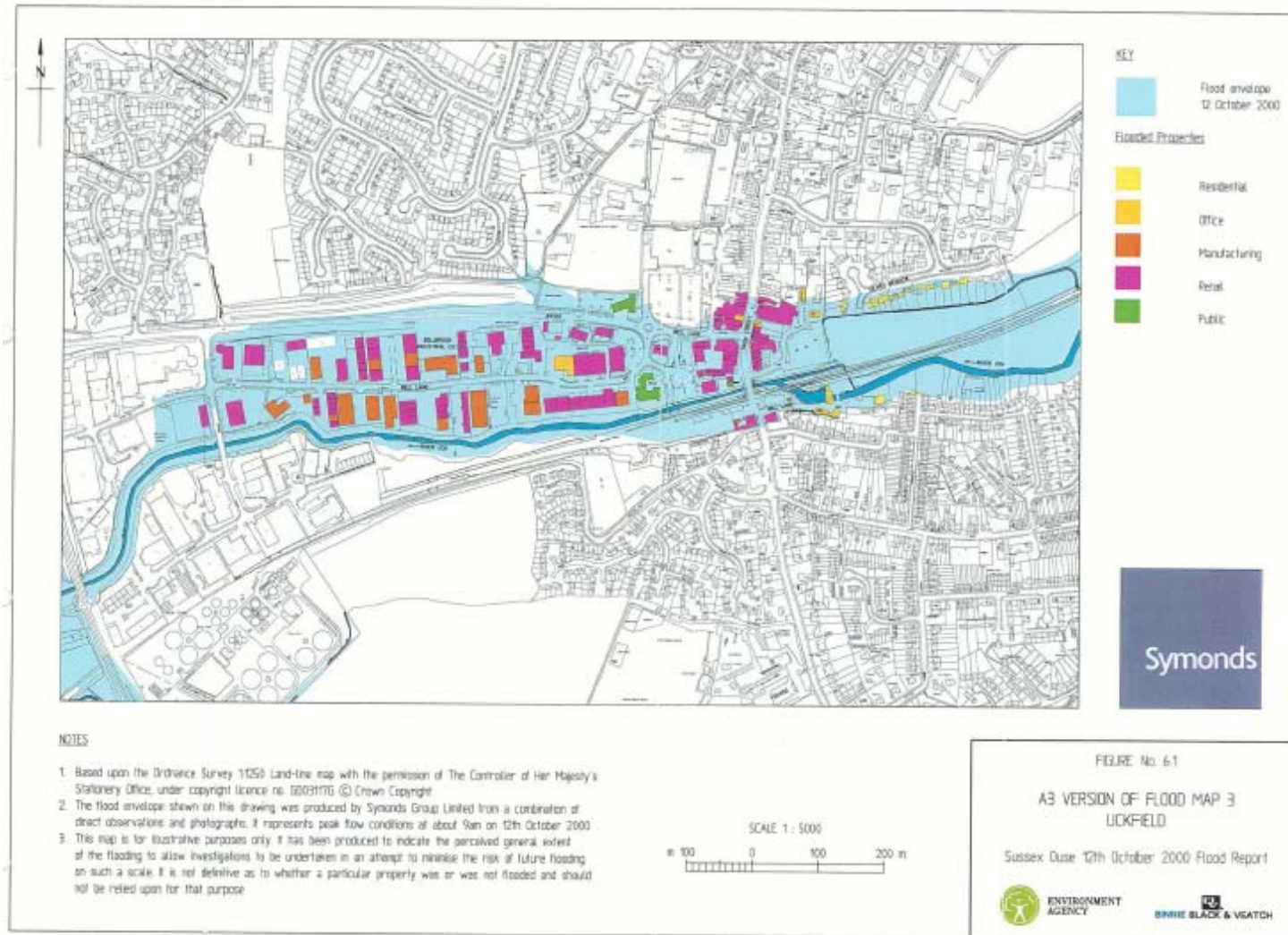
Figure 3.5. (Environment Agency 2001). The flood map produced for the town of Uckfield for the 2000 flood event.

3.4 Flood protection

As a consequence of the 2000 floods, and following detailed consultation, a flood wall was built to protect approximately 30 properties (Environment Agency 2009). The wall is designed to prevent flood waters flowing into the high street, and to return water to the river channel (Figure 3.6). However the flood wall is thought to provide defence against approximately a 1 in 10 year flood event, and therefore would offer insufficient defence in the case of a flood near the magnitude of the event in October 2000.

Figure 3.6. Uckfield flood wall, facing roughly east

3.5 Conclusion

The study catchment and its characteristics have been described, as well as the 2000 flood event. The 2000 flood event is the basis for the modelling work in this study in terms of model calibration and investigation of the effects of CRIMs on a flood hydrograph. The Overflow model will be discussed in more detail in the following chapter. The effects of catchment interventions are investigated based on the model simulation of the flood event.

Chapter Four   Model description

A full, detailed account of the Overflow model (Odoni and Lane, in prep) is provided in Appendix A. A summary of Overflow will therefore be presented here. The reasoning behind its use (Section 4.6) and the implications of applying such a model (4.7) will also be discussed.

4.1   Model overview

Overflow is a reduced complexity, spatially distributed hydrological model that aims to simulate catchment hydrological processes associated with rapid runoff. The model is designed to illustrate the effects of a variety of spatially diffuse flood risk reduction measures on downstream flood risk. Potential intervention measures include altering channel width, depth, sinuosity and roughness, and adjacent floodplain roughness. In this study, the effects of increasing channel and adjacent floodplain roughness in reaches throughout the Uck catchment are explored. Such changes are designed to represent the introduction of woody debris dams and riparian vegetation to the channel and floodplain areas respectively, with the aim of delaying flow during extreme flow events.

A number of assumptions and simplifications are incorporated in the model structure. The use of simplified physical properties allows model simulations to be simple and quick to run, thus allowing Overflow to be used as an effective exploratory tool with uncertainty analysis. The ease with which numerous flood interventions can be simulated allows a focus on the spatial arrangement of such intervention measures, indicating key areas throughout the catchment where such interventions are likely to be most effective. Once key areas are identified the effects of interventions may be explored in more detail using a more physically-based model.

4.2   Model structure summary

A number of simplifications are incorporated within the model structure of Overflow. Land surface cover and channel hydraulic geometry are represented through setting a Manning's n value, which indicates the surface roughness associated with a particular land cover type or channel condition.

The perennial channel network is defined by applying a rainfall rate that results in bankfull discharge at the catchment outlet. When discharge in a cell exceeds a set threshold, it is defined as a channel cell.

The hydrology and hydraulics in Overflow are simplified by creating several 'time maps' based on hypothetical rainfall rates and the Manning's equation. The time map used has an impact on flow speeds in the catchment and hence Overflow captures the event-dependent speeding up of the catchment as it becomes wetter and a greater proportion of flow is delivered by rapid runoff. Thus, the approach mirrors that of a spatially-distributed unit hydrograph approach (e.g. see Miadment et al. 1996; Olivera and Maidment, 1999; Saghafian et al., 2002; Liu et al. 2003; Du et al., 2009) but allowing for a dynamic evolution of runoff rates. Cell passage times (t_{cell}) are given by

$$t_{cell} = \frac{l}{v} = \frac{l}{\dfrac{S^{0.3}}{n^{0.6}}\left(\dfrac{Q}{w}\right)^{0.4}}$$

Eq. (4.1)

Where l is the distance of travel, v is the flow velocity, S is the bed slope, n is Manning's roughness coefficient, Q is the cell discharge and w is cell or channel width.

Once individual cell passage times are calculated, the flow time to the catchment outlet can be subsequently calculated for every cell in the catchment, working from the catchment outlet upwards. For example, if cell a flows into cell b, which flows into cell c, which in turn flows into the catchment outlet, the time map value for cell a is the sum of the passage times for cells a, b and c. Isochrones can subsequently be drawn for each rainfall rate. The isochrones indicate the areas in the catchment where flow time to catchment outlet is the same. Two examples are shown in Figure 4.1a and b, with different hypothetical rainfall rates applied. Changes in values used in Eq. (4.1), for example due to a woody debris dam increasing the hydraulic resistance along a channel reach, alter the isochrones.

The actual runoff that is routed is not the rainfall rate, but a runoff rate, determined by subtracting the estimated percentage loss (due to evaporation and loss to groundwater) from the rainfall rate. To calculate the appropriate percentage loss, and thus the effective runoff rate, a comparison is made between the estimated total flood volume and estimated total rain volume to estimate a percentage runoff. The runoff percentage is varied as the rain event progresses to reflect the rainfall intensity.

Runoff in the catchment is routed differently depending on a cell being defined as a slope or channel cell. Flow routing can be modified to allow headward extension of channelized flow and to allow flow to be routed across the floodplain when discharge exceeds the capacity of the channel to convey flow. Cell passage times are altered according to the proportion of overbank flow in the catchment to produce a revised isochrones map.

Figure 4.1. Time maps created for equilibrium flow rainfall rates of 30mm/day (4.1a) and 180mm/day (4.1b). Each different coloured 'band' indicates the time that water within its area will take to reach the catchment outlet.
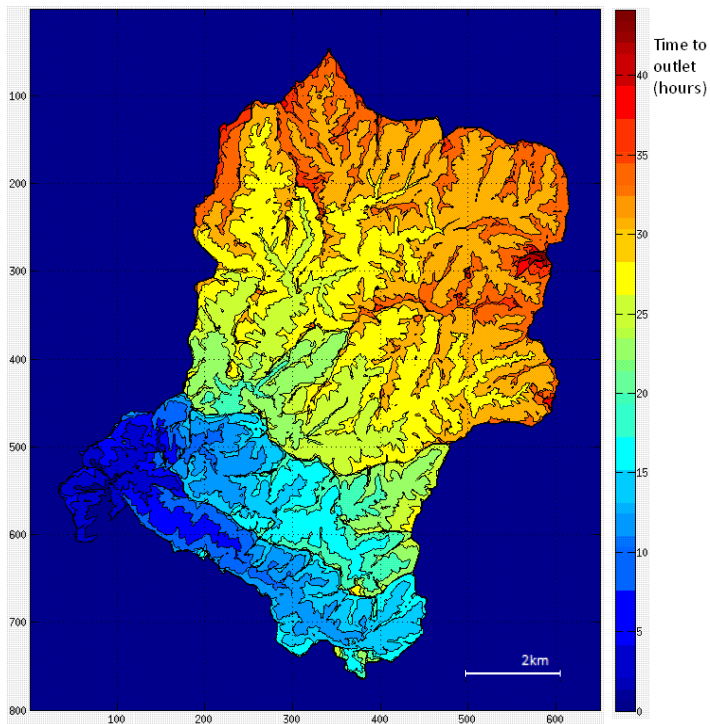
Figure 4.1a.
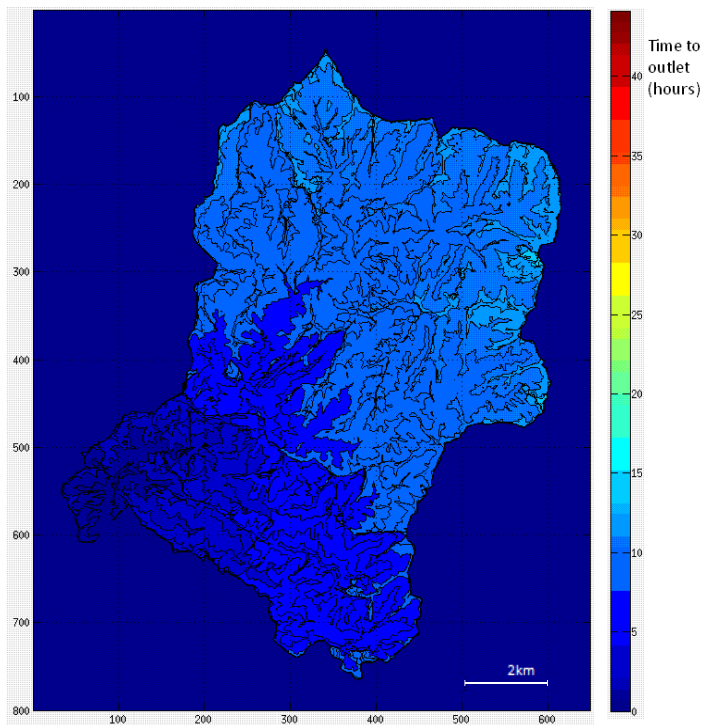
Figure 4.1b.

Different time maps can be applied at each hourly time step. Therefore Overflow must be calibrated in order to determine the order in which the time maps are selected.

Channel geometry is estimated using the following equations developed by Leopold and Maddock (1953). To calculate channel width:

$$w = 1.4Q^{0.45} \quad \text{Eq. (4.2)}$$

and channel depths (bank heights):

$$d = Q^{0.32} \qquad \text{Eq. (4.3)}$$

where w is the width of the perennial channel and d its depth. The discharges, Q for each cell are estimated after applying the rainfall rate used to define the perennial channel network.

There is a potential for more detailed physics to be implemented within the Overflow model itself, if required. There are also a number of opportunities for members of the Uckfield Flood Research Group to make suggestions to help improve the models representation of the catchment.

The model is applied in two broad steps. The first determines the time maps for each rainfall rate. The second calibrates the model by selecting from the set of available time maps to produce hydrographs for downstream locations where gauge data are available. This means that Overflow is not suitable for application in an ungauged catchment and that the gauge used in the analysis must be as reliable and accurate as possible.

4.3   Data sources

The following data sources were applied; (1) 20m resolution 'Nextmap' DEM data from Intermap (Figure 4.2). (2) Hourly river gauge data recorded at Isfield, downstream of Uckfield, in cubic metres per second (m^3s^{-1}), for a 120 hour period starting at 00:00 hours on the 9th October 2000 (Figure 4.3). No accurate hydrograph for Uckfield during the 2000 event was available (Environment Agency 2001). (3) Rainfall data in mm/hour for the October 2000 event, from various gauges in the Uck catchment, detailed in the Geographical Association report (Environment Agency 2001) (Figure 4.4).
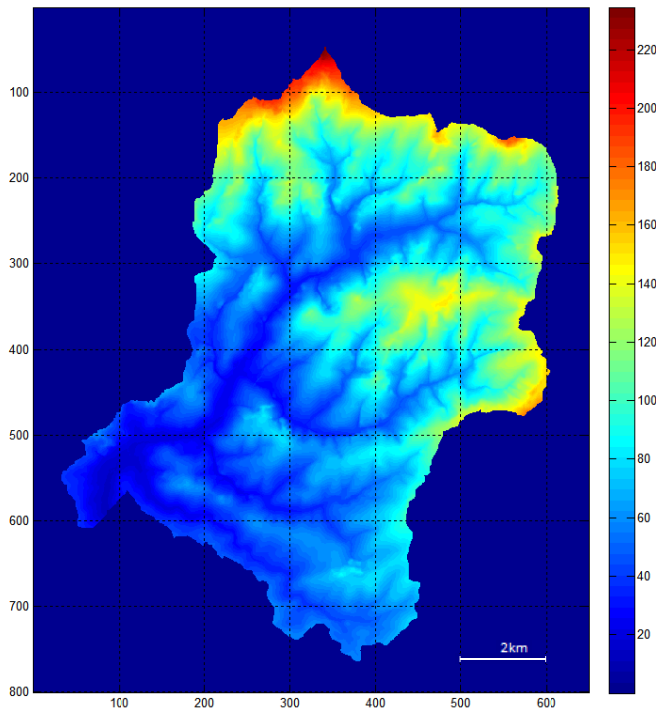
Figure 4.2. Contour plot of the River Uck catchment, resampled from 5m Intermap 'Nextmap' data. Elevations in metres, spatial resolution is 20m per cell, grid squares 2km x 2km.
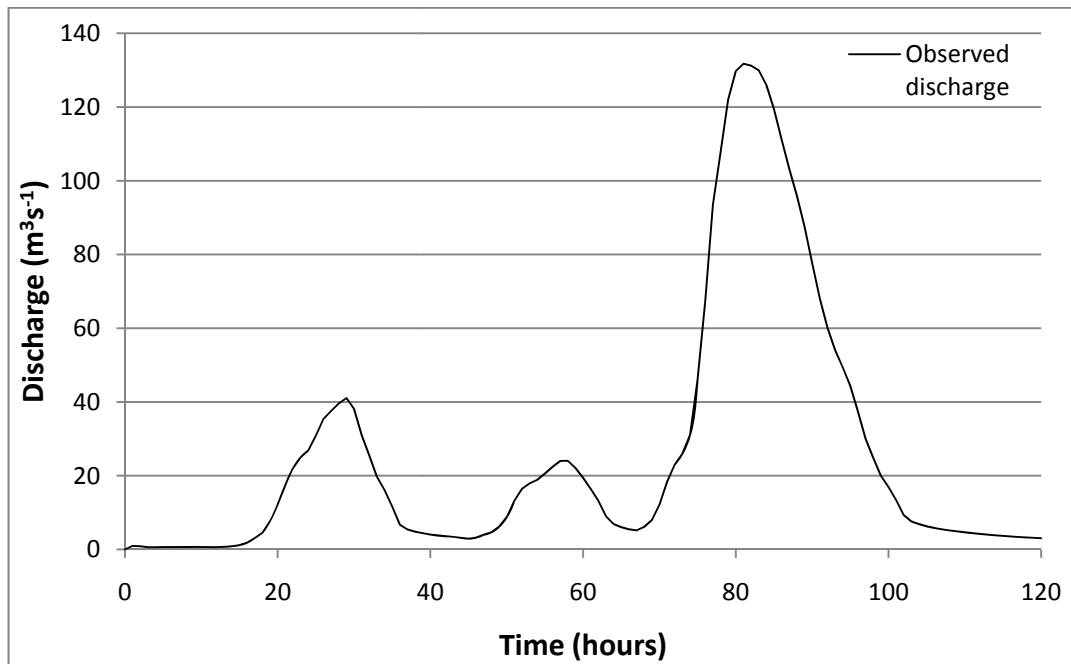
Figure 4.3.Observed discharge recorded at Isfield gauging station during the 2000 flood. 0 hours equtes to 00.00 hours on 9th October 2001.
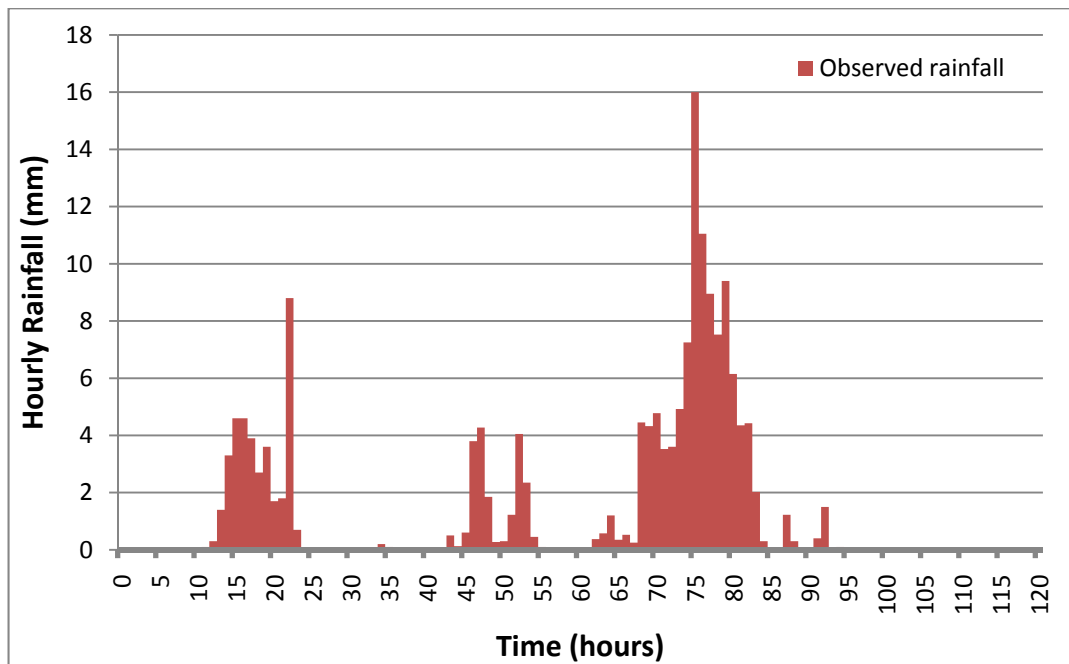
Figure 4.4 Observed rainfall recorded at Popeswood and Barcombe rain gauges. 0 hours equates to 00.00 hours on 9th October 2001. (Source: RAINARK).

4.4 Model Elements

Model parameters are values estimated, through model calibration, to represent catchment characteristics or processes which cannot be measured directly. There is therefore a degree of uncertainty associated with the use of model parameters (Vrugt et al. 2002). With a detailed investigation of model parameters (through sensitivity analysis, Chapter 5, and uncertainty analysis, Chapter 6), and consideration of uncertainty however, important results can be obtained from hydrological models. Overflow contains a number of parameters which are detailed below.

4.4.1 Parameters

- The unit Q that defines the channel network (i.e. how much Q makes it a channel and not a slope cell)
- The diffusion exponents for both hillslope and spill flows
- The parameters in the hydraulic geometry relationships (Eq. 4.2 and 4.3)
- The slope coefficient, used to calculate bank height elevation in the spill flow procedure
- The Manning's n values for both hillslopes and channels
- Parameters associated with estimation of the runoff percentage (Effective runoff), acoounting for evaporation and groundwater losses.

24

- The fixed baseflow contribution

Due to time restrictions, not all model parameters were included in the sensitivity and uncertainty analyses. This allowed detailed analysis of those parameters which were chosen. The parameters associated with channel, floodplain and catchment land roughness, runoff generation and catchment wetness (rainfall rate time map) were chosen for analysis as they were identified as they represent important simplifications in the model structure and previous work by Nicholas Odoni had confirmed that model predictions were particularly sensitive to these parameters (N. Odoni, Durham University, pers. comm.). The following sections expand on these parameters where appropriate.

4.4.2   Rain time maps.
Time maps were determined for 24 equilibrium flow rain rates, up to a maximum of 200mm per day. 24 rates were chosen to allow for a range of rates to be represented between 1 and 200mm per day. The parameter alters cell passage times for flow and thus allows the creation of 'time band zones' which show the flow time to the catchment outlet.

4.4.3   Effective runoff coefficients
These are used in two ways. To estimate the time maps, effective runoff is set at 61% of observed rainfall. This is determined by mass balance calculations based on observed rainfall and observed discharge at Isfield during the 2000 event (Odoni and Lane, in prep.).

Second, for the calibrated version of Overflow, the 2000 event is split in to four phases to reflect changes in the catchment as a result of rainfall events. 4 different runoff percentages are applied throughout the storm event to calculate the volume of water entering the catchment;

Unaltered (as there is no rainfall input during this period)

− hours 0-10

42 x (gross hourly rain rate/100) – hours 11 - 41

48 x (gross hourly rain rate/100) – hours 42 - 60

83 x (gross hourly rain rate/100) – hours 61 – 120

These figures are estimates of effective runoff rate during the storm event based on mass balance calculations (see Odoni and Lane, in prep.), examination of the relevant 2000 storm data and a combination of local knowledge and Environment Agency (EA) and Centre for Ecology and Hydrology (CEH) catchment data. The values differ from the figure of 61% to allow the model to account for variation in effective runoff rate as the storm event progresses (see Odoni and Lane, in prep.).

4.4.4   Manning's n roughness. The Manning's roughness is set for all hillslopes, floodplains and channels. Default roughness for the three broad land covers is 0.06 for hillslopes and floodplains and 0.035 for channels. Chow (1959) (Table 4.1) was consulted extensively throughout the study to inform selection of appropriate Manning's n roughness values.

4.5   Model data output

The model output consists of a flood hydrograph for two locations; Isfield gauging station and the meadows area in Uckfield (Figure 4.5). A hydrograph is simulated for a 240 hour (10 day period). Hours 1-120 represent a 'warm-up period' where only a steady baseflow is applied to the catchment. This warm-up period confirms the model is behaving as it should, before a rainfall input is added to the catchment. In this study, a focus lies on the flood hydrograph over the second 120 hour (5 day) period, with hour 120 corresponding to 00:00 hours, 9th October 2000 for all following figures.
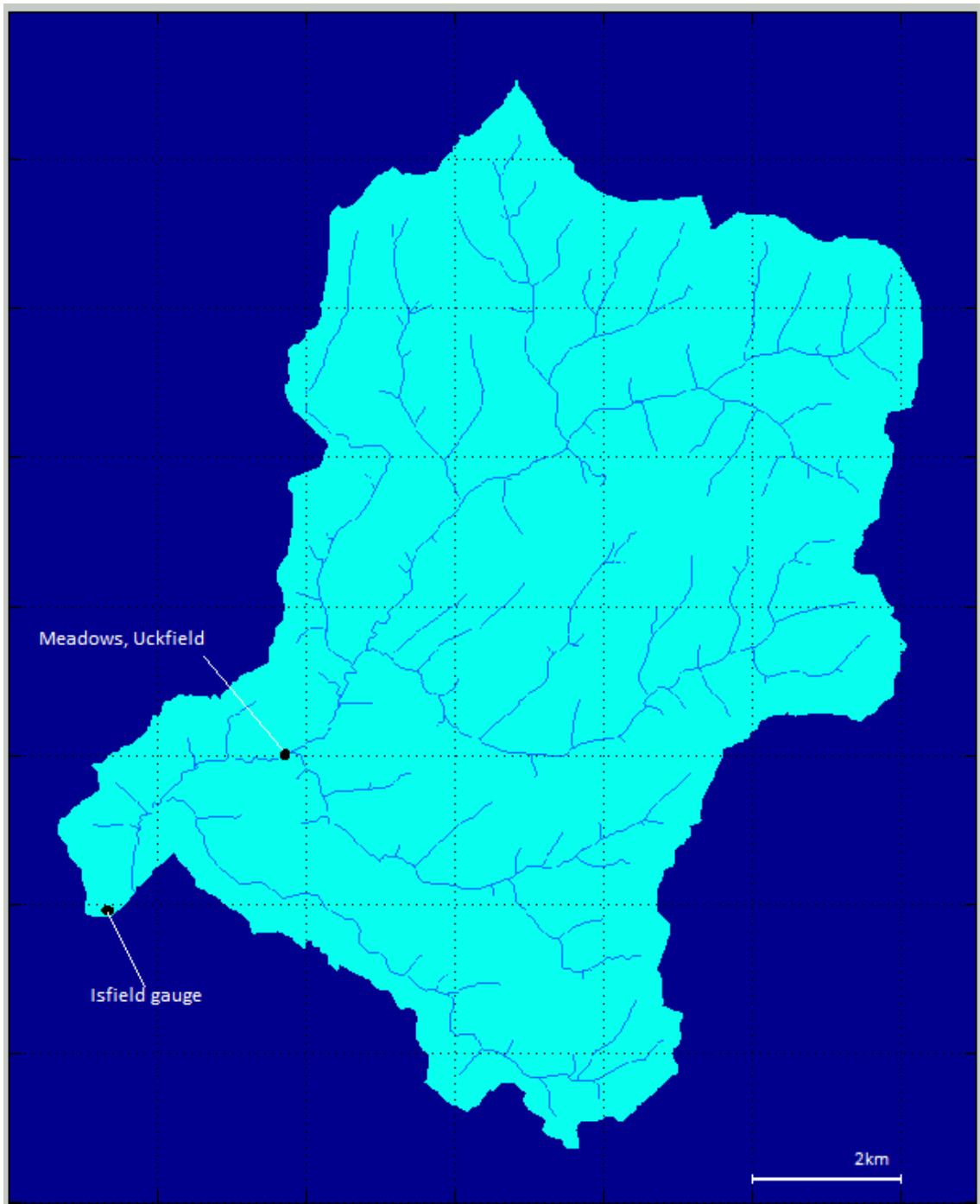
Figure 4.5. An outline of the Uck catchment indicating the approximate location of the Isfield gauge and Meadows area, Uckfield

Table 4.1. Manning's n values for channels and floodplains (Chow 1959)

Type of Channel and Description	Minimum	Normal	Maximum
Natural streams - minor streams (top width at floodstage < 100 ft)			
1. Main Channels			
a. clean, straight, full stage, no rifts or deep pools	0.025	0.030	0.033
b. same as above, but more stones and weeds	0.030	0.035	0.040
c. clean, winding, some pools and shoals	0.033	0.040	0.045
d. same as above, but some weeds and stones	0.035	0.045	0.050
e. same as above, lower stages, more ineffective slopes and sections	0.040	0.048	0.055
f. same as "d" with more stones	0.045	0.050	0.060
g. sluggish reaches, weedy, deep pools	0.050	0.070	0.080
h. very weedy reaches, deep pools, or floodways with heavy stand of timber and underbrush	0.075	0.100	0.150
3. Floodplains			
a. Pasture, no brush			
1.short grass	0.025	0.030	0.035
2. high grass	0.030	0.035	0.050
b. Cultivated areas			
1. no crop	0.020	0.030	0.040
2. mature row crops	0.025	0.035	0.045
3. mature field crops	0.030	0.040	0.050
c. Brush			
1. scattered brush, heavy weeds	0.035	0.050	0.070
2. light brush and trees, in winter	0.035	0.050	0.060
3. light brush and trees, in summer	0.040	0.060	0.080
4. medium to dense brush, in winter	0.045	0.070	0.110
5. medium to dense brush, in summer	0.070	0.100	0.160
d. Trees			
1. dense willows, summer, straight	0.110	0.150	0.200
2. cleared land with tree stumps, no sprouts	0.030	0.040	0.050
3. same as above, but with heavy growth of sprouts	0.050	0.060	0.080
4. heavy stand of timber, a few down trees, little undergrowth, flood stage below branches	0.080	0.100	0.120
5. same as 4. with flood stage reaching branches	0.100	0.120	0.160

4.6   Motivation for use of Overflow

The key aims of the study were to explore the effect of intervention measures placed throughout the catchment. The optimal channel reaches, defined as those where the adding of an intervention measure had the greatest effect in reducing downstream peak discharge, were to be identified and then an intervention strategy suggested. An additional important aspect was communicating work and results to members of the Uckfield Flood Research Group, which consisted of members from various backgrounds.

The features of Overflow described previously in the chapter were well suited to these aims for a number of reasons. The simple representation of land cover and channel hydraulic geometry allows the effects of different combinations of intervention measure to be explored with relative ease. In this study a focus was made on the potential of woody debris dams and riparian vegetation to slow flows during flood events. Such interventions could be simulated through simply altering the Manning's n values along the reach to be investigated.

The simplifications in the model structure also have the advantage of restricting the time required to run model simulations. In the case of the Uck catchment there are approximately 200 reaches upstream or flowing into the town of Uckfield. This represents a large number of channel reaches where interventions can potentially be sited. One simulation took approximately 12 minutes to complete. Therefore to simulate an intervention in each reach individually, this would require ~2400 minutes or ~40 hours. When looking at combinations of interventions, a very large number of simulations may be required. The use of Overflow reduces model running time and hence allows a more thorough investigation.

The combination of the above two features makes Overflow ideal as an exploratory tool, specifically to explore the spatial arrangement of interventions, with the aim of identifying key sites with flood mitigation potential. Once potential sites are identified more detailed analysis of the effects of flood intervention measures on the downstream flood hydrograph can be carried out with the use of a more physically-based model.

Throughout model development the potential for incorporation of local knowledge is emphasised. Input from local groups has previously informed work applying Overflow to the catchment of Pickering Beck (Odoni and Lane 2010). For example local observations indicated particular sections of the catchment contributing a relatively small amount of runoff to the 2007 flood. Such observations informed runoff percentage and baseflow calculations (Odoni and Lane, in prep). In the application of Overflow to the Uck catchment, local knowledge informed adjustments to the generation of the perennial channel network. The nature of Overflow has enabled effective communication of methods and results back to local members (see Appendix B: Research blog). The engagement of stakeholders in terms of allowing input in

the development of the model and effectively communicating results back has fulfilled the aims of the Uckfield Flood Competency Group of including the public in the flood research process.

4.7   Implications of using Overflow

The most notable feature of Overflow is the presence of a number of model parameters, for which default values are set. A number of parameter values are based on analysis of the Uck catchment and the 2000 flood event. The unit discharge parameter, for example, defines the perennial channel network and is based on the application of an effective rainfall designed to produce bankfull discharge at the catchment outlet. Values for other parameters such as land and channel Manning's n are estimated so as to fulfil the two criteria: realistic values and those which achieve an adequate fit between observed and simulated hydrographs. However it is apparent that spatially homogenous roughness values do not reflect small-scale variations in land cover.

Such simplifications in the model structure are justified, however, as they fulfil adequately the aims of the study. A complex model may not produce results that are any more certain than a reduced complexity model if the required data is absent or lacking in quality (Soulsby et al. 2006; Odoni and Lane, in prep; Research blog, Appendix B). Examples of sources of uncertainty, even in complex physically-based hydrological models include potential errors in runoff data, rainfall data and scale issues associated with data, and parameter uncertainty. The principle of Ockham's razor states that when faced with two satisfactory explanations of a system, it is right to favour the simpler (Barker 1961 in Smith and Smith 2007). A key reason for this principle is that a more complex model may be more uncertain if it requires data or parameters that are not available. Further, a simpler model may have a greater potential to be understood by various groups such as, in the case of this study, members of the public.

With the study blog representing a key component (Appendix B), a key argument in this study is that if uncertainty is acknowledged and clearly explained, it does not have to prevent important findings from being produced (Beven and Binley 1992). Instead, if the uncertainty of results can be understood and even embraced (Wheaton et al. 2008), the use of the Overflow model as a simple exploratory model can be recognised.

A clear acknowledgement of uncertainty subsequently requires a good understanding of how model simplifications affect the model output. Thus it is important to see how the selection of a default value for the parameters in question is going to affect the model output (flood hydrograph).

Such an exploration is carried out in the sensitivity analysis detailed in the following chapter. The sensitivity analysis indicates which parameters influence downstream discharge to the greatest degree. The values of the most sensitive parameters are likely to be more important (Smith and Smith 2000) and therefore the sensitivity analysis can help focus work on improving key parameters or areas of the model (Saltelli 2000).

The investigation of the effects of parameters in combination is carried out in Chapter 6. The uncertainty analysis allows a greater understanding of the "degree of belief" in different parameter sets (Beven 2001). During such a procedure different values for parameters can result in similar model output. Equally, similar parameter values can result in very different model output due to the influence of other model parameters. This is likely to be the case with Overflow due to the homogenous parameter values.

As stated previously model simulations take relatively little time to run, and therefore a large number of simulations can be run for the Uncertainty Analysis. This is beneficial as it allows a good exploration of the parameter space.

4.8 Conclusion

The conceptual model has been detailed in the chapter as has the method by which a flood hydrograph is simulated. The input data, parameters and model output are also shown. The reasons for using the Overflow model in this study have been discussed, as have the implications of its use. In the following chapter the sensitivity of model output to variation in model parameters is explored.

Chapter Five   Sensitivity Analysis

5.1   Introduction

In Chapter 4 the model Overflow was described. The key model parameters have been identified. In this chapter a sensitivity analysis is carried out. Sensitivity analysis allows the model user to explore the sensitivity of model output, in this study discharge, to changes in certain model parameters (Wainwright and Mulligan 2004). This in turn indicates which parameters are the most important.

First the methodology followed for the sensitivity analysis is presented (Section 5.2). The results of variation in the flood hydrograph as parameter values are varied one at a time is then presented (5.3). The subsequent change in goodness-of-fit between the observed and simulated hydrographs for the 2000 flood event is quantified by the objective functions. The results are discussed in 5.4.

5.2   Methodology

First, the initial qualitative analysis is described (5.2.1). Second the methodology for investigation of sensitivity to parameters is detailed. The key model parameters whose sensitivity will be assessed, and the range over which their values will be varied is identified (Section 5.2.3-5.2.7). The objective functions employed to quantify model output variation are described and discussed (5.2.9-5.2.10).

5.2.1   Initial graphical analysis

The first analysis of the performance of the model was through graphical analysis, identified as an important initial step in model evaluation by Green and Stephenson (1986) and Smith and Smith (2007). Model simulations of discharge can be compared to observations made at the Isfield gauging station along the downstream section of the River Uck, in the days preceding and following the 2000 flood event. This method of investigation into the model behaviour is both subjective and qualitative (Green and Stephenson 1986). However it allows an important preliminary understanding of the model behaviour to be gained. By varying key parameter values, an initial analysis can be made of how they affect model output (discharge).

5.2.2   One-at-a-time sensitivity analysis

Sensitivity analysis was subsequently carried out, whereby the variation in model output is analysed as key parameter values are varied (Saltelli 2000). Key input variables were identified

and varied one-at-a-time (OAT), whilst all other parameters remained constant (Hamby 1994; Saltelli 2000), fixed at their default values. The variation in output was then recorded.

5.2.3   Parameter selection

The following parameters were chosen to be varied for sensitivity analysis;

- Rainfall rate time map. Each time map sets cell passage times for a flow that is assumed to be fully adjusted to a given rainfall rate. This parameter does not alter the rain input in either volume or rainfall rate. Instead, by using a series of time maps the effects of the changing wetness of the catchment on flow translation speeds is determined. A higher rainfall rate time map sets flow velocities higher, and therefore reduces cell passage times. This results in water being routed through the catchment faster.

- Effective runoff rate. Runoff rate was varied between 75 and 125%. This accounts for any errors in rain and discharge gauge data. Effective runoff rate allows for adjustments to account for evaporation, groundwater losses and baseflow. Varying the effective runoff rate offers a more simple method of varying the runoff in the catchment.

- Floodplain Manning's n – the roughness values of *all* areas in the catchment designated as floodplains

- Channel Manning's n – the roughness values of the *entire* channel network

- Land surface Manning's n – the roughness values of the *entire* catchment excluding the channel network and areas designated as floodplains

- Hydrograph timing. When applying the objective functions used in this chapter (Section 5.2.10), individual simulated data points are compared directly to one other observed data point. The result is that even if discharge peaks are simulated to a relatively high accuracy, but their timing is erroneous, the model may be seen to perform very poorly. By simply shifting the simulated hydrograph so that the timing of the peaks in comparison with the observed data is altered, the effect of timing errors on objective function output can be explored. This is therefore not a model parameter but needs to be factored into the consideration of Objective Functions.

The selection of parameters was informed by the graphical analysis discussed above and previous work with the Overflow model (Odoni and Lane, in prep) to identify the most important parameters for this study. Due to time constraints, however, some parameters were not included in the sensitivity analysis, namely those linked to channel width and depth equations. The time constraints arose from the current model formulation which did not

facilitate sensitivity analysis for these parameters. This is potentially a limitation to the sensitivity analysis as such parameters could have a great influence on model output and the sensitivity of model output to other parameters.

5.2.4   Selection of method for parameter value variation

Once the parameters, whose values were to be varied in the sensitivity analysis, were decided upon, a second key feature of the experiment design was the decision of how to vary such parameter values. There are several different approaches to the selection of parameter value ranges discussed in the literature.

Saltelli (2000) stated that in one-at-a-time (OAT) sensitivity analysis a 'standard' value is chosen for each parameter, which is often based on an assessment of relevant literature. This standard value is then often assigned as the "midway", with two extreme values chosen either side of it. This method is used by Campolongo et al. (2000). Such a method is found to have a number of disadvantages.

First it does not allow a fine resolution analysis of the parameter space (Beven 2001). If a small variation in the value of a particular parameter results in a very large variation in the model output, this behaviour may very likely be missed as only 3 parameter values are used. If the output response to parameter variation is non-linear, this response will be poorly explored using the above method. Second the values chosen using this method may be relatively arbitrary and therefore not necessarily suitable. If extreme values are chosen with the nominal value as a midway the extreme values may lie outside of realistic parameter values. For example in this study the default floodplain Manning's n is 0.06. If extreme values of 0.01 and 0.11 were chosen, the former would represent an unrealistically low roughness and the latter would not allow the effect of very rough floodplains to be explored. This method also relies too strongly on the assumption that the initial value of 0.06 for the floodplain Manning's n is suitable. Whilst in this study the value of 0.06 for floodplain roughness has been chosen following previous work in the Uck and Pickering catchments (Odoni and Lane 2010), such a value has been chosen as an estimation to best represent the *entire* catchment and therefore not necessarily appropriate to base the sensitivity analysis around.

This reliance on the assumption that the default value is appropriate highlights the disadvantage of a second method of parameter value variation whereby the parameter value is varied by a fixed % of the default value (Lenhart et al. 2002).

5.2.5   Chosen method for parameter value variation

The range of parameter values were selected from the full distribution of feasible values based on an evaluation of the relevant literature. As roughness values were a key feature of this

sensitivity analysis, a strong focus on the work of Chow (1959) was deemed appropriate. This is an important step, as highlighted by Wainwright and Mulligan (2004). For example if the ranges of variable values are in no way realistic (when applied to a natural system) then their effect on the model output is largely irrelevant. Additionally at this stage it was thought to be important to explore the behaviour of the model parameters over their full potential range.

Beven (2001) stated that even using 10 increments for each parameter tested does not allow a thorough assessment of the parameter space. Due to the nature of the Overflow model it was possible to run several simulations every hour. This relatively low computational demand meant that it was practical to vary parameter values at increments of 5% of the realistic range. This allowed 21 increments per parameter. Lenhart et al. (2002) found that varying parameter values by a fixed % of the full parameter range did not give significantly different results to the method by which values are varied by a fixed % of the default value. Despite this there are several disadvantages to this technique and therefore the method chosen was selected as the most robust possible.

5.2.6 Parameter values for OAT sensitivity analysis

Table 5.1 shows the parameter values chosen. Whilst the values of all other parameters tested could be varied using percentage increments, discrete values were used for the time map parameter. The rain rate time maps were created to control cell passage times based on specified rainfall rates and so these specified rainfall rates were used as the basis of the OAT analysis.

Table 5.1 Model parameters and the range of values selected for use in the Sensitivity Analysis

Parameter	Parameter values	Range	Increments
Rain rate time map (rainfall mm/day)	1, 2, 4, 6, 8, 10, 12, 14, 16, 18, 20, 24, 30, 36, 42, 50, 60, 80, 100, 120, 140, 160, 180, 200		
Effective runoff rate	75-125% of default rainfall volume		
Channel Manning's n	0.025-0.15	0.125	0.00625
Floodplain Manning's n	0.02-0.2	0.18	0.009
Land Manning's n	0.02-0.2	0.18	0.009
Hydrograph timing (hours)*	(+) and (-) 20 hours of default timing	40hrs	2 hours

*Timing errors will occur if the rainfall input is routed through the catchment to slowly or too quickly. The effect of errors in the timing of the simulated flood peaks will also be explored. This will be done, not through changing a model parameter, but by simply shifting the simulated hydrograph either forwards or backwards in time. This analysis is therefore only used to identify bias in the objective functions used to quantify goodness-of-fit.

5.2.7   Rain time map to be used

As discussed in the graphical analysis section of the results (5.3.1), and as expected, the rain time map applied to the catchment has a large impact on the simulated hydrograph. This leads to a difficult decision regarding which rain time map should be used as the default when carrying out sensitivity analysis. Indeed, as the calibration goes on to show (Chapter 7) the required rain time map should vary as a function of time. To explore the effects of different rain rates on model sensitivity, different rain time maps (30 mm/day and 180 mm/day) were set as the default, as each roughness parameter and the effective runoff rate parameter was varied one at a time.

5.2.8   Figure scales

A normalised scale was created to allow parameters with different units and ranges of values to be compared on the same graphs. Whilst this does have the disadvantage of showing figures without dimensional parameter values, it does allow the variation in objective function

to be compared easily for all parameters. This method proves to be vastly better than using a logarithmic scale.

The parameter values were normalised by calculating the value, V by;

V = (Pi – Pmin) / (Pmax – Pmin)
where;
Pi = original parameter value, i
Pmax = maximum parameter value
Pmin = minimum parameter value

However, as previously stated, discrete values were used for the rain rate time map parameter. Additionally there are 24 rain time maps, as opposed to the 21 values for the other parameters. Therefore the above formula does not produce identical normalised scales for roughness and rain time map parameters. It can be seen by plotting a linear number pattern (y-axis) against the normalised scales for roughness and effective runoff rate parameters and rain time map parameter (Figure 5.1), that the two scales do not show a similar pattern. The rain time map scale shows a clustering of points close to each other between 0 and 0.2.
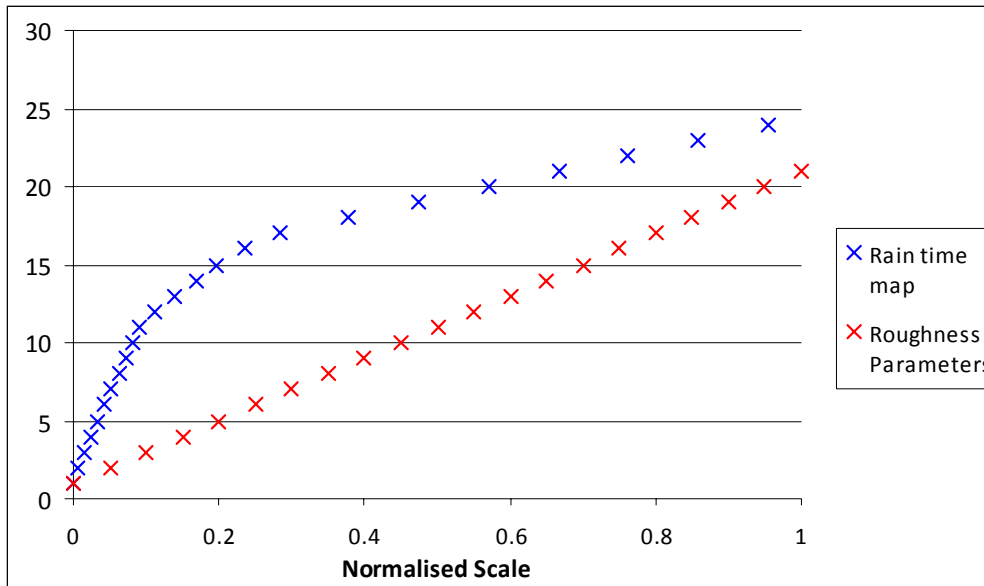
Figure 5.1. A figure plotting a linear trend against the normalised parameter scales. It can be seen that there are 21 points for the roughness parameters and 24 points for rain time map.

5.2.9   A Note on Objective Functions

McCuen (1973) and Diskin and Simon (1977) stated that the choice of objective function to be used to compare simulated and observed data is a largely subjective one; it is the choice of the

modeller. However both McCuen (1973) and Green and Stephenson (1986) emphasised the importance of selecting the appropriate goodness-of-fit statistic, or objective function, for the particular purpose it is intended for as different measures "may give more weight to certain aspects of the disagreement between simulated output and observed data" (Green and Stephenson 1986: 397). For example Nash-Sutcliffe Model Efficiency and sum of squared residuals, two objective functions frequently used in studies to compare two hydrographs, are biased towards errors in extreme values (Legates and McCabe 1999), in this study, simulated high flows or flood peaks.

As this study is focusing on the reduction of flood peaks in Uckfield this may be viewed as acceptable (Green and Stephenson 1986) as errors in the highest flood peak are more likely to be important in further investigation in this particular study, and therefore potentially should be emphasised. However such objective functions can potentially suggest that a model is not performing as well as it is, if errors are largely found at high flows. Therefore results can be misleading, suggesting that a model is not behavioural when for the most part it is. In addition to this Beven (2001) stated that disadvantages of the Nash-Sutcliffe and sum of squared errors are highly sensitive to error in the timing of predictions. The impact of this will be discussed later.

5.2.10 Objective function equations

(i) Nash-Sutcliffe Model efficiency

Nash-Sutcliffe model efficiency:

$$E = 1 - \frac{\sum_{t=1}^{T} \left(Q_o^t - Q_m^t\right)^2}{\sum_{t=1}^{T} \left(Q_o^t - \overline{Q_o}\right)^2}$$ Eq. 5.1

Where;

Q_o^t = observed flow rate at time t

Q_m^t = simulated flow rate at time t

$\overline{Q}_o$ = mean observed flow rate

(ii) % error in peak (PEP)

PEP = $\dfrac{q_{ps} - q_{po}}{q_{po}}$ x 100 Eq. 5.2

where;

q_{ps} = simulated peak flow rate

q_{po} = observed peak flow rate

(iii) Mean Absolute Error (MAE)

$$MAE = \frac{1}{n} \sum_{i=1}^{n} |e_i| . \qquad \text{Eq. 5.3}$$

where;

n = number of measures

$e_i = q_m{}^t - q_o{}^t$

$q_m{}^t$ = simulated flow rate at time t

$q_o{}^t$ = observed flow rate at time t

(iv) Root Mean Square Error (RMSE)

$$RMSE = \left(\frac{1}{n} \sum_{i=1}^{n} \{q_o(t) - q_s(t)\}_i^2 \right)^{\frac{1}{2}} \qquad \text{Eq. 5.4}$$

$q_s{}^t$ = simulated flow rate at time t

$q_o{}^t$ = observed flow rate at time t

n = number of measures

(v) Timing error

Time difference (in hours) between simulated and observed peak discharge

5.3   Results

First, visual, qualitative analysis of the hydrographs produced as parameter values are varied is presented. Subsequently the results of the quantitative sensitivity analysis are presented. The results are shown in order of the most sensitive parameters first, concluding with the effect of timing errors on the results.

5.3.1   Qualitative graphical analysis

It can immediately be observed from Figure 5.2, that for the default roughness parameter settings, and for certain rainfall rate time maps, a qualitative agreement can be observed

between model predictions and the observed hydrograph from the 2000 flood event; three peaks in discharge can be identified, though the timing of the flow peaks is not in precise agreement and the largest peak is greatly over-estimated in many cases.
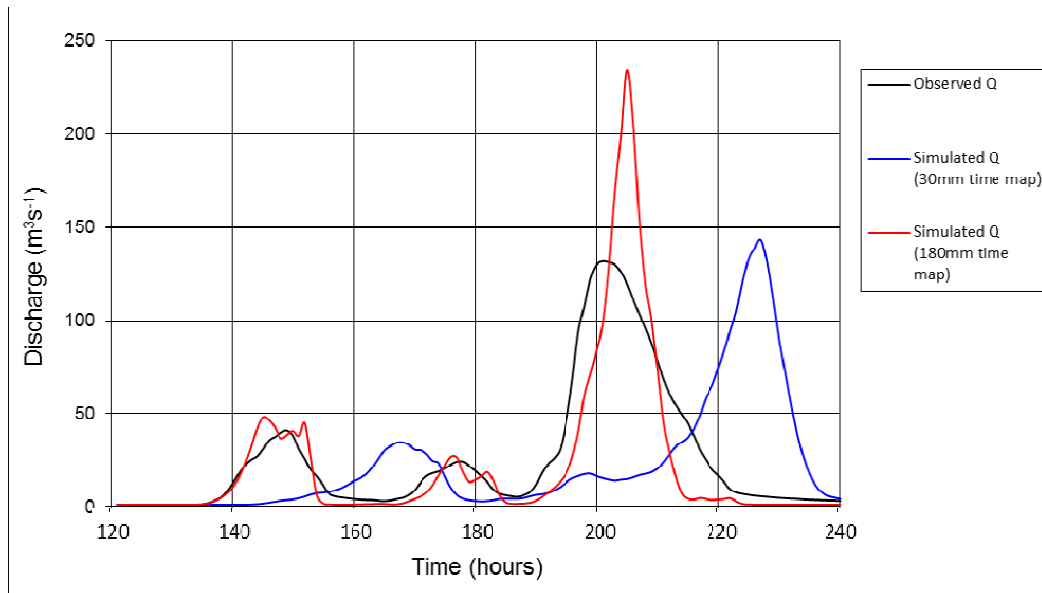
Figure 5.2. A comparison of observed discharge recorded at Isfield gauging station during the 2000 flood, with simulated discharge for 30 mm and 180 mm/day rain time maps.

Graphical analysis of the hydrographs produced applying 30 mm/day and 180 mm/day rain time maps (Figure 5.2) immediately highlights a number of key issues when working with the model;

First there are two main forms of hydrograph error immediately apparent:

- Timing errors in the three discharge peaks (most apparent in the third peak and for simulations using particular rain time maps)
- Peak flow error. Primarily an over-estimation of peak discharge, apart from for the lowest rain rates (24 mm/day or less), which greatly underestimate peak discharge.

Second it can be observed that the rain time map that is applied to the catchment (range 1 mm/day – 200 mm/day) has a very large effect on the shape of the hydrograph produced by the model. Figure 5.2 shows that when the 180 mm/day time map is applied the hydrograph produced shows a relatively good, qualitative agreement with the observed hydrograph in terms of the timing of the 3 peaks. The largest flood peak does show more error in timing, however. Secondly the discharge of the first two peaks shows a good fit with observed data, albeit with some additional oscillation in discharge. However the peak discharge for the event is greatly over-estimated. It is possible to argue that the 30 mm/day time map produces a qualitatively good simulation of observed discharge. The shape of the

40

observed and simulated hydrographs shows relatively good agreement. Secondly the peak discharge is close to that observed during the 2000 flood event. However the timing of the peaks is in error by approximately 20 hours.

Third it can be seen that the area under the flood curves is very similar for the different time maps. This is due to the effect of applying different rain time maps; the parameter does not affect rainfall volume. Instead it controls the routing of the rain input through the catchment. Therefore the same volume of water passes a fixed point, though at different times according to the rain time map applied.

5.3.2   Sensitivity Analysis

Figures (5.3-5.11) show the hydrographs produced as parameter values were varied one at a time. Variation in rain rate time map clearly affects the timing and shape of the flood peaks (Figure 5.3). When rain time maps 1-24 mm/day are applied, there is no resemblance between the observed and simulated hydrographs. As the time map rain rate is increased above 30 mm/day, peak discharge is overestimated to a greater degree though timing of the main flood peak becomes more accurate.

Variation in the effective runoff rate alters the flood volume but has no effect on any other features of the flood hydrograph (Figures 5.4, 5.5). For the 180 mm/day rain time map it can be seen that decreasing effective runoff rate reduced the greatly overestimated peak flow (Figure 5.5). Increasing effective runoff rate by a fixed % has a slightly greater effect on peak flow than decreasing effective runoff rate by the same amount. Increasing effective runoff rate by 10% leads to an increase in peak flow of 42.2 cumecs, whereas a 10% decrease leads to a decrease in peak flow of 38.8%.

As floodplain roughness is increased, the hydrograph is delayed and the main flood peak clearly reduced (Figures 5.6, 5.9). Delay in the hydrograph is greater when the 30 mm/day time map is applied. As channel Manning's n is increased the main peak flow is reduced (Figures 5.7, 5.10), though not delayed by as much as when floodplain roughness is increased. As with the floodplain roughness parameter, delay in the hydrograph as channel roughness increases, is greater for the 30 mm/day rain time map. Land surface roughness does not have a significant impact on the flood hydrograph (Figures 5.8, 5.11).
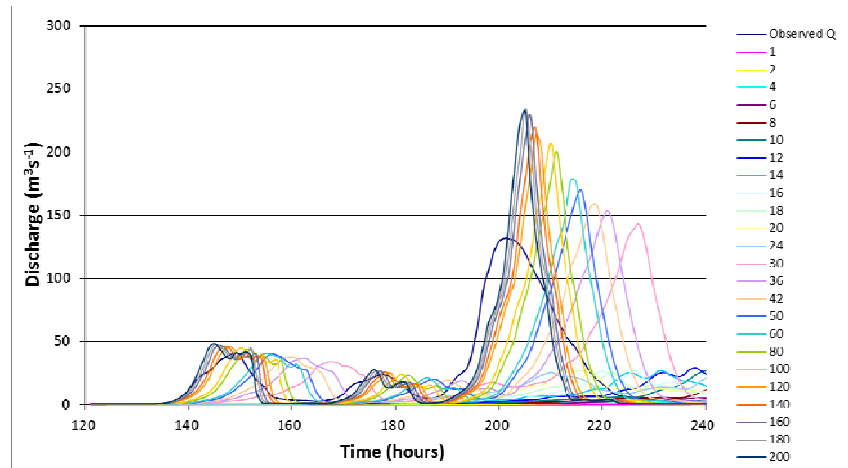
Figure 5.3. The hydrographs simulated as the rain time map is varied between 1 and 200 mm/day. The hydrograph in black shows the observed discharge at Isfield during the 2000 flood event.
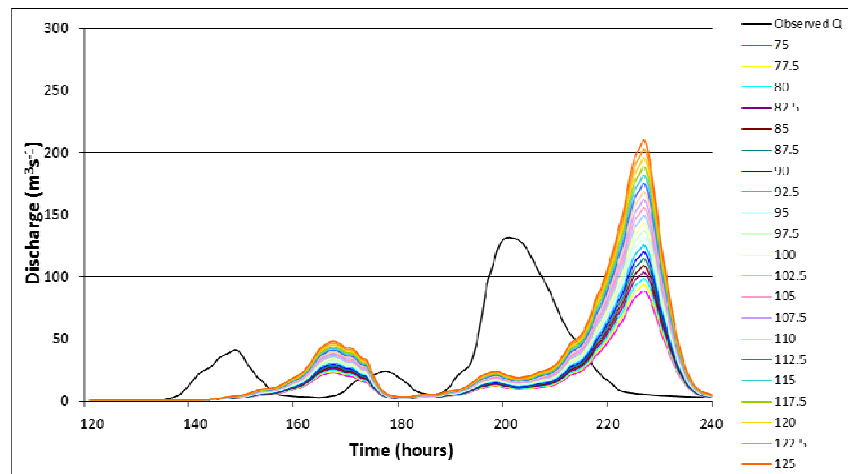
Figure 5.4. The hydrographs simulated as effective runoff rate is varied 75-125% of the default value. The hydrograph in black shows the observed discharge at Isfield during the 2000 flood event. Rain time map set at 30 mm/day.
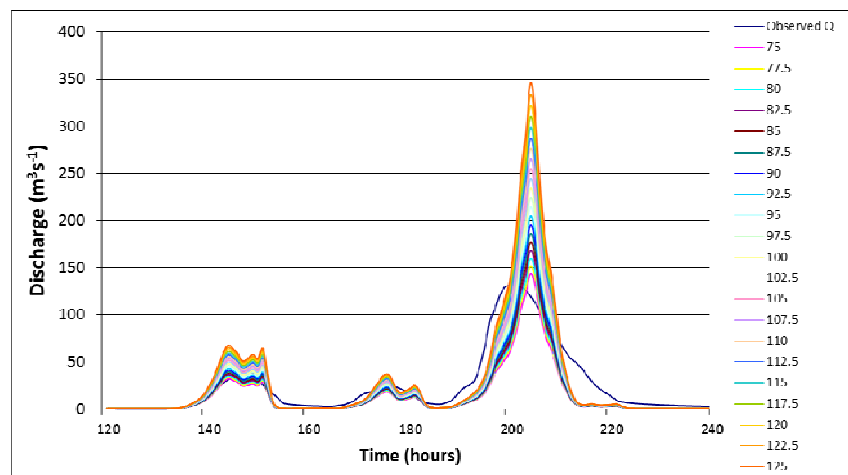
Figure 5.5. The hydrographs simulated as effective runoff rate is varied 75-125% of the default value. The hydrograph in black shows the observed discharge at Isfield during the 2000 flood event. Rain time map set at 180 mm/day.
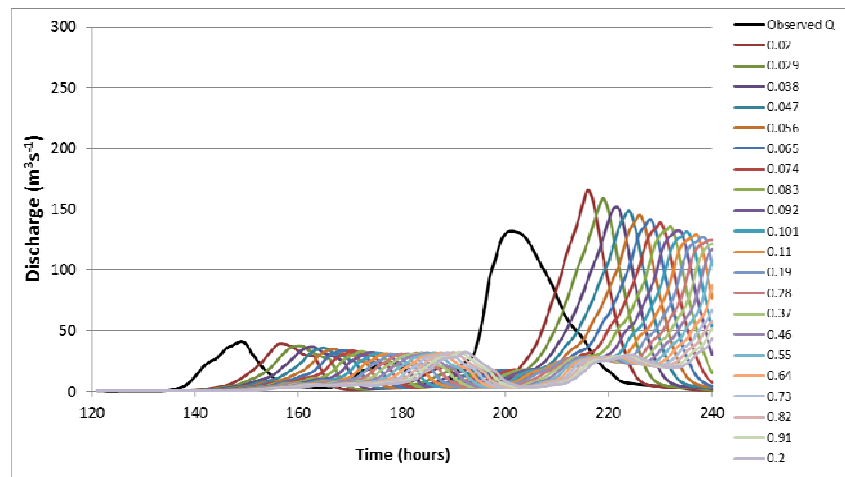
Figure 5.6. The hydrographs simulated as floodplain Manning's n is varied from 0.02 to 0.2. The hydrograph in black shows the observed discharge at Isfield during the 2000 flood event. Rain time map set at 30 mm/day.
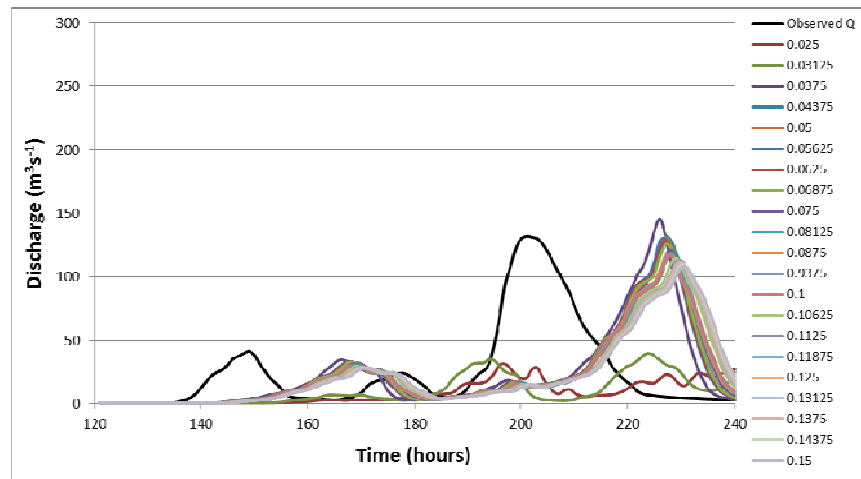
Figure 5.7. The hydrographs simulated as channel Manning's n is varied from 0.025 to 0.15. The hydrograph in black shows the observed discharge at Isfield during the 2000 flood event. Rain time map set at 30 mm/day.
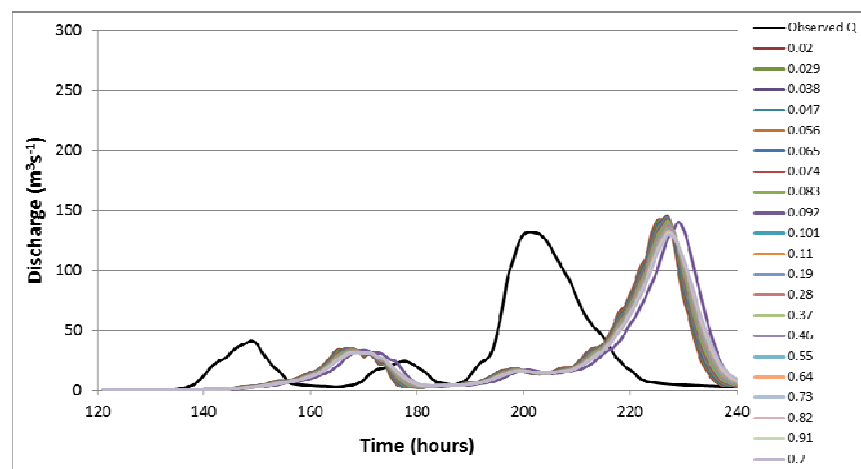
Figure 5.8. The hydrographs simulated as land Manning's n is varied from 0.02 to 0.2. The hydrograph in black shows the observed discharge at Isfield during the 2000 flood event. Rain time map set at 30 mm/day.
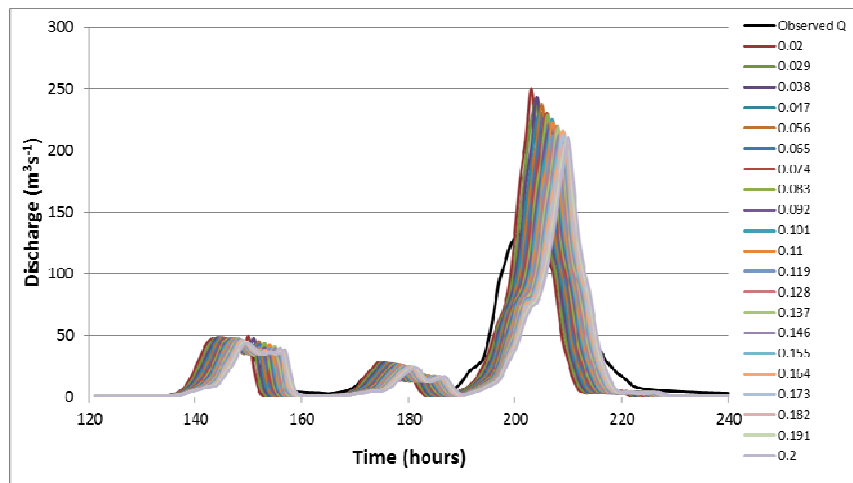
Figure 5.9. The hydrographs simulated as floodplain Manning's n is varied from 0.02 to 0.2. The hydrograph in black shows the observed discharge at Isfield during the 2000 flood event. Rain time map set at 180 mm/day.
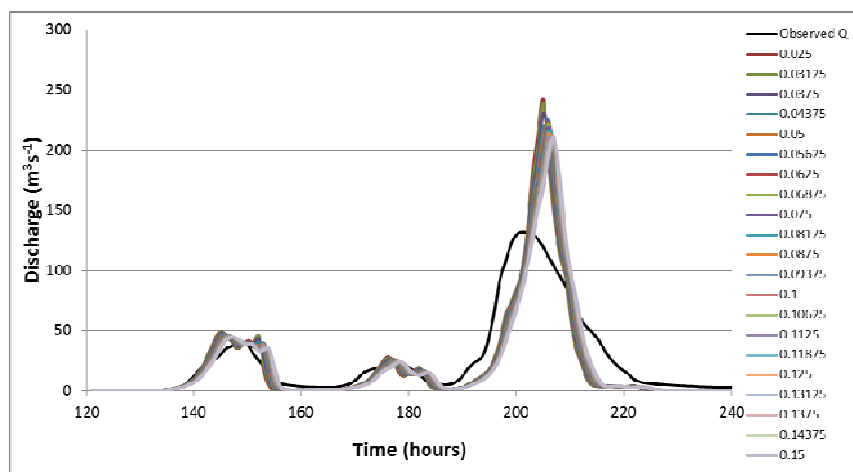
Figure 5.10. The hydrographs simulated as channel Manning's n is varied from 0.025 to 0.15. The hydrograph in black shows the observed discharge at Isfield during the 2000 flood event. Rain time map set at 180 mm/day.
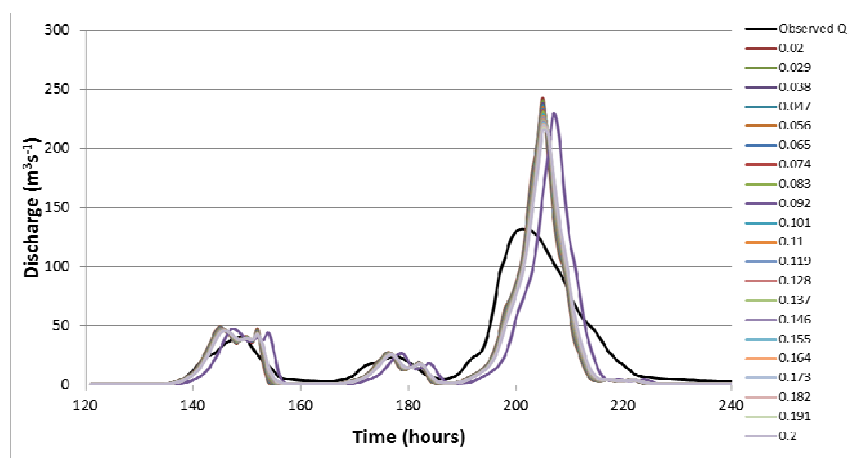
Figure 5.11. The hydrographs simulated as land Manning's n is varied from 0.02 to 0.2. The hydrograph in black shows the observed discharge at Isfield during the 2000 flood event. Rain time map set at 180 mm/day.

The results of the sensitivity analysis are shown in Figures (5.12-5.16), using both 30 mm and 180 mm/day as the default rain time maps when varying each roughness parameter one at a time. Figures 5.12-5.16 will be described in the next section. Data tables in Appendix C.
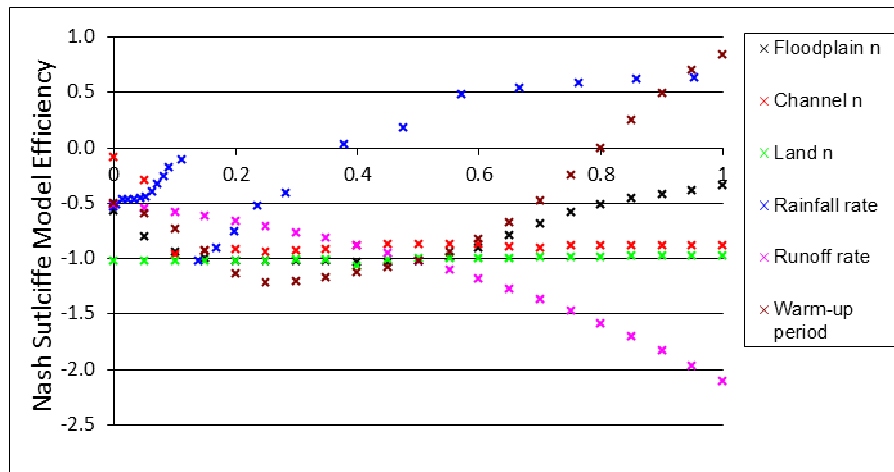
Figure 5.12a. Variation in Nash-Sutcliffe model efficiency against a normalised parameter scale. Rain time map fixed at 30 mm/day for roughness parameters
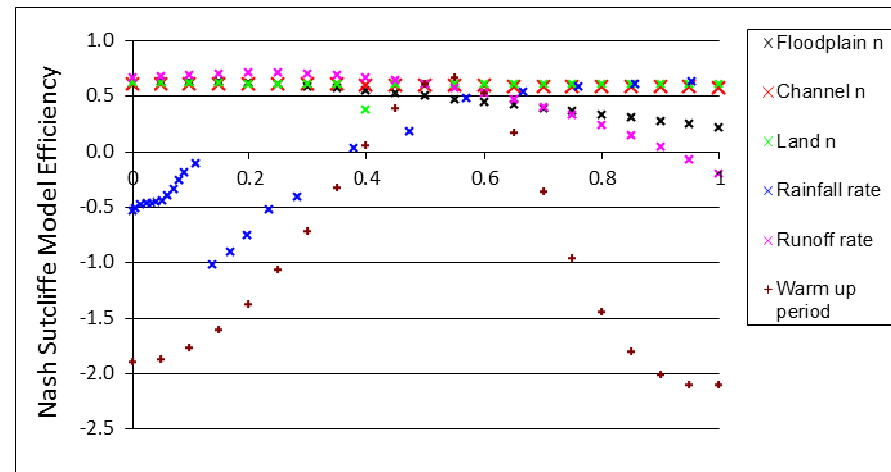
Figure 5.12b. Variation in Nash-Sutcliffe model efficiency against a normalised parameter scale. Rain time map fixed at 180 mm/day for roughness parameters
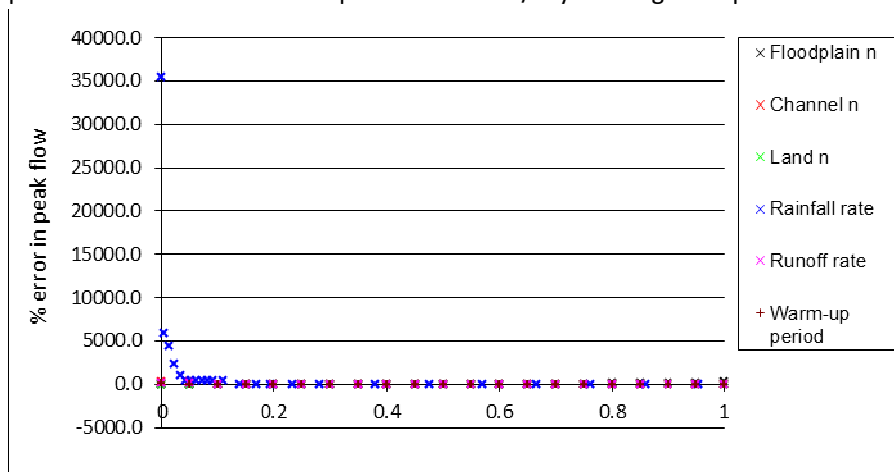
Figure 5.13a. Variation in % error in peak discharge against a normalised parameter scale. Rain time map fixed at 30 mm/day for roughness parameters
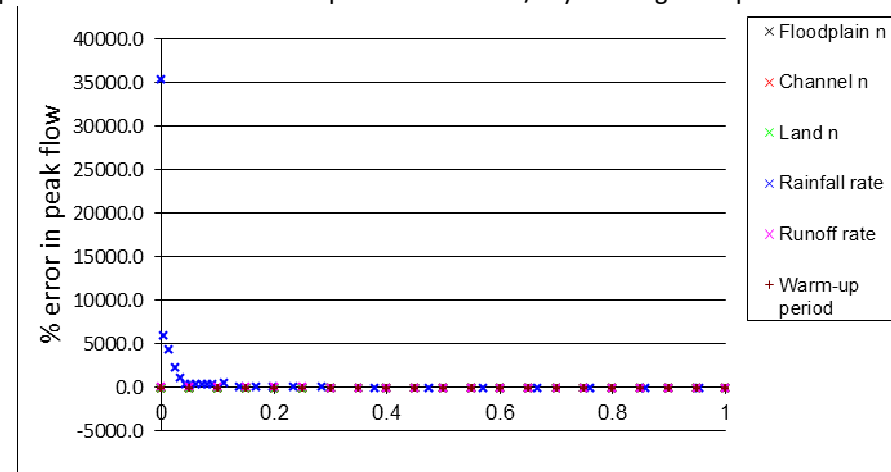
Figure 5.13b. Variation in % error in peak discharge against a normalised parameter scale. Rain time map fixed at 180 mm/day for roughness parameters
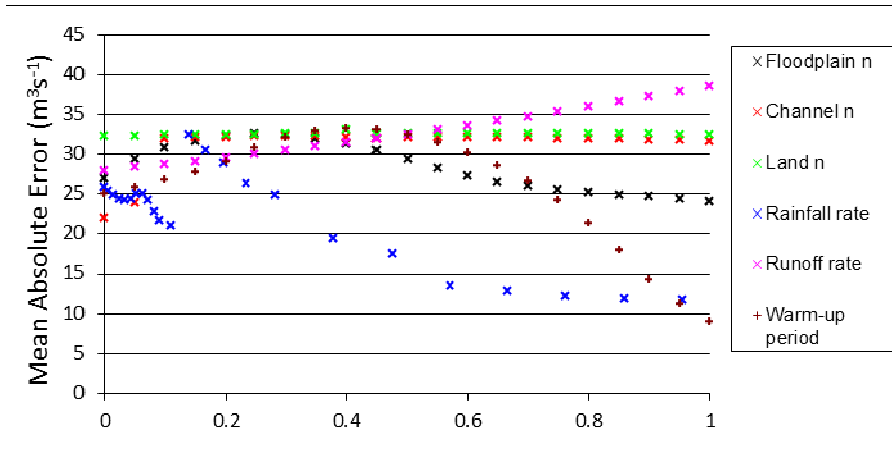
Figure 5.14a. Variation in Mean Absolute Error against a normalised parameter scale. Rain time map fixed at 30 mm/day for roughness parameters
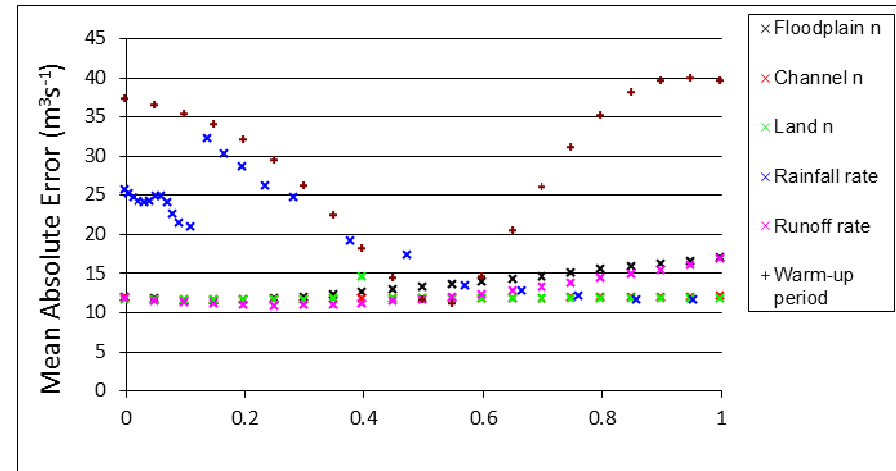
Figure 5.14b. Variation in Mean Absolute Error against a normalised parameter scale. Rain time map fixed at 180 mm/day for roughness parameters
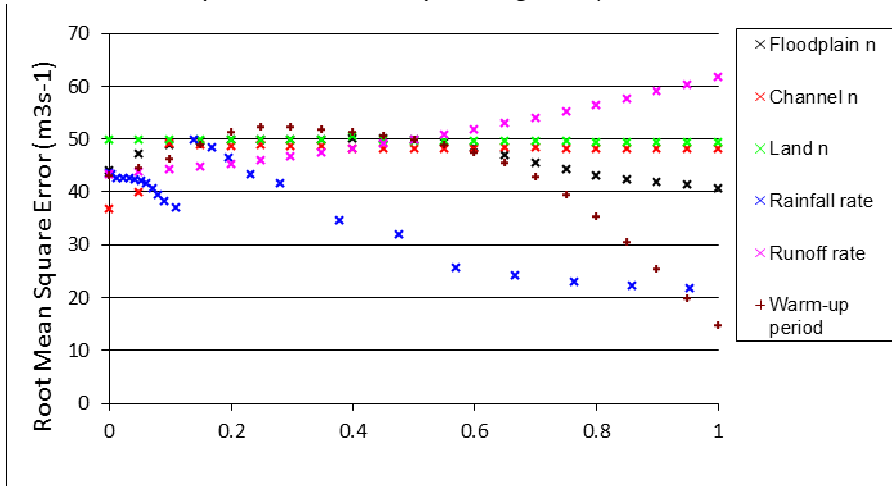
Figure 5.15a. Variation in Root Mean Square Error against a normalised parameter scale. Rain time map fixed at 30 mm/day for roughness parameters
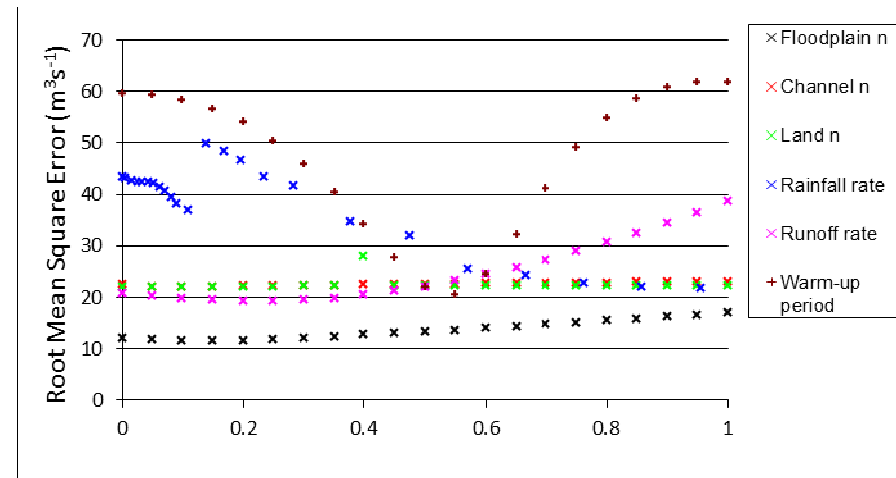
Figure 5.15b. Variation in Root Mean Square Error against a normalised parameter scale. Rain time map fixed at 180 mm/day for roughness parameters

47
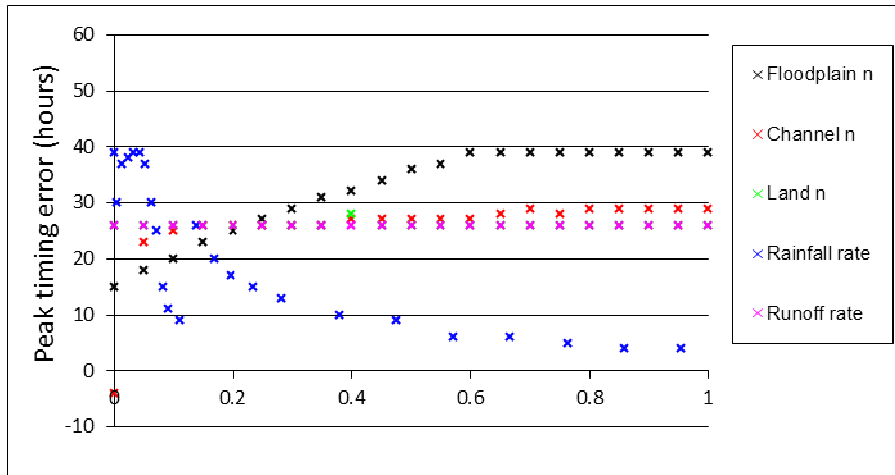
Figure 5.16a. Variation in Peak timing error against a normalised scale.
Rain time fixed at 30 mm/day for roughness parameters
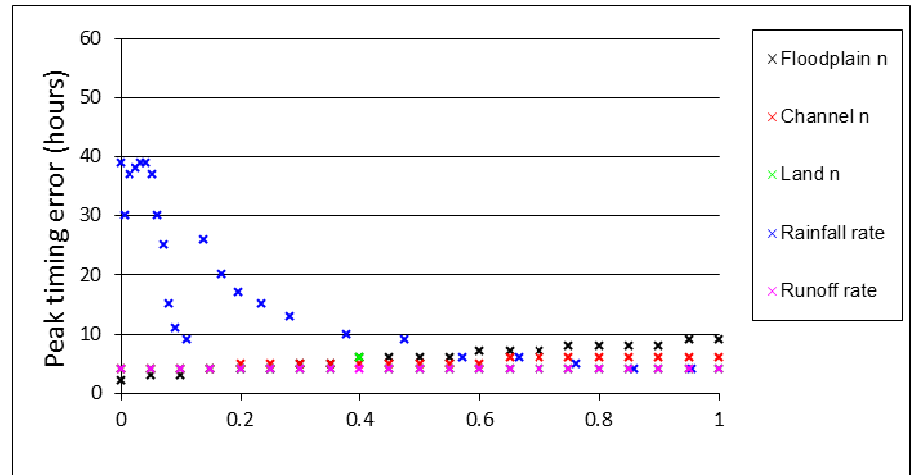
Figure 5.16b. Variation in Peak timing error against a normalised parameter scale.
Rain time map fixed at 180 mm/day for roughness parameters

5.3.3   Rain time map

Model output is most sensitive to the rain rate time map and effective runoff rate parameters; the goodness-of-fit, as quantified by the objective functions detailed in (Section 5.2.10) varies by the greatest amount as each of the two parameters is varied one at a time (Figures 5.12-5.16). The results of the former are presented first due to the importance of deciding on a default rainfall rate when other parameters are varied (Section 5.3.1).

Figures 5.12a and b show that positive Nash-Sutcliffe values are only found for the highest rain rate time map, at least whilst all other parameter values are fixed at their default values. Over the full range of rain rate time maps, resulting extremes in NSME values are -1.03 (30 mm/day) and 0.62 (200 mm/day). The lowest and highest NSME values occur when timing errors in peak Q are at their highest and lowest respectively. Results are reflected for MAE and RMSE; the largest errors are apparent when the 30 mm/day time map is applied and the smallest errors when the 200 mm/day time map is applied.

The % error in peak discharge (PEP) statistic shows the greatest indication of the sensitivity of the rain time map parameter (Figures 5.13a and b). The closest fit between observed and simulated hydrographs in relation to peak discharge occurs when the 30 mm/day time map is applied.

A threshold can be identified between the 24 mm/day and 30 mm/day time maps, at which point model performance is seen to change sharply (Figure 5.17). For example, error in peak discharge varies from 410.8% when the 24 mm/day time map is applied, compared to 8.0% for the 30 mm/day time map. Error in peak discharge magnitude then increases as larger time maps are applied. A similar pattern is also apparent for the other objective functions. However, in contrast to the PEP, all other objective functions show an increase in error moving from a 24 to 30 mm/day time map (for example NSME value -0.12 for the 24 mm/day and -1.03 for the 30 mm/day time maps), with error subsequently decreasing as larger time maps are applied (NSME 0.62 for 200 mm/day time map).

5.3.4   Effect of rain time map on quantification of goodness of fit

Model output is not only highly sensitive to the rain time map applied, but the response of model output to variation in other parameters is greatly affected by the choice of default rain time map. Because of the nature of the simulated hydrographs, the statistics can show different signals when different time maps are used. The difference in the sensitivity of model parameters when different default time maps are applied will be discussed in the following sections.
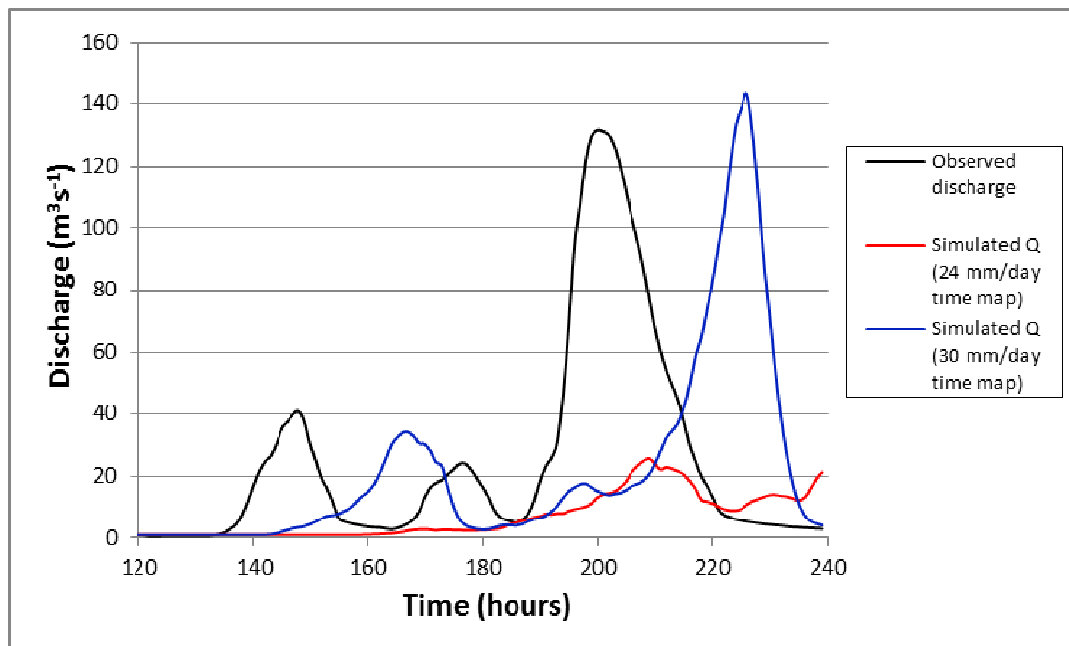
Figure 5.17. A comparison of model output with all parameters fixed, but with a 24 mm/day and 30 mm/day rain time map applied. A clear difference can be identified between the two hydrographs produced.

5.3.5 Effective runoff rate

The best fit between observed and simulated hydrographs occurs when effective runoff rate is at its lowest values (a minimum of 75% of the default amount) for both 30 mm and 180 mm/day rain time maps. Overall model output is more sensitive to variation in effective runoff rate when the 30 mm/day time map is set as the default. A flatter response for the higher rainfall rate can be observed. For all objective functions excluding PEP, there is little variation in model performance between 0 and 0.4 on the normalised scale when the 180 mm/day time map is applied (Figure 5.12-5.16).

For all effective runoff percentages, NSME values are higher when a 180 mm/day time map is applied (Figure 5.12b. At the same time MAE and RMSE values are lowest for the higher rain rate time map (Figures 5.14, 5.15). As discussed, error in peak flow timing is unaltered by variation in effective runoff rate (Figures 5.16a and b). Error in the timing of peak flow is 26 hours and 4 hours for the 30 mm/day and 180 mm/day time maps respectively. As with the rain time map parameter, the highest NSME values and lowest MAE and RMSE values occur when timing error is lowest.

5.3.6 Floodplain roughness

Figures 5.12-5.16 show that the roughness parameters are not as sensitive as the rainfall rate time map and effective runoff rate parameters. The only objective function which does not suggest this is peak flow timing error, which does not vary as effective runoff rate is varied.

Model output shows a higher sensitivity to floodplain roughness when Manning's n values are highest (Figures 5.12-5.16), though the Manning's n values at which model output becomes sensitive to floodplain roughness vary depending on the objective function used.

It can be seen that as floodplain roughness increases, the goodness-of-fit between observed and simulated hydrographs differs for the two rainfall rate time maps used. Overall floodplain roughness is most sensitive when the lower rain rate time map is applied. When the 180 mm/day rain time map is applied, NSME values decrease and MAE and RMSE values increase as floodplain roughness is increased. In contrast, when the 30 mm/day time map is applied, MAE and RMSE values decrease and NSME values increase towards 0 as floodplain roughness increases above 0.5 on the normalised scale (Manning's n, 0.11). However the trend is not linear when the 30 mm/day time map is applied. From 0 to 0.25 on the normalised scale (n values, 0.02-0.065), error values increase as floodplain roughness increases.

5.3.7   Channel roughness

Model output is relatively insensitive to variation in channel roughness in comparison to the response behaviour when floodplain roughness is varied. Figures 5.18a-e further highlight this. For example, as floodplain roughness is varied, MAE varies from 23.9-32.2 cumecs and 11.5-17.0 cumecs for 30 and 180 mm/day rain time maps respectively (Figures 5.14a and b; Appendix C). As channel roughness is varied, MAE varies from 21.9-32.1 cumecs and 11.7-12.0 cumecs for 30 and 180 mm/day rain time maps. However for the 30 mm/day rain time map, only 2 channel parameter values produce MAE below 30 cumecs (Figure 5.14a). This highlights the higher sensitivity of model output to variation in floodplain roughness. A similar signal is shown by RMSE (Figure 5.15a and b). Peak timing error varies to a greater degree when floodplain roughness is varied, in contrast to channel roughness. The variation in the timing of the peak discharge as floodplain roughness is varied has been shown (Figures 5.6, 5.9).

Model output shows slightly more sensitivity to variation in channel roughness when the 30 mm/day time map is applied, primarily when channel roughness is low. When channel roughness is low errors in simulated peak flow are very high (>200%).

Figure 5.18a-e. A comparison of the sensitivity of model output to one-at-a-time variation in channel and floodplain roughness for all 5 objective functions. The x-axes are the normalised scale, as with Figures 5.12-5.16
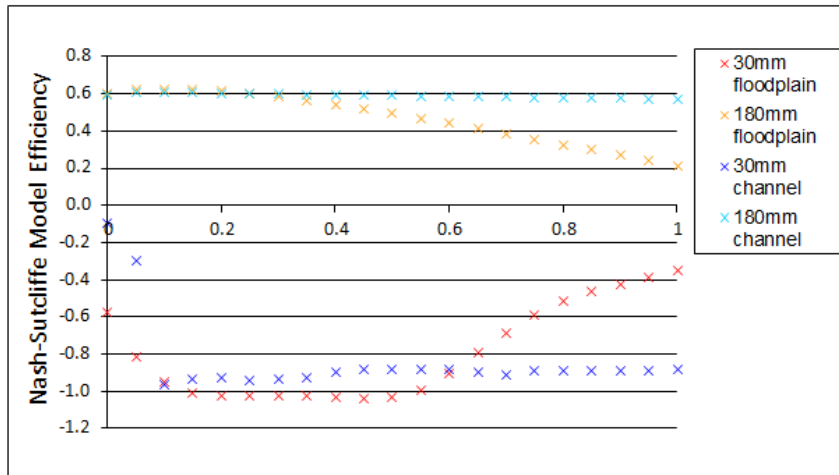
Figure 5.18a. Variation in Nash-Sutcliffe Model Efficiency
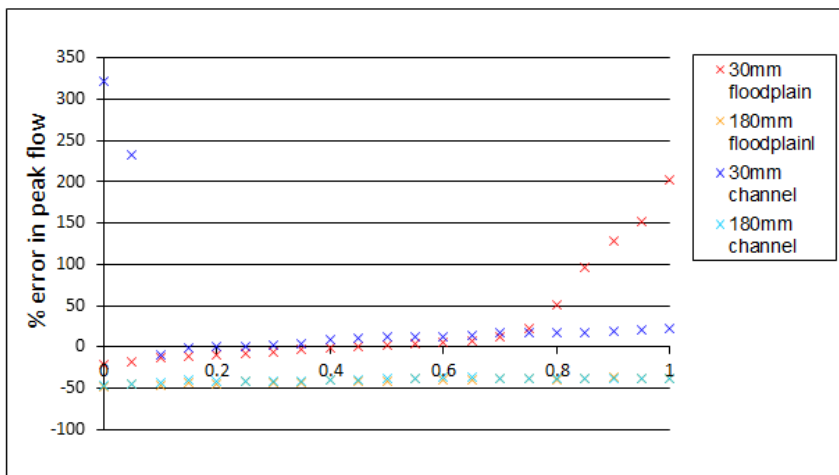
Figure 5.18b. Variation in % error in peak discharge
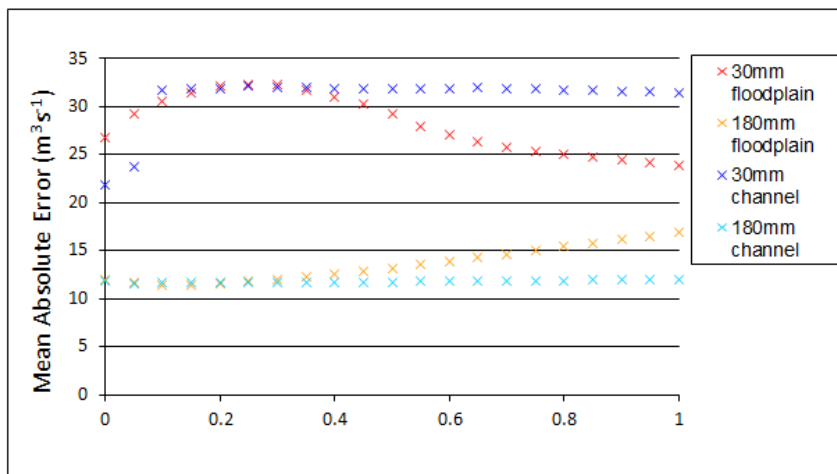
Figure 5.18c. Variation in Mean Absolute Error
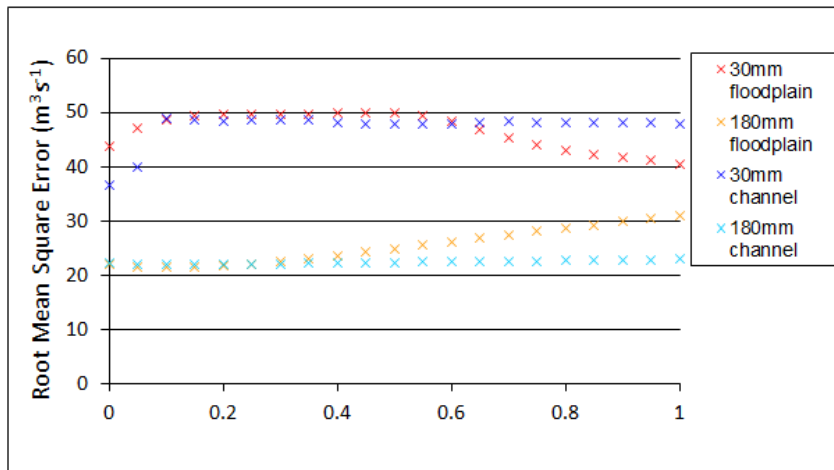
Figure 5.18d. Variation in Root Mean Square Error
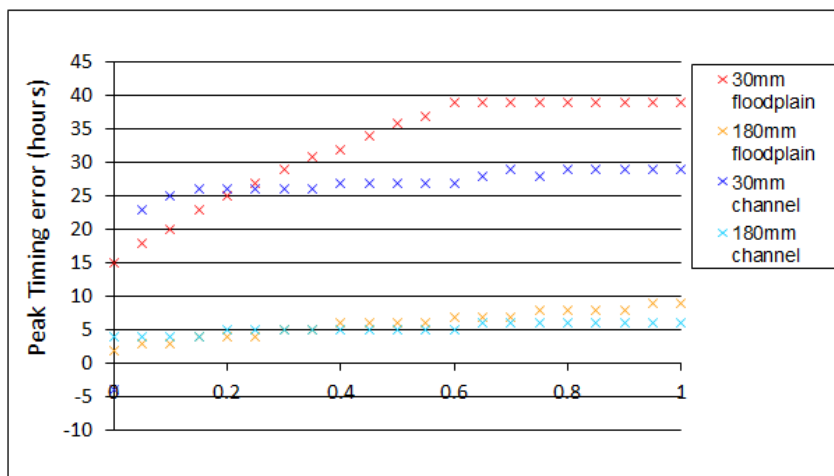
Figure 5.18e Variation in Peak timing error

5.3.8 Land surface roughness

Figures 5.12-5.16 show that land roughness is the least sensitive of the roughness parameters. It can be seen for all statistical tests that whilst there is some variation in the model output as land roughness values are varied across their realistic range, this variation is less than the other parameters. There is one anomalous point in the output, indicated by Nash-Sutcliffe Model Efficiency (NSME), Mean Absolute Error (MAE) and Root Mean Square Error (RMSE), located at point 0.4 on the normalised scale. However this does not affect the conclusion that of the 5 parameters tested, model output is least sensitive to land surface roughness. This indicates that whilst the model output is affected by the roughness of the catchment land cover, it is affected to a greater degree by the roughness of the floodplain and channel, and the rain time map applied.

5.3.9   Timing error effect on statistics/spin-up (warm-up time)

Table 5.2 shows the results of the objective functions for the hydrographs presented in Figures 5.19a and b. The results allow an understanding of the effect of the timing errors that are present in a number of the simulated hydrographs presented earlier in Section 5.3.2.

Table 5.2. The variation in goodness-of-fit for the same simulated hydrograph, but with hydrograph timing varied. It can be noted that for 30 mm/day, lower error is suggested for +20h timing. This is attributable to the fact that peak flow is delayed to such a degree that it does not influence the objective functions.

30 mm/day time map

Timing (hours)	NSME	MAE	RMSE	Peak timing error
+20	-0.51	24.9	43.0	46
+10	-1.22	30.6	52.2	36
Default	-1.03	32.3	49.8	26
-10	-0.26	24.2	39.3	16
-20	0.82	8.8	14.8	6

180 mm/day time map

Timing (hours)	NSME	MAE	RMSE	Peak timing error
+20	-1.91	29.4	59.7	24
+10	-1.08	37.3	50.4	14
Default	0.60	11.7	22.1	4
-10	-0.97	31.0	49.1	6
-20	-2.12	39.7	61.8	16

As previously shown in Section 5.3.1, the hydrograph simulated when the 180 mm/day time map is applied shows a better goodness-of-fit with the observed hydrograph. However, if the timing error was reduced, the hydrograph simulated when the smaller rain time map (30 mm/day) was applied, would show a better fit. Indeed for both time maps the closest fit, as quantified by the objective functions, occurs when timing errors are at their smallest.

Moving the hydrograph simulated for the 30 mm/day time map can result in much smaller errors. However Figure 5.20 shows that doing the same for the 180 mm/day time map would cause the simulated peak flow to occur either before or at the same time as the peak rainfall. This illustrates that such a procedure can only be carried out to further understand the results observed and cannot be treated as a model parameter.
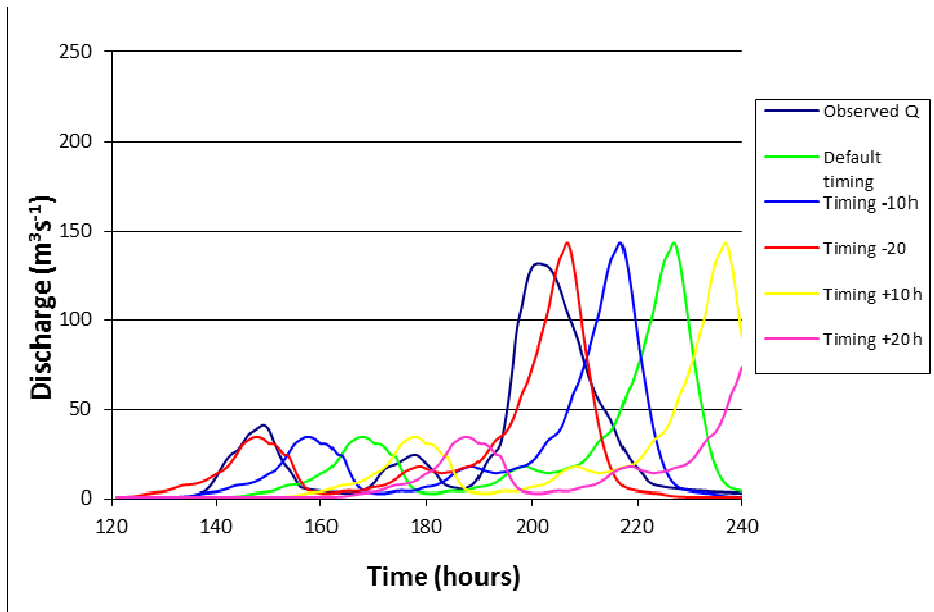
5.19a. 30 mm/day time map
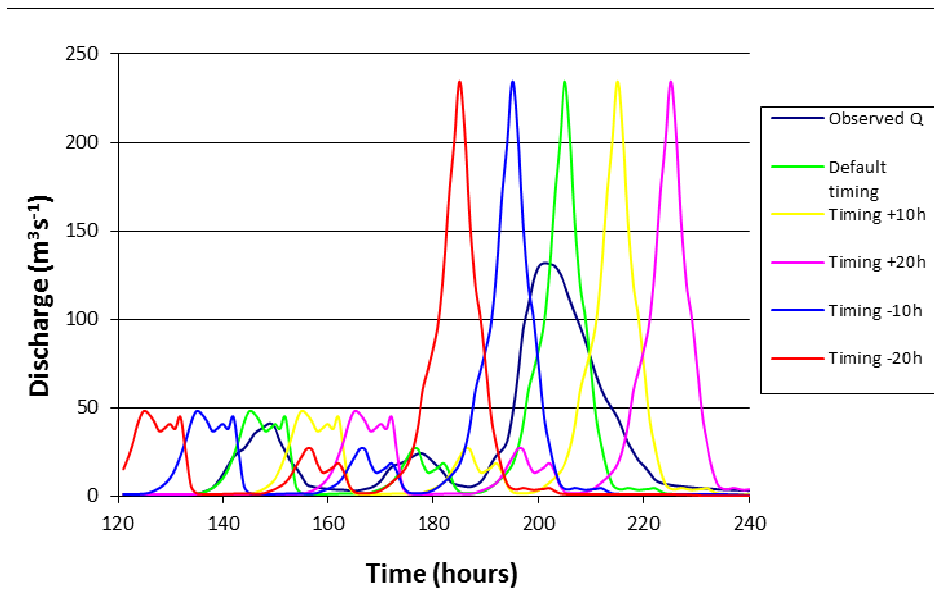
Figure 5.19b. 180 mm/day time map

Figure 5.19a and b. The simulated hydrographs are presented when a 30 mm/day and 180 mm/day time map is applied. The same hydrograph shifted 10 and 20 hours is also shown to highlight how the timing of the flood peaks in relation to the observed hydrograph influences the goodness-of-fit as shown in Table 5.2
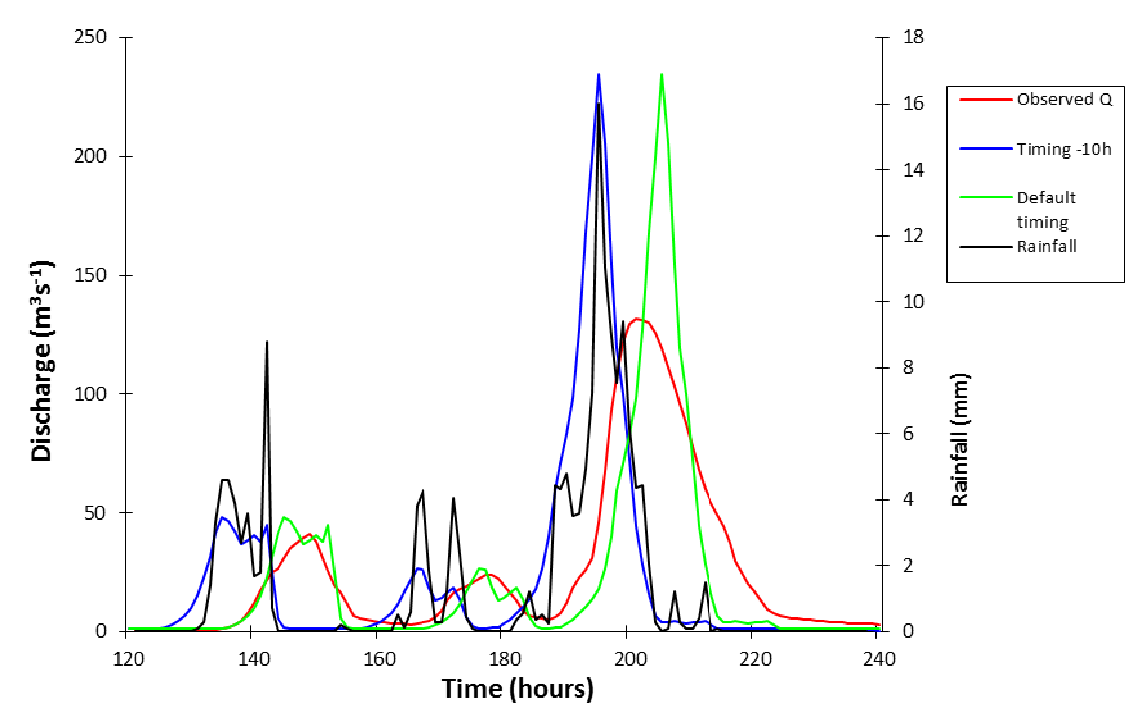
Figure 5.20. An illustration of the inappropriateness of shifting the simulated hydrograph, beyond the aim of exploring the objective function results. Shifting the hydrograph simulated, in this case, for the 180 mm/day time map would cause the flow peak to coincide with peak rainfall.

5.4   Discussion

5.4.1   Qualitative graphical analysis

Qualitative graphical analysis indicates errors in the simulated hydrographs. However, importantly it is possible to identify some *qualitative* agreement between simulated and observed hydrographs for some rain rate time maps. Therefore it is important not to reject the model straight away on the grounds of it being non-behavioural. Indeed, the key issue here is whether or not the model responds sensibly to parameter variation.

By looking at the hydrographs produced when using different rain time maps (Figure 5.2), an important issue arises. A decision is needed as to whether a hydrograph similar to that produced using a rain time map in the region of 180 mm/day or 30 mm/day is a more accurate (or realistic) simulation of the observed 2000 flood hydrograph (Figure 5.2), whilst also being realistic in relation to the hydrological response of the catchment as the storm event progresses. It is worthwhile considering whether, in the presence of hydrograph error which hydrograph characteristics are most essential for useful results to be acquired. Is it more desirable for a parameter set to produce model output so that; (A) the most accurate peak discharge is simulated and, whilst having a good qualitative agreement with the observed

hydrograph, timing of discharge peaks is most erroneous, or; (B) a hydrograph is simulated so that there is a good qualitative agreement with observed discharge, but the peak discharge is greatly over-estimated?

It can be seen that neither case is ideal and that such error is likely to be problematic further in the study. In relation to the results in this chapter this becomes more of an important issue when using objective functions whilst carrying out model sensitivity analysis due, amongst other factors, to the effect of timing errors.

5.4.2   Sensitivity analysis

5.4.3   Rain time map

It is not unexpected that model output is most sensitive to the rain time map applied. It can be expected that varying the rainfall rate from 1 mm/day to 200 mm/day will have a great impact on the simulated flood hydrograph.

As a higher equilibrium flow rainfall rate (time map) is applied, discharge in a cell at any given time will increase. As a result, for a flow of constant width and depth, flow velocity will increase, as shown by eq. 5.5;

$$v = \frac{Q}{wd} = \frac{1}{n} R^{\frac{2}{3}} S^{\frac{1}{2}}$$

Eq. 5.5

Cell passage time is then related to velocity by;

$$t_{cell} = \frac{l}{v}$$

Eq. 5.6

Where l = distance to travel, v = velocity

Changes in flow velocities occur as different time maps are applied. Eq. 5.5 shows that flow velocities will be much higher, and therefore cell passage times much shorter (Eq. 5.6) when a relatively high rainfall rate time map is applied. Figure 4.1a and 4.1b (Page 21) shows the time maps calculated for 30 mm/day and 180 mm/day equilibrium rain rates.

For the 30 mm/day time map, the time to outlet from the most distal areas of the catchment is at least twice that for the 180 mm/day time map. When a rain input is applied, depending on the time map, water will be routed through the catchment at very different speeds greatly affecting the flood hydrograph simulated. There will be a much shorter lag between peak rainfall and peak discharge when a higher rain rate time map is applied. The resultant hydrographs therefore show a great variation in shape and peak flow. This supports

the previous statement and explains the great variation in the objective functions as the rainfall rate time map is varied.

There is also a non-linear response in model output to changes in rainfall rate time map. A threshold in model output can be seen when rain time map is varied one step from 24 mm/day to 30 mm/day (Figure 5.17). The non-linear response in goodness-of-fit is explained by the nature of the hydrographs simulated (Figure 5.3). With rain time maps representing an equilibrium flow of 24 mm/day or less, the hydrograph is relatively flat with no substantial flow peaks. When the 30 mm/day rain rate time map is applied, a hydrograph more qualitatively similar to that observed during the 2000 storm event is simulated.

5.4.4   Effect of rain time map on objective functions

As discussed in Section 5.3.1, due to the high sensitivity of model output to the rain time map applied, the hydrographs produced vary greatly for different rainfall rate time maps. As the results of the objective functions vary greatly over the entire range of rain time map, the choice of one rain time map as the default setting will have an very important conditioning effect on model output and subsequently goodness-of-fit between observed and simulated hydrographs. This is indeed the case, with model output having a different response to changes in parameters when a different default rain time map is used.

It is therefore still problematic to use one single rain time map as the default for the sensitivity analysis. This informed the decision to use more than one rainfall rate during the sensitivity analysis (see Section 5.2.7). Following on from initial graphical and sensitivity analysis these results are the first indication that this study will be one in which the issue of applied rainfall rate time map will be key. This issue is made all the more important by the initial decision to apply a temporally and spatially constant rainfall rate time map throughout the simulated storm event for the purpose of sensitivity analysis. The decision hinges on the trade-off between model simplicity, the results obtained from the model and the uncertainty associated with these results. This will be discussed further in the uncertainty analysis.

5.4.5   Effective runoff rate

The variation in model output as effective runoff rate is varied is uncomplicated; as the total volume of rain applied to the catchment is reduced, peak discharge is also reduced. This decreases errors in the simulated peak flow for the 180 mm/day time map. As stated in 5.2.9, the NSME and RMSE statistics are biased towards error in the largest flows. This explains the great variation in the goodness-of-fit. It has already been stated that the timing of the flow peaks for the higher rain rate time map are relatively accurate. For the 30 mm/day time map timing errors remain large as the effective runoff rate parameter is varied. As a result the

largest errors are likely to occur in the largest flow peak, as it is compared to observed flow after the flow peak. A reduction in simulated peak flow therefore affects the goodness-of-fit.

5.4.6   Roughness parameters

Variation in the roughness parameters can be seen to have an impact on flow velocity, given a constant channel geometry, or cell width (Eq. 5.5). It might be expected that model output would be more sensitive to variation in channel roughness variation than floodplain roughness. Increased channel roughness is likely to reduce velocity and increase flow depth for a channel of constant geometry. Likelihood of overbank flow is subsequently increased, affecting downstream discharge (model output) (Wolff and Burgess 1994; Anderson et al. 2006). Floodplain roughness is only likely to have a significant effect when there is significant overland flow. However model output is more sensitive to floodplain n. At such high rain rates there is a possibility, particularly for the 180 mm/day time map, that flow is already out of bank, with the result that floodplain n has a large effect even when channel n is not increased. Such an explanation is supported by the low sensitivity to channel roughness when the 180 mm/day time map is applied. This again suggests that water is overbank in a large proportion of the catchment as altering channel roughness has very little impact. The small influence of channel roughness for the lower rain time map suggests that overbank flow is not initially occurring throughout the entire catchment.

Model output also appears to show less sensitivity to variation in floodplain roughness when the rain time map is set at 180 mm/day as opposed to 30 mm/day, when discharges are higher. Such a result is perhaps also unexpected as the higher rainfall rate is more likely to increase likelihood of overland flow at which point floodplain roughness will have a greater impact on flow conveyance. However when a large volume of water flows out of bank, overbank flow depth will be increased, reducing the sensitivity to n (see eq. 5.5). A number of studies have found this to be the case, when large volumes of water flow overbank flow velocities are greatly increased (Anderson et al. 2006).

An additional explanation may be offered through analysis of the simulated hydrographs. It was shown in Figures 5.6 and 5.9 that changing channel roughness has the effect largely of reducing the peak flow, whereas floodplain roughness has a delaying effect on the largest flood peak. This latter effect increases timing errors. The largest errors indicated by objective functions have been found to be associated with the largest timing errors (Section 5.2.9) potentially explaining the greater variation in the results of the goodness of fit statistics. This highlights the importance of considering closely why the statistics are showing the variation in model output that they do. The sensitivity of model output to variation of parameters has been discussed. Further analysis of the behaviour of the model will now be

discussed. This analysis has relevance for both explaining the results of the sensitivity analysis further and also highlighting issues associated with the model.

5.4.7   Timing error effect on statistics

Timing errors in the simulated hydrograph have been highlighted throughout this chapter. The largest errors between observed and simulated hydrographs appear to occur when timing errors are at their greatest, despite any apparent qualitative agreement between the hydrographs. The potential effect of error in timing of flood peaks on statistical results has also been detailed in Section 5.2.9 (Beven 2001). The effects of shifting the timing of the simulated hydrographs on the results of the objective functions are quantified in Section 5.3.9 for the 30 mm and 180 mm/day time maps. Whilst there are exceptions for the largest timing errors, it is clear that the best fits, when quantified by the objective functions used in this chapter, between observed and simulated hydrographs occur when timing errors are at their smallest.

The association between the poorest goodness-of-fit and the largest timing errors is largely due to the nature of the objective functions used i.e. the calculation of the difference between individual flow values. Therefore if simulated peak flow is delayed by a number of hours to coincide, for example with the falling limb of the observed hydrograph, the largest simulated flow values will be compared to much lower observed flow values.

Therefore the hydrograph simulated when the 30 mm/day time map is applied appears to have the best *qualitative* agreement in terms of shape and peak discharge with the observed hydrograph. However the large error in the timing of the peak discharge (26 hours, the greatest of all time maps when all other parameters are fixed, Figure 5.19, Appendix C) results in large errors.

Positive NSME values are only observed for higher rain time maps. This is an important aspect, as in many previous studies (Beven 2001) all parameter sets which produce negative Nash-Sutcliffe values are rejected as non-behavioural. There is therefore the problem that what appears, albeit qualitatively, to be the most suitable rainfall rate in terms of producing a simulated hydrograph most similar to the observed hydrograph, is also suggested to be non-behavioural in terms of NSME results. This highlights the importance of both initial qualitative graphical analysis and the use of numerous objective functions to analyse the sensitivity of model output to parameter variation. However, importantly, the only statistic that suggests the 30 mm/day time map as appropriate is the % error in peak discharge statistic. When the 30 mm/day time map is applied an error of -8.01% is produced, indicating that the simulated peak discharge is over-estimated by 8.01% of the observed peak discharge.

5.5   Conclusion

From the results presented above it is clear that model output is most sensitive to the rain time map used. The rain time map is varied over a wide range (1 mm/day to 200 mm/day), which is likely to explain to a degree the extent of output variation, as reflected by the objective function analysis. However initial graphical analysis highlighted how the shape of the hydrograph and features such as peak discharge and timing of the peak discharge vary to a large degree with smaller variation of the rain time map. Most notable is the threshold observed between rainfall rates of 24 mm/day and 30 mm/day. This leads to the conclusion that whilst other parameters may be important, the selection of the rainfall rate applied throughout the storm event is key. Effective runoff rate also has an important impact on model output, secondary to rain rate time map.

The objective functions show that model output is then most sensitive to floodplain, channel and land surface roughness parameters in that order. However it can be seen that model output response to variation in these parameters, particularly floodplain roughness, varies depending on the rain time map applied. This again emphasises the importance of rainfall rate on model output.

There is a degree of uncertainty associated with the presented results. As discussed above the selection of rain time map is important. This means that the results discussed here could vary to those found if rain time maps different to 30 mm/day and 180 mm/day were chosen. Indeed the selection of the two rain time maps used in the chapter is subjective. This is where uncertainty analysis offers a key advantage by looking at the effects of variation of all roughness values and effective runoff rate as the applied rain time map changes.

Indeed one at a time sensitivity analysis does not show the effects of interactions between parameters, merely the main effects of parameters (Campolongo 2000). By selecting two different time maps as the default, the interaction between rainfall rate and other parameters has been explored, although only briefly. Therefore there are limitations to the conclusions that can be made regarding parameter sensitivity. However as mentioned above, it is apparent that the rain time map used will affect the model output far greater than any other parameter tested. The interactions of parameters will now be explored by analysing the effect on model output of variation of all parameters at the same time (Chapter 6).

<u>**Chapter Six   Uncertainty Analysis**</u>

6.1   Introduction

The aim of the uncertainty analysis in this chapter is to attempt to produce an estimate of the belief we have in different model realisations using different combinations of parameter values (Beven 2001).

In this chapter the methodology followed for the uncertainty analysis is described, with the method for sampling parameter values presented (Section 6.2). In contrast to the sensitivity analysis presented in the previous chapter, parameters were varied simultaneously. As with the sensitivity analysis, objective functions were used to quantify the goodness-of-fit between simulated and observed hydrographs. The findings presented (6.3) and subsequently discussed (6.4).

6.2   Methodology

First the parameters and the range of values to be to be sampled from, are detailed. Second, the method by which the parameters were sampled is shown, followed by a description of the methods used to present the results. It was decided to carry out uncertainty analysis using a methodology similar to Generalised Likelihood Uncertainty Analysis (GLUE) first presented by Beven and Binley (1992) and further discussed by Beven (2001; 2009). This method allows the interactions of parameters to be assessed, already identified as an important factor in the previous chapter.

6.2.1   Parameters to be varied

The interactions of 5 parameters were analysed; (1) spatially and temporally constant rain rate time map (cell passage times for set equilibrium flow rainfall rates, mm/day); (2) effective runoff rate (A % of the observed rainfall during the 2000 flood event), varied to account for adjustments allowing for estimated evaporation, groundwater losses and baseflow, providing an effective runoff rate. This represents a simple method of altering the volume of water in the catchment; (3) channel roughness (Manning's n); (4) floodplain roughness (Manning's n); and (5) catchment land roughness (Manning's n).

Due to computational and time restrictions, not all model parameters were included in the uncertainty analysis (and sensitivity analysis, previous chapter). The full list of model parameters is provided in Chapter 4 (Section 4.4.1) and Appendix A (Odoni and Lane, in prep). The parameters listed above were identified as important simplifications in the model

structure and particularly sensitive on the basis of the results in Chapter 5. A greater understanding of the roughness parameters was deemed important before altering roughness values to simulate flood risk reduction measures. The applied rain time map and effective runoff rate parameters were chosen as, through previous work with Overflow, they were thought to be highly important in the model structure. The effects of hydrograph timing are not explored here, as in Chapter 5, as it is not a model parameter and was simply used to explore objective function bias in the previous chapter.

6.2.2 Parameter values for Uncertainty Analysis

Beven (2001) stated that computational time can be saved when following the GLUE methodology by narrowing the range of possible parameter values, by excluding areas of the parameter space previously identified as having low goodness-of-fit measure values, if these are known. In the previous chapter, the choice of default rain rate time map was found to have a strong effect on model sensitivity to other parameters. Goodness-of-fit between simulated and observed hydrographs varied greatly depending on rainfall rate time map and timing errors. Therefore there was a significant degree of uncertainty associated with narrowing the range of values of rainfall rates and, to a lesser extent, effective runoff rates.

However it was possible to limit the range of roughness values through a consideration of realistic values to be found within the Uck catchment. Chow (1959) was consulted to provide realistic Manning's n values. For example, a Manning's n value of 0.07 was considered as a reasonable maximum roughness of the channel network in the Uck catchment, prior to introduction of Catchment Riparian Intervention Measures (CRIMs). Based on this assessment of realistic catchment characteristics the following parameter ranges are used.

Time map (rainfall mm/day)

1, 2, 4, 6, 8, 10, 12, 14, 16, 18, 20, 24, 30, 36, 42, 50, 60, 80, 100, 120, 140, 160, 180, 200

Channel manning's n

0.025-0.07 (range, 0.045)

Floodplain manning's n

0.02-0.1 (range, 0.08)

Land manning's n

0.02-0.2 (range, 0.18)

Effective runoff rate

75-125% of measured rain input before adjustments for estimated evaporation, groundwater losses and baseflow. Effective runoff rate is varied to >100% in order to account for the effects of errors in rain gauge and discharge gauge data. Error in such data will affect the calculation

of effective runoff %, which is based on a comparison of rain and discharge volume during the 2000 storm event. The Uck catchment became very wet during the storm event and therefore effective runoff was likely to be close to 100%. Varying effective runoff to >100% accounts for the potential errors discussed, which are almost certain to be present to some degree (Beven 2001: 217).

As in the Sensitivity Analysis, the rain rate time map parameter was varied in a different way to all other parameters. Discrete time maps had to be created for certain fixed rain rates, as shown above. This meant that for each simulation, a time map had to be randomly selected from the predetermined list, as opposed to being varied entirely randomly within a fixed range, as with all other parameters.

6.2.3   Sampling method

The uncertainty analysis was carried out using a Monte Carlo sampling-based method as discussed by Saltelli (2000) and Smith and Smith (2007). Here, 2000 simulations were run using parameter values randomly selected from the set distribution (Section 6.2.2). The method was chosen due to its simplicity and low computational cost. For example, using a full factorial design, if 10 increments were chosen for each parameter, 100000 simulations would be required (Campolongo et al. 2000). With the method chosen for this analysis, whereby sampling was randomised, 2000 simulations were deemed to be sufficient to provide a good exploration of the parameter space.

6.2.4   Objective functions

Nash-Sutcliffe Model Efficiency (NSME), Mean Absolute Error (MAE) , Root Mean Squared Error (RMSE) and % error in peak flow (PEP) were all calculated to analyse the variation in goodness of fit between observed and simulated discharge at Isfield as all other selected parameters were varied simultaneously. The objective functions are defined in Section 5.2.10.

6.2.5   Dotty plots

Scatter plots or dotty plots (Beven 2001) were produced. For each individual parameter, parameter value was plotted against each of the four objective functions. Each point on the dotty plots represents one model simulation (Beven 2001).

6.2.6   Probability distribution functions (PDFs)

The results of the uncertainty analysis, as shown by the dotty plots, were then plotted as two dimensional probability distribution function with a 0.01 x 0.01 probability resolution. Creation of the PDFs allows a better identification of the concentration of data points in the parameter

space. It also indicates the probability of a certain objective function value based on random variation of the model parameters.

6.2.7   Classification of 'best' simulations

A performance threshold was set for each objective function. This allows a sample of the model simulations with a relatively good fit with observed data, to be analysed, without identifying a single 'optimal' simulation. Model simulations with a NSME value above 0.7 were sampled. The same procedure was followed for each objective function separately. Performance thresholds were set for MAE, RMSE and PEP at <10 cumecs, <20 cumecs and <10% respectively. These values were chosen as they represent something of a compromise between an indication of model accuracy and values which allow a sample suitable for analysis. Ideally thresholds would be set based on suitable error terms, however in this case error is relatively high. Selecting the 5% of simulations with the best goodness of fit was not deemed any less arbitrary, as though a simulation may show a better fit with observed data than 95% of the simulations, its goodness-of-fit may be in reality still very poor.

A different number of model simulations were subsequently sampled for each objective function, as a different number of simulations passed each threshold for the objective functions. The range of parameter values over which the best simulations occurred was analysed.

6.3   Results

First an overview of the objective function results will be presented, without consideration of parameter values selected. Subsequently the trends between parameter values selected and the goodness-of-fit will be shown.

6.3.1   Overview of statistics

Table 6.1 shows that just above one quarter of model realisations have a Nash-Sutcliffe value of above 0. This means that ~25% of model realisations are performing better than the random case. From the PDFs produced for parameter value against NSME it is clear that the majority of points have values ≤0 (Figures 6.6a-6.10a). All negative points are assigned a 0 on the PDF figures. This explains the very dense collection of points at 0 on the y-axis (NSME values). Only 18% of the 2000 parameter sets have a mean error of less than 10 cumecs, whilst 10.6% simulate peak flow magnitude with an error of less than 10% (~13 cumecs error) of observed peak discharge. Using MAE, 87% of models had an error >12.9 cumecs, 50% of the average discharge observed at Isfield during a 120 hour period during the 2000 flood event.

It can be seen on the dotty plots (Figures 6.1-6.5), and clearly highlighted by the PDFs (Figures 6.6-6.10) that there is a dense area of points, within a smaller range of objective function values, running horizontally across the figures. This indicates a concentration of simulations of very similar performance across all parameter values for channel, floodplain and land roughness. Through analysis of the objective function statistics it is possible to identify approximately the upper and lower limits of this concentration of points (Table 6.2). % error in peak flow (PEP) does not show such a clear clustering of points.

While the full range of MAE and NSME values is 27.36 cumecs and 2.40 respectively, it can be seen that 1104 (57%) points lie within a range of $5m^3s^{-1}$ for MAE and 938 (46.9%) within a range of 0.3 for NMSE. This represents a much smaller range of values.

Table 6.1. A summary of the objective function values recorded by comparing observed and simulated discharge at the Isfield gauge for 2000 model simulations

Nash-Sutcliffe value	>0	>0.5	>0.75	>0.8	
% of model realisations	27.7	12.3	3.5	0.2	
MAE (cumecs (m^3s^{-1}))	<20	<15	<10	<5	
% of model realisations	28.8	18.0	4.9	0	
RMSE (cumecs)	<40	<30	<20	<10	
% of model realisations	54.55	17.9	7.3	0	
% error in peak Q (PEP)	<100	<50	<20	<10	<5
% of model realisations	91.8	34	15.5	7.4	4.4

Table 6.2. An indication of the concentration of model simulations with similar objective function values. The range of objective function values, and the number of model simulations which fall within this range are shown for NSME, MAE and RMSE.

Objective function	Value range selected for each objective function	Number of simulations within selected range
NSME	(-)0.2 – (-)0.5	938 (46.9%)
MAE	22 - 27 cumecs	1104 (57%)
RMSE	38 - 44 cumecs	1020 (51%)

6.3.2   Dotty plots

Figures 6.1-6.5 show dotty plots (Beven 2001), which plot each parameter included in the uncertainty analysis (Section 6.2.1) against the four statistical tests selected (Section 6.2.4). For all plots the best simulations are towards the top of the figure. Figures 6.6-6.10 show probability distribution functions (PDFs). The PDFs show the concentration of data points in the parameter space. Figures 6.1-6.10 are described in the following sections.
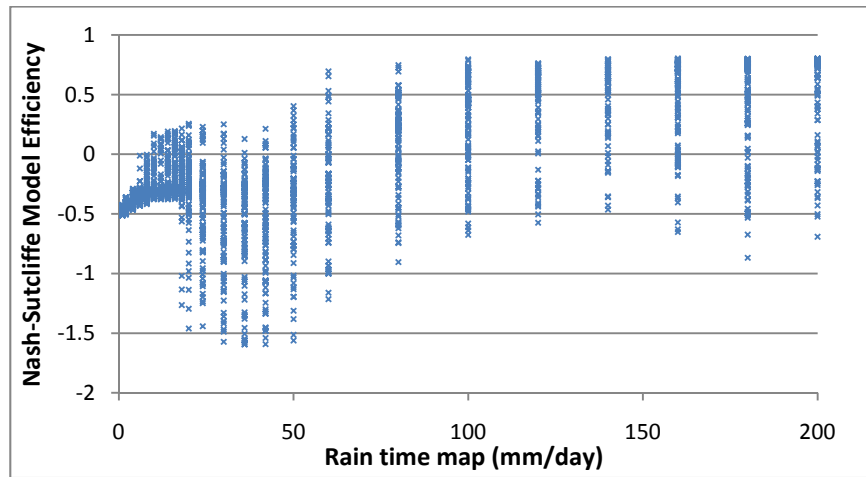
Figure 6.1a. Dotty plot of Nash-Sutcliffe Model Efficiency measure against rain time map. Each dot represents one model run as parameter values were varied randomly.
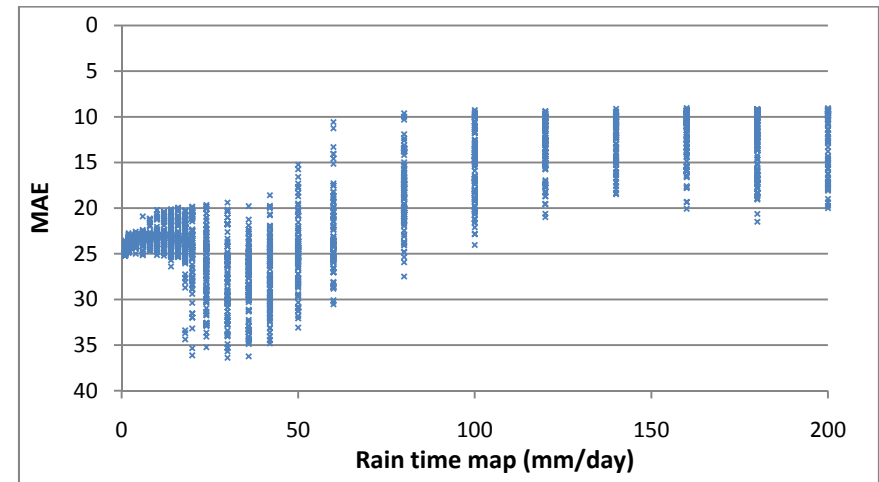
Figure 6.1b. Dotty plot of Mean Absolute Error against rain time map.
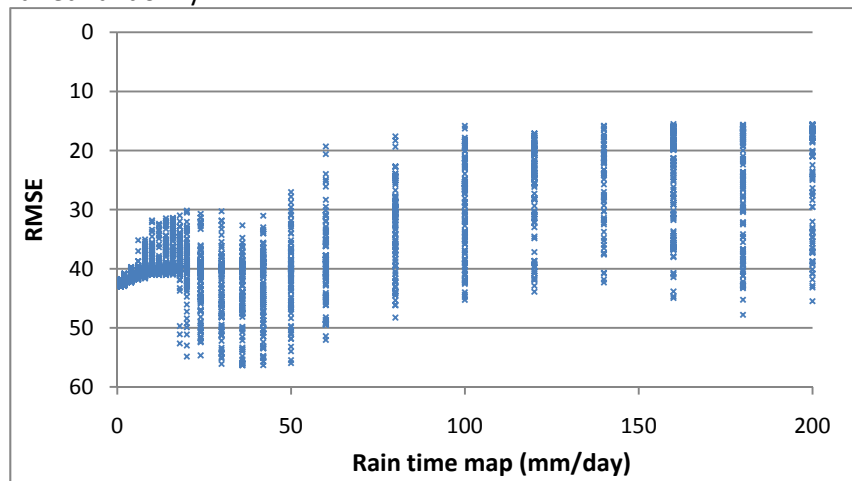
Figure 6.1c. Dotty plot of Root Mean Squared Error against rain time map.
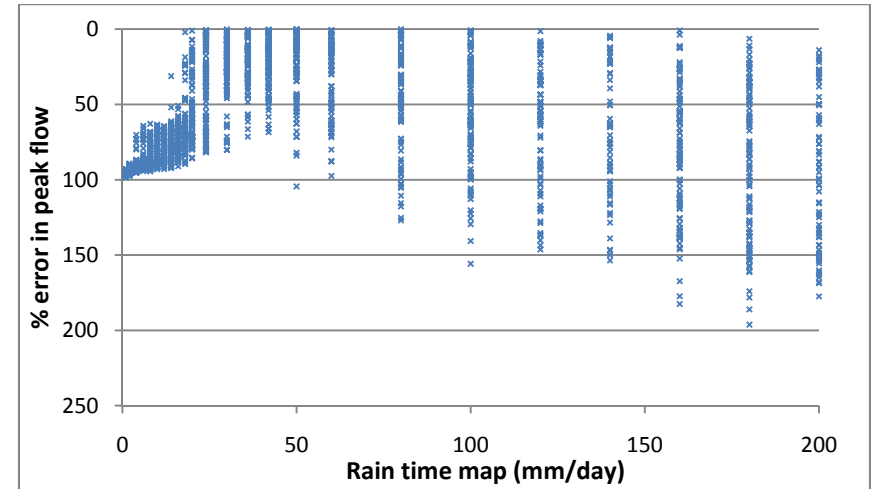
Figure 6.1d. Dotty plot of % error in peak flow against rain time map.
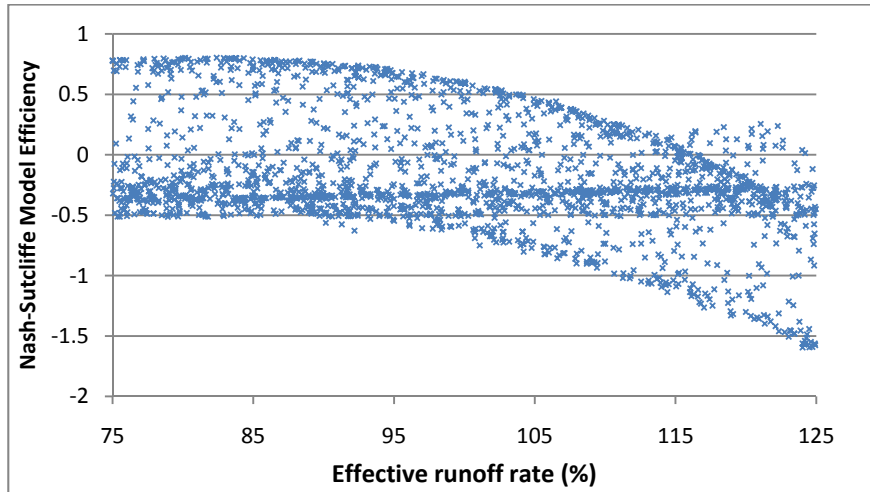
Figure 6.2a. Dotty plot of Nash-Sutcliffe Model Efficiency measure against effective runoff %.
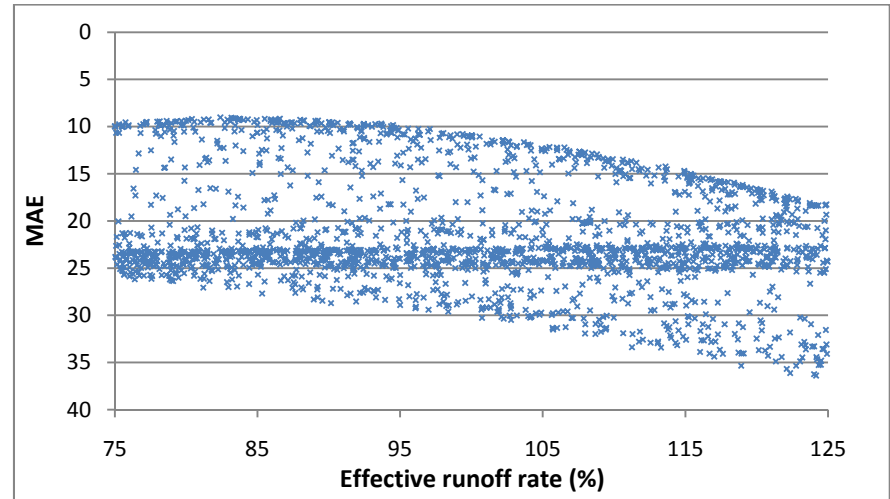
Figure 6.2b. Dotty plot of Mean Absolute Error against effective runoff %.
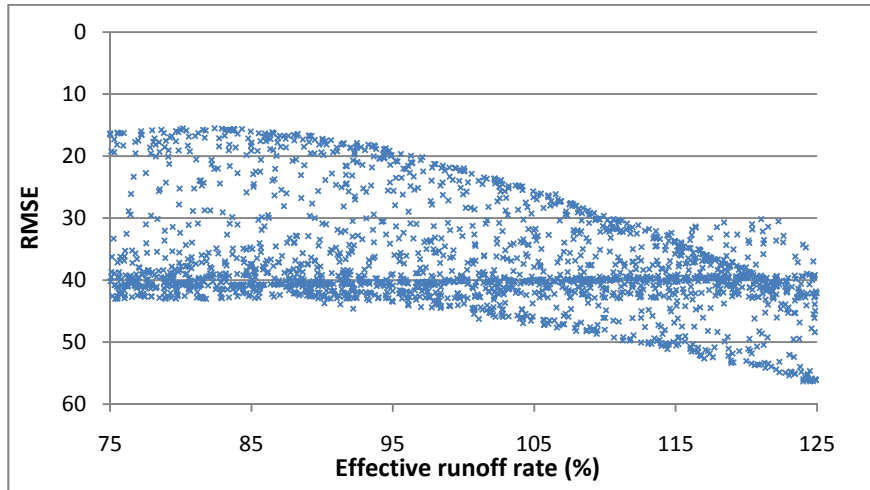
Figure 62c. Dotty plot of Root Mean Squared Error against effective runoff %.
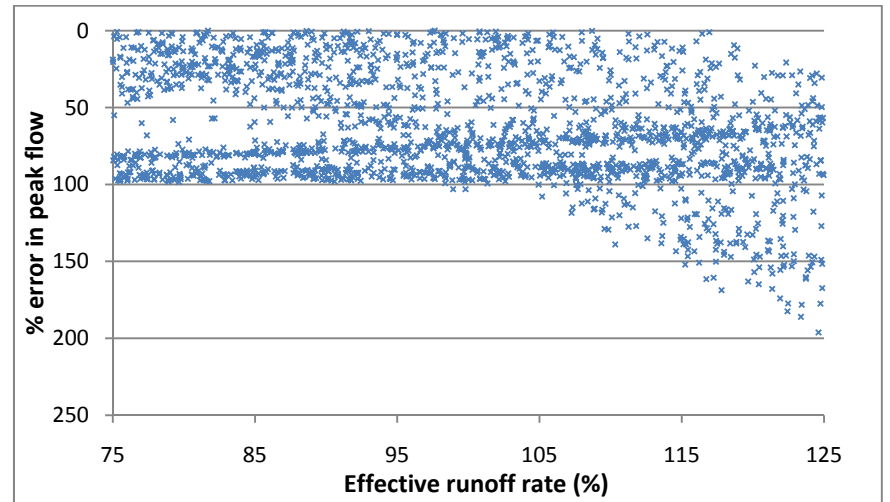
Figure 6.2d. Dotty plot of % error in peak flow against effective runoff %.
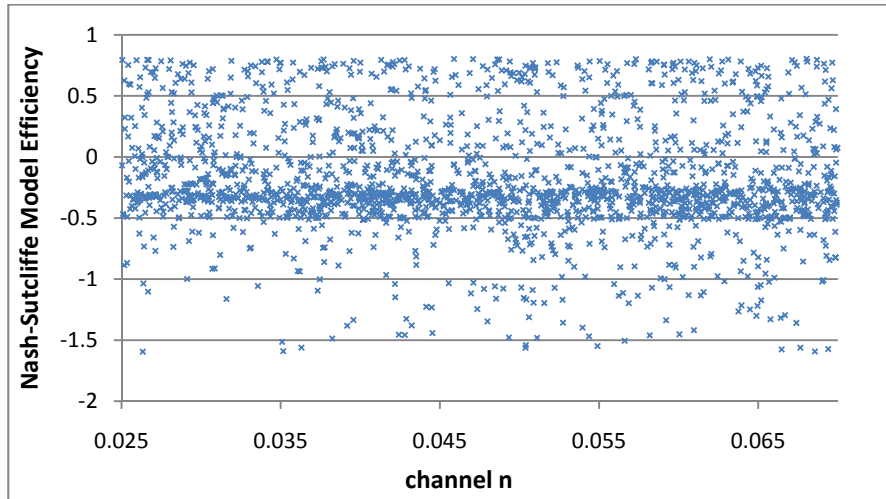
Figure 6.3a. Dotty plot of Nash-Sutcliffe Model Efficiency measure against channel manning's n.
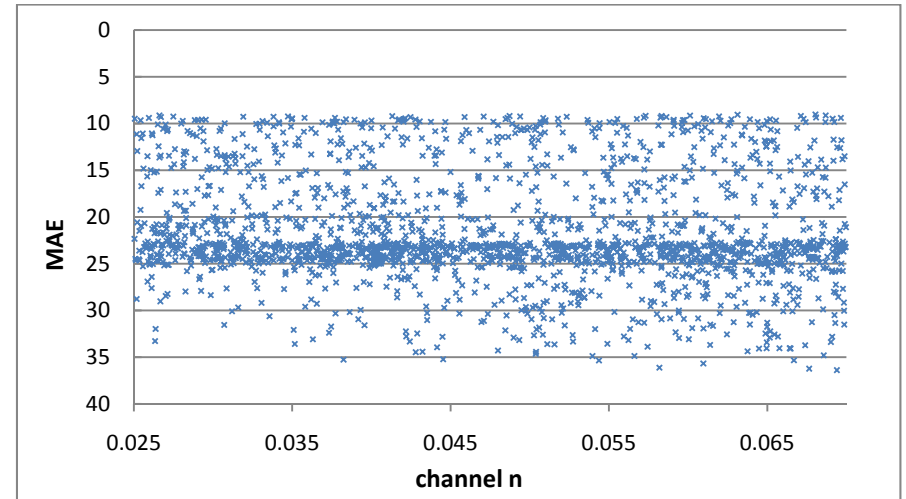
Figure 6.3b. Dotty plot of Mean Absolute Error against channel manning's n.
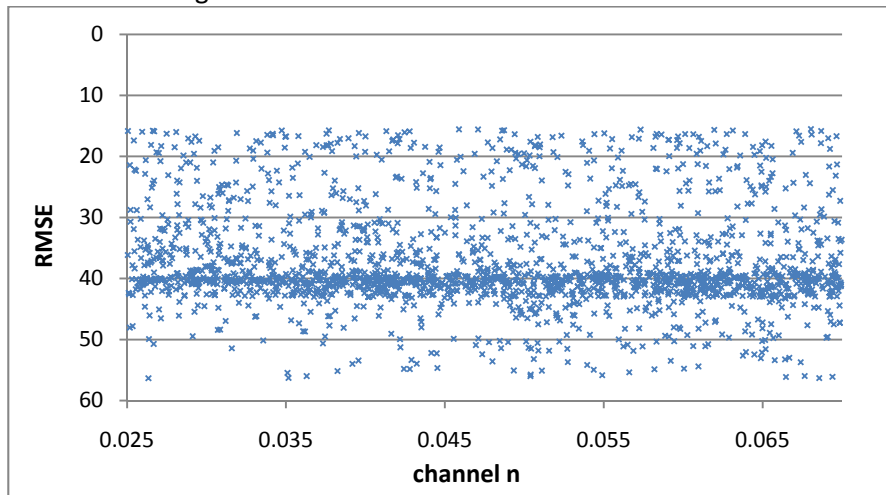
Figure 6.3c. Dotty plot of Root Mean Squared Error against channel manning's n.
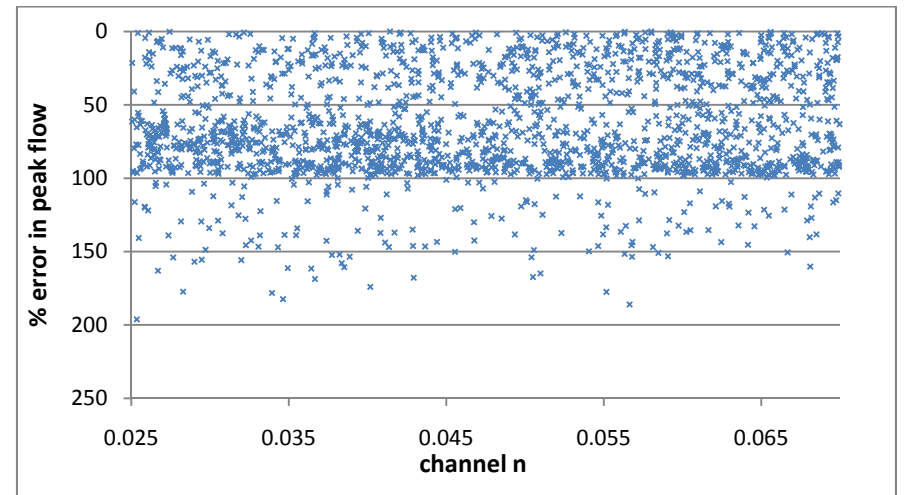
Figure 6.3d. Dotty plot of % error in peak flow against channel manning's n.
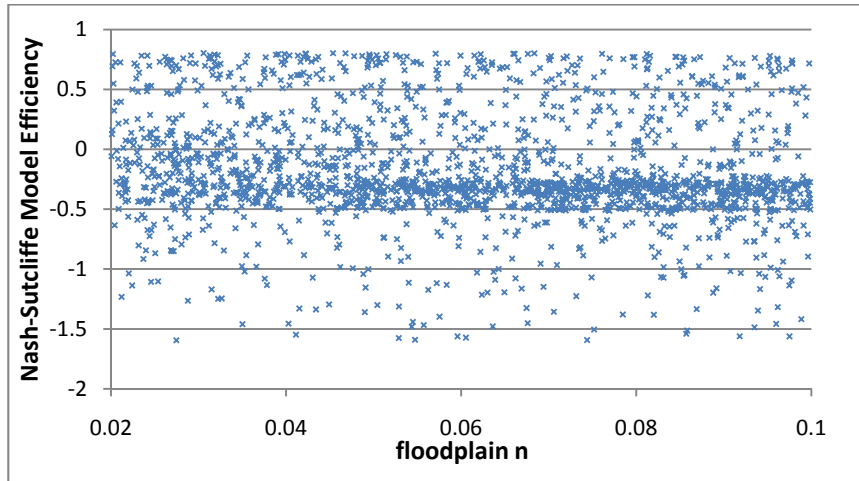
Figure 6.4a. Dotty plot of Nash-Sutcliffe Model Efficiency measure against floodplain manning's n.
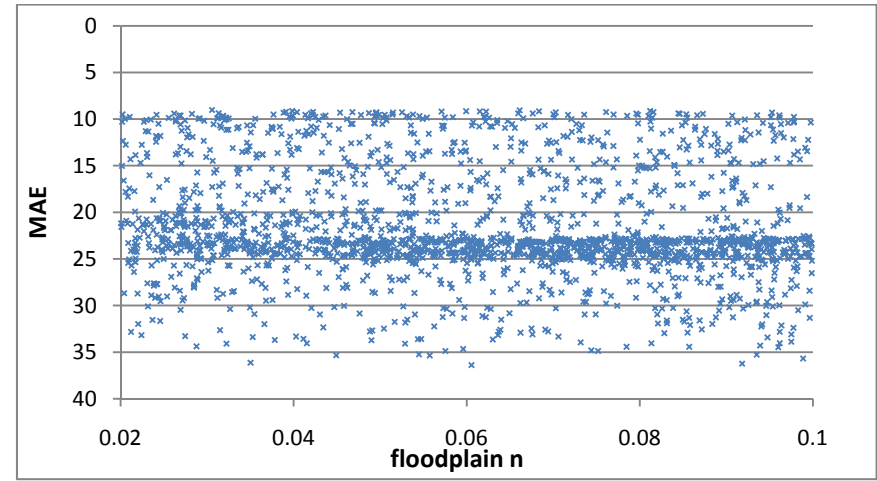
Figure 6.4b. Dotty plot of Mean Absolute Error against floodplain manning's n.
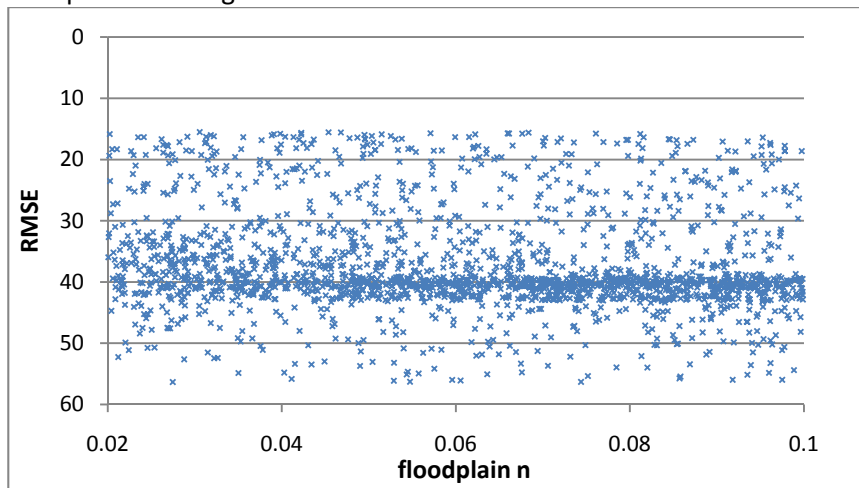
Figure 6.4c. Dotty plot of Root Mean Squared Error against floodplain manning's n.
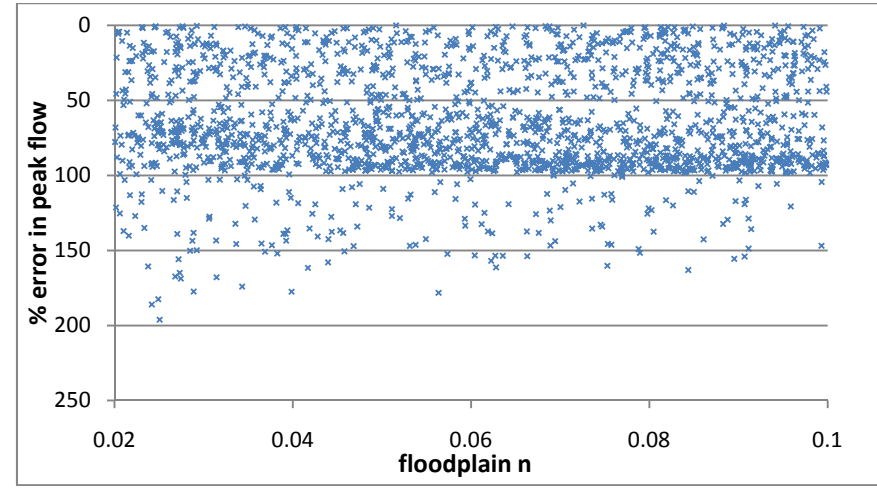
Figure 6.4d. Dotty plot of % error in peak flow against floodplain manning's n.

71
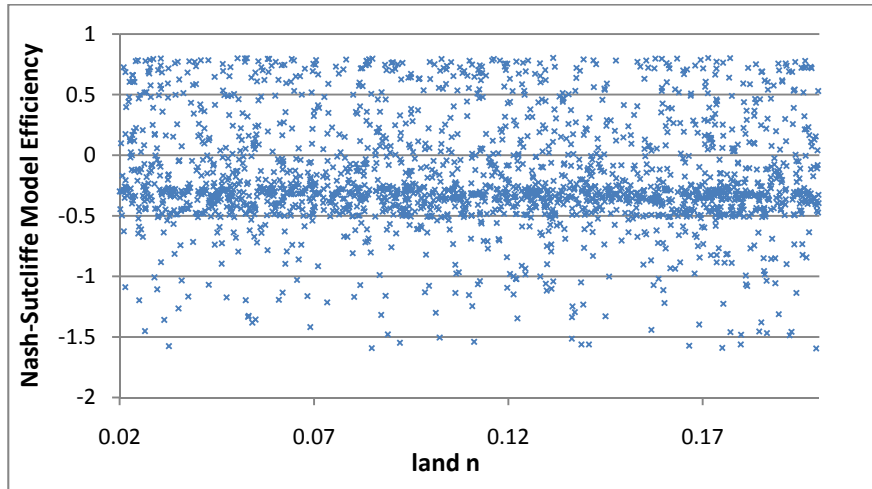
Figure 6.5a. Dotty plot of Nash-Sutcliffe Model Efficiency measure against land manning's n.
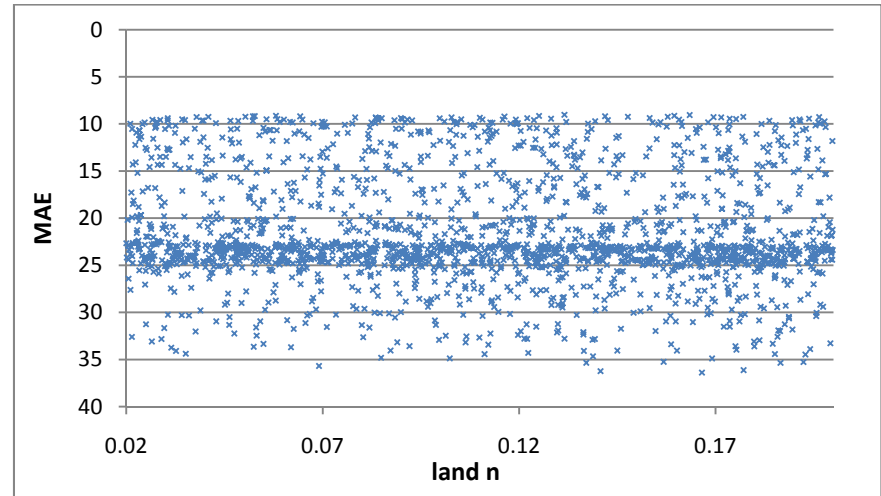
Figure 6.5b. Dotty plot of Mean Absolute Error against land manning's n.
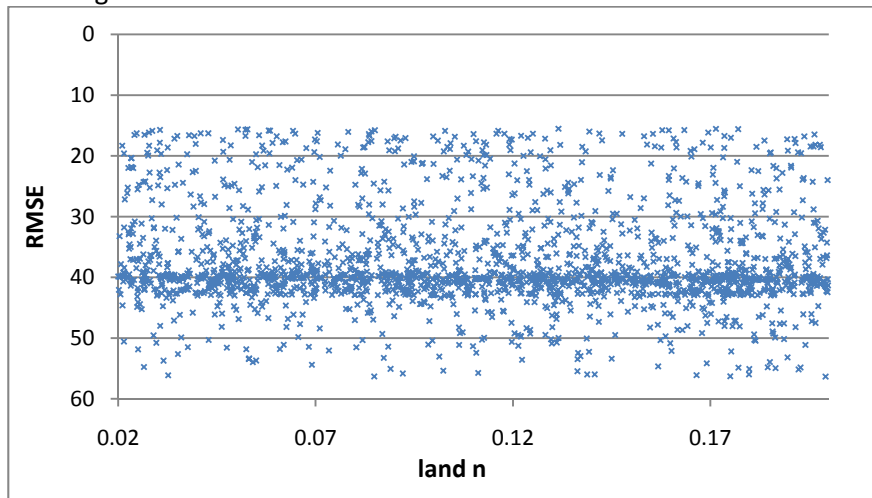
Figure 6.5c. Dotty plot of Root Mean Squared Error against land manning's n.
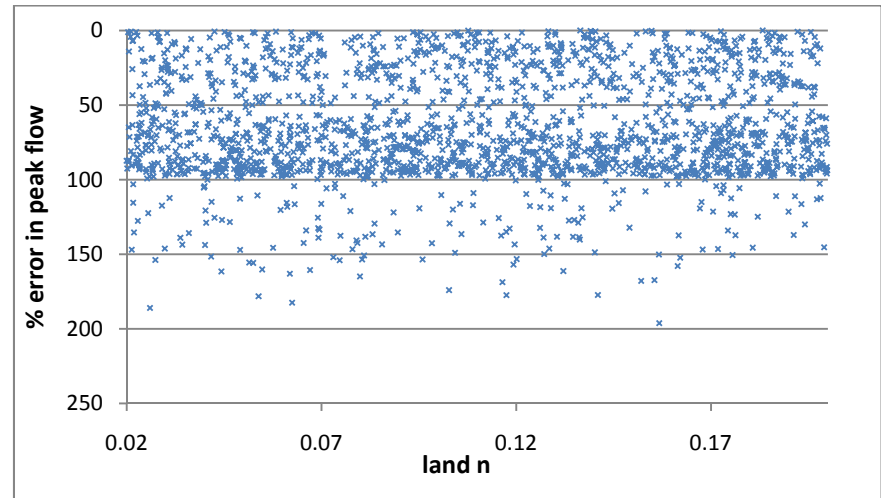
Figure 6.5d. Dotty plot of % error in peak flow against land manning's n.

72
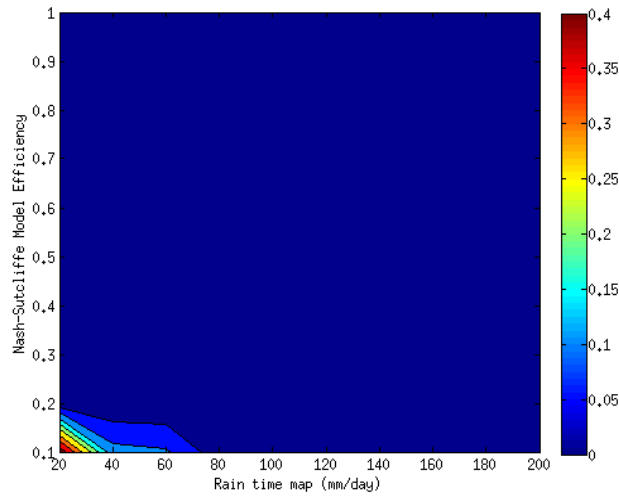
Figure 6.6a. PDF of Nash-Sutcliffe Model Efficiency against rain time map.
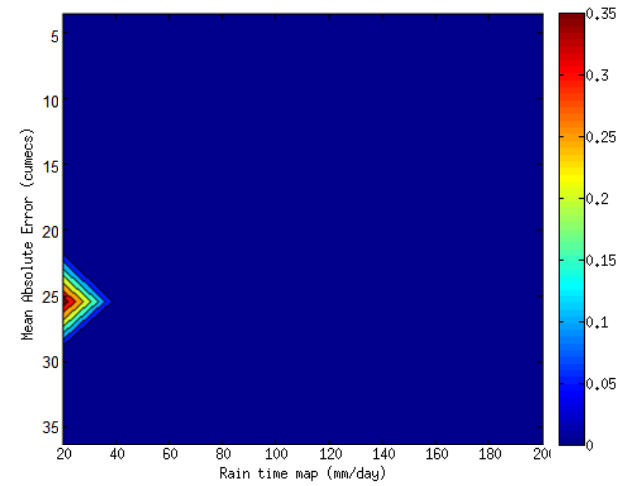
Figure 6.6b. PDF of Mean Absolute Error against rain time map.
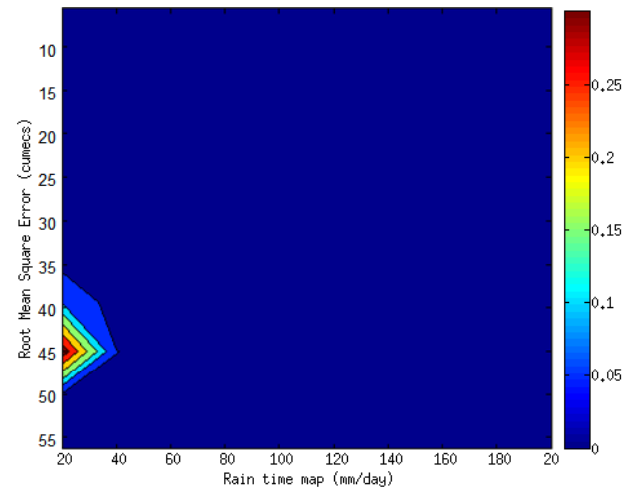
Figure 6.6c. PDF of Root Mean Square Error against rain time map.
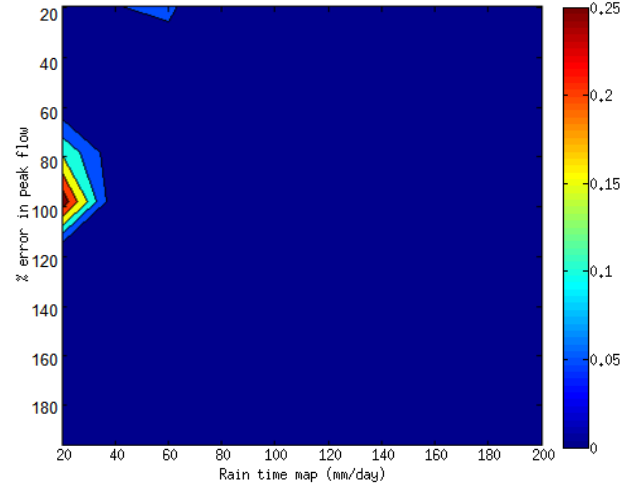
Figure 6.6d. PDF of % error in peak flow against rain time map.
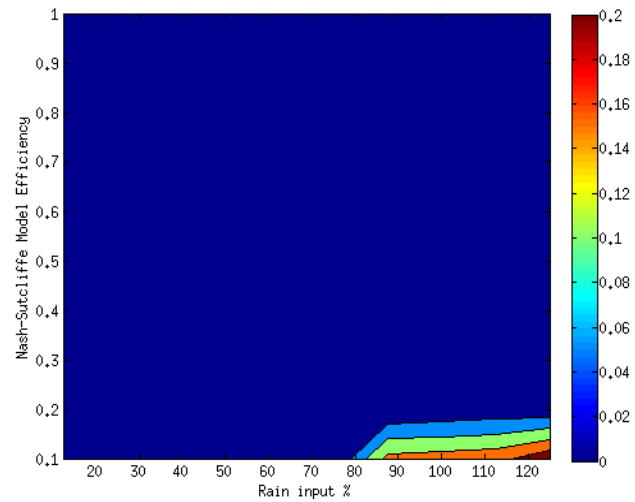
Figure 6.7a. PDF of Nash-Sutcliffe Model Efficiency against effective runoff rate
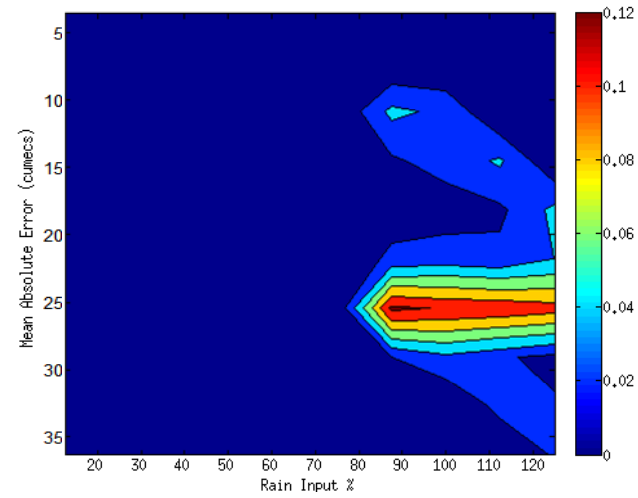
Figure 6.7b. PDF of Mean Absolute Error against effective runoff rate
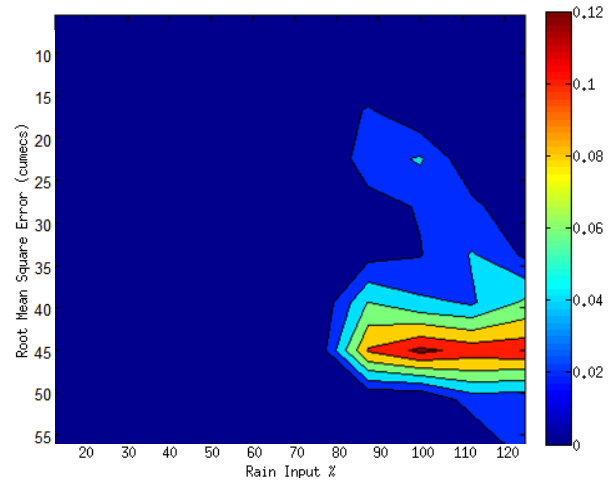
Figure 6.7c. PDF of Root Mean Square Error against effective runoff rate
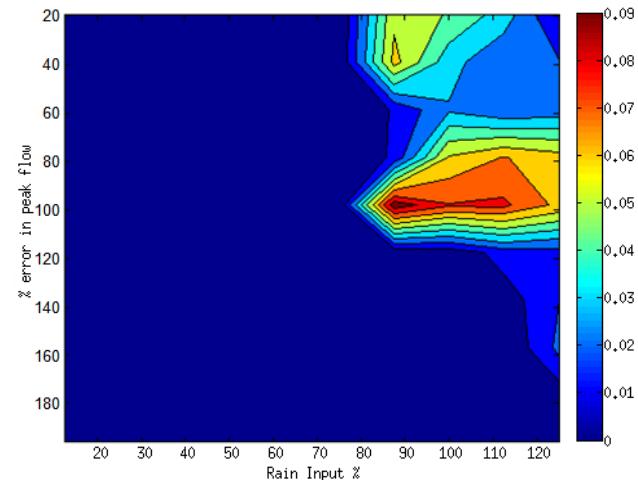
Figure 6.7d. PDF of % error in peak flow against effective runoff rate
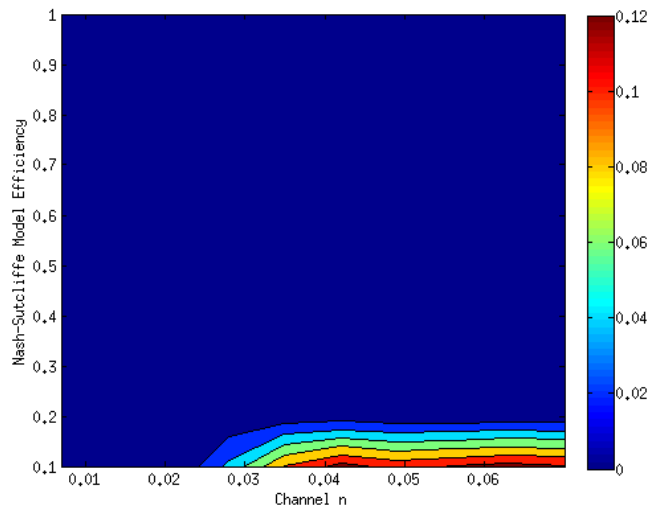
Figure 6.8a.PDF of Nash-Sutcliffe Model Efficiency against channel Manning's n
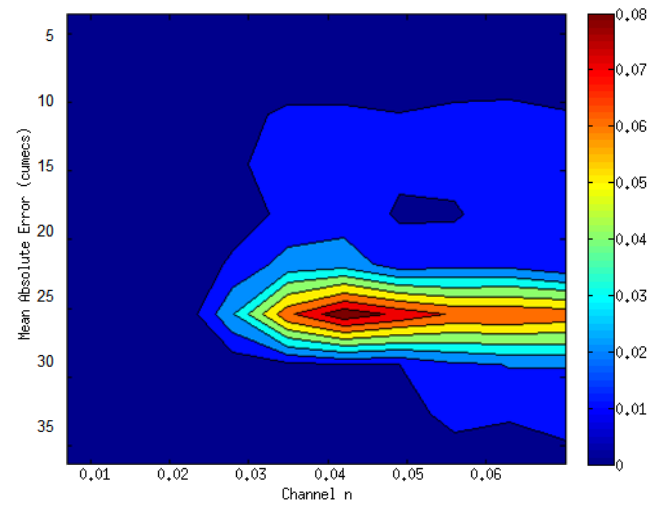
Figure 6.8b. PDF of Mean Absolute Error against channel Manning's n
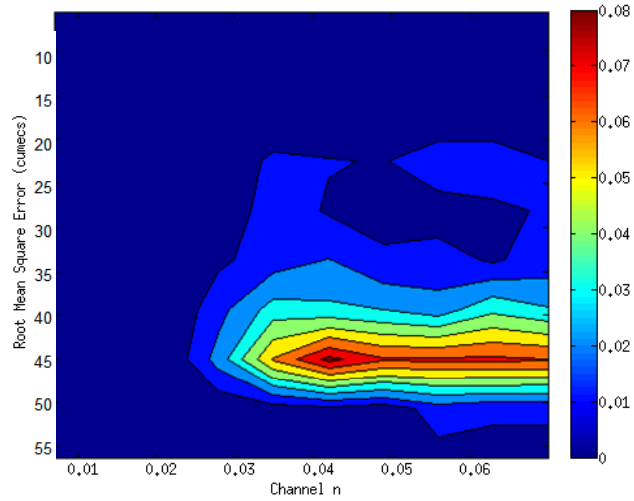
Figure 6.8c. PDF of Root Mean Square Error against channel Manning's n
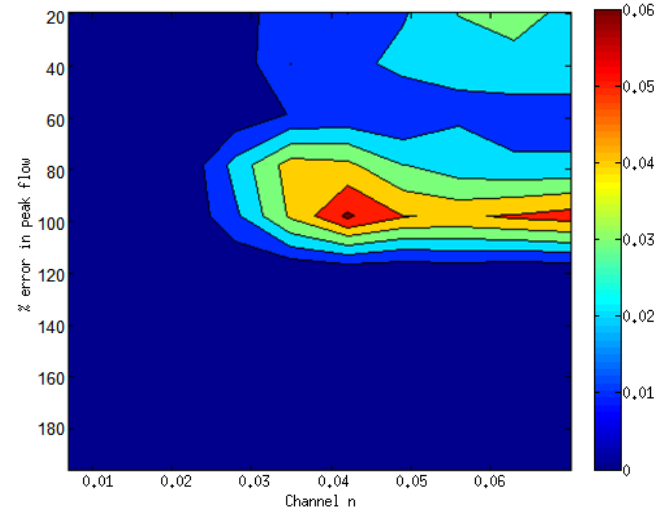
Figure 6.8d. PDF of % error in peak flow against channel Manning's n

75
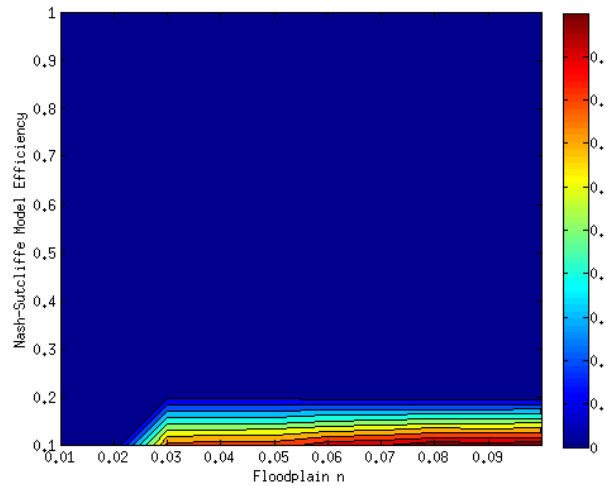
Figure 6.9a. PDF of Nash-Sutcliffe Model Efficiency against Floodplain Manning's n
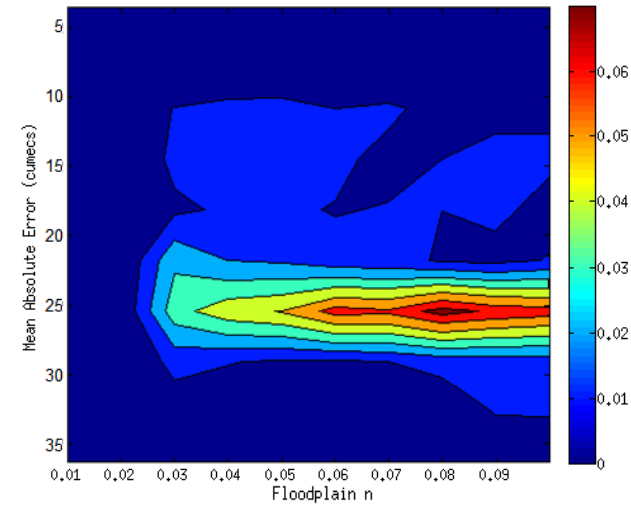
Figure 6.9b. PDF of Mean Absolute Error against Floodplain Manning's n
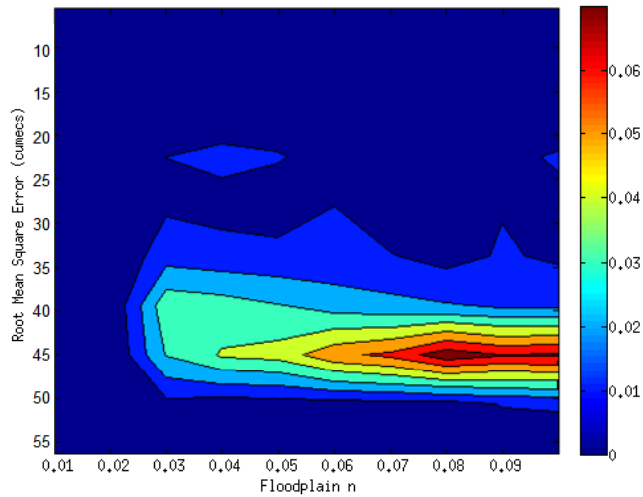
Figure 6.9c. PDF of Root Mean Square Error against Floodplain Manning's n
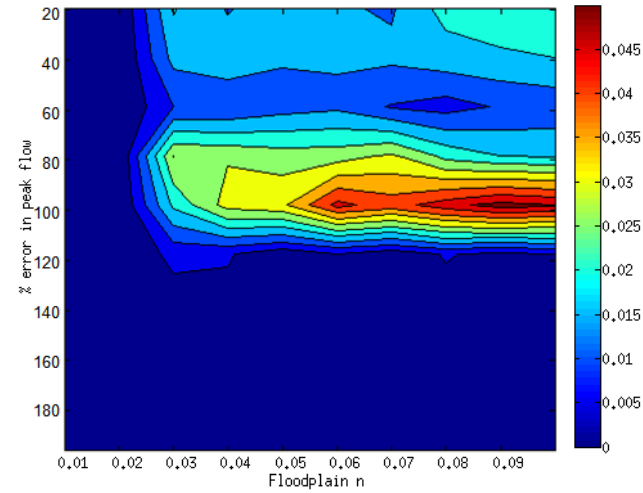
Figure 6.9d. PDF of % error in peak flow against Floodplain Manning's n

76
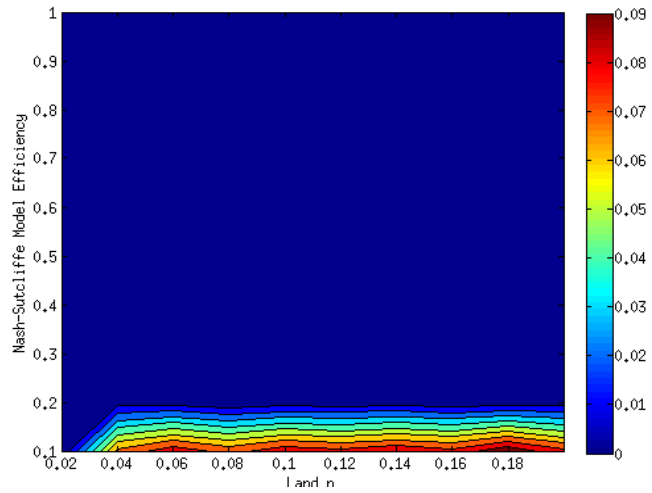
Figure 6.10a. PDF of Nash-Sutcliffe Model Efficiency against Land Manning's n
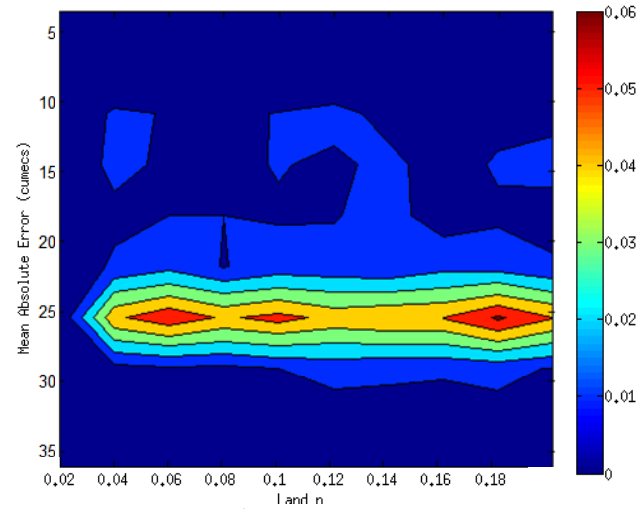
Figure 6.10b. PDF of Mean Absolute Error against Land Manning's n
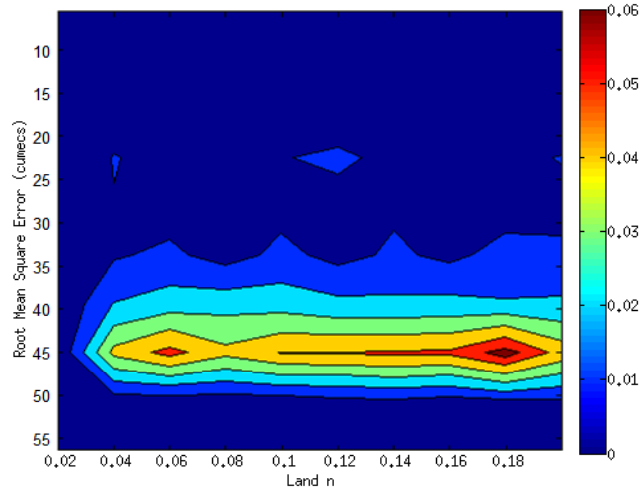
Figure 6.10c. PDF of Root Mean Square Error against Land Manning's n
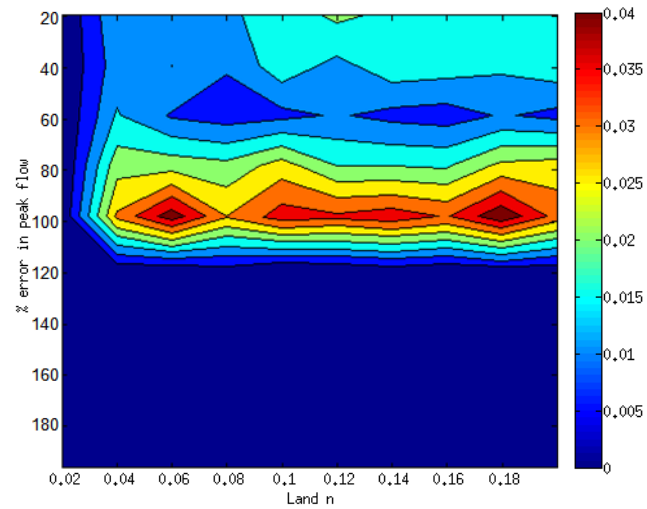
Figure 6.10d. PDF of % error in peak flow against Land Manning's n

77

6.3.3   Rain rate time map

A distinction can be made between the effects of variation of roughness parameters and rain time map and effective runoff parameters on model performance. Results associated with the latter two parameters will be presented first. The best models, above set performance thresholds, are not found across the entire range of rain time maps (Figures 6.1a-d). Table 6.3 shows that the range of rain time maps which produce the best models varies depending on the objective function used to quantify goodness-of-fit. From the 'best' models, the ranges of time maps sampled are 80-200 mm/day for NSME and MAE, 60-200 mm/day for RMSE and 18-200 mm/day for PEP, and not over the full potential range of time maps.

Table 6.3. A table showing the number of simulations above the set performance threshold for each objective function. The maximum, minimum and % of potential range of rain time maps for these model simulations are shown for rain rate time map. Figures marked with * indicate the potential extreme value i.e. largest and smallest possible rain time map

Objective function	Threshold	Sample size (% of 2000 model simulations)	Rain rate time map (mm/day)		
			Max	Min	% of potential range
NSME	>0.7	122 (6.1)	200 *200	80 *1	60
MAE	<10 (cumecs)	98 (4.9)	200	80	60
RMSE	<20 (cumecs)	146 (7.3)	200	60	70
PEP	<10%	148 (7.4)	180	18	81

The poorest models are found approximately within the range of rain time maps; 20-50 mm/day using NSME (Figure 6.1a), 20-36 mm/day using MAE (Figure 6.1b), 30-50 mm/day using RMSE (Figure 6.1c), whilst the greatest % error in peak flow is observed for the largest rain time maps (Figure 6.1d). Importantly, model simulations with high error occur for all rain time maps. For all rain time maps, at least 1 model simulation achieves a NSME value of <0 (Figure 6.1a). Similarly error values of >10 and >20 cumecs and >50% for MAE, RMSE and PEP (Figures 6.1b-d) respectively are found for all rain time maps. This implies that there is parameter interaction and that an inappropriate value of the rainfall rate time map may be compensated for by other parameter effects.

The PDFs show a clear concentration of points at high error values. There is a concentration of points towards the lowest rainfall rate time maps (Figures 6.6a-d), however this is due to the nature of the time map values used (Section 6.2.2), with a cluster of time maps of low rain rates. The PDF produced for the PEP statistic indicates a concentration of low

simulated peak magnitude error values approximately between rain time maps of 40 and 60 mm/day. The PDF assigned all negative NSME values as 0 (Figure 6.6a). Therefore, as with all parameters tested, the PDF shows a very high concentration of data points with NSME values close to 0.

From the 2000 simulations, the deviation from the mean objective function value associated with each rain rate time map was calculated (Figure 6.11). The degree of deviation from the mean shows a different trend depending on the objective function used. Standard deviation for RMSE shows an increasing trend as the rain time map increases (Figure 6.11c). The same occurs for NSME (Figure 6.11a) and MAE (Figure 6.11b) up to a rain time map of approximately 50 mm/day after which standard deviation oscillates. Variation in standard deviation of PEP values as rain time map varies does not show a clear trend. In general, for the NSME, MAE and RMSE statistics the highest rainfall rate time maps show a greater deviation from the mean than for the very smallest rain time maps. This shows a different trend to that of equifinality. This trend shows different objective function values occur for the same objective function values. Again this suggests parameter interaction effects.

6.3.4   Effective runoff rate

Model output does not show a clear trend when plotted against variation in the effective runoff rate (Figures 6.2a-d). Table 6.4 shows that the best simulations, as indicated by NSME, MAE and RMSE statistics occur when effective runoff rate is varied between 75 and 97%. This represents less than half of the potential range of values set for the uncertainty analysis. The peak discharge can be best simulated over close to the full range of effective runoff % (75-119%).

Table 6.4. A table showing the number of simulations above the set performance threshold for each objective function. The maximum, minimum and % of potential range of effective runoff values for these model simulations are shown for effective runoff rate. Figures marked with * indicate the potential extreme value i.e. largest and smallest possible effective runoff rate

Objective function	Threshold	Sample size (% of 2000 model simulations)	Effective runoff rate (%)		
			Max	Min	% of potential range
NSME	>0.7	122 (6.1)	94.76 *125	75.00 *75	39.5
MAE	<10 (cumecs)	98 (4.9)	94.50	75.00	39
RMSE	<20 (cumecs)	146 (7.3)	96.28	75.00	42.6
PEP	<10%	148 (7.4)	118.68	75.09	87.2
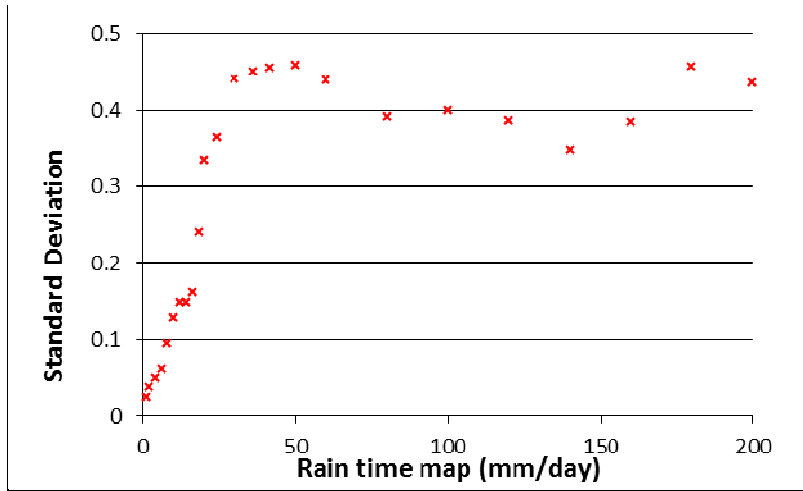
Figure 6.11a. A plot showing variation in standard deviation from the mean Nash-Sutcliffe Model Efficiency values for each rain time map
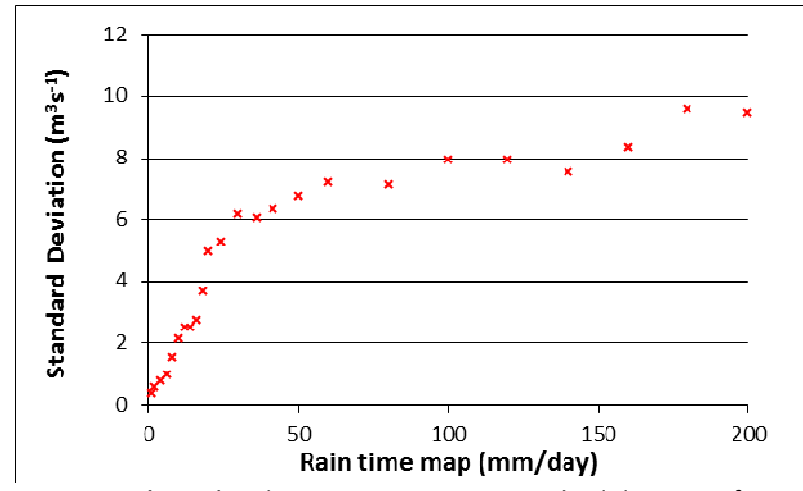
Figure 6.11b. A plot showing variation in standard deviation from the mean Root Mean Square Error for each rain time map
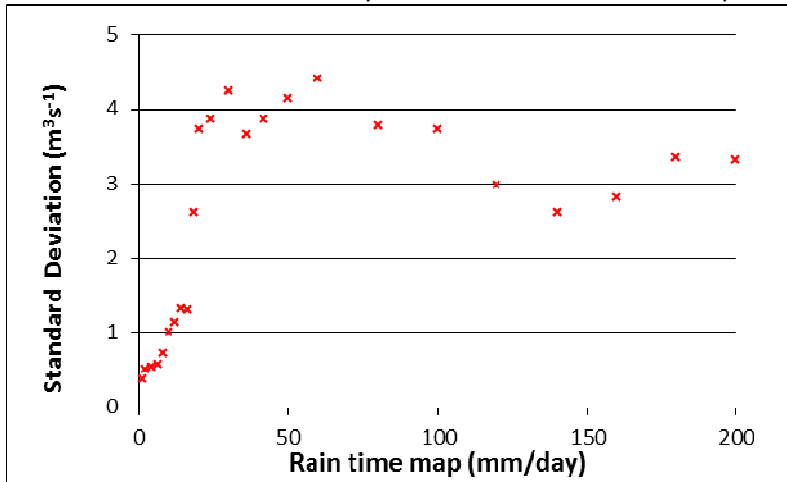
Figure 6.11c. A plot showing variation in standard deviation from the mean Mean Absolute Error for each rain time map
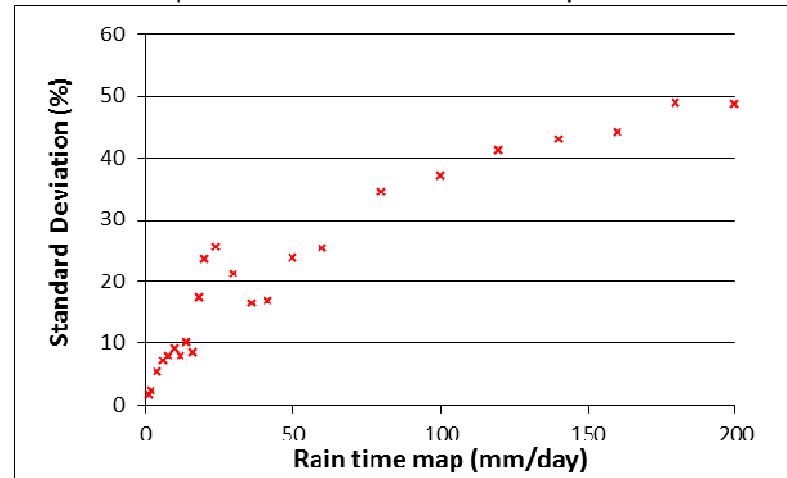
Figure 6.11d. A plot showing variation in standard deviation from the mean % error in peak flow for each rain time map

When variation in effective runoff rate is plotted against NSME, MAE and RMSE (Figures 6.2a-c) a curved band of data points bounded by the best and worst model performance values can be clearly observed. There is a general downward trend in model performance as effective rainfall rate is increased. Within the upper and lower bounds it is possible to identify a clustering of points which indicate very little variation in model performance with variation in effective runoff rate percentage. The PDFs produced clearly highlight this (Figures 6.7a-c).

The PDF produced for the % error peak flow (Figure 6.7d) reveals a more complex pattern. In addition to the concentration of points running horizontally across the figure clearly observed for NSME, MAE and RMSE, there is also a second concentration of model simulations indicating a much lower error in peak flow. As with the PDF produced for the rain time map parameter against NSME, there is a clear concentration of points with values close to 0 (Figure 6.7a). However the trend towards higher error at higher rain input percentages, as discussed previously, is reflected by the densest concentration to the right of Figure 6.7a.

6.3.5   Roughness parameters

The trends observed for all three roughness parameters; channel, floodplain and land manning's n, are very similar to each other, but different to the two previously discussed parameters. A relatively good fit between observed and simulated discharge can be achieved when parameter values are selected at or close to their extreme ranges.

6.3.6   Channel roughness

The dotty plots showing model performance against the channel roughness parameter (Figures 6.3a-d) indicate that for all four objective functions, values indicating the best fit between observed and simulated hydrographs are found across the full range of parameter values. Table 6.5 shows that the full range of channel roughness values can result in a model simulation exceeding the set threshold. For example, a model simulation can achieve a NSME value of >0.7 when channel roughness is set at close to either the maximum or minimum possible range (Manning's n 0.07 and 0.025). Similarly such extremes in channel roughness can result in simulations achieving MAE, RMSE and PEP values of <10 cumecs, <20 cumecs and <10% respectively. The PDFs indicate a relatively small number of simulations with a good fit with the observed discharge hydrograph at Isfield, indicated by the dark blue colour at lower error values (Figures 6.8a-c). The PDF for PEP (Figure 6.8d) indicates the best simulations are slightly concentrated towards higher channel roughness values.

A relatively sparse scatter of the very poorest model realisations can be observed for all objective functions (Figures 6.3a-d). However, importantly, the poorest models still occur across approximately the entire range of values for channel roughness values defined for the

analysis (Section 6.2.2). The observed trends show a contrast to the more complex trends presented for the two rain parameters.

As presented in Section 6.3.1, the densest concentration of data points, indicating relatively poor goodness-of-fit, runs horizontally across the range of channel roughness values.

Table 6.5. A table showing the number of simulations above the set performance threshold for each objective function. The maximum, minimum and % of potential range of channel roughness values for these model simulations are shown for channel roughness. Figures marked with * indicate the potential extreme value i.e. largest and smallest possible roughness values

Objective function	Threshold	Sample size (% of 2000 model simulations)	Channel roughness (Manning's n)		
			Max	Min	% of potential range
NSME	>0.7	122 (6.1)	0.070 *0.07	0.025 *0.025	100
MAE	<10 (cumecs)	98 (4.9)	0.070	0.025	100
RMSE	<20 (cumecs)	146 (7.3)	0.070	0.025	100
PEP	<10%	148 (7.4)	0.070	0.025	97.8

6.3.7   Floodplain roughness

The floodplain roughness parameter shows similar behaviour to the channel roughness parameter (Figures 6.4a-d and 6.9a-d). As with channel roughness, the majority of model simulations show high error between observed and simulated hydrographs across all roughness values. The best model simulations also occur across the entire range of floodplain roughness values (Table 6.6).

Table 6.6. A table showing the number of simulations above the set performance threshold for each objective function. The maximum, minimum and % of potential range of floodplain roughness values for these model simulations are shown for floodplain roughness. Figures marked with * indicate the potential extreme value i.e. largest and smallest possible roughness values

Objective function	Threshold	Sample size (% of 2000 model simulations)	Floodplain roughness (Manning's n)		
			Max	Min	% of potential range
NSME	>0.7	122 (6.1)	0.100 *0.1	0.020 *0.2	0.080 (0.08)
MAE	<10 (cumecs)	98 (4.9)	0.098	0.020	97.5
RMSE	<20 (cumecs)	146 (7.3)	0.100	0.020	100
PEP	<10%	148 (7.4)	0.099	0.020	98.8

6.3.8 Land roughness

Trends in land roughness parameter are very similar to the other roughness parameters (Figures 6.5a-d and 6.10a-d). The best model simulations occur across the full range of land roughness values sampled (Table 6.7).

Table 6.7. A table showing the number of simulations above the set performance threshold for each objective function. The maximum, minimum and % of potential range of land roughness values for these model simulations are shown for land roughness. Figures marked with * indicate the potential extreme value i.e. largest and smallest possible roughness values

Objective function	Threshold	Sample size (% of 2000 model simulations)	Land (Manning's n)		
			Max	Min	% of potential range
NSME	>0.7	122 (6.1)	0.198 (0.2)	0.021 (0.02)	98.3
MAE	<10 (cumecs)	98 (4.9)	0.198	0.021	98.3
RMSE	<20 (cumecs)	146 (7.3)	0.198	0.021	98.3
PEP	<10%	148 (7.4)	0.197	0.020	98.3

6.4   Discussion

6.4.1   Overall model performance

Only approximately one quarter of model realisations achieved NSME values of above 0. A NSME value of 1 indicates a perfect fit between observed and simulated hydrograph (Table 6.1). A value of 0 indicates that the model realisation in question is the same as a "no knowledge model that gives a prediction of the mean of the observations for all time steps" (Beven 2001: 223). This indicates a large proportion of model simulations show a poor fit with the observed hydrograph. MAE and RMSE are dimensional measures of goodness of fit (Green and Stephenson 1986; Willmott and Matsuura 2005) and show a similarly high degree of error associated with all of the 2000 parameter sets.

Such results are not unexpected. As discussed in the previous chapter, varying rainfall rate time map by between 1 mm/day and 200 mm/day is naturally expected to result in a large variation in the shape of the hydrograph at the catchment outlet. Even when other parameters are varied at the same time, as in GLUE analysis, the wide variation in rain time map and effective runoff rate parameters is likely to greatly influence the hydrograph simulated. If it is assumed that a temporally constant rain time map can adequately represent the hydrological response of the catchment throughout the 2000 flood event, there is likely to be a small range of appropriate rainfall rates which will result in a good fit between observed and simulated discharge. Additionally, varying the effective runoff rate would naturally greatly affect the simulated hydrograph. As shown in the results section, both rain time map and effective runoff rate parameters have a large impact on model output.

It is important to note that the poor performance of a majority of simulations does not necessarily indicate a poor model, merely that the model realisations in question are poor. Indeed, the optimum NSME value is 0.80 (2 d.p.), which indicates relatively good model performance, despite temporally and spatially uniform parameter values. It should be noted that 25% of models perform better than the random case. This can be viewed as positive considering the homogenous parameters, and the wide range over which the parameter values are varied. The range of parameter values randomly selected during the uncertainty analysis will have an impact on the proportion of simulations which show a good fit with observed discharge during the 2000 flood event. However, MAE of all model simulations exceeded 9 cumecs, which is significant.

6.4.2   Rain time map and effective runoff rate

It was found in the sensitivity analysis (Chapter 5) that model output was sensitive to the rain time map and effective runoff rate applied. This is also the case in the uncertainty analysis,

though effective runoff is possibly more sensitive. Model performance shows great variation as the two parameters are varied. The conclusions from these results must be similar to those drawn from the sensitivity analysis. The rainfall rate and also effective rainfall rate are important controls on model performance. Again, this may be explained by the degree of variation in both parameters, which may exert a large influence on the model output and the response of other parameters. This factor is also discussed in Chapter 5. It is shown in Tables 6.3 and 6.4 that only certain values for the rain time map and effective runoff rate parameters result in the best models, potentially due to the wide range of possible values. Indeed the results suggest that it is not necessary to apply an effective runoff rate exceeding 100% in order to compensate for any potential errors in gauge data. This however does not mean that no such errors exist; in fact they are almost a certainty (Beven 2001: 217).

However, it can be seen that for those time maps selected from the simulations exceeding set objective function values i.e. the highest rainfall rate time maps, there is a degree of equifinality (Table 6.3). A relatively wide range of effective runoff rates (75-97%) also indicates equifinality.

The highest rain time maps show a different trend to equifinality, with a high standard deviation from the mean objective function values for each rainfall rate. This indicates that very different objective function values can result from applying the same rain time map. This supports the conclusion that parameter interactions have an effect on parameter behaviour.

6.4.3   Roughness parameters

The effect of varying roughness parameters is not as clear as for the rain parameters. There are no clear trends indicating a tendency for those models exceeding the set performance thresholds when certain roughness values are set. Instead, the model output as roughness parameters are varied shows a high degree of equifinality, more so than for the rain parameters; different combinations of parameter values can results in the same or similar model output. Whereas the rain parameters have a large control on model output, the effect of a certain channel, floodplain or land roughness value on model output depends largely on the values randomly selected for the other model parameters. As stated in the previous section, this may potentially be due to the variation of the rain parameters over very large ranges.

The high degree of equifinality observed for the roughness parameter values, indicated by the occurrence of the best models across the full range of parameter values (Figures 6.3-6.5 and 6.8-6.10), may also be partly explained by the nature of the model. The spatially homogenous roughness values for land and floodplain cover and in-channel roughness represent a key simplification in the model structure. It is clear that one single

Manning's n value for each of these parameters will not represent in great detail the roughness of the entire catchment, which will be highly heterogeneous at various scales. Therefore the statement that no optimum parameter set exists (Beven and Binley 1992) is particularly relevant. Equifinality may suggest that roughness does not matter to a great degree in comparison to the selection of a rain time map and rain input %. This may have important implications for model development and analysis of results uncertainty. Within the context of using a reduced complexity model, results potentially suggest that assumptions regarding roughness values are not so important so as to make model predictions of no use.

6.4.4   Effect of objective function

There is a large amount of literature discussing the use and appropriateness of objective functions in assessing model performance (Green and Stephenson 1986; Beven 2001; Willmott and Matsuura 2005; Schaefli and Gupta 2007). There is an emphasis on applying a number of objective functions due to the bias associated with every objective function (Green and Stephenson 1986). The dotty plots suggest a similar pattern of model performance for the objective functions; NSME, RMSE and MAE, whereas those using PEP show a slightly different pattern. This is most likely due to the fact that the PEP measures the goodness of fit of only one aspect of the hydrograph; the agreement between observed and simulated peak flow magnitude. The % error in peak flow is not affected by timing errors between the simulated and observed hydrographs, identified as important in the previous chapter. It is apparent that the exact range of parameter values within which the best models are found depends on the objective function used.

Beven (2001: 224) stated that "different performance measures will usually give different results in terms of the 'optimum' values of parameters and the relative sensitivity of different parameters". This is indeed the case when the focus of analysis is shifted from performance of all parameter sets to optimum parameter sets. This highlights the inappropriateness of attempting to identify an 'optimal' parameter set. However it is also important to note that even if only one objective function was used to analyse model performance, the parameter set chosen could vary greatly (as discussed above; Section 6.3) due to equifinality.

Following discussion of the trends observed in the results it is worth noting that, to a degree, some trends may be due to the sample size in the uncertainty analysis. Whilst the sampling method used is random, with 2000 simulations run there is some evidence of clustering of points within certain parameter ranges. Some rain time maps, as well as values for other parameters, are selected more than others. Therefore a concentration of data points in particular areas in the parameter space may be due simply to a higher sampling in this area.

Such sampling bias does occur to a small degree in this analysis. To avoid such uncertainty due to sampling bias in future a larger number of simulations can be run (>2000), however this is likely to be a minor factor.

6.4.5 Significance of uncertainty analysis

The primary aim of the uncertainty analysis detailed above is to assess the performance of the uncalibrated Overflow model, randomly selecting sets of parameter values (Campling et al. 2002). Whilst the sensitivity analysis presented in the previous chapter analysed the variation in model output whilst parameter values were varied one at a time, the GLUE analysis shows the effects of parameter interactions on model output (Saltelli 2000; Wainwright and Mulligan 2004). Such interactions are clearly important in this uncertainty analysis, for example the importance of rain time map parameter in relation to other parameters.

It is stated by McCuen (1973) that studies which aim simply to define an optimal parameter set through sensitivity analysis are "limited", though McCuen (1973) then proceeded to attempt to define such an optimal parameter set. Beven and Binley (1992) went further in disputing the existence of a true optimal parameter set. Much further work has been carried out by Beven on the theory of equifinality (Beven 2006), whereby multiple model realisations can give relatively good fits to observed data. Uncertainty analysis allows an exploration of parameter equifinality. The results presented indeed show the absence of a single 'optimal' value for each parameter.

Acreman et al. (2003: 83) in reference to Kirkby et al. (1993), stated that "models are, by definition, simplifications of reality that retain only certain characteristics of the system under study". Beven and Binley (1992) and Beven (2001) cited a number of sources of error for hydrological and hydraulic models. Errors in model structure, parameterisation, initial and boundary conditions and observed data for calibration result in uncertainty in model output. It is also important to note uncertainty due to the approach to sensitivity and uncertainty analysis, such as the choice of objective functions to be used (Diskin and Simon (1977). The focus in this chapter is on parameter uncertainty, whereby different sets of parameter values may be equally likely as simulators of a catchment (Beven and Binley 1992). As discussed, results in this chapter suggest a large degree of equifinality, particularly for the roughness parameters. This suggests uncertainty in selection of particular parameter values. Another source of uncertainty lies in the objective functions, which are found to be biased towards some aspects of the hydrograph, as discussed in the previous chapter. The choice of objective function used is also subjective.

Wheaton et al. (2008) stated that quantification of uncertainty and subsequent communication to the public or stakeholders is often ignored in research studies. Addressing

the uncertainty associated with predictions is a key aspect of this study. The power of the reduced complexity model is in the simple modelling procedures which can allow reduced simulation time. They can also have the benefit of being simpler to explain to those with a vested interest in the output of such models (Odoni and Lane 2010). Wainwright and Mulligan (2004: 59) identified error as "an important part of the modelling process". This study is certainly no exception. Therefore uncertainty of predictions must be made clear (Wainwright and Mulligan 2004). The investigation of model equifinality is particularly important due to the nature of the model. As the model incorporates a number of simplifications and assumptions it is important to have sufficient understanding of the effects of these assumptions on model predictions. For example, a key simplification lies in the representation of land cover and the channel network through assignment of spatially homogenous roughness values. Whilst a default manning's n of 0.035 is set for the channel network, similarly good predictions of model output are made when very different channel roughness values are applied.

6.5 Conclusion

It can be seen that there is a high degree of equifinality between parameter sets for all roughness parameters. Equifinality is also apparent for rain rate time maps and effective runoff rate parameters, though less so. There is also evidence from the results of the influence of parameter interactions. Model output appeared to be more sensitive to rain time map and rain input percentage. These results suggest that selection of a homogenous roughness value may be an acceptable model simplification, with not too great an impact on model output, particularly in comparison to the other tested parameters.

Relatively good models can be observed across a wide range of parameter values for all parameters. Some model realisations performed relatively well, particularly as homogenous parameters have been set. However the rain time map was found to be important. Overall model performance was poor, primarily due to the wide range of parameter values sampled from. Of note is that all simulations had an error of >9 cumecs.

The overall performance of the model in the GLUE analysis may be due in part to the nature of the analysis; in model runs where a rain time map of 1 mm/day was applied, the likelihood of a similar simulated magnitude and pattern of discharge passing the gauge at Isfield to the observed event was low no matter what roughness parameters were applied.

The above two findings; relatively poor model performance, with large errors even for simulations with the best goodness-of-fit with observed discharge, and a high sensitivity of rain rate time map were clear indications that using a single, constant rain time map throughout the storm event was not an acceptable simplification. However the key justification for the

decision to calibrate the Overflow model, applying a varied temporal rain time map throughout the storm event, was that it is well known that precipitation, and catchment hydrological response varies as a function of time. It was therefore thought beneficial to allow improved representation of the wetting up and drying of the catchment as the rainfall event progressed. The newly calibrated Overflow model and its performance in terms of goodness of fit with observed discharge will now be discussed in the following chapter.

<u>**Chapter Seven   Calibration of Overflow**</u>

This Chapter discusses the performance of the calibrated model developed following the results of the uncertainty analysis discussed in Chapter 6. Issues associated with the uncalibrated model are presented in Section 7.1.1, followed by the methodology followed for calibration of the model (Section 7.1.2). Qualitative and quantitative comparison of the simulated hydrographs produced by the calibrated and uncalibrated Overflow models is then detailed (7.2.1). Finally, features of the calibrated model are described in more detail (7.2.2).

7.1   Calibration of Overflow

7.1.1   Issues with the uncalibrated Overflow

In the sensitivity analysis and uncertainty analysis in Chapters 5 and 6 respectively, a number of issues associated with the uncalibrated Overflow model are presented. First, the model output (discharge) is highly sensitive to variation in the rainfall rate time map applied. Second, the use of a single rain time map throughout the storm event, which lasts 5 days, represents an important simplification. This is reflected in the relatively poor performance of the model in all of the 2,000 simulations in the Uncertainty Analysis. Third, and as a consequence of the two previous points, there is difficulty in selecting one single rain time map throughout the 5 day storm event.

7.1.2   Methodology

In the uncalibrated version of the Overflow model, a single rain time map was applied to represent the wetness, and thus the cell flow passage times, in the catchment. The actual observed rainfall is then applied to the catchment. Whilst rainfall varies temporally, a single rain time map is set for the entire event. To calibrate the Overflow model the order of time maps was varied, allowing improved temporal representation of the hydrological response of the catchment as the rainfall event progresses. 200 sets of different time map ordering were created.

To determine the temporal ordering of the rain rate time maps, a number of steps were followed. Odoni and Lane (in prep, Appendix A) provide a more detailed description of the model and calibration procedure. A Monte Carlo technique is applied to perform the calibration, whereby rain time maps are randomly and then strategically sampled (Odoni and Lane, in prep). For each 1 hour time step, of which there are 120, a rain time map is randomly selected from the full distribution (1-200 mm/day). This procedure is repeated 200 times to produce 200 hydrographs. For each time step, the range of potential time maps to be sampled

from is then narrowed by calculating which rain time maps produce a complete flood hydrograph with the best possible Nash Sutcliffe Model Efficiency (NSME). This procedure is then repeated, but sampling from the narrowed range of time maps for each time step, until 200 model simulations are produced achieving a NSME exceeding 0.98 (Odoni and Lane, in prep). The mean of the 200 time map orderings is shown in Figure 7.1. Peaks in observed rainfall precede peaks in the rain time map. However the lag in the rain time map peak remains relatively consistent and does appear to reflect variation in observed rainfall rate.
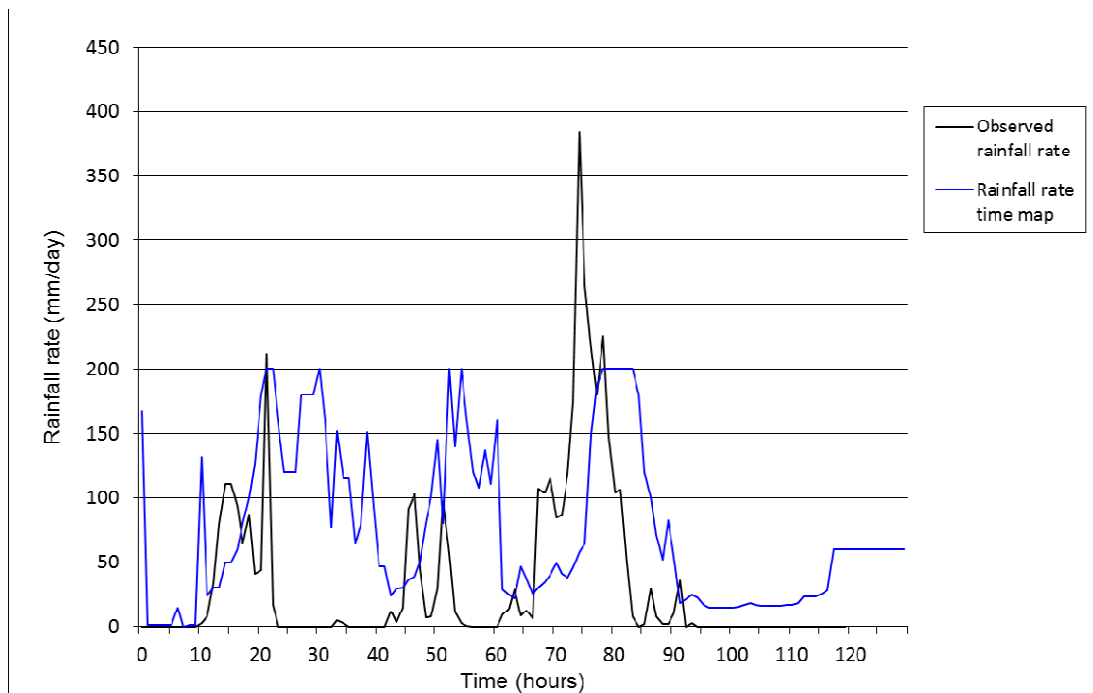
Figure 7.1. A figure comparing observed rainfall during the October 2000 storm event with the temporal ordering of rain rate time maps. Observed rain is converted into an equivalent daily rain rate in order to allow comparison with the rain time map.

In the following chapter, where the effects of flood interventions on peak flow are explored, a single hydrograph is used as the 'base case', the simulated hydrograph at Uckfield when no interventions are simulated. The base case hydrograph is calculated as the mean of the 200 simulated hydrographs which achieve a NSME of >0.98, and is shown in Figure 7.2.

It should be noted that this is not a full calibration procedure, as ideally all effective parameters would be calibrated (Odoni and Lane, in prep). A full calibration was not carried out due to time constraints. However, as discussed, the rain rate time map was viewed as an essential parameter for calibration. Following this procedure, a hydrograph with a much improved goodness-of-fit with observed data was simulated.

7.2   A brief analysis of the calibrated Overflow model

7.2.1   Comparison of uncalibrated and calibrated Overflow

Figure 7.2 shows the performance of the calibrated version of Overflow, with comparison statistics shown in Table 7.1. Figure 7.3 shows the performance of the uncalibrated version of Overflow as a comparison, with relevant statistics shown in Table 7.2. In Figure 7.2, the discharge at the Isfield gauge observed during the 2000 flood event is compared to the simulated discharge, for both Isfield and the Meadows area at Uckfield. The simulated discharge at Isfield is shown as it can be directly compared statistically to the discharge observed at Isfield flood gauge. The simulated discharge at Uckfield is shown as the effects of Catchment Riparian Intervention Measures (CRIMs) on the hydrograph at Uckfield are to be explored in following chapters.

Figure 7.2 shows that the calibration has been effective. There is a good qualitative agreement between the observed and calibrated hydrograph at Isfield. Table 7.1 allows a quantitative analysis of agreement. A Nash-Sutcliffe Model Efficiency (NSME) value of 0.99 and error values of 0.74 cumecs and 3.84 cumecs are recorded for the Mean Absolute Error (MAE) and Root Mean Square Error (RMSE) statistics respectively. The good performance of the calibrated version of Overflow is particularly apparent in comparison to the uncalibrated model.

Graphical analysis in Figure 7.3 clearly shows a poor fit between the observed hydrograph and the hydrographs simulated for many time invariant rain time maps, regardless of the value of rainfall rate used. This is reflected in the statistics shown in Table 7.3. Error between observed and simulated discharge is high for every rain time map applied. The hydrograph with the best fit as indicated by the objective functions is simulated when a rain time map of 200 mm/day is applied. The simulated hydrograph achieves a NSME value of 0.62 and MAE and RMSE of 11.56 cumecs and 21.68 cumecs respectively. The error in simulated peak flow is large, however. The results indicate a high degree of error between observed and simulated hydrographs.
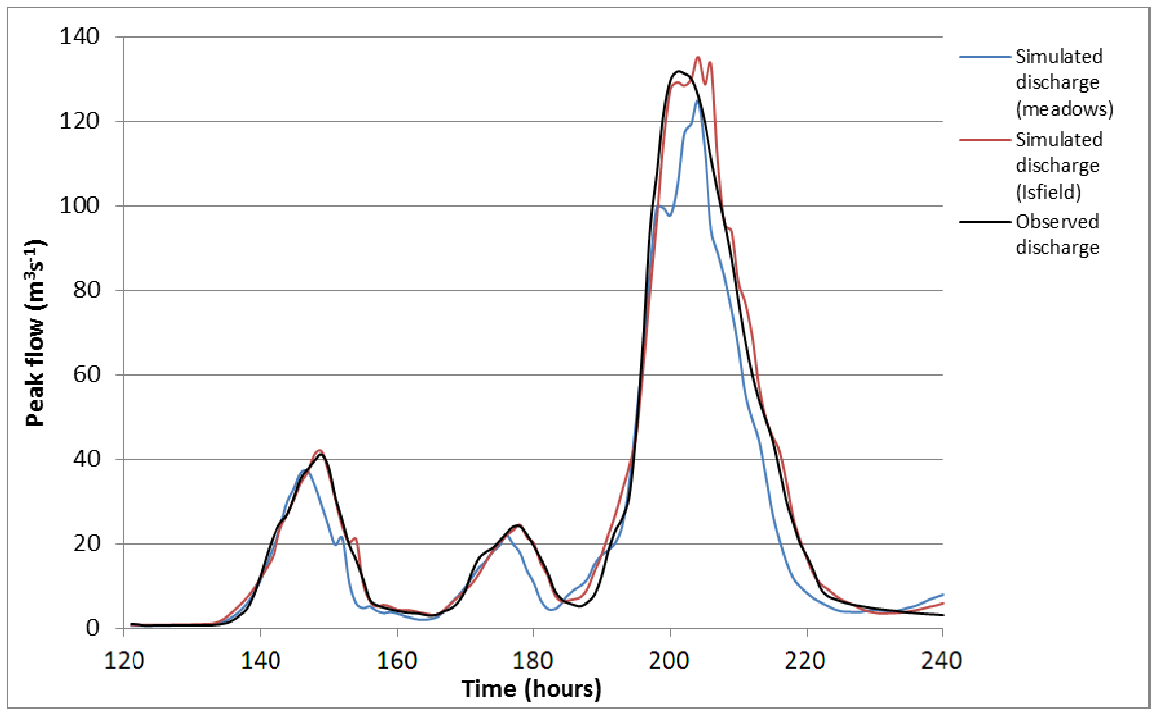
Figure 7.2a. A comparison of observed discharge during the 2000 flood event at Isfield with simulated discharge at Isfield and Meadows (upstream of Uckfield) using the calibrated version of Overflow.
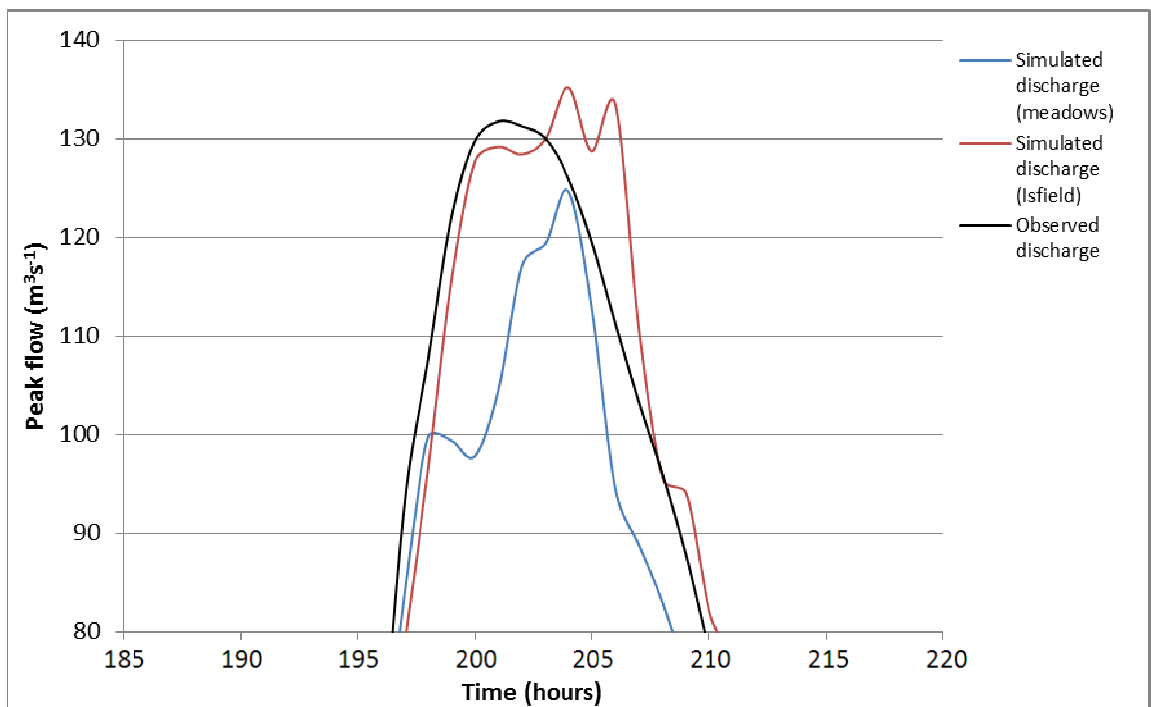
Figure 7.2b. A replica of Figure 1a with a focus on the highest flows

Table 7.1. The results of objective functions showing the goodness-of-fit between the observed and the simulated hydrograph at Isfield. The simulated hydrograph (shown in red in figure 7.2) was produced using the calibrated version of Overflow.

NSME	RMSE (cumecs)	MAE (cumecs)	% error in peak	Peak timing error (hours)
0.99	3.84	0.74	2.54	2
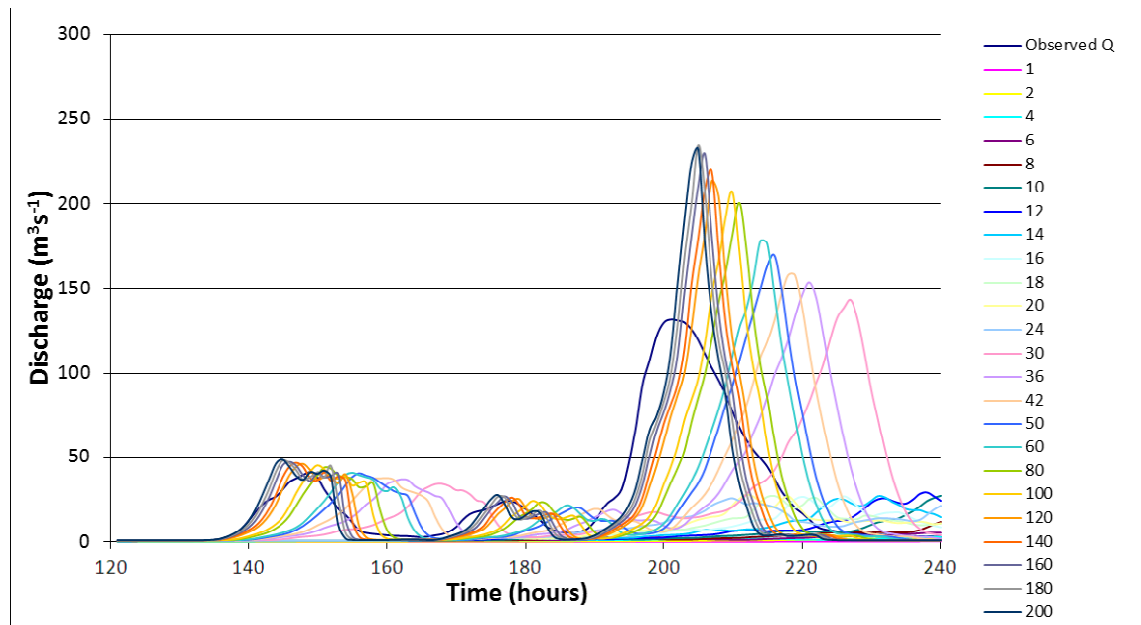
Figure 7.3. A comparison of the hydrograph observed at Isfield during the 2000 flood event with hydrographs simulated using the uncalibrated version of Overflow. All parameters, with the exception of the rain time map parameter, were set at default values. The 24 simulated hydrographs were created by applying a different rain time map.

94

Table 7.2. The results of objective functions showing the goodness-of-fit between the observed and simulated hydrographs at Isfield. Hydrographs (as shown in Figure 7.2) are simulated applying different rain time maps for the uncalibrated version of Overflow.

Rain time map (mm/day)	NSME	RMSE (cumecs) (m^3s^{-1})	MAE (cumecs) (m^3s^{-1})	% peak error	Peak timing error (hours)
1	-0.54	43.44	25.67	35343.85	39
2	-0.52	43.17	25.25	5942.20	30
4	-0.48	42.61	24.72	4344.80	37
6	-0.48	42.48	24.30	2277.71	38
8	-0.47	42.46	24.04	1009.24	39
10	-0.47	42.34	24.21	382.89	39
12	-0.45	42.13	24.88	350.90	37
14	-0.41	41.49	24.90	386.64	30
16	-0.35	40.56	24.03	389.08	25
18	-0.27	39.39	22.56	385.03	15
20	-0.20	38.24	21.49	372.16	11
24	-0.12	36.96	20.89	410.82	9
30	-1.03	49.84	32.29	-8.01	26
36	-0.92	48.41	30.29	-14.35	20
42	-0.77	46.51	28.71	-16.66	17
50	-0.53	43.32	26.15	-22.38	15
60	-0.42	41.62	24.65	-25.98	13
80	0.02	34.60	19.22	-34.28	10
100	0.17	31.89	17.30	-36.32	9
120	0.47	25.57	13.38	-38.26	6
140	0.52	24.14	12.73	-39.81	6
160	0.58	22.78	12.05	-42.43	5
180	0.60	22.08	11.67	-43.80	4
200	0.62	21.68	11.56	-43.15	4

7.2.2   Issues with the calibrated Overflow model

Whilst the fit between the observed hydrograph and the hydrograph simulated with the calibrated version of Overflow is good, there are a number of issues. The most apparent discrepancy between the observed and simulated hydrographs at Isfield is observed during the highest flows (Figure 7.2b). The simulated flow peak is maintained, and indeed increases slightly, for approximately 2 hours after the observed discharge begins to decrease. There is also a slight inconsistency in the recession limb. However, as indicated by NSME values close to 1, the simulated hydrograph is a good estimation of that observed during the 2000 flood event.

No observed hydrograph at Uckfield exists for the 2000 flood event, therefore no direct comparison between the simulated hydrograph at this location and existing data can be made. However it is possible to make informed observations of the nature of the hydrograph simulated at the Meadows area. An unexpected fall in discharge along the rising limb preceding the peak flow can be observed. This has the effect of delaying the simulated peak flow, which occurs at the same time as peak flow downstream at Isfield. As the Meadows area is located several kilometres upstream of the Isfield site, it would be expected that there would be a lag between peak flow simulated at the upstream and downstream sites, even with the presence of a major contributing tributary located downstream of Uckfield. This qualitative analysis suggests a source of uncertainty associated with the simulated hydrograph at the Meadows area just upstream of Uckfield.

7.3   Conclusion

The procedure followed to calibrate Overflow, as described, does not represent a full calibration of the model. Ideally all uncertain parameters would be included in the calibration process. That aside, the objective functions used suggest that the newly calibrated model performs well when compared to observed data, and in comparison to the uncalibrated model. For example, the model achieves a Nash-Sutcliffe Model Efficiency value of 0.99. However, there is some uncertainty associated with the simulated hydrographs at Isfield and Uckfield. This may in turn lead to some uncertainty in results exploring the effects of adding Catchment Riparian Intervention Measures (CRIMs) to the Uck catchment on the simulated hydrograph. Such an exploration will be detailed in Chapter 8.

Chapter Eight   Impact of Catchment Riparian Intervention Measures (CRIMs) on peak flow

at Uckfield

In Chapter 7 the calibration of the Overflow model was discussed. In this chapter the effects on the flood hydrograph of adding Catchment Riparian Intervention Measures (CRIMs) throughout the catchment are explored. Initially, a screening process is carried out to identify reaches in the Uck catchment where adding a single CRIM has a positive impact in terms of reduction in peak flow downstream at Uckfield (Section 8.2). The results of the screening process are discussed in Section 8.3. The impact on the flood hydrograph downstream of adding CRIMs in combination is then presented (8.4), along with a consideration of conditioning factors (8.5).

8.1   Methodology

First the methodology for the screening process (8.1.1), and then the exploration of CRIMs in combination (8.1.5), is presented.

8.1.1   Initial screening

Before the effect of combinations of CRIMs on the downstream hydrograph could be investigated, it was necessary to carry out screening simulations. The screening runs involved increasing the roughness of the floodplain and channel sections along one individual reach at a time, keeping all other parameter values throughout the catchment at their default values. This represents the effects of adding of a CRIM to the particular reach in question. From these results it was possible to identify the individual effect on peak flow upstream of Uckfield of adding a CRIM to different reaches.

Reaches downstream of Uckfield, and also those above a critical width were excluded from the screening runs. Reaches with a width above 7m were deemed too wide for debris dams to be added (T. Nisbet, Forest Research, pers. comm.). Adding CRIMs to reaches downstream of Uckfield would naturally not have an effect on the flood hydrograph just upstream of the town. Following this process, 199 separate reaches were identified as potential sites where CRIMs could be added.
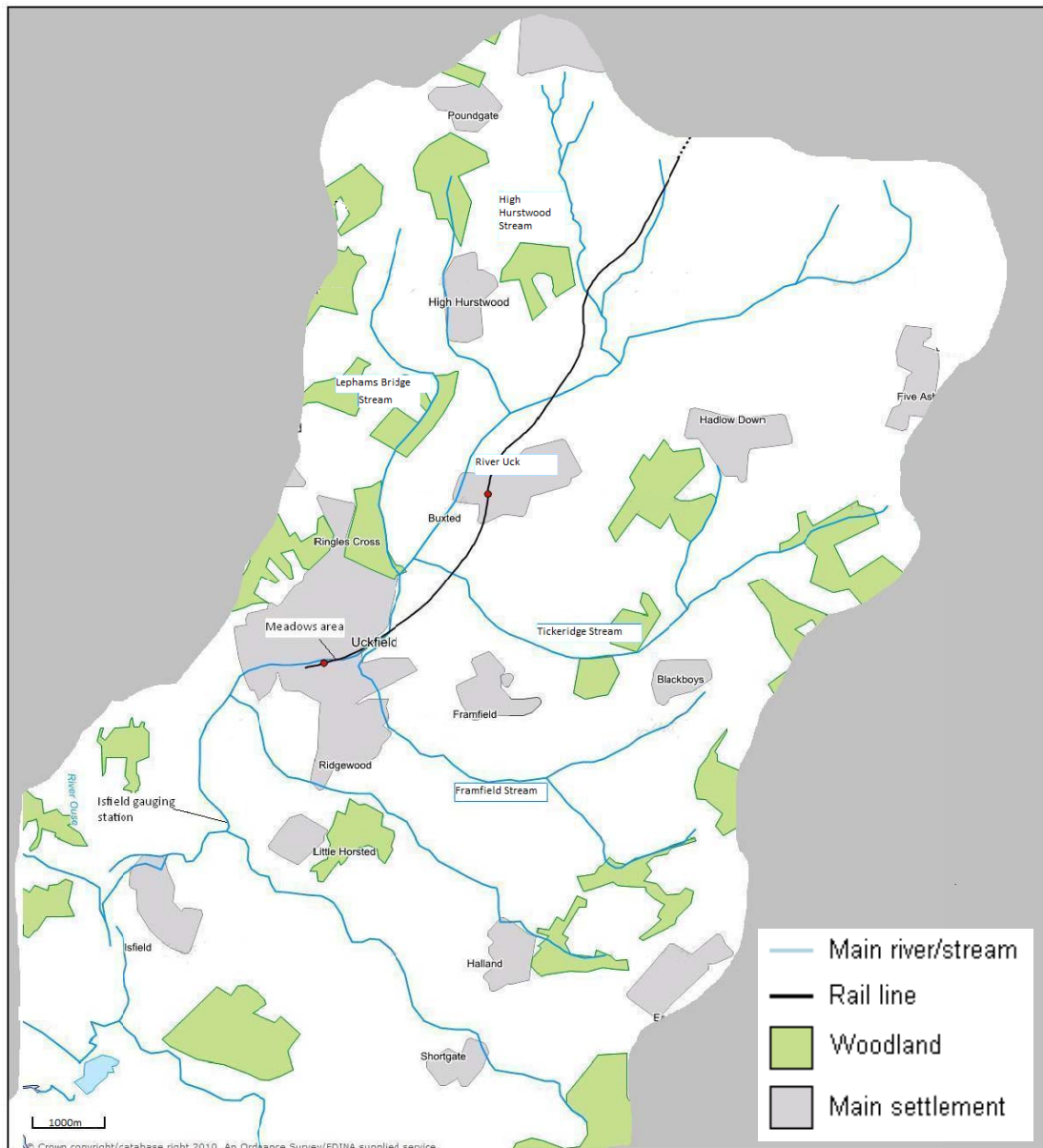
Figure 8.1. The Uck catchment. Main tributaries and the location of the two sites where hydrographs are simulated throughout the study; Isfield and the Meadows (Uckfield).

199 simulations were carried out. For each simulation the roughness of one reach was increased to Manning's n values of 0.16 and 0.14 for the floodplain and channel respectively. These values were based on the 'central' values suggested by Odoni and Lane (2010). Chow (1959) suggested a Manning's n value of 0.16 represents the extreme floodplain roughness associated with medium to dense brush or timber. 0.14 is close to the extreme value for very weedy, blocked channels. The Manning's n values of all other reaches remained at their default values (0.06 and 0.035 for floodplain and channel respectively).

8.1.2   Classification of reaches

The peak flow for the hydrograph simulated just upstream of central Uckfield (Meadows, Figure 8.1), with no CRIMs added throughout the catchment (the 'base case') was compared to the peak flow for all 199 hydrographs produced when a CRIM was simulated in one single reach. The effects of increasing reach hydraulic roughness on downstream peak flow were initially defined as positive and negative. Reaches with a positive effect reduced downstream simulated peak flow by >0 cumecs, whereas negative reaches increased peak flow by >0 cumecs. However, as with previous work in this study, the methodology used was to an extent influenced by the results obtained (Section 8.2.1). Due to the large number of positive reaches following the screening simulations, it was decided that not all reaches which reduce peak flow by >0 cumecs would be included in the list of positive reaches as introducing such a large number of CRIMs would be unfeasible. It was decided that the 100 reaches which reduced the peak flow by the greatest amount would be included in the list of positive sites. Those which reduced peak flow by less were classed as neutral reaches. Those which increased flow peak remained classed as negative.

8.1.3   Classification maps

To gain further information on the spatial pattern of positive, neutral and negative sites, a map was produced showing the locations of the different classified reaches throughout the catchment.

8.1.4   Reach properties/statistics

The influence of reach properties on downstream peak flow, as a CRIM was added to one reach at a time, was analysed. Reach properties, as represented in Overflow, were extracted from the model. For a full description on how these properties were formulated (see Chapter 4: model description, and Odoni and Lane, (in prep) (Appendix A)).

The reach properties that were analysed in this study are;

Median channel reach width (m)

Median channel reach depth (m)

Median channel reach slope

Channel reach natural length (m)

Floodplain width (m)

Floodplain slope

The average floodplain width was calculated by dividing the total floodplain area along the reach by the natural reach length. Whilst channels in the Uck catchment are as wide as 8m, cell resolution is 20m. Therefore channel cells will often contain a large area of floodplain in

addition to the channel. This will lead to an under-estimation of the floodplain width. However the calculated floodplain width is felt to be an appropriate approximation.

Floodplain slope can be calculated in two ways; as the steepest flow path or the slope to the lowest neighbouring cell. However the choice of method is found not to have a considerable impact. Here the latter method is chosen and the results presented.

8.1.5 Combination of CRIMs

The positive reaches were subsequently ranked in order of greatest effect on the peak flow; this was the order in which CRIMs would be added in combination. Initially a CRIM was added to the site with the greatest peak flow reduction effect. The reduction in peak flow for this first CRIM was equal to its individual effect. A CRIM was then added to the site with the second greatest effect on flow peak so that there were two separate sites with CRIMs. A model simulation was run and the new simulated hydrograph upstream of Uckfield analysed. The cumulative effect of the CRIMs on peak flow was recorded. This process was repeated going down the positive reach list so that more CRIMs were added in combination. If the cumulative peak flow reduction was negatively affected (i.e. downstream peak flow increased from the previous simulation) as a result of the addition of a CRIM in combination, this reach was excluded and the process continued. This recognised that the effect of a CRIM in isolation might be different to that when a CRIM was included along with other CRIMs.

8.2 Results (1) - Impact of CRIMs in single reaches

8.2.1 Positive and negative impacts

Table 8.1 summarises the effects of increasing the floodplain and channel roughness of single reaches on the peak flow of the simulated hydrograph upstream of Uckfield. Table 8.1 shows that there is a considerably larger number of reaches where an increase in roughness has a reducing, as opposed to an increasing effect on the peak flow just upstream of Uckfield. Adding a CRIM to a reach reduces downstream peak flow with 127 reaches whereas 72 reaches increase downstream peak flow. There is an even greater disparity between the magnitude of this peak flow reduction and the magnitude of peak flow increase. When a CRIM is simulated, of the 199 reaches explored, only 2 reaches increase downstream peak flow by over 1 cumec. In contrast 13 reaches reduce peak flow by over 1 cumec. No reaches have an effect of increasing peak flow by over 2 cumecs. The greatest reduction in peak flow as a result of adding a CRIM to a single reach was 3.86 cumecs (3.1% of initial peak flow). In contrast the greatest increase in peak flow was 1.96 cumecs (1.6% of initial peak flow).

Table 8.1. The number of reaches in the Uck catchment where, if applied to 1 individual reach, a CRIM would modify flood peak by more than 3, 2, 1, 0.5, 0.1 and 0 cumecs. CRIMs were applied to a total of 199 separate reaches.

Reduction in peak flow (cumecs)	>3	>2	>1	>0.5	>0.1	>0
Number of reaches	3	6	13	31	72	127
Increase in peak flow (cumecs)		>2	>1	>0.5	>0.1	>0
Number of reaches		0	2	7	32	72

127 reaches had a 'positive' effect in terms of flow peak reduction. This represents nearly two thirds of the 199 reaches determined as valid for the screening process, as discussed in Section 8.1. Only 31 of these 127 'positive' reaches reduced the downstream peak flow by over 0.5 cumecs. 55 reaches had an effect of reducing peak flow by between 0.1 and 0 cumecs. These results influenced the selection of reaches to be used to explore the effects of the combination of CRIMs (Section 8.1.2). As a consequence, the 27 'positive' reaches with the lowest magnitude effect on the downstream flow peak were assigned as neutral sites.

8.2.2   Spatial patterns of positive and negative impacts

Figure 8.2 shows a complex spatial pattern of positive, neutral and negative reaches throughout the catchment, though it is possible to identify some patterns. Positive sites are located along the entire length of the main Uck channel, with the exception of the most peripheral reaches in the north-east of the catchment. It can also be observed that reaches along the Uck leading towards Uckfield were excluded from the screening simulations as they exceeded a critical width of 7 metres (Section 8.1.1). Two main tributaries; High Hurstwood Stream and Tickeridge Stream (Figure 8.2) contain a large proportion of reaches with a reducing effect on the peak flow downstream. However there are a number of peripheral reaches flowing into the two tributaries, particularly Tickeridge Stream, which have the effect of increasing peak flow downstream when a CRIM is simulated. It is the case in several areas of the catchment that main tributaries contain a number of both positive and negative sites. In a number of main tributaries the negative sites are concentrated in more peripheral reaches and as mentioned earlier, are just upstream of positive reaches.
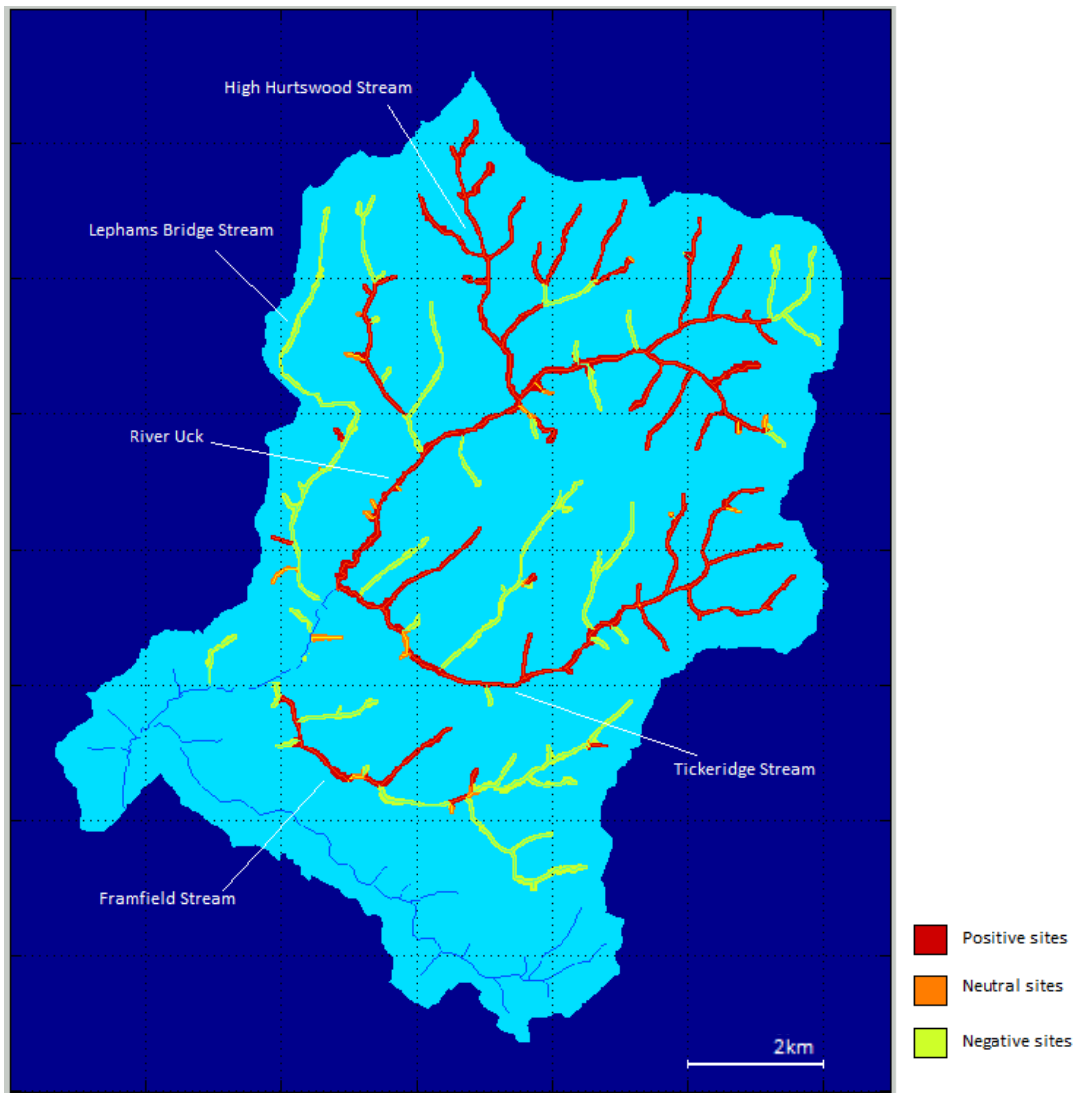
Figure 8.2. A map showing the location of positive, neutral and negative sites when a CRIM is added. All sites not highlighted were not suitable for intervention, either due to the width of the channel, or due to being situated downstream of Uckfield.

However, this is not the case in all tributaries. In some tributaries, such as Framfield Stream, reaches alternate between being classed as positive and negative as they move downstream. There is a concentration of negative sites located in Lephams Bridge Stream and Framfield Stream (Figure 8.2). However of note is the particularly long channel reach along Lephams Bridge Stream, the consequence of which is there are a small number of separate reaches along the tributary.

Figure 8.2 also shows that nearly all of the neutral sites are relatively short. However, analysis of Figure 8.2 does not indicate any clear patterns regarding the length of positive and negative reaches. Visual analysis of individual reaches in this case is difficult as separate reaches are not distinguishable on Figure 8.2 when one flows directly in to the other. However it is possible to identify a small number of negative and positive sites which are of comparable

length to the neutral sites. These patterns will be indicated more clearly below. Neutral sites are located throughout the catchment and do not show any clear spatial pattern.

As discussed previously the initial results from the screening simulations informed the choice of the 100 reaches which had the greatest individual effect on downstream flow peaks when a CRIM was applied to each reach one at a time. Figure 8.3 maps the location of the positive reaches, in 5 classes of 20 reaches based on the magnitude of their effects.

The majority of the 20 reaches with the greatest effect on downstream simulated peak flow are located along the main channel of the Uck, and a number of major tributaries. There are reaches with a lower magnitude effect along the main channel. These reaches are characterised by their short length, qualitatively similar to the neutral sites in Figure 8.2. The 40 reaches with the lowest effect on downstream flow peak are largely short or peripheral reaches. By just showing positive reaches, Figure 8.3 highlights and supports the statement that a large proportion of the negative sites are located in the two tributaries which feed into the Uck close to Uckfield. This is shown by the absence of many positive sites in these two tributaries, especially the Lephams Bridge Stream. However it may also be important to note the large number of positive reaches located along Tickeridge Stream which flows into the Uck just upstream from this tributary.

8.2.3   Local controls on CRIM impact

Figures 8.4-8.9 show selected reach properties plotted against the downstream peak flow when a CRIM is added to a particular reach. Two sets of CRIM values are used; Set 1 (in red): Floodplain n 0.16, Channel n 0.14; Set 2 (in blue): Floodplain n 0.16, Channel n 0.08. Set 2 offers a comparison to the main set of roughness values (Set 1) used in this study, based on 'central cases' used in Odoni and Lane (2010). The characteristics of all 199 reaches included in the screening simulations are plotted.

Figures 8.4 and 8.5 suggest a trend whereby adding a CRIM to the widest and deepest channels results in the greatest decrease in downstream peak flow. The lower peak flows as a result of increasing channel and floodplain roughness occur along reaches with the lowest slope (Figure 8.6). However it can also be observed that the highest peak flows also occur when CRIMs are added to reaches with the lowest slopes. Importantly it can be seen that in channels with larger slopes, increasing channel and floodplain roughness has little impact. Even with roughness increased along a reach, in the steepest reaches there is little change in the downstream flow peak. This is particularly the case in reaches steeper than 0.05.
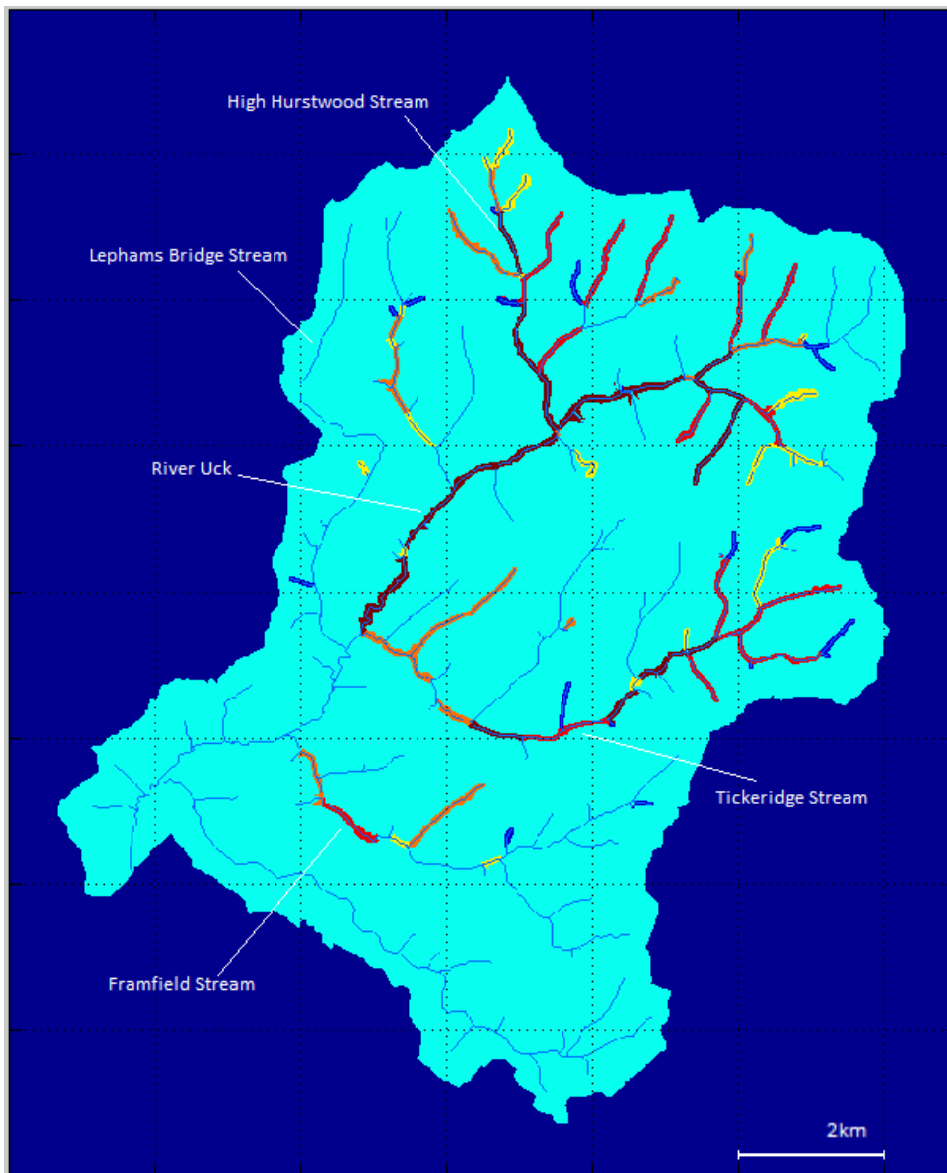
Figure 8.3. A map showing the distribution of the 100 reaches which reduce flow peak by the greatest amount when roughness is increased, in 5 classes;

A 20 reaches with greatest positive impact on peak flow

B 21-40

C 41-60

D 61-80

E 81-100
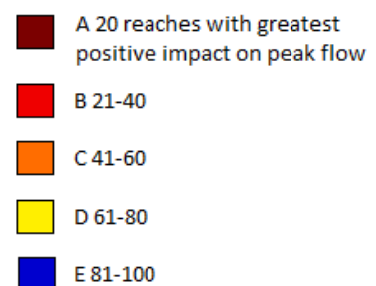
No clear trends can be identified when peak flow is plotted against channel length (Figure 8.7). However a cluster of points indicating little change in peak flow occur for the shortest channel reaches, supporting the earlier observation that neutral sites appear short in length.

A relationship between downstream peak flow and floodplain characteristics can be identified to an extent (Figures 8.8 and 8.9). Whilst the relationship is less clear than for channel width, depth and slope, it can be observed that the lowest downstream peak flows appear to occur in the reaches with the widest floodplains with the lowest slopes.

Plots were produced isolating the properties of the 20 best and worst reaches in terms of the effect on downstream peak flow of adding a CRIM along its length (Figures 8.10-8.15). The trends identified above relating peak flow to channel width, depth and slope are further supported by Figures 8.10-8.12. The 20 reaches where adding a CRIM decreases downstream peak flow by the greatest amount are shown to have, in general, deeper and wider channels with shallower slopes, compared to the worst 20 reaches. The majority of 20 best and worst reaches have floodplains of between 40 and 80m in width. This does not suggest a clear trend in terms of positive/negative reach characteristics but does in terms of the most effective positive sites.

Analysis of the 20 'best' reaches suggests that whilst there is a trend towards CRIMs being most effective in the widest channel, this is not the absolute rule. 5 of the 6 reaches with the greatest median width are included in the 20 reaches where CRIMs are most effective. Similarly 11 of the 26 widest channels are amongst the 20 reaches where CRIMs are most effective. This shows that CRIMs do not have the greatest impact in all of the widest reaches.

Figures 8.4-8.9 show that the most extreme peak flows occur when the rougher channel is simulated (Manning's n value of 0.14 as opposed to 0.08).
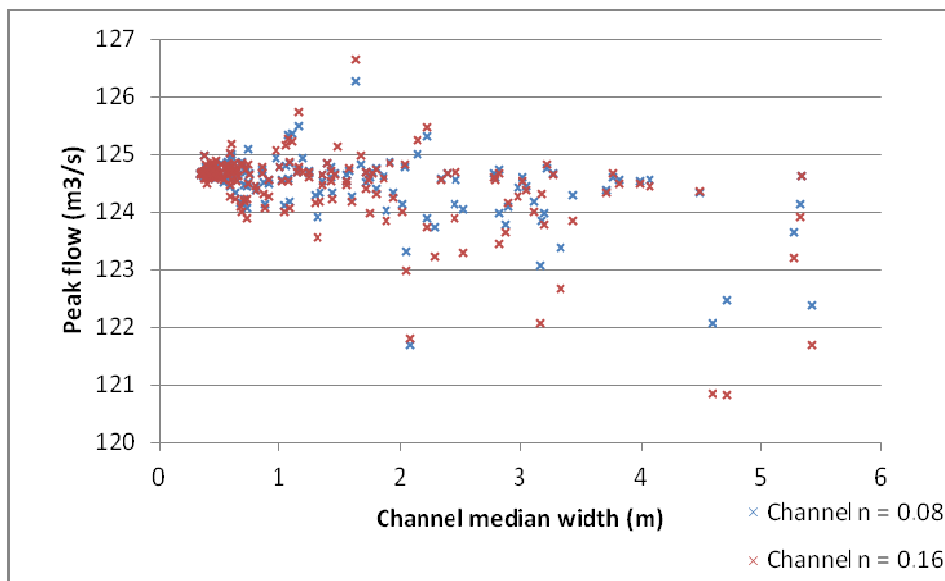
Figure 8.4. Channel median width of 199 reaches against downstream peak flow. Each point represents the width of one reach and the downstream peak flow when a CRIM is added to that reach. Two sets of values were used for the CRIMs; Set 1 (in red): Floodplain n 0.16, Channel n 0.14; Set 2 (in blue): Floodplain n 0.16, Channel n 0.08.
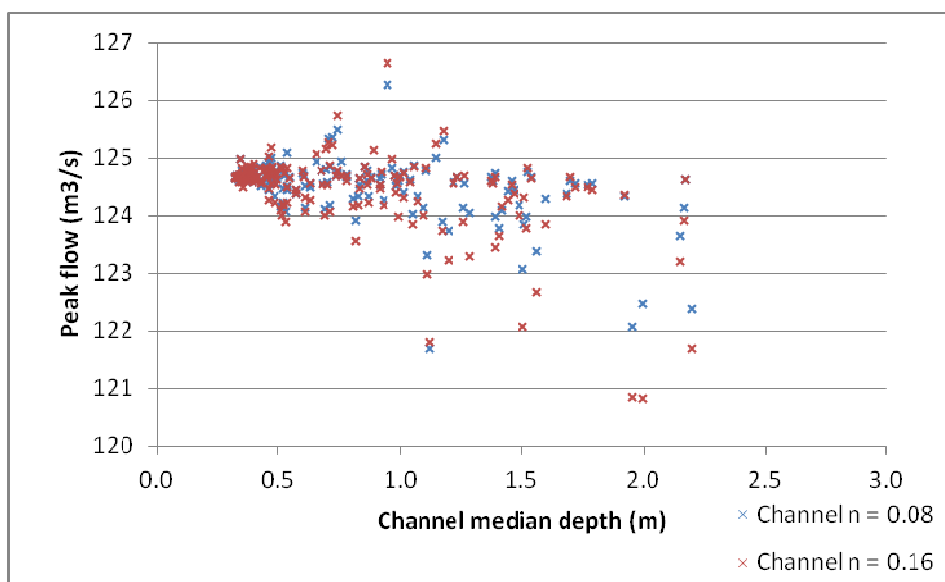
Figure 8.5. Channel median depth of 199 reaches against downstream peak flow. Each point represents the width of one reach and the downstream peak flow when a CRIM is added to that reach. Two sets of values were used for the CRIMs; Set 1 (in red): Floodplain n 0.16, Channel n 0.14; Set 2 (in blue): Floodplain n 0.16, Channel n 0.08.
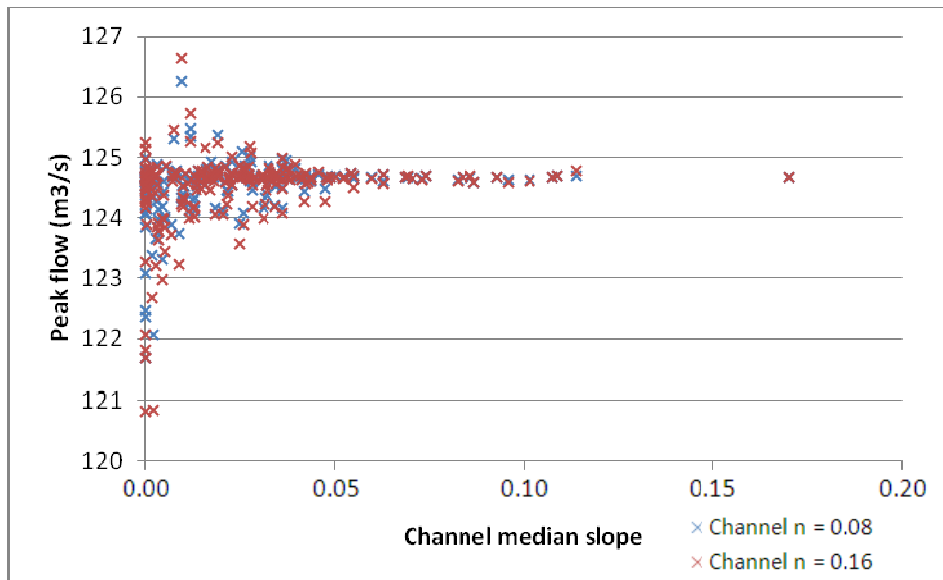
Figure 8.6. Channel median slope of 199 reaches against downstream peak flow. Each point represents the depth of one reach and the downstream peak flow when a CRIM is added to that reach. Two sets of values were used for the CRIMs; Set 1 (in red): Floodplain n 0.16, Channel n 0.14; Set 2 (in blue): Floodplain n 0.16, Channel n 0.08.
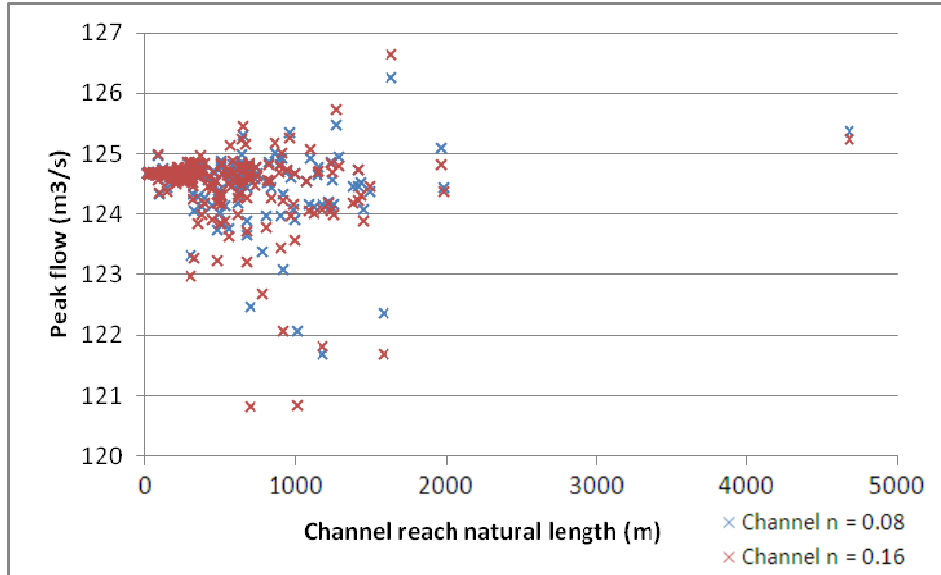
Figure 8.7. Channel reach natural length of 199 reaches against downstream peak flow. Each point represents the length of one reach and the downstream peak flow when a CRIM is added to that reach. Two sets of values were used for the CRIMs; Set 1 (in red): Floodplain n 0.16, Channel n 0.14; Set 2 (in blue): Floodplain n 0.16, Channel n 0.08.
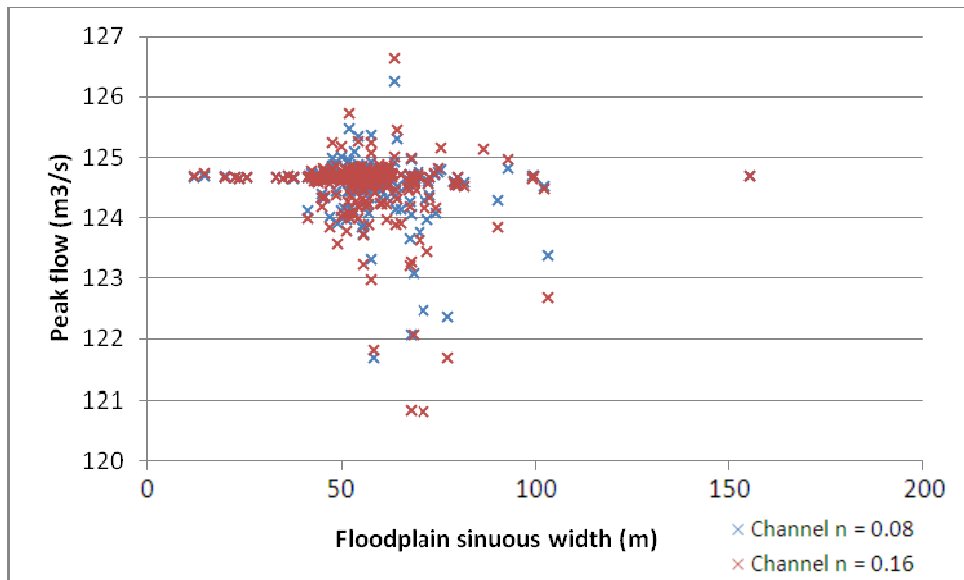
Figure 8.8. Floodplain width of 199 reaches against downstream peak flow. Each point represents the width of one reach and the downstream peak flow when a CRIM is added to that reach. Two sets of values were used for the CRIMs; Set 1 (in red): Floodplain n 0.16, Channel n 0.14; Set 2 (in blue): Floodplain n 0.16, Channel n 0.08.
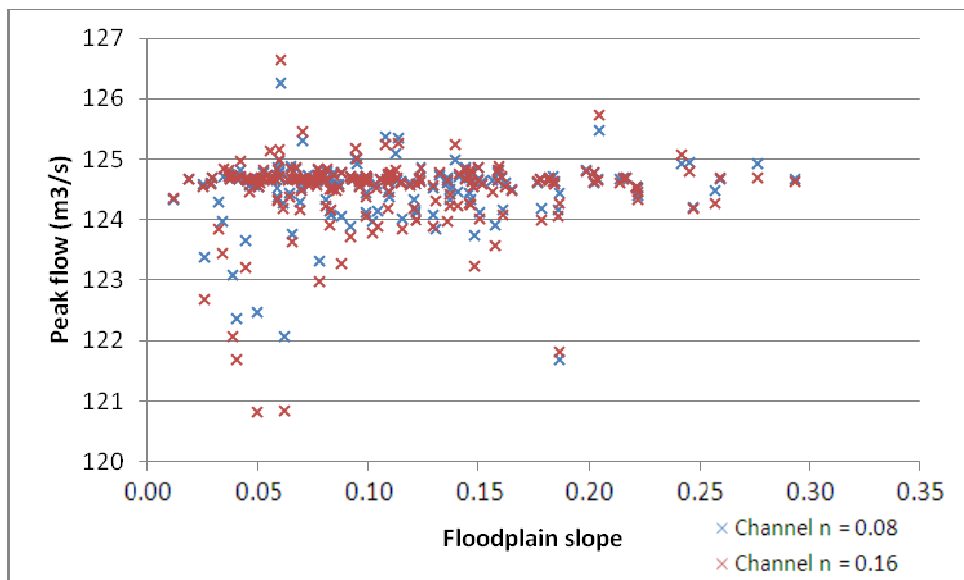
Figure 8.9. Floodplain slope of 199 reaches against downstream peak flow. Each point represents the slope of one reach and the downstream peak flow when a CRIM is added to that reach. Two sets of values were used for the CRIMs; Set 1 (in red): Floodplain n 0.16, Channel n 0.14; Set 2 (in blue): Floodplain n 0.16, Channel n 0.08.
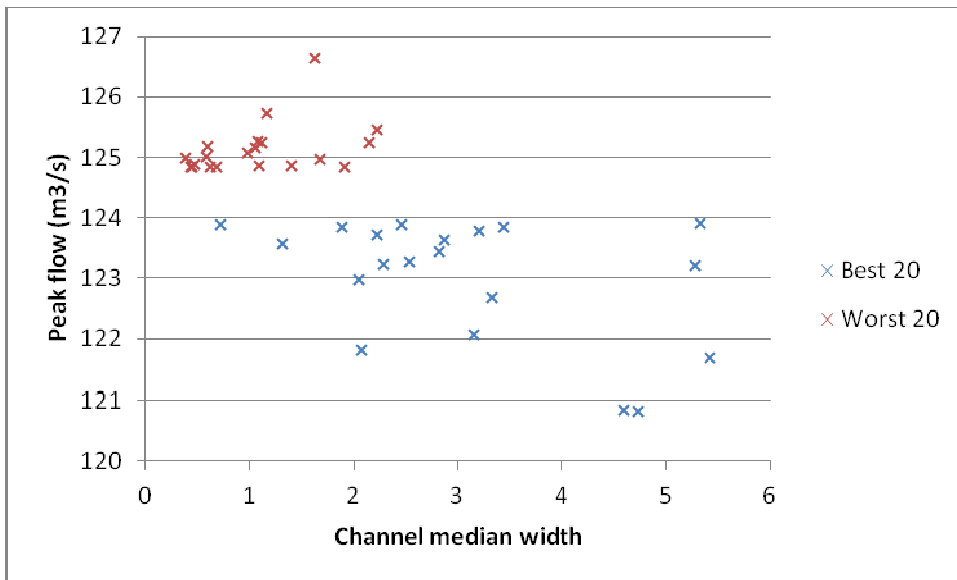
Figure 8.10. Median channel width of 20 best and worst reaches in terms of effect on downstream peak flow when a CRIM is added. Each point represents the width of one reach and the downstream peak flow when a CRIM is added to that reach.
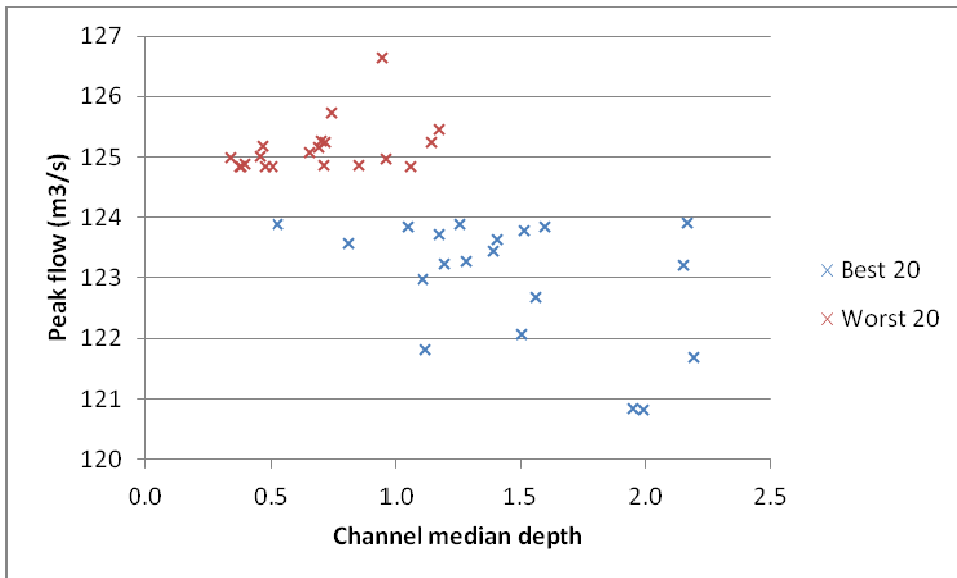
Figure 8.11. Median channel depth of 20 best and worst reaches in terms of effect on downstream peak flow when a CRIM is added. Each point represents the width of one reach and the downstream peak flow when a CRIM is added to that reach.
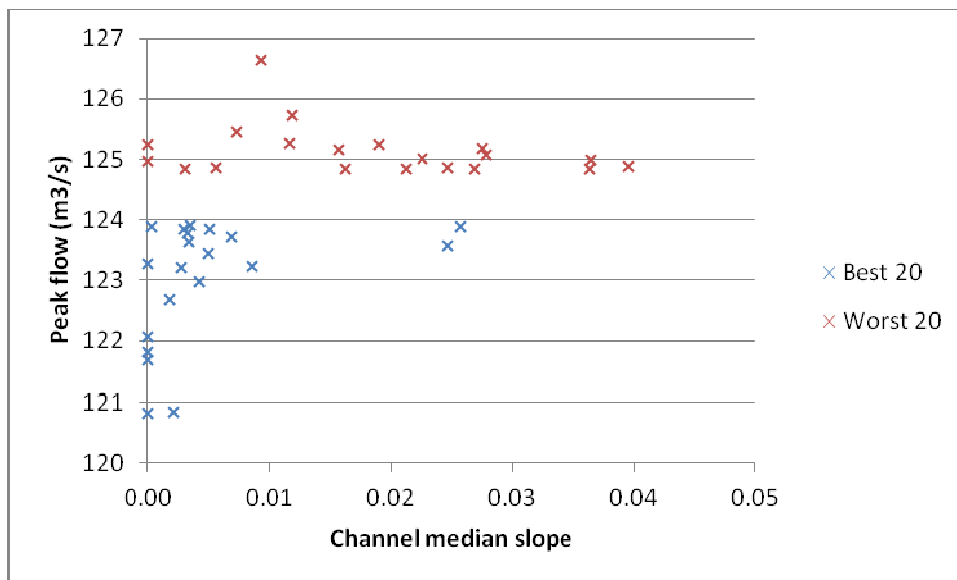
Figure 8.12. Median channel slope of 20 best and worst reaches in terms of effect on downstream peak flow when a CRIM is added. Each point represents the width of one reach and the downstream peak flow when a CRIM is added to that reach.
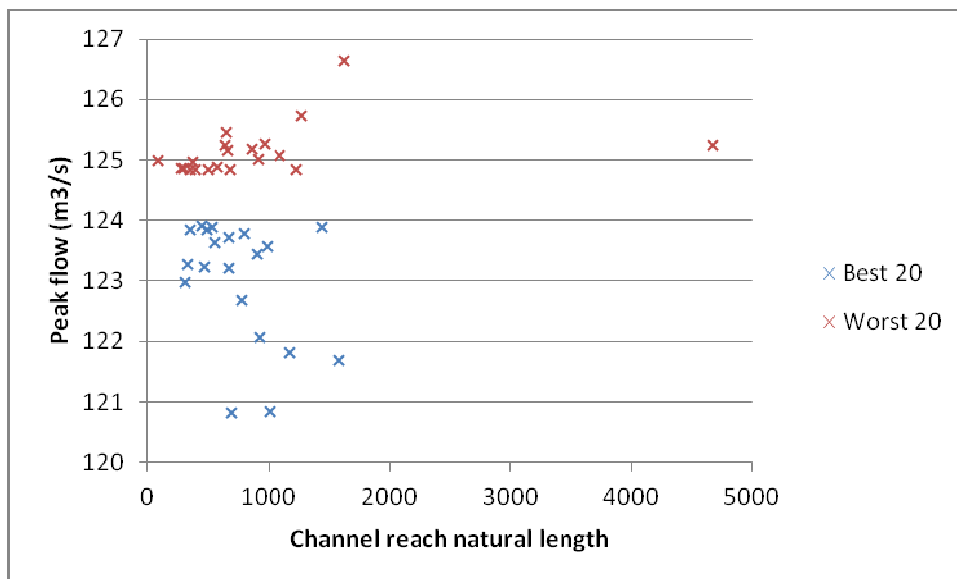
Figure 8.13. Natural channel length of 20 best and worst reaches in terms of effect on downstream peak flow when a CRIM is added. Each point represents the width of one reach and the downstream peak flow when a CRIM is added to that reach.
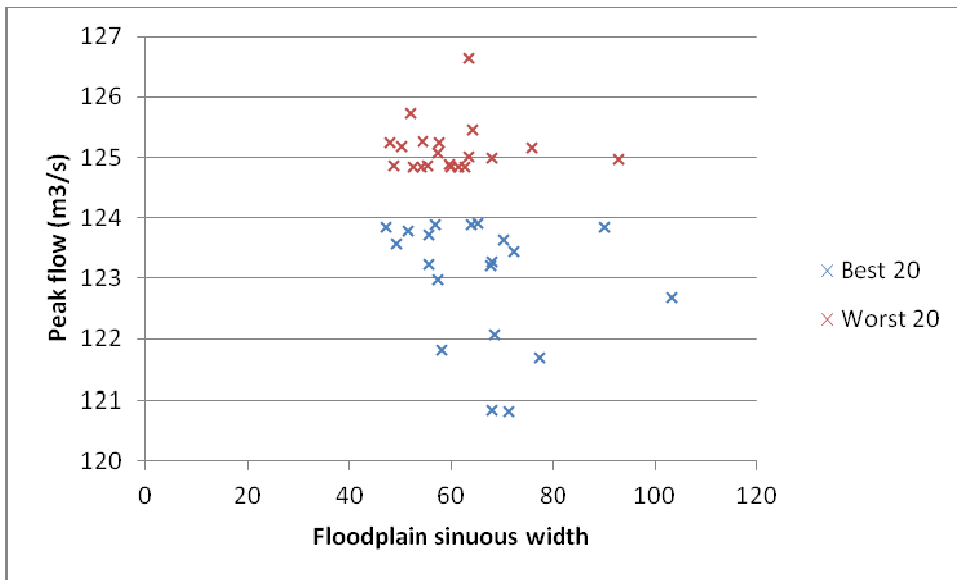
Figure 8.14. Floodplain sinuous width of 20 best and worst reaches in terms of effect on downstream peak flow when a CRIM is added. Each point represents the width of one reach and the downstream peak flow when a CRIM is added to that reach.
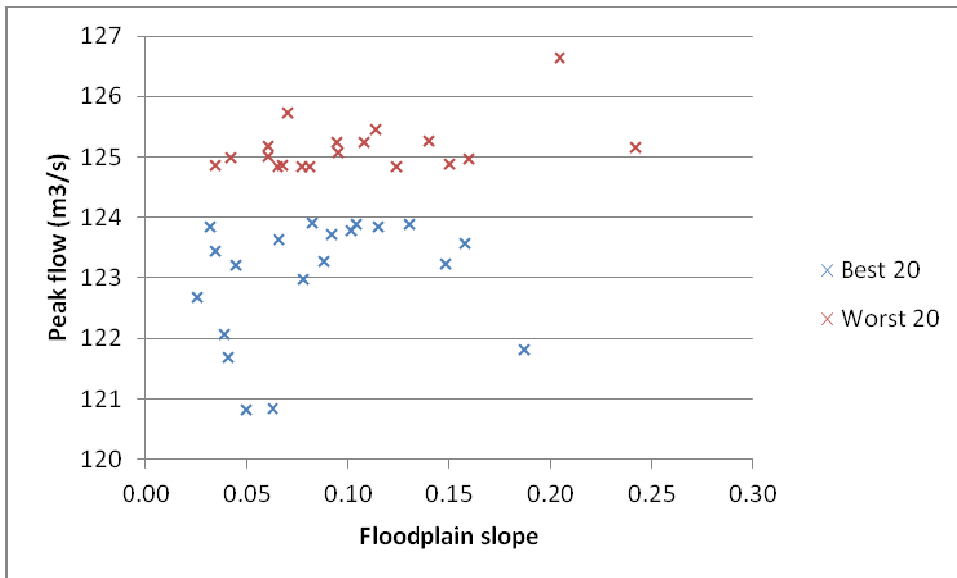
Figure 8.15. Floodplain slope of 20 best and worst reaches in terms of effect on downstream peak flow when a CRIM is added. Each point represents the width of one reach and the downstream peak flow when a CRIM is added to that reach.

8.3   Discussion (1) – Impact of CRIMs in single reaches

8.3.1   Positive and negative impacts

For a large number of reaches in this study, the effect of increasing roughness (to simulate the adding of a CRIM) has the effect of reducing downstream peak flow. By increasing Manning's n along a channel reach, channel conveyance is reduced due to the increased resistance to flow (Knighton 1998; Järvelä 2002). This increase in roughness simulates the adding of woody debris into the channel network, which results in a less "hydraulically efficient" channel (Anderson et al. 2006). Dudley et al. (1998) and Rhee et al. (2008) stated that discharge capacity and flood risk are directly linked to increases in flow resistance. The Manning's equation shows this;

$$v = \frac{Q}{wd} = \frac{1}{n} R^{2/3} S^{1/2} \qquad\qquad \text{eq. 8.1}$$

Where Q is the channel discharge, w is channel width, d is channel depth, v is the mean velocity, n is the Manning's roughness coefficient, R is hydraulic radius and S is slope of the water surface. The left hand side of the equation can be re-arranged to give

$$d = Q / wv \qquad\qquad\qquad \text{eq. 8.2}$$

Roughening the channel leads to a reduction in *v* for in-channel flows, so resulting in a greater *d* for a given *Q*. This greater *d* increases the likelihood of overbank flow and hence attenuation of *Q*: shallow overbank flow tends towards a low velocity due to the nature of the flow and the increased roughness of the floodplain. Such conditions "maximise attenuation" (Woltermade and Potter 1994: 1935).The planting of riparian vegetation further increases roughness (Thomas and Nisbet 2007; Tang and Knight 2009), in turn further delaying overbank flow. This leads to increased flood storage, a common result of which is to reduce and delay the peak flow leaving the reach (Nisbet and Thomas (2006).

If we interpret eq. 8.1, however, there are a number of contributing factors to the results shown in Table 8.1 and Figures 8.2-8.3. First, in relation to the reach scale, Wolff and Burges (1994) stated that in addition to hydraulic roughness, geometry influences effective storage of the reach and therefore the reduction in peak flow. Channel width and slope (Wolff and Burgess 1994), as well as floodplain width (Wolff and Burgess 1994; Woltermade and Potter 1994) have been found to influence peak flow.

Indeed, eq. 8.2 shows that the effects of reducing *v* on *d* will also depend upon *w*. Depth increases will be greater for channels of smaller width such that channels upstream will

impact upon peak flow reduction to a greater degree than those downstream. This has been well-established (e.g. Anderson *et al.*, 2006; Defra, 2006; Lane and Thorne, 2007).

But, second, the magnitude of discharge in channel segments upstream will be proportionately lower as compared to downstream and the effect of any intervention may itself be subject to attenuation. For instance, Ghavasieh et al. (2006) stated that in addition to factors reflecting the characteristics of reaches, the proximity of reach interventions to the focus area for flood mitigation is an important control on the success of such a strategy. Investigating the effect of roughened strips along a short section of floodplain (~4km), Ghavasieh et al. (2006) found that attenuation of the flood peak decreased rapidly downstream. Liu et al. (2004) found that the reduction in velocity as a result of river rehabilitation was not maintained downstream of the affected reaches. These observations are reflected in the individual CRIM simulation results as some CRIMs have only a marginal effect on the flow peak, even those not far upstream of Uckfield.

Third, there are some reaches where adding a CRIM has the effect of *increasing* peak flow upstream of Uckfield (negative sites). Although the number of negative sites was found to be lower than the number of positive sites, the number of negative sites was not insignificant. As discussed above, at the reach scale it might be expected that an increase in hydraulic roughness would decrease and delay the peak flow along the extent of all reaches in the Uck catchment. However, there is a key potential reason that an increase in roughness along these reaches does not reduce peak flow many kilometres downstream. At the catchment scale, the relative timing of flood waves can become an important factor in relation to downstream peak flow generation (Pattison et al. 2008). However it is important to note that the findings of this paper are based on a much larger catchment than the Uck; 2288km^2 as opposed to the 104km^2 of the Uck catchment (Figures 8.1 and 8.2).

8.3.2   Channel properties

Analysis of the relationship between reach properties and downstream peak flow when a CRIM is added highlights the potential influence of different contributing factors (Section 8.2.1.5). It can be seen that there is a trend towards the lowest downstream peak flows resulting from adding a CRIM to reaches of larger channel width. This is contrary to the behaviour expected based on eq. 8.2. Increases in depth as a result of a decrease in velocity are expected to be smaller in wider channels given a certain discharge. As discussed, greater increases in water depth increase the likelihood of overland flow, thus increasing the potential for storage. This may lead to a greater decrease in downstream peak flow. However, this does not appear to be the case. This may be explained by a number of factors.

First, only one of the 20 reaches where adding a CRIM has the largest effect on downstream flow, has a Strahler stream order number of 1. A large proportion of these reaches have a relatively high stream order. Therefore this suggests that whilst increases in depth would be lower in these reaches for constant Q, the magnitude of discharge will be proportionately larger (Knighton 1998).

Second, the effect of the addition of a CRIM will also be proportionately larger in a wider channel. A debris dam placed in a wider channel will have a greater influence on the downstream movement of water.

Finally whilst there is a trend whereby placing a CRIM in the widest channels has the greatest effect on peak flow downstream, it is not the absolute rule. This may be explained by their location in the catchment – i.e. wide channels of low order so lower Q.

A similar spatial pattern can be observed for the location of the deepest channels to that for the widest channels. The effect of CRIMs in these reaches is to have a greater effect in terms of increasing the likelihood of overbank flow in these reaches. Reconnecting the channel and floodplain will result in increased storage of flood waters, in turn impacting on downstream peak flow (Harman et al. 2002).

The significance of the length of the neutral sites is in their ability to store large enough magnitudes of water to have an effect on the downstream peak flow. As stated by Wolff and Burges (1994) the effective storage of a reach influences the reduction in peak flow. A short reach is less likely to have a large effective storage, though this is also influenced by reach geometry, for example floodplain width. This may explain the concentration of points at the lowest reach lengths on Figure 8.7. It can be seen that peak flow is lower when CRIMs are added to reaches with wider floodplains. This again relates to the effective storage of the floodplain (Wolff and Burges 1994).

Importantly it can be seen that CRIMs have little impact when placed in reaches with a steeper floodplain, and particularly channel slope. This is thought to be due to higher in-stream and overbank flow velocities (Knighton 1998; eq. 8.2).

With such large increases in roughness values for the channel and floodplain (an increase in channel and floodplain roughness of 400% and 267% from default values), channel and floodplain geometry would be expected to become proportionately less important (eq. 8.1). However it can be seen that geometry still has a conditioning effect on the relationship between placing of CRIMs and downstream peak flow. Analysis of the contrasting impact of different roughness values for CRIMs suggests that the different roughness has a conditioning effect on the response to reach geometry. Downstream peak discharge change is more sensitive to channel and floodplain properties when channel roughness is set at a Manning's value of 0.16, as opposed to 0.08, though this trend is not systematic.

Whilst trends have been identified, it is thought that a relatively low percentage of explanation of variability in CRIM success is attributable to local factors.

8.3.3   Timing of flood waves

It was noted above that increased roughness is expected to increase flood storage at the reach scale, conditioned by the local geometry of the channel and floodplain. However analysis of reach properties does not explain the presence of reaches where the addition of a CRIM increases downstream peak flow. This suggests that the effects of relative timing of flood waves from tributaries are likely to be an important process affecting changes in peak discharge at the catchment scale. The flow velocity may be reduced, and overbank storage of flood water increased, at the reach scale. When the spatial scale is broadened to the scale of the tributary, the increase in flood storage, or simply a decrease in in-channel velocity will delay the delivery of flood water to a downstream confluence. At the catchment scale, an increase in flow peak at a given downstream point can occur if flood waves from two of more tributaries arrive concurrently due to a delaying of the flood wave from a tributary. Such catchment flood response behaviour can be seen in a number of studies. Turner-Gillespie et al. (2003), employing a distributed hydrologic and 2-D hydrodynamic model in their study of a ~10km reach in the USA, found that increasing the delay in flood wave delivery in tributaries feeding into the reach increased flood peaks at the downstream gauge. Similarly, Saghafian and Khosroshani (2005: 274) found that "hydrograph synchronization" as a result of flood control measures was a very important factor. These studies show the potential impact of varying flood response times in tributaries and suggest a potential explanation for the 'negative' effects on downstream peak flow of introducing a CRIM to a reach. The spatial location of positive, negative and neutral sites may partly explain the above results, and will be discussed next.

The previous discussion suggests the relative timing of flood waves as a possible hypothesis for the presence of reaches where an increase in hydraulic roughness has a negative effect (i.e. an increase) on downstream peak flood. Figure 8.2 starts to highlight the specific pattern of reaches throughout the Uck catchment where this may be the case.

The presence of a large number of negative sites in tributaries flowing into the Uck upstream of Uckfield (Lephams Bridge and Framfield Streams) may be due to the delaying effect of CRIMs on the flood wave, as discussed previously. Without the presence of a CRIM, the flood wave from tributaries proximal to the main channel just upstream of Uckfield may arrive before those from more peripheral tributaries due to the slightly increased travel distance of the latter.

However if the arrival of the flood wave is delayed due to local scale flooding as a result of adding a CRIM along a reach section, it may coincide with the flood wave of other more distal tributaries. This would have the effect of increasing the peak flow during a flood event. It is important to note that this hypothesis relies on the assumption that because a flood wave has further to travel to Uckfield it will arrive later. This relies on a great simplification which excludes processes at the reach and tributary scale which affect the conveyance of the flood wave and assumes they have no impact. In addition to this it can be seen that negative sites are not limited to reaches relatively proximal to Uckfield, but indeed can be observed throughout the catchment (figure 8.2). Tickeridge stream contains a large number of positive reaches as well as negative sites. Its confluence with the Uck is a very short distance upstream from another confluence with largely negative sites. This suggests that the above assumptions may be slightly flawed in this case.

As noted in the report on the 2000 flood event (Environment Agency 2001), the tributaries draining into the Uck upstream of Uckfield are of similar length, and the catchment roughly circular. This means that peak flows from the tributaries often arrive at Uckfield concurrently. This also reduces confidence in the explanation presented above explaining the large number of negative sites in tributaries flowing into the Uck just upstream of Uckfield.

Whilst it is likely that the pattern of results observed is due in part to the effects of relative timing of tributary hydrographs, it can be seen that the spatial pattern is complex. Following this discussion it is clear that an explicit identification of the timing of the flood wave from each tributary would provide further insight into the effects on downstream peak flow of adding CRIMs to reaches, either one at a time, or in combination (as discussed below).

8.3.4   Positive reaches

As discussed, just upstream of the confluence of the Uck and Tickeridge Stream, along the channel of the River Uck are sites with the largest positive effect (Figure 8.3). The point upstream of the Tickeridge-Uck confluence can be qualitatively assigned as the 'upper section' of the catchment. This qualitative discretization can have a beneficial illustrative use. It can be observed that a delay in the flood wave from this upper section would have a potentially highly beneficial effect on the downstream peak flow. An increase in the travel time of the flood wave from this 'upper section' could have the effect of further increasing the time between the arrival at Uckfield of the flood peaks of tributaries in the lower half and upper half of the catchment. As noted above, the roughly circular characteristic of the Uck catchment results in peak flows from tributaries often arriving downstream concurrently (Environment Agency 2001). A delay in arrival of peak flows from this 'upper section' would therefore be beneficial.

Discharge will be relatively large in the main channel, which also potentially explains the greater impact of the placement of a CRIM.

8.3.5   Summary

The analysis above suggests that to judge the effects of a CRIM, it is necessary to consider where the CRIM is located in the catchment with respect to attenuation effects, and flood wave interaction, at the catchment scale as well as the local conditioning effects associated with the particular CRIM location i.e. the channel and floodplain geometry.

8.4   Results (2) Impact of CRIMs in combination

8.4.1   Flow peak impacts

Figure 8.16 shows the effects of simulating the addition of CRIMs to several reaches at the same time on the flow peak just upstream of Uckfield. As stated previously, the simulated peak discharge just upstream of Uckfield is 124.7 cumecs when all parameters are at their default values, the 'base case'. Adding CRIMs to all positive reaches (i.e. the best 100) in combination throughout the catchment reduces flow peak by over 12 cumecs, after which the impact of adding more CRIMs is relatively insignificant. Points in blue indicate reaches which, when added in combination had a negative effect on the cumulative flow reduction.

Figure 8.17 compares the effect on downstream peak flow of adding a CRIM to a particular reach in isolation and in combination, with CRIMs along other reaches. It can be observed that for all reaches, the adding of a CRIM has a smaller effect on peak flow when CRIMs are also placed in other reaches throughout the catchment than when a CRIM is placed on its own. When the *individual* effects of the 100 CRIMs are cumulated, the result is a reduction in peak flow of 52.6 cumecs. In combination, *including* the effect of negative reaches, the 100 CRIMs have a cumulative effect of 7.5 cumecs. It is noted that due to the inclusion of the rejected reaches, the figure is lower than when only positive reaches (in combination) are included, as stated above. However, beyond the trend of reduced impact in combination, no clear overall trend can be identified. The effect of a CRIM added in combination cannot be predicted by its effect in isolation (Figure 8.17). Both Figures 8.16 and 8.17 show that adding a CRIM to a number of reaches has an adverse effect on the cumulative peak flow reduction.

48 of the 100 reaches initially classed as positive were rejected when used in combination as each of these reaches had a negative effect on the cumulative peak flow reduction when a CRIM was added along its extent in rank order of individual CRIM performance. Adding CRIMs to 52 reaches in combination resulted in a reduction in the flow

peak at Uckfield of 12.5 cumecs, reducing peak flow to 112.2 cumecs. This will in future be referred to as the 'intervention case'. This equates to a decrease in peak flow of 10.0%. Figure 8.18 shows the spatial distribution of the reaches and Appendix D shows the full table of results and provides further detail as to why each reach was excluded. The implication of these results is that, in combination, 48 of the reaches previously deemed as having a positive impact in terms of reduction of the peak discharge, now have a negative effect on peak reduction.
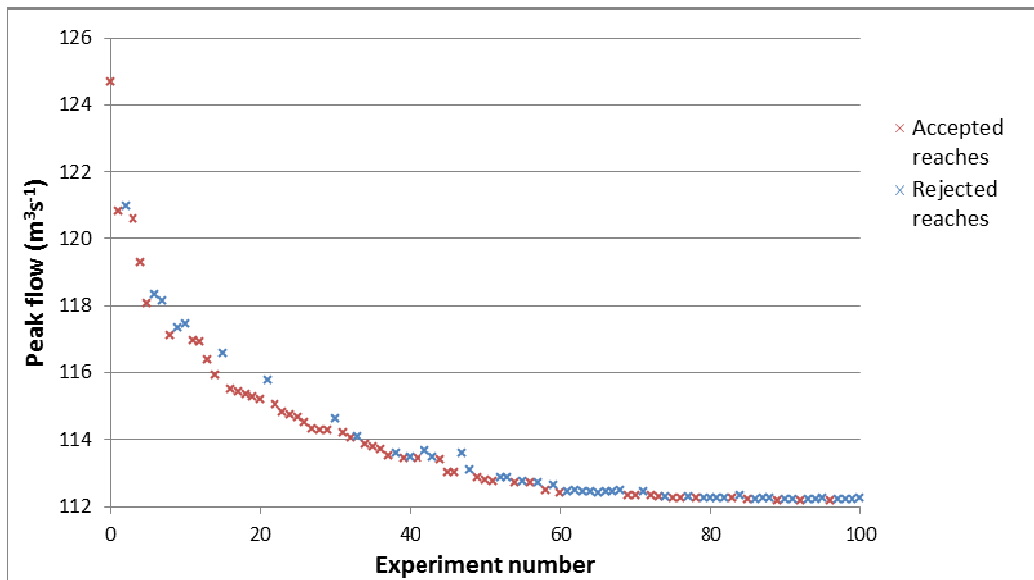
Figure 8.16. A scatter plot showing the cumulative effect on the flood peak just upstream of Uckfield of adding CRIMs to numerous reaches throughout the catchment. Experiment number also relates to the ranking of positive reaches so that the point at 1 on the x axis shows flow peak after adding a CRIM to the reach with the largest effect on the flow peak. Point 2 shows the effect of combining CRIMs at the 2 reaches with the largest effect. Points in blue indicate a decrease in cumulative downstream peak flow reduction; these reaches were rejected.
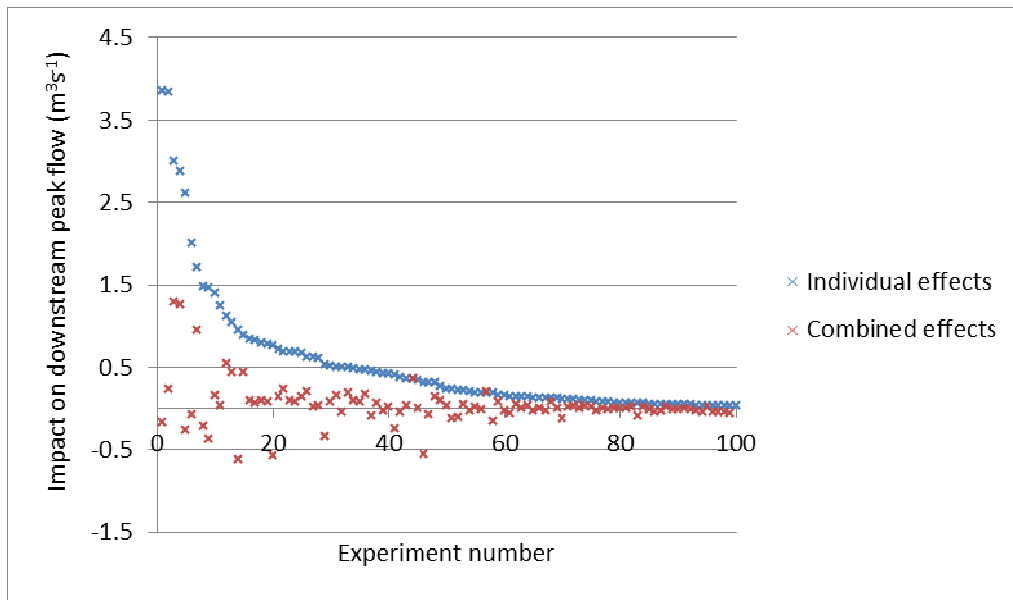
Figure 8.17a. A comparison of the effect of adding a CRIM to a reach in isolation and in combination. Adding a CRIM to a particular reach may have a positive effect on downstream peak flow reduction when added in isolation. However, in combination with CRIMs in other reaches, it may have a reduced positive or even negative effect.
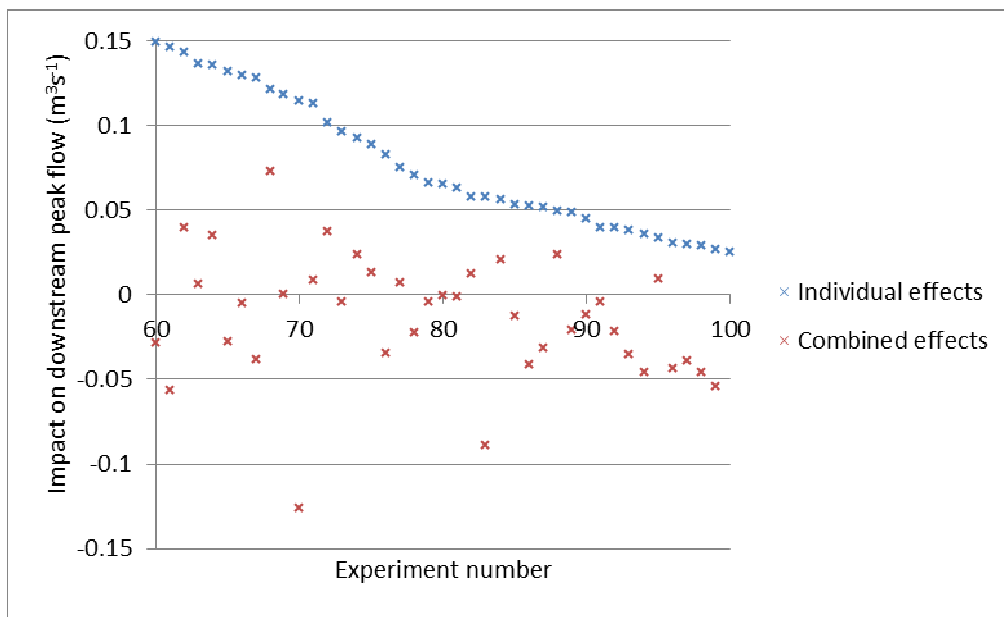
Figure 8.17b. A replica of Figure 17a, but focused on reaches 60-100 in the intervention list
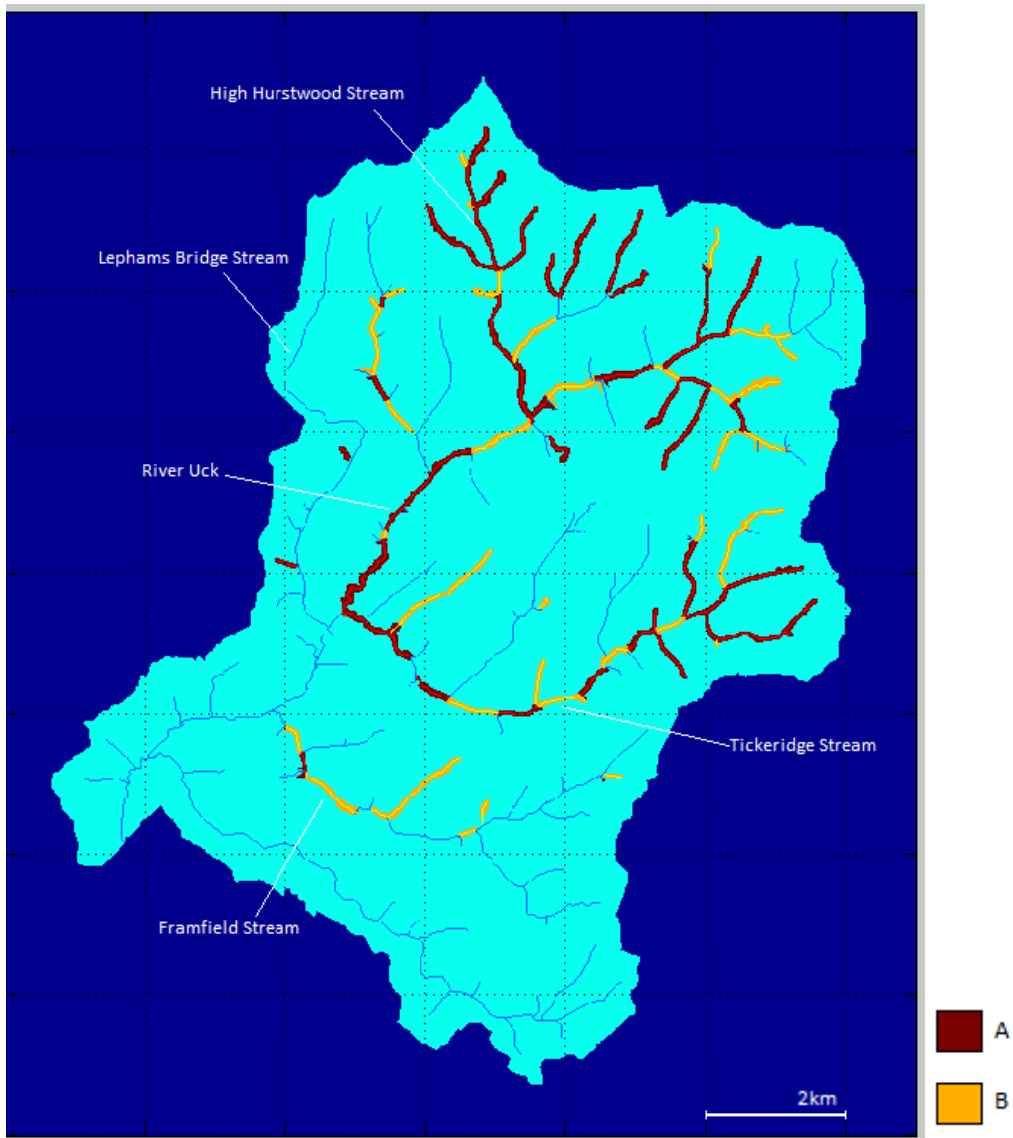
Figure 8.18. The spatial distribution of reaches where the simulation of a CRIM has a positive and negative effect on downstream peak flow when added in combination. A – positive reaches. B – negative reaches; when a CRIM was added to this reach in combination the reduction of downstream peak flow was reduced.
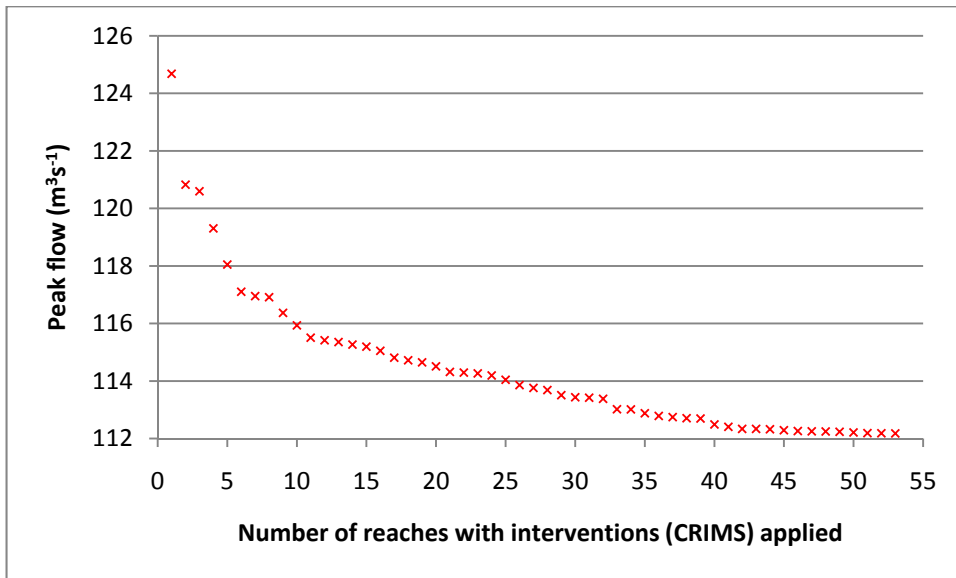
Figure 8.19 Cumulative effect on the flood peak at Uckfield, with data points from rejected reaches excluded. This shows the reduced positive impact of increasing the number of reaches with CRIMs simulated. The x-axis shows the number of reaches where a CRIM has been applied. Just over half of the 100 'positive' reaches are included.

Figure 8.19 shows the cumulative effect on peak flow of only those reaches which had a positive cumulative effect. As the number of reaches with interventions increase, the cumulative effect on the peak flow downstream can be observed. Initially a small number of CRIMs has a relatively large effect on the peak flow. Over 50% of the total peak flow reduction occurs when CRIMs are applied to only 4 reaches. The remaining reduction in peak flow occurs as a result of adding CRIMs to 48 more reaches. Over 80% of the peak flow reduction is accounted for by adding CRIMs to 18 reaches. This behaviour is indicated by the slow levelling out of the data points in Figure 8.19.

   A ratio of number of reaches with interventions applied : effect on peak flow (cumecs (m^3s^{-1})) can yield further information (Table 8.2).

Table 8.2. A table showing the reduction of peak flow when CRIMs are added to 4, 18 and 52 reaches. The ratio of number of CRIMs to reduction in peak flow is also shown.

No. CRIMs applied	Cumulative effect (reduction in peak flow, cumecs (2d.p.)	Ratio number CRIMs : peak flow reduction
4	6.63	1:1.66
18	10.04	1:0.56
52	12.50	1:0.24

When 4 CRIMs are simulated, each CRIM reduces downstream peak flow by an average of 1.66 cumecs. This average reduces to 0.56 cumecs when 18 CRIMs are simulated and finally 0.24 cumecs when 52 CRIMs are simulated.

It can also be seen that the cumulative peak flow reduction does not show a smooth curve, as is observed when the effect of the CRIMs when applied one at a time, is summed (Figure 8.20). In addition to this, Figure 8.20 also shows that the cumulative reduction in peak flow is much less than the sum of the effects of adding CRIMs to single reaches at a time.

It can be seen that there is a much larger proportion of reaches which do not have a positive effect on the cumulative peak flow reduction in experiment 51-100 as opposed to 1-50 (Figure 8.16). Of the first 50 reaches 17 are rejected, as opposed to 35 of the last 50.
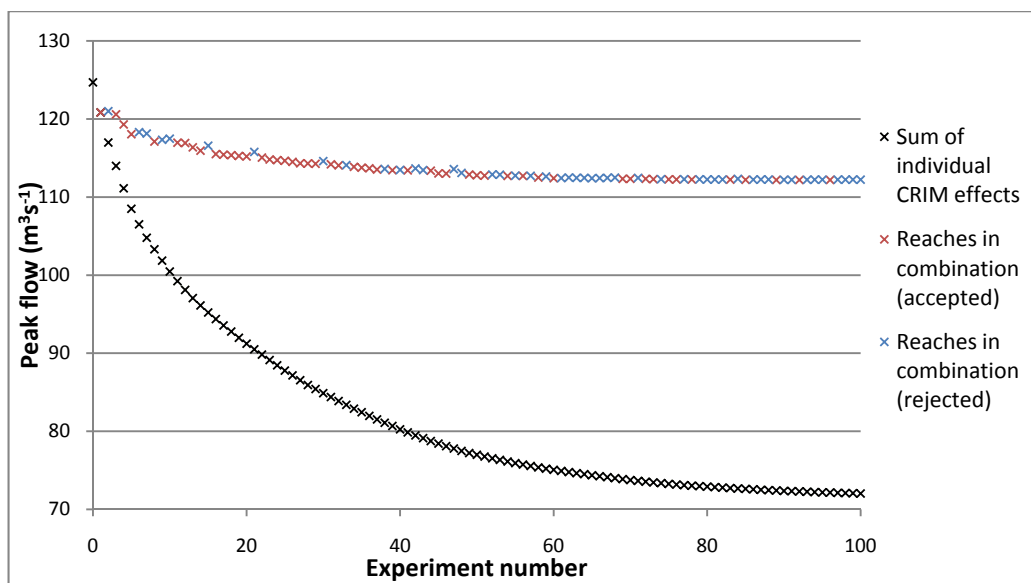
Figure 8.20. The cumulative peak flow reduction curve produced with accepted CRIMs in red and rejected CRIMs in blue compared to the curve produced by summing the individual effect of all 100 'positive reaches'

8.4.2   Downstream peak flow timing

Whilst adding CRIMs throughout the catchment resulted in a decrease in peak flow from 124.7 cumecs to 112.2 cumecs, an unexpected characteristic is the lack of a delay in peak flow at the location just upstream of Uckfield (Figure 8.21). Indeed, instead of a delay, the flow peak occurred 2 hours earlier when CRIMs were added throughout the catchment, compared to the base case. It is possible to identify a delay of 2 and 1 hours for the 1st and 2nd smaller peaks respectively and indeed a slight reduction in peak flow for both peaks preceding the major flood event. More significantly, it is possible to observe a delay in the rising limb of the intervention case. This delay is approximately 1 hour when discharge is approaching 100

cumecs; this is where an inflection can be observed in the rising limb of the base case hydrograph.
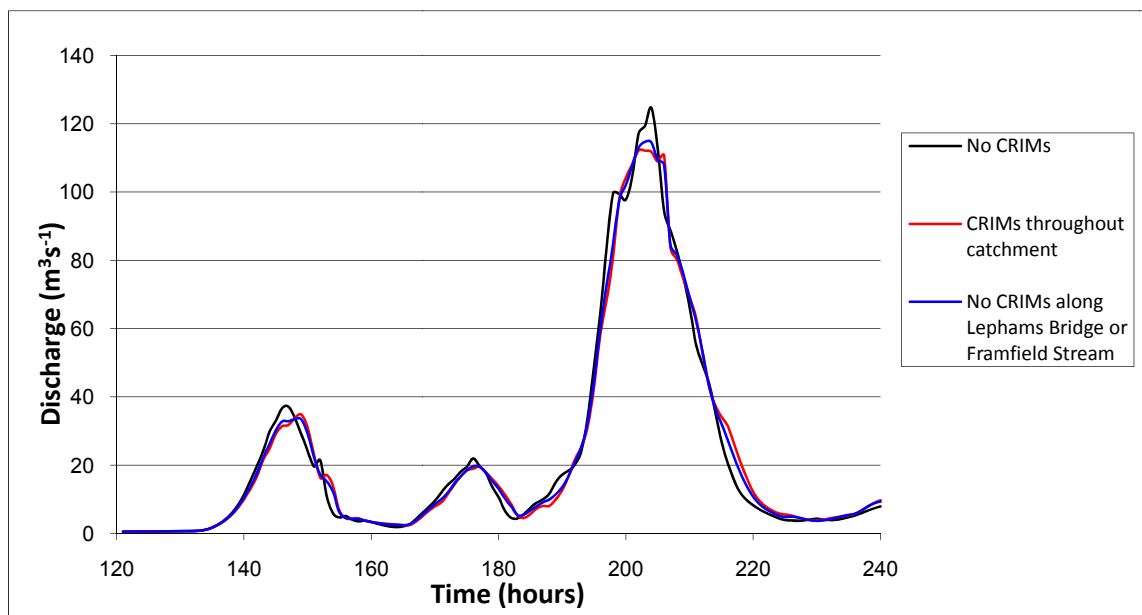
Figure 8.21a. A comparison of the hydrographs simulated just upstream of Uckfield when no CRIMs are introduced (the base case) and when 52 CRIMs are simulated throughout the catchment.
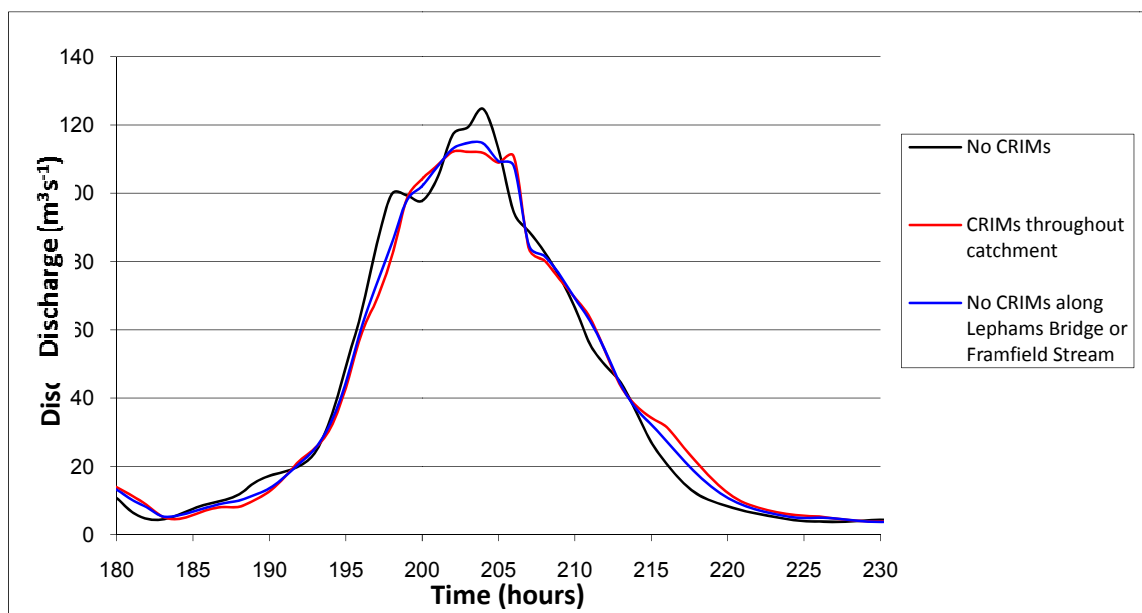
Figure 8.21b. A replica of figure 21a, but focused on the largest flow peak between 60 and 110 hours

Following this inflection, the base case shows a lag for a short period. The effect of the introduction of interventions is to create a relatively flat peak in comparison to the base case. The peak flow in the intervention case occurs 2 hours before the peak flow for the base case. A

clear signal for the falling limb of the main peak is less clear until discharge is below 40 cumecs, then a clear delay is observed for the intervention case. The peak flow is maintained at approximately the same level for longer in the intervention hydrograph (Figure 8.21).

To further analyse the effect of the spatial distribution of CRIMs on the hydrograph, CRIMs located in the two most downstream tributaries were removed from the intervention case. 32 CRIMs were applied, as opposed to the 52 in the intervention case. Due to the reduced number of CRIMs, downstream peak flow was 114.7 cumecs, approximately 2.5 cumecs greater than when 52 CRIMs are applied. However, peak flow occurred 1 hour earlier than that for the base case hydrograph, 1 hour later than when CRIMs were also applied in the two most downstream tributaries.

8.5   Discussion (2) Impact of CRIMs in combination

8.5.1   Flow peak effects

Previous discussion of the effects of adding a CRIM to a particular reach was in reference to the effects of adding an intervention to a *single* reach at any one time. The results presented above give an indication of the behaviour of the flood peak when CRIMs are added to numerous sites at the same time. The effects of increasing channel and floodplain roughness represents a considerable reduction in peak flow, though this is a result of placing a large number of CRIMs throughout the catchment. Nonetheless this does suggest a significant potential for storage of flood water in the headwaters and other reaches upstream of Uckfield as a means of reducing downstream peak flow. It is possible also to observe that there is a limit to the number of interventions throughout the catchment before the additional effects become relatively insignificant in comparison to the peak flow. It can be seen that adding CRIMs to a relatively small number of reaches results in a comparatively large attenuating effect on the downstream flood peak, whilst it can be observed that the reduction of flow peak shows a levelling off after >50 CRIMs have been applied. However the results suggest that the effectiveness of additional CRIMs reaches a low level before this, with implications for any decision making by stakeholders and authorities. Due to the large impact of adding CRIMs to the most favourable sites it is likely to be important to identify a balance between the reduction in peak flow and the number of reaches in which it is practical to intervene. This can be viewed in terms of time/cost effectiveness. For this purpose the observation of the effects of the most effective 4, or even 18 reaches is deemed useful. It can be clearly seen that the most efficient results in terms of peak flow reduction per CRIM added are observed when a small number of CRIMs are added. This efficiency decreases as the number of reaches introduced to the catchment increases. However, if an intervention scheme were based

entirely on this, only one CRIM would be added. To achieve the greatest reduction in downstream peak flow a much larger number of CRIMs must be added to reaches. This highlights the trade-off that may exist if the decision was made to add CRIMs or other similar interventions to the catchment.

Figure 8.20 shows the difference between the cumulative peak flow reduction when CRIMs are added in combination and the sum of the effects of adding CRIMs to these reaches one at a time. These results are not unexpected. Wolff and Burges (1994) and Anderson et al. (2006) found that attenuation increased downstream along a reach of several tens of kilometres when hydraulic roughness was increased all the way along the reach. It can be seen that for a number of areas adding CRIMs to consecutive reaches has a positive effect (Figure 8.18). However there is little possibility of the effects being the same as the sum of their effects when a CRIM is added one at a time as the influence on flow of adding a CRIM upstream will affect the influence of the downstream CRIM.

It is clear that important interaction effects have to be considered when adding interventions to a catchment. The spatial distribution of reaches *in combination* and the impact on downstream peak flow must be analysed. Figure 8.18 shows that the behaviour of the flood hydrograph downstream as a consequence of adding a CRIM to a reach is dependent on its location in the catchment and also the location of other interventions throughout the catchment.

8.5.2 Downstream peak flow timing

Whilst the key focus of the analysis in this chapter was on the effect of CRIMs on downstream peak flow, analysis of the peak flow timing is important in providing more information on the nature of the effects of CRIMs as well as the nature of the model itself. It is also of worth to note the benefits of peak flow delay in terms of flood warning times (Thomas and Nisbet 2007). The arrival of peak discharge two hours earlier as a result of the placement of CRIMs throughout the catchment is perhaps unexpected. Indeed based on the relevant literature it would be expected that the effect of increasing storage of flood water on upstream floodplains would be to delay the arrival of the flood peak a number of kilometres downstream (Liu et al. 2004; Ghavasieh et al. 2006; Thomas and Nisbet 2007). The local effects of increasing channel and floodplain roughness have been discussed, in reference to findings from relevant modelling studies (Wolff and Burgess 1994; Liu et al. 2004; Anderson et al. 2006). Ghavasieh et al. (2006) stated that whilst attenuation decreased rapidly downstream of roughened floodplain strips, the delay in the flood peak was maintained, or even increased with distance downstream of the intervention. There are two potential causes for the lack of a peak flow delay upstream of Uckfield.

8.5.3 Interaction between flood waves

As discussed previously, if flood waves from tributaries are altered to arrive concurrently this can have a negative effect on the downstream hydrograph in relation to peak flow (Turner-Gillespie et al. 2003; Saghafian and Khosroshani 2005). The same processes may also alter the time of peak flow occurrence. It can be seen from Section 8.4.2 that applying CRIMs throughout the catchment, excluding the two most downstream tributaries, affected the peak flow magnitude and timing. The peak flow magnitude is not reduced as greatly as when 52 CRIMs are applied, though peak flow occurred 1 hour later. This indicates that the interaction of the flood waves is important in relation to flood peak timing.

8.5.3 Uncertainty associated with simulated flood peak

The nature of the simulated hydrograph for the base case (no interventions) was discussed qualitatively previously (Chapter 7). A dip in the discharge along the rising limb occurs. This characteristic is not expected of the hydrograph and has the effect of delaying the peak discharge. This delaying of peak discharge due to a potential inaccuracy in the model could also, at least in part, explain the apparent lack of a delay in arrival of flood peak upstream of Uckfield when CRIMs are simulated throughout the catchment.

As discussed above, increased storage of flood water on upstream floodplains is expected to result in a delay in peak flow downstream. Evidence of a delay throughout the intervention case hydrograph (Figure 8.21) suggests that the lack of a timing delay in the peak flow is largely due to the effect of the inflection in the rising limb of the final flood peak of the simulated base case hydrograph. This highlights a source of uncertainty in the interpretation of results, whilst it is important to consider the objective function statistics suggesting that the model is a good representation of the 2000 flood event. It is likely that the nature of the simulated hydrograph and interaction of the flood waves both contribute to the occurrence of the flow peak 2 hours earlier when CRIMs are added throughout the catchment.

Finally it may be considered that the lack of a delay is partly due to the experiment methodology. When accepting and rejecting reaches in combination, no consideration was made for the effect on the occurrence time of the peak flow.

Thomas and Nisbet (2007) briefly stated that desynchronisation of flood waves from tributaries may result in longer duration flood events. Whilst the exact desynchronisation of the flood waves is not entirely clear, such an effect can be observed (Figure 8.21). The peak flow is maintained for longer for the intervention case, though the benefit in terms of peak flow magnitude reduction is clear. Due to the uncertainty associated with the simulated base case flood peak it is not possible to make any certain conclusions.

8.5.4 Uncertainty in selection of CRIMs

As discussed in Section 8.1.5, to explore the effects of CRIMs in multiple reaches, a CRIM was initially added to the reach where a CRIM had the greatest effect on downstream peak flow in isolation. A CRIM was then added to the reach where a CRIM had the next greatest impact in isolation. A reach was rejected if adding a CRIM negatively affected the cumulative peak flow reduction. However the 100 reaches classed as 'positive' may be altered if different roughness values are applied to represent the adding of a CRIM (in this study 0.16 and 0.14 for floodplain and channel respectively, based on previous work by Odoni and Lane (2010)).

Second, selection of different roughness values may also impact on the ranking of reaches based on the impact of adding a CRIM in isolation. If CRIMs were added to reaches in a different order, it is possible that different reaches would be rejected. For example, the first reach added will always be accepted, as its individual effect is already known.

The two points presented highlight the potential impact on the reaches classed as having a positive effect on peak flow reduction in combination. This highlights the importance on the study of the choice of default channel and floodplain roughness values. For example, in the following chapter, uncertainty analysis is carried out, varying channel and floodplain roughness in the 52 reaches classed a 'positive' in combination in this chapter (Figure 8.19).

8.6 Conclusion

Increasing channel and floodplain roughness (to simulate the adding of a CRIM) has an important and varied effect on downstream peak flow attenuation and delay. It can be seen that there are a large number of reaches throughout the catchment where increased roughness has a negative effect on the downstream peak flow. Simulating a CRIM along these reaches increases the peak flow downstream. It is suggested that modification of the relative flood wave timing is responsible for this behaviour. Whilst trends can be identified relating peak flow reduction to local factors associated with channel properties, a relatively low percentage of variability in CRIM success is attributable to local factors.

A reduction in downstream peak flow of 12.50 cumecs (10.0% of initial peak flow) is achieved when CRIMs are simulated in 52 reaches in combination throughout the Uck catchment. A clear levelling out of the cumulative peak flow reduction curve highlights the increasingly negligible effect of adding more CRIMs to reaches. This suggests a necessary decision to be made as to how many reaches require CRIMs before the cost of the CRIMs outweighs the flood peak reduction benefit.

It can be seen that the spatial pattern of reaches classed as positive, negative and neutral is complex. In addition to this, the effect of increased roughness in reaches varies when

modelled individually and in combination; 48 out of the 100 'positive reaches' identified from the screening process had a negative effect on downstream peak flow reduction when added in combination. The effect of a CRIM in combination cannot be predicted from its impact in isolation.

This highlights the complexity of diffuse flood mitigation schemes at the catchment scale, as well as the potential for the Overflow model to allow the investigation of this. The uncertainty associated with the results presented in this chapter will now be presented and discussed in the following chapter.

Chapter Nine   Catchment Riparian Intervention Measure (CRIM) uncertainty analysis

Chapter 8 detailed the results of an exploration of the effect on the downstream hydrograph of adding CRIMs throughout the Uck catchment. Adding CRIMs to 52 reaches led to a reduction in peak flow of 12.5 cumecs, from an initial peak of 124.7 cumecs. In this chapter an uncertainty analysis is carried out exploring the variation in downstream peak flow reduction as different roughness values are used for the 52 CRIM sites. First, the methodology used is shown (Section 9.1). The results are split into a statistical overview (9.2.1) followed by a more detailed analysis of model output against channel and floodplain roughness (9.2.2). The results are then discussed (9.3).

9.1   Methodology

The CRIMs to be used for the uncertainty analysis were set in the 52 reaches where CRIMs had a positive effect in combination (Figure 9.1). As the effect of varying CRIM properties was to be investigated; only floodplain and channel roughness along the reaches was altered. Uncertainty analysis was carried out with three sets of simulations varying floodplain and channel roughness along 20, 40 and all of the 52 reaches. This allows an analysis of the varying uncertainty as CRIMs are added to more reaches.

9.1.1   Range of parameter values

The parameter distribution was selected based on a reasonable minimum and maximum roughness associated with potential interventions, based on consultation of Chow (1959).

Channel Manning's n

0.08-0.15 (range, 0.07)

Floodplain Manning's n

0.01-0.2 (range, 0.1)

9.1.2   Sampling method

The sampling method was similar to that used in Chapter 6. A Monte-Carlo sampling method was followed, whereby the roughness of the channel and floodplain along the 52 reaches was randomly selected from the set parameter distribution, above. 1,500 simulations were run for each set of reach sites i.e. 1,500 simulations varying roughness in 20, 40 and 52 reaches. A total of 4,500 simulations were therefore run.
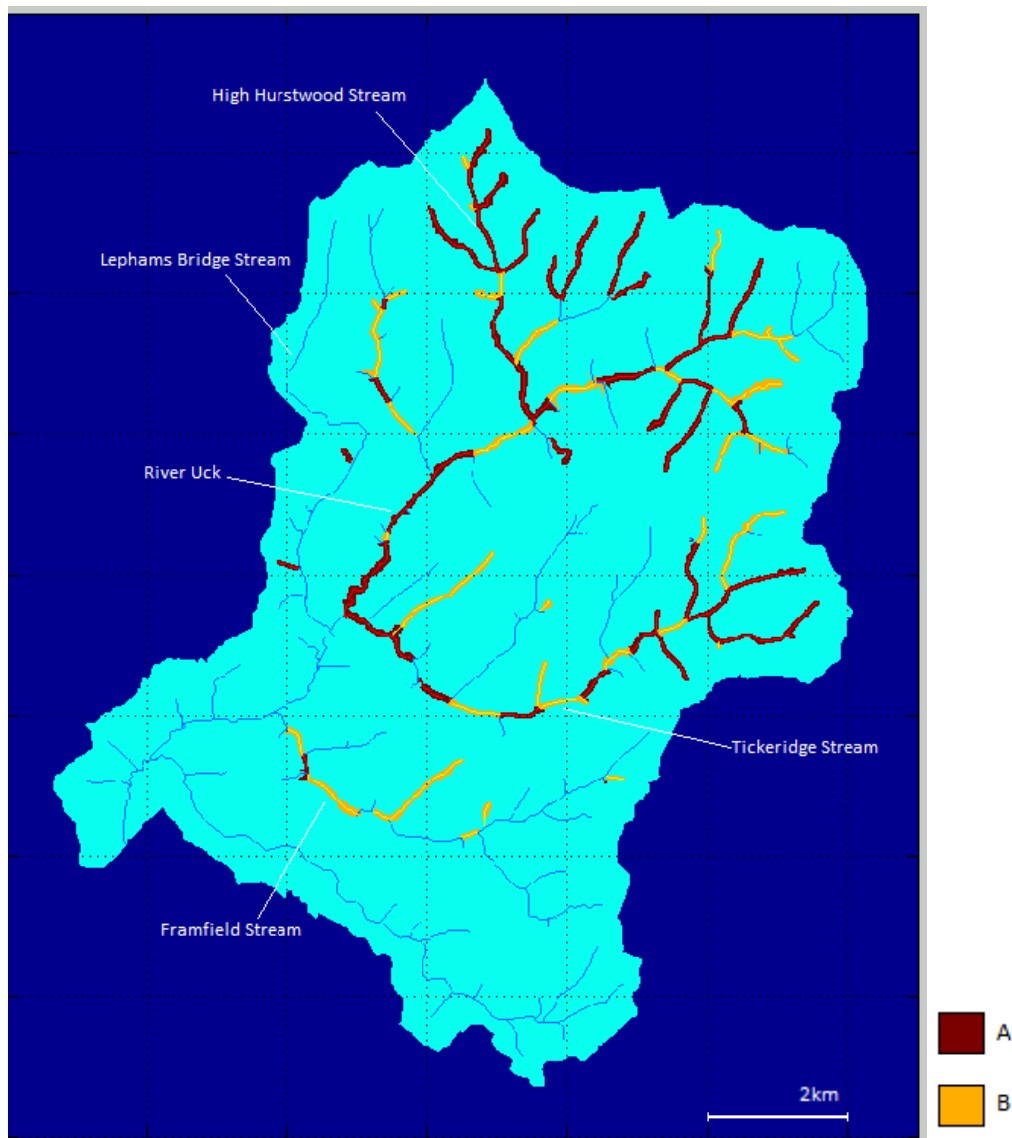
Figure 9.1. The spatial distribution of reaches where the simulation of a CRIM has a positive (A – in red) and negative (B – in orange) effect on downstream peak flow when added in combination. When a CRIM was added in combination to a positive reach, the cumulative peak flow was further reduced. The 52 'positive' reaches are used in the Uncertainty Analysis

9.1.3 Assessment

The uncertainty associated with the effects of CRIMs on downstream flood risk at Uckfield was to be assessed. Therefore the variation in discharge at Uckfield was analysed and subsequently could not be compared to observed discharge at Isfield. This meant that the use of objective functions was not appropriate as the simulated hydrograph could not be directly compared to the observed flood hydrograph during the 2000 event. Therefore the variation in peak discharge was the focus of this analysis, as in the previous chapter.

9.1.4   Dotty plots

Dotty plots similar to those produced in Chapter 6 were created, though only peak discharge was plotted. Each data point represents one model simulation.

9.2   Results

9.2.1   Statistical overview

Simulated peak discharge at Uckfield (Meadows) was 124.7 cumecs when roughness parameters were set at their default values (floodplain and channel n values 0.06 and 0.035). As discussed in Chapter 8, when added in combination, 52 reaches out of 100 had a 'positive' cumulative effect on downstream discharge. The peak discharge at Uckfield was reduced to 114.31, 112.41 and 112.18 cumecs when CRIMs (simulated by increasing floodplain and channel Manning's n to 0.16 and 0.14 respectively) were added to 20, 40 and 52 reaches (Table 9.1).

Here, the statistics are presented showing the effect of varying roughness values along reaches (Table 9.1). The median peak flow from 1,500 simulations decreases as the number of reaches with CRIMs is increased from 20 to 40 to 52**.** The mean peak flow is clearly lower when 40 and 52 CRIMs are simulated, though the mean when 40 CRIMs are added is 0.04 cumecs lower than when 52 CRIMs are added.

The minimum peak discharge (i.e. greatest reduction in peak flow) occurs when CRIMs are added to 52 reaches. The maximum peak flow (the model run where peak flow was reduced by the smallest amount) does not show any clear pattern. The standard deviation from the mean peak flow increases as roughness is varied in an increasing number of reaches.

9.2.2   Trends in uncertainty analysis

Plots of channel and floodplain roughness against downstream peak flow are presented (Figures 9.2-9.4).

Channel n

Simulated downstream peak discharge shows much less variation when channel n is at its highest values (above ~0.12 Manning's n), though when 40 and 52 CRIMs are added throughout the catchment, variation in peak discharge subsequently increases slightly when channel Manning's n values are increased above approximately 0.13 (Figures 9.3a and 9.4a). It can be observed that for all three sets of reaches (20, 40 and 52), there is a general trend of decreasing downstream peak flow as channel roughness increases. The lowest peak flows (greatest *reduction* in downstream peak flow) occurs when channel n values are highest, approximately between 0.13 and 0.15, though also when channel n values are ~0.10. Figure

9.5 highlights this trend by showing the channel roughness values randomly sampled for the 100 simulations where downstream peak flow was lowest. Channel roughness values are concentrated around 0.10 and 0.14-0.15. A key point, however, is that when channel roughness is around 0.10, results are dependent on other parameters, namely floodplain n.

Of note is that the spread of peak flow values is much lower when channel n values are highest (as mentioned above). In contrast, when channel n values are around 0.10, whilst some simulations result in a large decrease in peak flow, a much smaller reduction can also occur. This indicates that at lower channel roughness values, variation in floodplain roughness has a greater influence.

Table 9.1. Statistical analysis of downstream peak flow as channel and floodplain roughness is randomly varied along 20, 40 and 52 reaches in the Uck catchment.

Number of CRIMs added	20	40	52
	Discharge (cumecs (m^3s^{-1}))		
Test case (FP 0.16, Channel 0.14)	114.31	112.41	112.18
Uncertainty analysis			
Mean	114.93	113.03	113.07
Median	114.49	112.57	112.48
Min	114.16	112.04	111.91
Max	118.45	118.21	118.44
Range	4.29	6.16	6.53
Standard Deviation	0.92	1.10	1.33

Floodplain n

A similar pattern can be observed when peak discharge is plotted against floodplain n. The overall range of peak flow values decreases as floodplain n increases. This is the case when 20,

40 and 52 CRIMs are added. Uncertainty in the downstream peak flow as a result of a particular floodplain n whilst channel n is varied is lower for higher floodplain n values. There is a slight trend, when CRIMS are added to 40 and 52 reaches, towards the greatest reduction in peak flow when floodplain roughness is highest (~>0.16) (Figures 9.3b and 9.4b). Figure 9.5 highlights this trend. However, Figures 9.2b, 9.3b and 9.4b show that a similar reduction in downstream peak flow is achieved when floodplain roughness is varied across the full set range (Manning's n 0.1-0.2). As with channel n, when floodplain roughness values are lower, peak flow is also dependent on channel roughness.
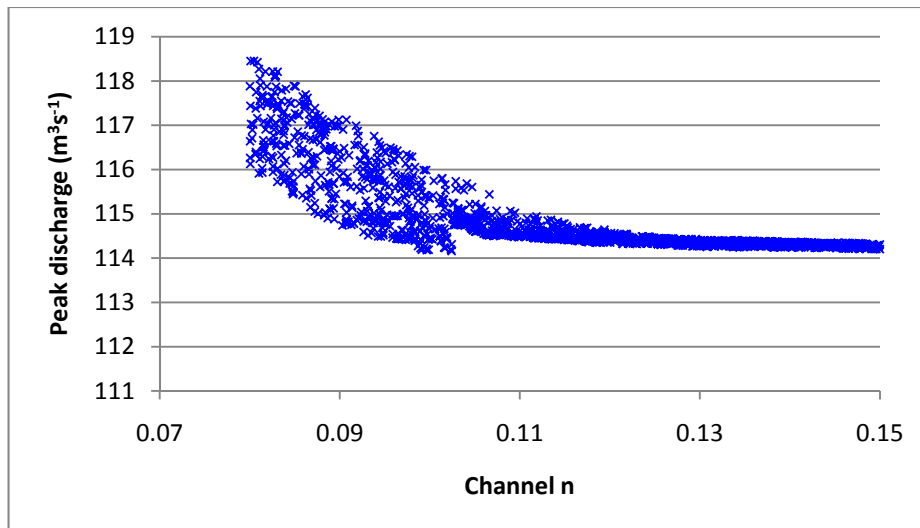
Figure 9.2a. A plot of channel manning's n against peak flow downstream at Uckfield as floodplain and channel roughness was varied along 20 reaches. Each point represents one simulation, of which there were 1,500
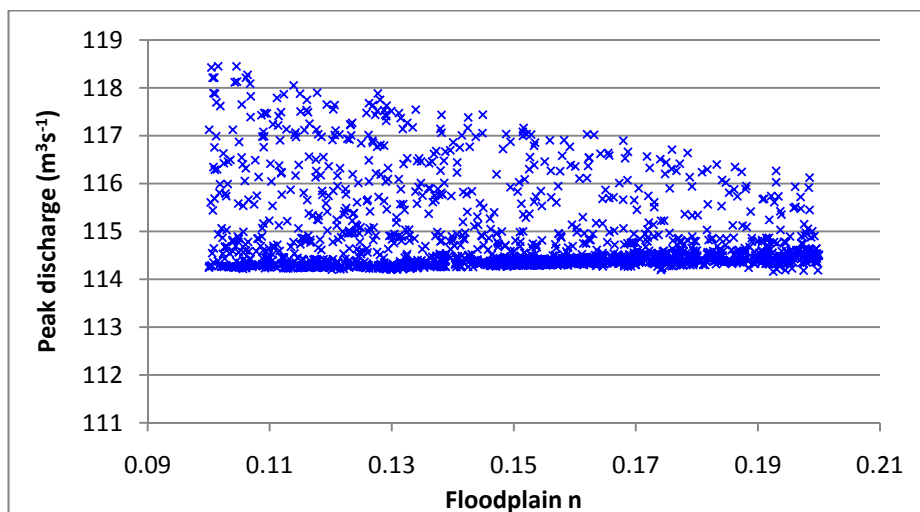
Figure 9.2b. A plot of floodplain manning's n against peak flow downstream at Uckfield as floodplain and channel roughness was varied along 20 reaches. Each point represents one simulation, of which there were 1,500
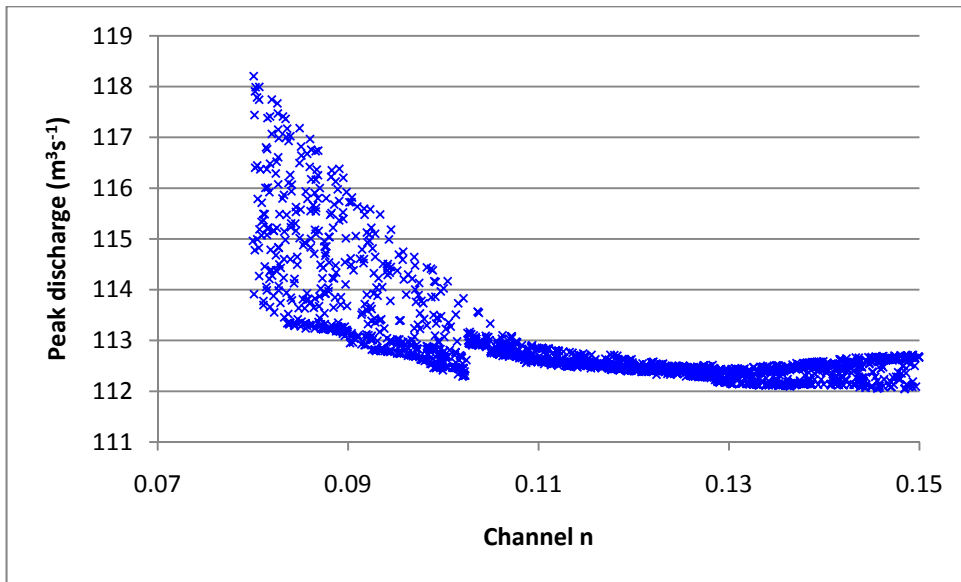
Figure 9.3a. A plot of channel manning's n against peak flow downstream at Uckfield as floodplain and channel roughness was varied along 40 reaches. Each point represents one simulation, of which there were 1,500
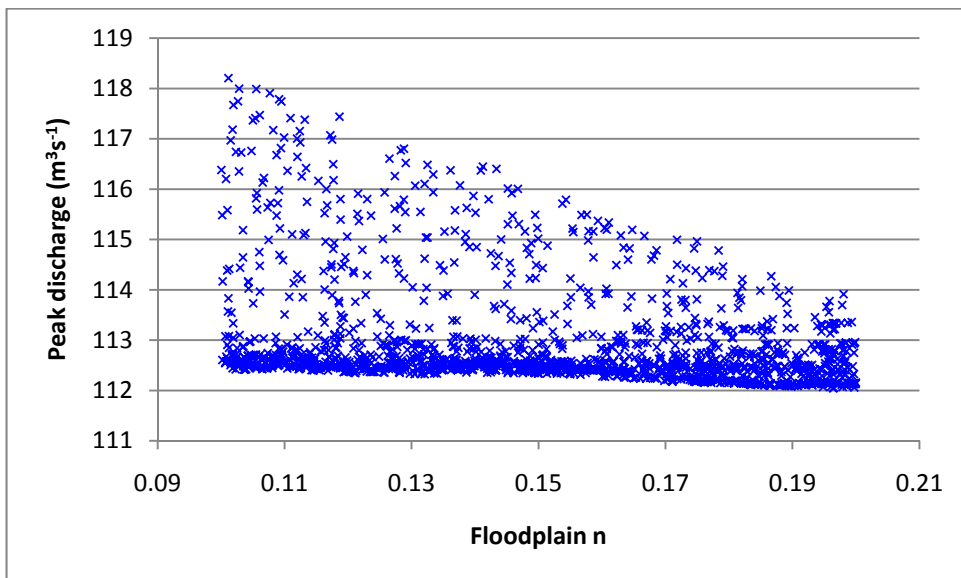
Figure 9.3b. A plot of floodplain manning's n against peak flow downstream at Uckfield as floodplain and channel roughness was varied along 40 reaches. Each point represents one simulation, of which there were 1,500
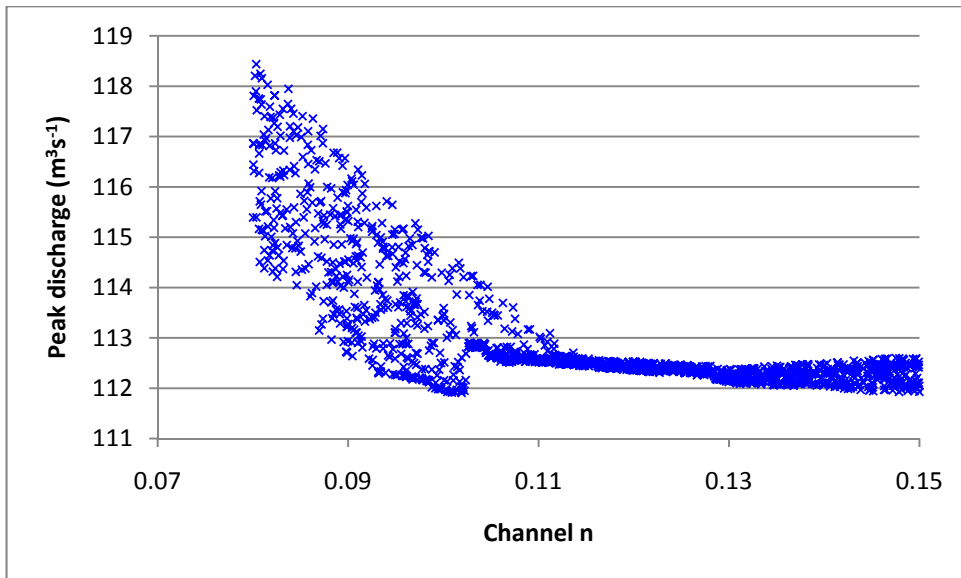
Figure 9.4a. A plot of channel manning's n against peak flow downstream at Uckfield as floodplain and channel roughness was varied along 52 reaches. Each point represents one simulation, of which there were 1,500
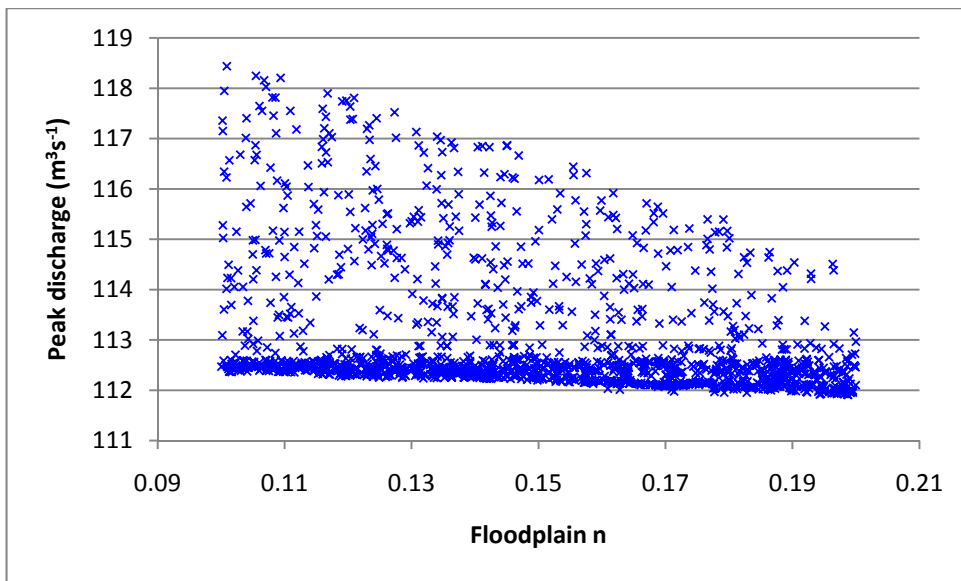
Figure 9.4b. A plot of floodplain manning's n against peak flow downstream at Uckfield as floodplain and channel roughness was varied along 52 reaches. Each point represents one simulation, of which there were 1,500
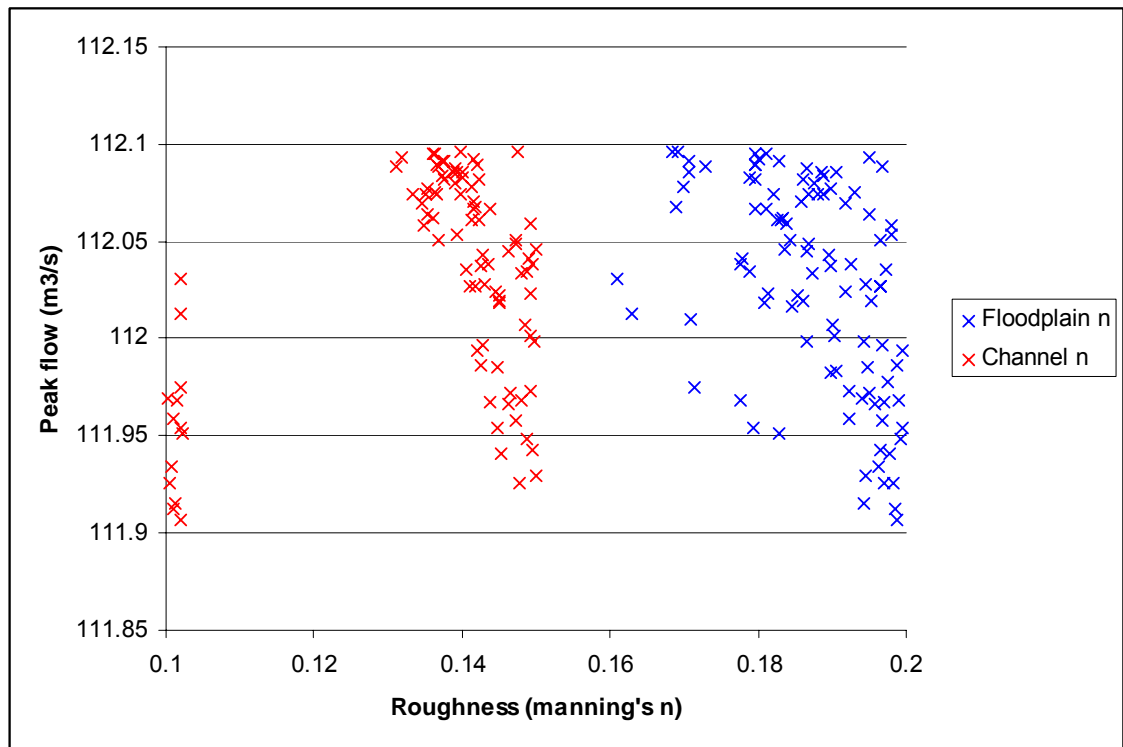
Figure 9.5. Channel and floodplain roughness values along 52 CRIM sites plotted against downstream peak flow. 100 model realisations are presented where simulated peak flow was the lowest.

9.3   Discussion

9.3.1   Uncertainty in selection of reaches for CRIM uncertainty analysis

Before discussing the uncertainty analysis relating to the effects of the choice of roughness values used to represent CRIMs, it is important to discuss the uncertainty associated with the choice of CRIM sites to be tested. As discussed in the previous chapter (Section 8.5.4), the identification of reaches where a CRIM has a positive effect on downstream peak flow in combination may be impacted on by the initial choice of roughness values used to represent a CRIM (in this study, 0.16 and 0.14 for floodplain and channel). Naturally this would impact on the reaches used for the uncertainty analysis in this chapter. Therefore it is worth noting that the analysis in this chapter is dependent to an extent on previous decisions made in the study.

9.3.2   Statistical Overview

A trend is apparent whereby an increased number of CRIMs simulated throughout the catchment results in a greater decrease in peak flow downstream; indicated by the median and lowest peak flow statistics. This is expected, as well established in the previous chapter, due to increased channel roughness the likelihood of overbank flow at the reach scale is

136

increased along a larger number of reaches (Knighton 1998; Järvelä 2002). A larger volume of water will therefore be stored on the floodplain (as long as discharge is large enough to exceed bankfull discharge). Discounting interaction of flood waves, which will have an important effect, peak flow downstream is likely to be lower. The flood event is likely to be lengthened however (Woltemade and Potter 1994; Thomas and Nisbet 2007).

The mean suggests little advantage is gained by adding CRIMs to 52, as opposed to 40 reaches. This may be due to the fact that the extra 12 reaches were at the end of the intervention list created in the previous chapter and therefore were reaches which had a relatively small positive effect in terms of downstream peak flow reduction in isolation.

The range of peak flow values and standard deviation from the mean peak flow increases as the number of CRIMs increases. This suggests that there is greater uncertainty associated with an estimate of the downstream peak flow based on random variation of the roughness values. This may be due to increased interaction effects of tributaries as their flow patterns are altered more.

9.3.3 Trends in uncertainty analysis

Channel n

The results obtained from the CRIM uncertainty analysis suggest that little is to be gained, in terms of peak flow reduction downstream, in increasing channel n above a value of ~0.10. However, it can be seen that increasing channel roughness to this level will lead to greater uncertainty associated with choice of floodplain n in comparison to if channel roughness was increased to values above ~0.11.

The results are logical; the influence of floodplain roughness, relative to channel roughness, on downstream peak flow is likely to increase as channel roughness decreases if flows are overbank. This is not likely to always be the case, and will be dependent on the magnitude of the rainfall event. In a particular storm event, a reduction in channel roughness may reduce the likelihood of overbank flow, thus also reducing the influence of the floodplain. However, for this particular rainfall event, it can be assumed that flows are very high, and likely to be overbank in most reaches when channel roughness is above 0.10. Such an assumption is based on results from the sensitivity analysis in this study (Section 5.4.6).

Figure 9.6 shows the floodplain roughness values randomly selected for the simulations where channel roughness was randomly selected between 0.10 and 0.11, and the subsequent peak flow downstream. The figure shows that if channel n were to be set as low as 0.10-0.11, floodplain roughness would need to remain high (>~0.16) to still achieve the largest reductions in downstream peak flow.
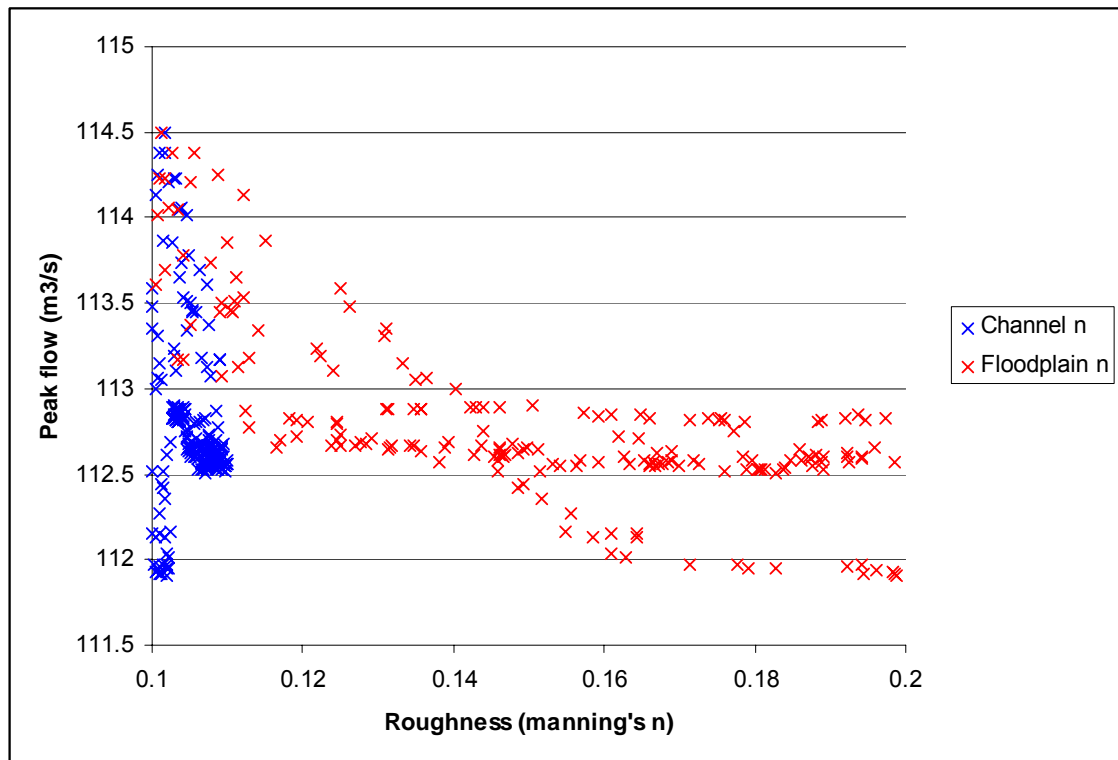
Figure 9.6. A plot of peak flow against pairs of channel and floodplain roughness values, when channel n values are between 0.1 and 0.11. The plot indicates the optimum floodplain roughness when channel n is constricted.

Floodplain n

Similar to results for channel roughness, the results suggest that there is no clear benefit to increasing floodplain roughness above 0.1. However the downstream peak flow reduction will still rely on the channel roughness selected. The results show that either floodplain or channel roughness can be reduced below the values of 0.16 and 0.14 respectively chosen to represent a CRIM in this study, whilst maintaining similarly positive results. However if the roughness of one parameter is lower, the roughness of the other will need to remain high for optimal results in terms of peak flow reduction. For example in one model simulation, a low downstream peak flow of 112.0 cumecs was achieved as a result of setting channel and floodplain roughness to 0.10 and 0.16 (2dp). Whilst this is simply one simulation it highlights the potential for reducing the extent of channel blockage in a CRIM scheme, providing floodplain roughness is high.

9.4   Conclusion

The analysis constrains the range of roughness values which need to be considered for an intervention scheme. They suggest that whilst good results in terms of peak flow reduction are likely to occur when channel n is close to the value of 0.14 used in the previous chapter, similar

results may be obtained if channel n were lower, provided floodplain interventions are also appropriate. Indeed the best result occurs when channel n ~0.10-0.11. However it is important to note that if channel roughness cannot be increased above ~0.10, floodplain roughness will have to be increased in order to achieve the best flood peak reduction effects. Similarly, if floodplain roughness cannot be increased close to a Manning's n of ~0.16, channel roughness will need to be increased significantly from a natural state.

For a practical intervention scheme, it is apparent that a channel with a relatively lower roughness and a floodplain with relatively higher roughness may achieve the best results. It may be easier to increase roughness on the floodplain without the need to block up the channel as much.

The study conclusions are discussed in the next chapter.

Chapter Ten   Conclusions

10.1   Introduction

This thesis had three aims (Chapter 1):

1. **To evaluate the performance of a suitable reduced complexity model for assessing the impacts of small scale riparian woodland interventions**

2. **To develop an intervention strategy with the aim to reduce downstream flood risk, taking into account feasibility**

3. **To provide a discussion, throughout the study, of uncertainty associated with methods and results**

This chapter summarises the findings of the study against these (Aims 1 and 2) and then evaluates the critical limitations, and related uncertainty (Aim 3), and key research directions that follow from the work reported.

10.2   Key findings

In Chapter 4 the Overflow model is described. Sensitivity and Uncertainty Analyses were subsequently carried out for the uncalibrated Overflow in Chapters 5 and 6 respectively. The analyses allowed an evaluation of the performance of Overflow. In the sensitivity analysis the effects of varying chosen model parameters one-at-a-time on model output is explored. Parameters chosen for the sensitivity analysis were land, floodplain and channel roughness, effective runoff rate and rain rate time map. It is clear that the rain rate time map parameter is the most sensitive and important of those tested in this study. The uncertainty analysis revealed that whilst the rain rate time map was important, parameter interactions were also apparent. A high degree of equifinality was observed for roughness parameters, suggesting that assumptions regarding roughness values are not so important so as to make model predictions of no use. It was also suggested that it is not necessary to increase effective runoff rate above 100% to account for input data error.

      Using the uncalibrated Overflow model, it became apparent that the choice of a single rain time map throughout the 5-day storm event simulated is problematic for a number of reasons.

First, the selection of a single rain rate time map is a key simplification of the uncalibrated Overflow model. However applying one rain rate time map throughout the storm event will not adequately represent the hydrological response of the catchment during a 5 day event. A single rainfall rate time map is likely to represent a catchment that is too wet during some periods of the storm event, and a catchment that is not wet enough during other periods.

Second, due to the high sensitivity of model output to the rain time map used, it is difficult to select an appropriate time map as the default when carrying out the sensitivity analysis, varying parameters one-at-time. This was a major issue during sensitivity analysis.

Finally, in the uncertainty analysis (Chapter 6), the goodness of fit between the observed flood hydrograph and simulated hydrographs appears relatively poor. This can be largely explained by the wide range of parameter values which were sampled from, particularly the rain rate time map parameter. With this in mind, it is observed that a number of model simulations achieve a relatively good fit with observed discharge, particularly considering the use of homogenous parameters. However it was deemed necessary to vary the applied rain rate time map throughout the storm event to allow a better representation of the hydrological response of the catchment, and to allow a much improved fit between simulated and observed hydrographs.

Given these points, a decision was made to carry out a partial calibration of the Overflow model (Chapter 7), through applying a different temporal ordering of rain time maps throughout the storm event to improve the temporal representation of the hydrological response of the Uck catchment. This was a partial calibration as ideally all uncertain parameters would be calibrated.

That aside, the calibration process followed resulted in a much improved fit between observed and simulated hydrographs at Isfield (Chapter 7). Due to the lack of an accurate observed hydrograph at Uckfield for the October 2000 flood event (Environment Agency 2001), the goodness of fit of the simulated hydrograph at Uckfield could not be directly assessed. However, the indication was that overall model performance was good. The calibrated model, with an improved fit between observed and simulated hydrographs, allowed an exploration of the effects of Catchment Riparian Intervention Measures (CRIMs) on the downstream hydrograph.

Such an exploration was carried out in Chapter 8. A suitable intervention strategy was also developed. First a screening process was carried out to identify the effects on downstream peak flow of CRIMs placed in one separate channel reach at a time. From these results it was possible to identify the individual effect on peak flow at Uckfield of adding a CRIM to different reaches. It was found that adding a CRIM to a reach had a varied effect

depending on the location of the reach in question. Simulating a CRIM in a single reach led to a reduction in downstream peak flow for 127 of the 199 reaches identified as potential sites. A CRIM increased downstream peak flow when placed in 72 reaches. A CRIM was found to increase downstream peak flow due to resynchronisation of tributary peak flow with the peak flow from other tributaries and thus initial exploration of the location of a CRIM was found to be important.

Following the screening process, 100 reaches were identified where adding a CRIM in isolation had the most positive effects in terms of downstream peak flow reduction. The effect of adding CRIMs to these reaches in combination was subsequently explored. As CRIMs were added to more and more reaches, downstream peak flow was reduced. However, the existing presence of a set of CRIMs had a conditioning effect on the addition of CRIMs in new reaches. Thus, the adding of a CRIM to a new reach often had an adverse effect on the cumulative peak flow reduction, and therefore that reach was rejected. This indicates the importance of exploring the spatial arrangement of multiple CRIMs in the Uck catchment. 48 reaches were rejected in total. Applying CRIMs to 52 reaches reduced simulated peak flow at Uckfield by ~12 cumecs from an initial peak flow of 124.7 cumecs. The sum of the effect of individual CRIMs in these 52 reaches was 52.6 cumecs, much greater than when CRIMs were added at the same time. Importantly, the effect of a CRIM in combination could not be predicted from its effect in isolation.

In Chapter 9 an uncertainty analysis was carried out exploring the effect of the roughness values chosen to represent a CRIM along a reach, the default being Manning's n values of 0.16 and 0.14 for the floodplain and channel (as used in Chapter 8). 1,500 simulations were run, randomly selecting floodplain and channel roughness values along the 52 reaches identified above. Floodplain and channel Manning's n values ranged from 0.1-0.2 and 0.08-0.15 respectively. The reduction in peak flow at Uckfield as a result of adding CRIMs to these 52 reaches varied significantly when roughness values were randomly varied. Peak flow at Uckfield varied from 111.9 cumecs to 118.4 cumecs dependent on the roughness values selected to represent CRIMs throughout the catchment.

Importantly, it was found that similarly fine results in terms of downstream peak flow reduction could be achieved when either floodplain or channel roughness values were lower than the default used in Chapter 8 (Floodplain n, 0.16; Channel n, 0.14). However, importantly, if the roughness of one is increased to a smaller degree above natural levels, the roughness of the other must be increased to a high degree. For example if channel roughness cannot be increased above n = ~0.10, then floodplain roughness must be close to n = ~0.16 for optimal flood peak reduction.

10.3   Critical analysis of the study

10.3.1 Model simplification and uncertainty

As a reduced complexity hydrological model, the key advantage to Overflow was the ease and speed with which different flood risk reduction measures could be simulated in different spatial arrangements. However, it is important to include a consideration of the simplifications inherent in the model.

Firstly, whilst the rain input is based on observed rainfall rates during the October 2000 storm event, and thus varies temporally, it is applied as a spatially homogenous rainfall rate. Along with errors in rain gauge data, this is likely to lead to some inaccuracy in the rain input. The effective runoff rate is determined based on comparison of the rainfall and discharge volume during the storm event. As there are likely to be errors in observed discharge data also, such a calculation is an estimate.

The effective runoff rate parameter accounts for evaporation, losses to groundwater and baseflow, which are not represented explicitly in the model. The previous paragraph indicates uncertainty in the calculation of effective runoff. The effective runoff rate parameter itself is also spatially homogenous, and largely temporally homogenous, with only 4 different runoff percentages set during a 120 hour period. Ideally a time dependent treatment of catchment runoff rate would be included in the model structure. This would reflect the hydrological response of the catchment as the rainfall input varies. A spatially homogenous runoff rate does not allow for local and small-scale variation in runoff. The percentage of rainfall entering the catchment that is transferred as runoff is likely to be in reality highly spatially heterogeneous.

Similarly the rainfall rate time maps created are spatially homogenous. Ideally the rainfall rate time maps would allow for different areas of the catchment drying and wetting at a particular time step, which would be reflected in the cell passage times.

 It is important to note that even if the rain time map and effective runoff parameters were spatially heterogeneous, uncertainty would remain due to a lack of data, errors in available input data and the input of rainfall that is not spatially distributed. It is important therefore to appreciate that a more complex, physically-based model will still be uncertain. However the factors discussed will have important impacts on the input of rain and the delivery of this rainfall as runoff through the catchment, ultimately impacting on downstream discharge calculations.

Another key model simplification is the treatment of catchment land cover by assigning a spatially homogenous Manning's n roughness coefficient of 0.06. The floodplains and channel network are also assigned spatially homogenous roughness values. The roughness

values in turn affect the velocity of flow throughout the catchment, and hence cell passage times.

Despite the simplified model structure, namely the use of homogenous parameters, the calibration procedure did produce relatively good results (Chapter 7). By varying the order of rainfall rate time maps applied, and thus improving the temporal representation of catchment hydrological response throughout the storm event, a good fit between observed and simulated hydrographs at Isfield was achieved.

The above discussion emphasises the importance of a consideration of the simplifications, and associated uncertainty inherent in the model structure used. Simultaneously, it must be noted that useful results can be produced by a reduced complexity hydrological model. The Overflow model performs well despite the use of homogenous parameters.

10.3.2   Uncertainty in the exploration of the use of CRIMs

As mentioned previously in the above section, and in Chapter 8, the selection of 'positive' CRIMs from the screening process had an important effect on the intervention strategy developed. This is largely due to the interaction effects which occur when a CRIM is added to more than one reach in the catchment. When exploring the effect of CRIMs in combination, the spatial arrangement of CRIMs already added to the catchment had an important effect on the effectiveness of any CRIMs added to new reaches. Therefore the order in which CRIMs were added in combination had an important influence on the intervention strategy proposed.

A potential improvement to the study methodology would be to repeat the screening process a number of times using different roughness values to simulate CRIMs. Such a process is likely to result in the selection of some different reaches where interventions are deemed beneficial. At the same time, certain reaches are likely to be consistently identified as optimal locations for the placement of CRIMs. This would allow an intervention strategy based on a consideration of the placement of CRIMs of different roughness levels.

Ideally a much more intensive exploration of CRIMs in combination would be carried out. By randomly selecting a number of reaches from a list of 'positive' reaches, and simulating CRIMs in those chosen reaches, the problem of adding CRIMs in a certain order would be removed. If this process was repeated numerous times, each time randomly selecting different combinations of reaches, those reaches which consistently produce good results in terms of peak flow reduction could be identified.

With reduced time constraints, all model parameters could be included in the sensitivity and uncertainty analyses. Instead, key model parameters were chosen based on a

previously developed understanding of the model. However, this is not as comprehensive an analysis as desired.

10.4   Future research

It has been previously stated that Overflow is effectively an exploratory tool, primarily for exploring the spatial arrangement of intervention measures. There is therefore a wide scope for further research in the future.

As discussed above, an intervention strategy has been developed for the Uck catchment. There is now the potential for further analysis of the effects on downstream flooding of such an intervention strategy, but utilising a more complex physically based model. Such research, however, will require suitable data of sufficient quality and quantity. Without such data, the use of a more complex model offers little advantage to Overflow, as results are likely to be at least as uncertain.

Second, there is a clear need to explore the effect of intervention measures on downstream flooding for a variety of storm events of different magnitude. There is likely to be a different response to interventions when the runoff in the catchment, and therefore in-channel discharge, varies. The current study suggests an intervention strategy that may have been effective in reducing peak flow during the 2000 flood event. However, to better inform stakeholders, an indication of the effectiveness of the intervention strategy for potential future flood events is important. Without observed discharge data, however, results are likely to be more uncertain.

In Chapter 9 the uncertainty associated with the roughness values used to simulate a CRIM was explored. It is likely that CRIMs representing a certain level of in-channel obstruction will have a varied effect for flood events of different magnitude and therefore would need to be investigated.

Third, a further exploration of Overflow itself would allow an improved understanding of the influence of model parameters on model output. In Chapter 5 and 6 it is stated that due to time constraints a number of parameters were not included in the sensitivity and uncertainty analyses. For example, the influence of the discharge threshold and geometry equations on the channel network was not explored. A sensitivity analysis of the calibrated Overflow model is also required. A larger number of simulations in the uncertainty analysis would also allow an improved exploration of model parameters and model uncertainty.

Fourth, as detailed in Chapter 7, a full calibration involving all effective parameters was not carried out, again primarily due to time constraints.

There is a balance to be met between improving the temporal and spatial treatment of catchment characteristics and processes, and maintaining the key features of Overflow; namely the ability to apply various flood risk reduction measures throughout the catchment with ease and quickly. Increasing the complexity of the model is likely to affect this. However the use of land use data would be beneficial in allowing improved spatial representation of land cover in Overflow. Key land cover types, and their associated roughness could be represented.

The study has indicated the potential for use of diffuse, small-scale interventions to reduce downstream peak flow. The potential for the use of Overflow as an exploratory tool has also been demonstrated. Uncertainty associated results must be considered when analysing results. More detailed work may now be carried out, as deemed appropriate.

References

Acreman, M.C., Ruddington, R., Booker, D.J. (2003) Hydrological impacts of floodplain restoration: a case study of the River Cherwell, UK, *Hydrological and Earth System Sciences*, 7, 1: 75-85

Anderson, B.G., Rutherfurd, I.D., Western, A.W. (2006) An analysis of the influence of riparian vegetation on the propagation of flood waves, *Environmental Modelling & Software*, 21: 1290-1296

Archer, D.R. (1989) *Floods: Hydrological, Sedimentological and Geomorphological Implications*, John Wiley & Sons, New York, 37-46

Archer (2003) Scale effects on the hydrological impact of upland afforestation and drainage using indices of flow variability: the River Irthing, England, *Hydrology and Earth System Sciences,* 7, 3: 325-338

Ball, T. (2008) Management approaches to floodplain restoration and stakeholder engagement in the UK: a survey, *Ecohydrological Processes and Sustainable Floodplain Management,* 8, 2-4: 273-280

Barker, S. F. (1961) On simplicity in empirical hypotheses. *Philosophy of Science,* 28: 162-171

BBC (2009) *The floods of 2000*, BBC Online, http://news.bbc.co.uk/local/sussex/hi/people_and_places/history/newsid_8330000/8330270.stm, accessed 5 October 2010

Beven, K. (2001) Rainfall-Runoff Modelling – The Primer, John Wiley and Sons Ltd., England

Beven, K. (2006) A manifesto for the equifinality manifesto, *Journal of Hydrology,* 320, 1-2: 18-36

Beven, K., J. (2009) Environmental modelling: an uncertain future?: An introduction to techniques for uncertainty estimation in environmental prediction, Taylor & Francis, New York

Beven, K.B., Binley, A. (1992) The future of distributed models: Model calibration and uncertainty prediction, *Hydrological Processes,* 6: 279-298

Bronstert, A., Niehoff, D., Burger, G. (2002). Effects of climate and land-use change on storm runoff generation: present knowledge and modelling capabilities, *Hydrological Processes,* 16, 2: 509-529.

Brown, J.D., Damery, S.L. (2002) Managing flood risk in the UK: towards an integration of social and technical perspectives, *Transaction of the Institute of British Geographers,* 27, 4: 412-426

Campling, P., Gobin, A., Beven, K., Feyen, J. (2002) Rainfall-runoff modelling of a humid tropical catchment: the TOPMODEL approach, *Hydrological Processes,* 16, 2: 231-253

Campolongo, F., Saltelli, A. Sorensen, T., Tarantola, S. (2000) Hitchhikers guide to sensitivity analysis. In Saltelli, A., Chan, K., Scott, E.M. (Ed.) *Sensitivity Analysis*, John Wiley and Sons Ltd., England: 15-48

Chang, H., Franczyk, J. (2008) Climate change, land use change and floods: Toward and intergrated assessment, *Geography Compass*, 2: 1549-1579

Chow, V.T. (1959) *Open channel hydraulics*, Mc-Graw-Hill, New York

Department for Environment and Rural Affairs (2005) *Making space for water: Taking forward a new Government strategy for flood management in England*, Defra Publications, London.

Diskin, M.H., Simon, E. (1977) A Procedure for the selection of objective functions for hydrological simulation models, *Journal of Hydrology,* 34: 129-149

Du, J., Xie, H., Hu, Y., Xu, Y., Xu, C-Y. (2009) Development and testing of a new storm runoff routing approach based on time variant spatially distributed travel time method, *Journal of Hydrology*, 369, 1-2: 44-54

Dudley, S.J., Fischenich, J.C., Abt, S.R. (1998) Effect of woody debris entrapment on flow resistance, *Journal of the American Water Resources Association,* 34, 5: 1189-1197

Environment Agency (2001) Sussex Ouse 12th October 2000 flood report, Binnie Black and Veatch

Environment Agency (2008) River Ouse Catchment Flood Management Plan – Draft Main Stage, http://www.environment-gency.gov.uk/static/documents/Research/1_es_and_int_ 2020599.pdf, accessed 20 July 2010

Environment Agency (2009) Uckfield flood protection gets a boost, http://www.environment-agency.gov.uk/news/106810.aspx?page=3&month=4&year =2009, accessed 5 September 2010

Evans, E.P., Ramsbottom, D.M., Wicks, J.M., Packman, J.C., Penning-Rowsell, E.C. (2002) Catchment flood management plans and the modelling and decision support framework, *Civil Engineering*, 150: 43–48

Geographical Association, http://www.geography.org.uk/resources/flooding/uckfield/, accessed 5 September 2010

Ghavasieh, A-R, Poulard, C., Paquier, A. (2006) Effect of roughened strips on flood propagation: Assessment on representative virtual cases and validation, *Journal of Hydrology*, 318: 121–137

Ganoulis, J. (2003) Risk-based floodplain management: A case study from greece, *International Journal of River Basin Management,* 1, 1: 41-47

Green, I.R.A., Stephenson, D. (1986) Criteria for comparison of single event models, *Hydrological Sciences,* 31, 3, 395-411

Hamby, D.M. (1994) A review of techniques for parameter sensitivity analysis of environmental models, *Environmental Modelling and Assessment,* 32, 135-154

Hannaford, J., Marsh, T.J. (2008) High-flow and flood trends in a network of undisturbed catchments in the UK, *International Journal of Climatology,* 28: 1325-1338

Harman, J., Bramley, M.E., Funnell, M. (2002) Sustainable flood defence in England and Wales, Proceedings of the ICE, *Civil Engineering*, 150: 3-9

Hooijer, A., Klijn, F., Pedroli, B.M., Van Os, A.G. (2004) Towards sustainable flood risk management in the Rhine and Meuse River Basins: Synopsis of the findings of Irma-Sponge, *River Research and Applications*, 20: 343-357

Hurkmans, R., T., W., L., Terink, W., Uijlenhoet, R., Moors, E.J., Troch, P.A., Verbung, P.H. (2009) Effects of land use changes on streamflow generation in the Rhine basin, *Water Resources Research,* 45, W06405, doi:10.1029/2008WR007574

Järvelä, J. (2002*) Determination of flow resistance of vegetated channel banks and floodplains.* In Bousmar, D. and Zech,Y. (Ed.) (2002) *River Flow*, Swets & Zeitlinger, Lisse, pp. 311–318

Järvelä, J. (2003) Influence on flow structure in floodplains and wetlands. In Sanchez-Arcilla, A., Bateman, A. (Ed.) *Proceedings of the 3rd Symposium on River, Coastal and Estuarine Morphodynamics*, IAHR, Madrid, 845-856.

Kirkby, M.J., Naden, P.S., Burt, T.P. and Butcher, D.P., (Ed.) (1993) *Computer Simulation in Physical Geography,* Second edition, Wiley, Chichester, UK. 190pp.

Knighton, D. (1998) Fluvial Forms and Processes, Arnold, London

Lane S.N. (2002) More floods, less rain: changing hydrology in a Yorkshire Context, *The Yorkshire and Humber Regional Review,* 11: 18–19.

Lane, S.N. (2007) Managing the rural landscape in Thorne, C.R., Evans, E.P, Penning-Rowsell, E.C. (Ed.) *Future flooding and coastal erosion risks*, Thomas Telford Publishing, London, pp. 297-319

Lane, S.N. (2008a) Climate change and the summer 2007 floods in the U.K, *Geography*, 93: 91-97

Lane, S.N. (2008b) Slowing the floods in the U.K. Pennine uplands…a case of Waiting for Godot? *Journal of Practical Ecology and Conservation*

Lane, S.N. & Thorne, C.R. (2007) River processes. In: Thorne, C. R. Evans, E. P. & Penning-Rowsell, E. C. *Future Flooding and Coastal Erosion Risks*. Thomas Telford, London; 2007:82-99

Legates, D.R., McCabe Jr., G.J. (1999) Evaluating the use of "goodness-of-fit" measures in hydrologic and hydroclimatic model validation, *Water Resources Research,* 35, 1: 233-241

Lenhart, T., Eckhardt, K., Fohrer, N., Frede, H.G. (2002) Comparison of two different approaches to sensitivity analysis, *Physics and Chemistry of the Earth, Parts A/B/C*, 27, 9-10: 645-654

Leopold, L.B., Maddock, T. (1953) The Hydraulic Geometry of Stream Channels and Some Physiographic Implications, *U.S. Geological Survey, Professional Paper,* 252

Linstead, C., Gurnell, A.M. (1999) Large woody debris in British headwater rivers: physical habitat role and management guide. Environment Agency R&D Technical Report W185.Environment Agency, Bristol.

Liu, Y.B., Gebremeskel, S., De Smedt, F., Hoffmann, L., Pfister, L. (2003) A diffusive transport approach for flow routing in GIS-based flood modelling, *Journal of Hydrology,* 283: 91–106

Liu, Y.B., Gebremeskel, S., De Smedt, F., Hoffmann, L., Pfister, L. (2004) Simulation of flood reduction by natural river rehabilitation using a distributed hydrological model, *Hydrology and Earth System Sciences,* 8, 6: 1129-1140

Maidment, D.R., Olivera, F., Calver, A., Eatherall, A., Fraczek, W. (1996) Unit hydrograph derived from a spatially distributed velocity field, *Hydrological Processes,* 10, 6: 831-844

McCuen, R.H. (1973) The role of sensitivity analysis in hydrologic modelling, *Journal of Hydrology,* 18, 1: 37-53

Nash, J.E., Sutcliffe, J.V. (1970) River flow forecasting through conceptual models, 1, A discussion of principles, *Journal of Hydrology,* 10: 282-290

Niehoff, D., Fritsch, U., Bronstert, A. (2002). Land-use impacts on storm-runoff generation: scenarios of land-use change and simulation of hydrological response in a meso-scale catchment in SW-Germany, *Journal of Hydrology,* 267, 1-2: 80-93.

Nisbet, T.R., Thomas, H. (2006) The role of flood control: a landscape perspective, Proceedings of the 14th annual IALE(UK) 2006 conference on Water and the Landscape, Eds. Davies, B., Thompson, S.: 118-125. IALE(UK), Oxford

Nisbet, T.R., Thomas, H. (2008) Restoring Floodplain Woodland for Flood Alleviation, Final Report

Odoni and Lane (2010) Assessment of the impact of upstream land management measures on flood flows in Pickering Beck using Overflow, http://www.forestry.gov.uk/website/forestresearch.nsf/ByUnique/INFD-7ZUCQY

Odoni and Lane (in preparation) OVERLOW 1: development of a spatially-distributed unit hydrograph method for testing diffuse land management interventions

Olivera, F., Maidment, D. (1999) Geographic Information Systems (GIS)-based spatially distributed model for runoff routing, *Water Resources Research*, 35, 4: 1155–1164

Parrott, A., Brooks, W., Harmar, O., Pygott, K. (2009) Role of rural land use management in flood and coastal risk management, *Journal of Flood Risk Management,* 2, 4: 272-284

Pattison, I., Lane, S.N., Hardy, R.J., Reaney, S. (2008) Sub-catchment peak flow magnitude and timing effects on downstream flood risk, *BHS 10th National Hydrology Symposium,* Exeter

Poulard, C., Lafont, M., Lenar Matyas, A., Lapuszek, M. (2010) Flood mitigation designs with respect to river ecosystem functions – a problem oriented conceptual approach, *Ecological Engineering*, 36, 1: 69-77

Posthumus, H., Hewett, C.J.M., Morris, J., Quinn, P.F. (2008) Agricultural land use and flood risk management: Engaging with stakeholders in North Yorkshire, *Agricultural Water Management,* 95, 7: 787-798

Quinn, P.F., Hewett, C.J.M., Dayawansa, N.D.K. (2008) TOPCAT-NP: a minimum information requirement model for simulation of flow and nutrient transport from agricultural systems, *Hydrological Processes,* 22: 2565-2580

Rhee, D.S., Woo, H., Kwon, B.A., Ahn, H.K. (2008) Hydraulic resistance of some selected vegetation in open channel flows, *River Research and Applications*, 24, 5: 673-687

Robson, A.J. (2002) Evidence for trends in UK flooding, *Philosophical Transactions of the Royal Society A:* 360, 1796: 1327-1343

Roughani, M., Ghafouri, M., Tabatabaei, M. (2007) An innovative methodology for the prioritization of sub-catchments for flood control, *International Journal of Applied Earth Observation and Geoinformation,* 9: 79–87

Saghafian, B., Julien, P.Y., Rajaie, H. (2002) Runoff hydrograph simulation based on time variable isochrone technique, *Journal of Hydrology,* 261, 1-4: 193-203

Saghafian, B., Khosroshani, M. (2005) Unit Response Approach for Priority Determination of Flood Source Areas, Journal of Hydrologic Engineering, 10, 4: 270-277

Saltelli, A. (2000) What is Sensitivity Analysis in Saltelli, A., Chan, K., Scott, E.M. (Ed.) *Sensitivity Analysis*, John Wiley and Sons Ltd., England, 3-14

Schaefli, B., Gupta, H.V. (2007) Do Nash values have value?, *Hydrological Processes,* 21: 2075-2080

Smith, J.U., Smith, P. (2007) An introduction to environmental modelling, Oxford University Press, Oxford

Soulsby, C., Tetzlaff, D., Dunn, S.M., Waldron, S. (2006) Scaling up and out in runoff process understanding: insights from nested experimental catchment studies, *Hydrological Processes*, 20, 11: 2461-2465

Sulaiman, W.N.A., Heshmatpoor, A., Rosli, M.H. (2010) Identification of Flood Source Areas in Pahang River Basin, Peninsular Malaysia, *Environment Asia*, 3: 73-78

Tang, X., Knight, D.W. (2009) Lateral distributions of streamwise velocity in compound channels with partially vegetated floodplains, *Science in China Series E: Technological Sciences*, 52, 11: 3357-3362

Thomas, H. and Nisbet, T. R. (2004) An assessment of the hydraulic impact of floodplain woodland. Forest Research, Alice Holt Lodge, Farnham, Surrey

Thomas, H. and Nisbet, T.R. (2007) An assessment of the impact of floodplain woodland on flood flows, *Water and Environment Journal*, 21, 2: 114-126

Turner-Gillespie, D.F., Smith, J.A., Bates, P.D. (2003) Attenuating reaches and the regional flood response of an urbanising drainage basin, *Advances in Water Resources,* 26, 6: 673-684

Vrugt, J.A., Bouten, W., Gupta, H.V., Sorooshian, S. (2002) Toward improved identifiability of hydrologic model parameters: The information content of experimental data, *Water Resources Research,* 38, 12: 1312, doi:10.1029/2001WR001118

Wainwright, J., Mulligan, M. (2004) Environmental modelling – Finding Simplicity in Complexity, John Wiley and Sons Ltd., West Sussex, England

Werritty, A. (2006) Sustainable flood management: oxymoron or new paradigm?, *Area,* 38,1: 16-23

Wharton, G., Gilvear, D.J. (2006) River restoration in the UK: meeting the dual needs of the European Union Water Framework Directive and flood defence?, *International Journal of River Basin Management*, 4, 4: 1-12

Wheaton, J.M., Darby, S.E., Sear, D.A. (2008) The Scope of Uncertainties in river Restoration. In Derby, S., Sear, D. (Ed.) *River Restoration: Managing the Uncertainty in Restoring Physical Habitat*, John Wiley & Sons, Ltd.

Willmott, C.J., Matsuura, K. (2005) Advantages of the mean absolute error (MAE) over the root mean square error (RMSE) in assessing average model performance, *Climate Research*, 30: 79-82

Wolff, C.G., Burgess, S.J. (1994) An analysis of the influence of river channel properties on flood frequency, *Journal of Hydrology*, 153, 1-4: 317-337

Woltermade, C.J., Potter, K.W. (1994) A watershed modelling analysis of fluvial geomorphologic influences on flood peak attenuation, *Water Resources Research*, 30, 6: 1933-1942

Wu, C.F.J., Hamada, M. (2000) Experiments: Planning, Analysis and Parameter Design Optimization, John Wiley & Sons, Inc., New York

APPENDIX

Appendix A (Odoni and Lane, in prep).

OVERLOW 1: development of a spatially-distributed unit hydrograph method for testing diffuse land management interventions

Abstract:

OVERFLOW has been developed as an exploratory model to demonstrate the effects of different channel and catchment intervention measures on flooding in rural areas caused by major rainfall events. The results generated by OVERFLOW are intended to be used as guidance to both practitioners and non-experts as to what types of measures - and particularly what spatial arrangements of them - should be studied in detail using the conventional, more strongly physically-based models commonly applied to flooding problems. These intervention measures include, with respect to channels, changes in channel depth, width, sinuosity, roughness, and associated floodplain roughness, the latter two implemented in OVERFLOW by simple adjustments to Manning's '*n*' values. Channel roughness changes are also used to simulate the incorporation of flow delay structures, such as large woody debris dams, in the streams. Similarly, the wider catchment interventions in OVERFLOW can potentially include changes in planting and cropping, building of ponds, digging or blocking of drains and ditches, planting of hedgerows, and the incorporation of low level bunds as temporary water storage zones across the floodplain or as smaller storage interventions in areas nearer the channel heads. The model uses simplified representations of land surface cover and channel (hydraulic) geometry in order to allow rapid inclusion in the model of any number and combination of the interventions potentially of interest in a particular catchment. This facility in using the model enables the significance of the spatial arrangements of those interventions, as a means to reduce flood risk, to be demonstrated and thus the more optimal solutions, both of intervention type and their spatial arrangement, to be identified. The underlying model simplifications of the hydrology and hydraulics are achieved by calculating flows according to a sequence of 'time maps', which are themselves first calculated from a set of hypothesised rainfall rates covering the range of those observed during a known rainfall event or events that have caused a major flood. In calibration of the model, the time maps are used in a temporal order that follows broadly the applied gauged rainfall, and the order is further adjusted to achieve high agreement between the observed and modelled discharges at one or more reference points of interest in the channel network. Once calibrated, the same time map order is then applied to the catchment when using the model to explore how different intervention arrangements affect the flood hydrograph. Each intervention case result is compared with the base modelled result in order to assess the efficacy or otherwise of the intervention case as a potential flood reduction solution. Evaporation, losses to groundwater and baseflow effects are also taken into account in a highly simplified way in the model set up and calibration. OVERFLOW is presently intended to be applied to flood related problems affecting small to medium-sized catchments (up to 150 km^2), at spatial resolutions 10-50 m^2, although work is in hand to adapt the model for application to larger catchments. Here we present a complete model description and the calibration of the model for the catchment of Pickering Beck, North Yorkshire, for two major flood events (2007 and 2000). Application of

the model to simulate these floods in Pickering Beck and the results generated by exploring different combinations for flood intervention measures are explained in part 2.

INTRODUCTION

There is considerable interest in the possibility that diffuse interventions in river catchments might provide an alternative methodology for reducing downstream flood risk. Field measurements at quite small scales (between 1 m^2 and 1 km^2) have confirmed that land management can impact locally upon the amount of runoff generation and its speed of transfer over the land surface (e.g. Heathwaite *et al.*, 1990; Marshall *et al.*, 2009). Small scale interventions have been shown to have considerable local benefits in reducing peak river flows during extreme events and such interventions have included: (1) small ponds (e.g. Wilkinson *et al.*, 2008); (2) localised tree planting and restrictions on livestock grazing (e.g. Marshall *et al.*, 2009); (3) field-scale land use change such as replacing arable cover with grass land (e.g. Boardman *et al.*, 2003).

However, there remains considerable uncertainty over the extent to which such small scale benefits might scale up to have larger scale impacts (O'Connell *et al.*, 2007). Further, if many interventions are introduced, each having beneficial local impacts upon the reduction of peak river flows, the interventions change the relative timings of sub-catchment responses and, possibly, increase peak river flows downstream. Indeed, statistical analysis has shown that in larger river basins (> 10 km^2), the relative timing of tributary peaks with respect to the main channel may explain between 10 and 20% of the variance in downstream peak river flow magnitudes (e.g. Lane, 2003). Even measures that are locally beneficial may be problematic at larger scales and need to be properly evaluated in a catchment-scale framework.

Unfortunately, this presents a major challenge for hydrological modelling. First, if an intervention produces with downstream impacts that depend upon the response of other parts of the catchment, the analysis needs to be spatially explicit. This obviates the use of effective runoff modelling tools such as those that use width functions or instantaneous unit hydrographs (Olivera and Maidment, 1999; Liu *et al.*, 2003). Second, there may be many possible types of interventions that might be considered in many possible different locations. Consider the following: (1) N possible types of interventions; (2) m possible stream reaches, where a reach is defined as either an order 1 stream or any subsequent stream segment bounded by an upstream and a downstream confluence; and (3) l possible intensities of intervention (e.g. densities of riparian woodland planting). Assessing all possible combinations of intervention would require $(l \times N)^m$ simulations which given that m might be expected to be > 100, represents an impossible computational problem unless either: (1) methods for reducing the number of simulations; or (2) computational simplicities; can be found. Third, many of the interventions have small-scale local impacts that can be sensitively dependent upon the detailed local characteristics of the system such as soil depth or channel width and depth. These are not necessarily measurable over large spatial scales with a sufficient spatial resolution and may need to be estimated or inferred from other variables. They may therefore be highly uncertain and this has implications for model complexity: there is little to be gained from having a model whose complexity necessitates data that are not available or a data precision that is not achievable.

Given these three constraints, this paper seeks to develop a reduced complexity hydrological model that could allow the testing of multiple, distributed interventions in river catchments with the aim of reducing downstream flood risk. Its companion paper (Odoni *et al.*, in review) explores the application of this model to flood risk reduction using channel and riparian interventions.

Model Conceptualisation: a spatially-distributed unit hydrograph treatment with time-dependent flow path evolution

The process by which complexity was reduced is an integral part of the model reported. Model development was undertaken as part of a wider project concerned with undertaking flood risk research in a collaborative collective where both academic natural and social scientists worked alongside local people to develop new flood risk reducing strategies (Whatmore, 2009; Odoni and Lane, 2010; Lane *et al.*, 2011). The particular focus of this project was rural areas in England which, under England's Department of the Environment, Food and Rural Affairs prioritisation policies, were unlikely to receive conventional flood defence investment. Thus, the model conceptualisation, and its associated complexity, was grounded in both: (1) those interventions that the collective decided might be feasible in the study catchments and which they felt merited further testing; and (2) the characteristics of hydrological response for the chosen catchment as perceived by local people and as shown in available rainfall and river discharge data for the study catchments. The conceptualisation in this paper focuses upon two types of intervention identified as feasible: (1) installation of woody debris dams within higher order streams to reconnect those streams with their floodplains; and (2) floodplain woodland expansion; both expected to lead to greater hydrological attenuation. Both interventions were expected: (1) to have benefits that were sensitive to where they were located in the catchment; (2) to require potentially many interventions to have a significant impact; and (3) to change the interactions, through relative timing effects, of runoff generation from different parts of the catchment. Thus, the model had to be both spatially-distributed and time dependent but also, to allow testing of different combinations of interventions in different locations, computationally efficient. Although these are the focus of this paper, there are other interventions that could readily be incorporated into the same model framework (e.g. stream remeandering).

The particular hydrological focus was upon the more extreme flood events measured in river catchments (typically with return periods greater than 50 years) in which the catchments have a high level of saturation as revealed by standard percentage runoff coefficients of greater than 70%. In turn this allowed for a major reduction in model complexity by focusing upon the response of rapid runoff generation routes and their contribution to flow peaks in particularly extreme events. The decision was taken to base the modelling upon a spatially-distributed unit hydrograph approach (e.g. Maidment, 1993; Maidment *et al.*¸1996; Olivera and Maidment,

1999; Saghafian *et al.*, 2002; Liu *et al.* 2003; Du *et al.*, 2009) that uses the time to equilibrium (t_e) approach pioneered by Saghafian and Julien (1995).

Initial applications of the spatially-distributed unit hydrograph method assumed: (1) a single continuous and time-invariant flow path (e.g. Maidment *et al.*, 1996); (2) a linear system response in which at higher flows, travel times are independent of the amount of runoff being routed (e.g. Kull and Feldman, 1998; Olivera and Maidment, 1999); and (3) independence of response where two locations share elements of the same flow path (e.g. Maidment *et al.*, 1996). Despite these assumptions, these early applications were found to reproduce measured hydrographs extremely effectively (e.g. Maidment *et al.*, 1996). Given the interventions we explore, these assumptions needed to be relaxed. For instance, a woody debris dam is designed to switch the local flow path from channel to floodplain once local bank heights are exceeded. Similarly, work that has followed Maidment *et al.* (1996) has shown that it is possible to introduce travel time treatments that change with the amount of runoff being generated and delivered from upstream contributing areas (Saghafian *et al.*, 2002). Thus, our conceptual model builds upon the work of Saghafian and Julian (1995) and Saghafian *et al.* (2002) by allowing for time dependent evolution of travel times but introduces an additional modification by which the flow path followed by water is also allowed to evolve as a function of time, so as to capture time-dependent, spatially collocated transitions from channel to overbank flow.

The time to equilibrium is defined as the time required for maximum potential runoff to be reached for a catchment under a constant rainfall intensity and which varies as a function of both intensity and catchment geometry and physical properties (see Saghafian and Julien (1995) for review). Saghafian and Julien (1995) develop a formulation for the time to equilibrium that allows for distributed rainfall and runoff generation as the basis of estimating 'travel time' maps, such as maps of equal travel times called isochrones (Saghafian and Julien, 1995). Saghafian and Julien (1995) show that a (flood) wave travel time (t_w) formulated for a kinematic wave approximation can be described by:

$$t_w = \int_{x_1}^{x_2} \frac{\gamma b_1}{(\beta - 1)\alpha^{1-\gamma}} \left(\frac{a_1}{Q_e}\right)^{\gamma} dx$$

with

$$\gamma = \frac{\beta - 1}{\beta + b_1 - 1}$$

[1]

where x_i is the distance between points $i = 1$ and $i = 2$; α and β are parameters that depend on form of the resistance law used; a, b = constants dependent upon local channel cross-section geometry; and Q_e = upslope discharge delivered to the upstream point; x = distance along flow path. With a Manning resistance equation, this can then be formulated for the treatment of both overland flow and channel flow (Saghafian and Julien, 1995).

Saghafian *et al.* (2002) moved away from the linear routing assumption by calculating travel time maps using [1] with a Manning resistance formulation for a number, *N*, of different rainfall intensities or, in effect, maps of runoff generation to produce *N* isochrone maps. These isochrone maps were then convolved to produce *N* incremental hydrographs, each of which were delayed by the time corresponding to each map, and then superimposed to obtain the final hydrograph.

Our model is based upon the Saghafian *et al.* (2002) approach. To address our need to understand the effects of riparian zone interventions such as floodplain forest, we modify this approach to allow for the explicit effects of flow from channels onto floodplains, as conditioned by both the local flow magnitude, channel geometry and channel and floodplain resistance.

Detailed model description

Determination of channel network

The DEM used in the analysis is initially pit-filled following the Planchon and Darboux (2003) method. Flow paths are then calculated using two methods according to whether a grid cell is labelled as a hillslope cell or a channel cell. In the case of a hillslope cell, the flow is routed using Quinn *et al.'s* (1991) FD8 algorithm, with a diffusion exponent of 3. In the case of channel cells, we use the steepest downslope flow path (i.e. D8) algorithm.

Clearly, we have no *a priori* definition of what is a hillslope cell and what is a channel cell. Thus, we approach the problem using a single, steady state, extreme, effective rainfall. This involves routing the runoff generated by an extreme rainfall event using the FD8 algorithm. We then apply a unit discharge threshold to the FD8 accumulated rainfall to identify the onset of channel routing across the landscape and apply the D8 routing to all cells downstream. We use an effective rainfall that gives a discharge at the catchment outlet that corresponds to bankfull, with a return period of *c.* 2 years.

For this, and for all subsequent calculations, following other applications of the spatially distributed unit hydrograph approach (e.g. Maidment *et al.*, 1996; Saghafian *et al.* 2002), we set the effective rainfall as a runoff, based upon the excess of net rainfall, after evapotranspiration and interception losses, over local infiltration rate. Thus, the effective rainfall rate is defined as the rainfall rate minus some assumed percentage loss, the runoff percentage. The runoff percentage is assumed to be spatially uniform and reflecting our observations that during the flood event simulated, the catchment was close to saturation. We explain below how we introduce some temporal variability into the runoff percentage.

Isochrones

Isochrones are determined for each member of a set of rainfall rates. We subtract the assumed percentage loss from each rainfall rate to get a runoff rate. This runoff rate is routed either by the FD8 method or the D8 method according to our definition of the channel network.

Modification of flow path routing for extreme rainfall rates

Thus far, much of what we have described has formed the basis of published work. The novelty in this paper is that we recognise that flow paths can evolve as a function of rainfall rate. There are two modifications: (1) to allow for headward extension of channelized flow within an event when a unit discharge threshold is exceeded; and (2) to allow for flow path routing across floodplains rather than entirely within the river channel.

The first modification is undertaken relatively easily by considering the first calculation of the FD8 and D8 routed discharges based upon the channel network and then allowing the D8 routing to extend headwards in situations where an estimated unit discharge exceeds the threshold for channelized flow. Note that this adjusts the flow path (from FD8 to D8) but does not extend headwards the physical expression of the river network as an incised channel. In other words, we continue to calculate cell velocities and travel times using the full cell width. We argue that this reflects the distinction between the more dynamic hydrological expansion

160

(and contraction) of a channel network, which we are addressing here, and the much slower geomorphological adjustment, which we assume is constant over the scale of a flood event.

The second modification is more complex but also more important because it is required so that we can explore diffuse land management interventions that increase the amount of flow locally on river floodplains. It is based upon a simplified representation of overbank flow mechanisms, reflecting the data uncertainties associated with catchment-scale modelling, especially in relation to channel geometry estimation (see below). Our goal is to correct the travel times estimated assuming channel flow and D8 routing for situations where some flow is routed across a floodplain.

In the first step of the analysis, we consider the initial D8-based Q estimates (by definition, channel cells) for each rainfall rate. These can be converted into estimated flow depths (d_{ij}^{ch}) using the Manning equation and estimated channel width (see below). We then calculate the estimated water surface elevation (z_{ij}^{w}) as

$$z_{ij}^{w} = z_{ij} + d_{ij}^{ch}$$

[2]

where z_{ij} is the elevation of the DEM cell that the river is passing through. In theory, we should only have to compare z_{ij}^{w} with adjacent non-channel cells to see if there could be flux of water into those non-channel cells. However, almost invariably except for rivers with widths much greater than the DEM resolution, the channel occupies only a proportion of the DEM cell and z_{ij} is a spatial average of elevations associated with that cell such that:

$$z_{ij}^{ch} < z_{ij} < z_{ij}^{f}$$

3]

where f indicates a floodplain cell. In process terms, this means that the z_{ij}^{w} from [2] may be higher than it should be and lead to a flux of water into the floodplain too readily. Thus, we introduce a correction term k which scales the estimated channel depth:

$$z_{ij}^{w} = z_{ij} + k d_{ij}^{ch}$$

[4]

We would expect the proportion of a cell that is floodplain to be greater for narrower channels which, by implication, have steeper slopes. Hence, we define k as

$$k = (1 + k_c S)^{-1}$$

[5]

noting that k_c is an adjustable parameter which could be parameterised using high resolution remotely sensed data but which, in the absence of such data in this study, is treated as an adjustable parameter whose effects on prediction uncertainty are explored. Note that this scaling effect should also show a DEM resolution dependence. We then label a channel cell (i,j) as an overbank channel cell if:

$$z_{ij}^{w} > z_{ij}$$

[6]

Once [6] has been applied to all cells containing a channel, and channel overbank cells identified, we identify the set of cells surrounding each channel overbank cells as floodplain spill cells by:

$$z_{ij} + k\,d_{ij}^{ch} > z_{i+x,j+y} \text{ for } x = -1{:}+1; \; y = -1{:}+1; \text{ excluding } x = y = 0$$

[7]

In the second stage of the analysis, we repeat the flow path, flow routing and flow accumulation but with modification for overbank channel and floodplain spill cells (taken together, these are labelled in combination as flood cells). This stage seeks to identify the flowpaths followed by water across the floodplain associated with the flow resulting from each rainfall rate. Commonly, floodplain flow routing is based upon the analysis of water surface gradients. The most simplified forms of floodplain routing treat the flow as a diffusion wave (e.g. Bates and de Roo, 2000; Horritt and Bates, 2001; Bradbrook *et al.*, 2004; Yu and Lane, 2006). Water is spread iteratively across the floodplain based upon flux apportionment but routing is only allowed to any two of the orthogonal cardinal flow directions in any one time step. Our aim is not to represent the progressive spreading of water within the floodplain during an event but to characterise the routes followed by water across the floodplain at a series of local flow discharges as defined by each rainfall rate. Thus, we do this by modifying the flow paths for flood cells in a way that makes them more diffusive under the assumption that, for floodplain flow, water surface gradient and momentum effects should reduce further the dependence of flow path upon topographic steering.

By definition, up until this point, a floodplain spill cell cannot be a channel cell, and so has the FD8 routing with the default diffusion exponent of $u = 3$. Given routing to eight possible cardinal directions from cell (i,j), flow is partitioned into fractions, f, defined as:

$$f_{i+x,j+y} = [\, s_{ij}^{i+x,j+y}\,]^{u} \left(\Sigma x\ \Sigma y\ [\, s_{ij}^{i+x,j+y}\,]^{u} \right)^{-1} \text{ for } x = -1{:}+1;\ y = -1{:}+1;\ \text{excluding } x = y = 0 ;\ \text{and}$$

$$s_{ij}^{i+x,j+y} < 0$$

[8]

In [8], u is effectively a measure of the sensitivity of routing of flow to topography: as u tends to infinity, the routing tends towards a channel type D8 routing, with water following the line of steepest descent. As u tends to zero, routing becomes progressively less sensitive to topography and progressively more diffusive, until at $u = 0$, routing is independent of topography. Hence, we introduce u as an adjustable parameter, with $u < 3$. Comparison with conventional floodplain diffusion wave routing algorithms is not straightforward as these only allow routing to any two cells at any one time period. However, if we take $u = 1$, then we become close to approximating the slope dependence used in diffusion wave models.

By applying this treatment to flood cells, we have to make a distinction between a channel overbank cell and a floodplain spill cell. A channel overbank cell is assumed to have two types of routing: D8 for the linear proportion of discharge that corresponds to in-channel flow:

$$z_{ij}^{w} \leq z_{ij}$$

[9]

and FD8 with $u = 1$ for that proportion that corresponds to out of channel or overbank flow:

$$z_{ij}^{w} \geq z_{ij} .$$

[10]

All floodplain spill cells have FD8 routing with $u = 1$ but [8] is modified so that we do not allow any diffusion from a floodplain spill cell into a channel overbank cell. We then iteratively identify additional floodplain spill cells, defined as those that are adjacent to existing floodplain spill cells except that: (1) we route water from the floodplain spill cell back into the main channel where a floodplain spill cell finds itself next to a channel cell that is not labelled as a channel overbank cell; and (2) where the discharge becomes very low (set here as the

163

critical discharge threshold for channel flow) and topographic influences are likely to become greater, we return to $u = 3$ in the FD8 algorithm. When water is returned to a channel cell, we check using [6] whether or not the new accumulated flow can still be accommodated within the channel, or whether this channel cell should also now itself become an overbank cell.

In theory, this process could be iterated many times, but we found that just one or two iterations led to typically stable flow paths for a given rainfall rate.

Following from the flow path modifications, the cell travel time calculations also need some adjustment. For floodplain spill cells we use the lowest neighbouring cell rather than the steepest flow path cell, although these are sometimes the same. We introduce this modification because, particularly for floodplain spill cells next to channel cells, the steepest flow path route is often immediately straight back into the channel. For overbank channel cells, we have to combine two controls on routing: (1) the within-channel proportion which we assume to follow the steepest path as defined by D8; and (2) the overbank proportion which should be routed to the lowest neighbouring cell. These routes may or may not be the same for the cell in question, and there is also still the problem that the flow velocities should be different, that of the in-bank channel flow being in likelihood much faster than that of the shallow water over the bank side areas. We handle these two routes in combination. The different flow components, within bank and overbank, are calculated. The flow depth for the channel component is always assumed to be the channel depth, the width of the flow the channel width, and the length of travel the distance in the steepest path direction. Also, the resistance to the flow, the Manning's n value, is that for the channel. For the overbank proportion, the flow depth is inferred from the full width of the channel overbank cell and the velocity is calculated applying this to lowest neighbour flow path, this time using the Manning's n value appropriate for the bank side. To simplify matters here, the bankside n value is assumed to be the same as that of the adjoining floodplain cells, but the model includes the possibility to set it to a different value if desired (for example, if modelling a narrow woodland buffer strip immediately alongside the channel and separating it from a pasture floodplain). Once the cell passage times for each flow type have been calculated, they are weighted according to the values for each type of flow, and an overall weighted average cell flow passage time is then calculated for the overbank channel cell using:

$$t_w = \frac{V_{inbk} t_{inbk} + V_{obk} t_{obk}}{V_{inbk} + V_{obk}}$$

[11]

where t_w is the weighted cell passage time, t_{inbk} and t_{obk} are respectively the cell passage times for the within bank and the overbank components of the cell flow, and V_{inbk} and V_{obk} are

respectively the values corresponding to the within bank and overbank flows found from the revised flow map.

Sampling the isochrones maps associated with each rainfall rate

With each rainfall rate modified for headward extension and overbank flow, the final step is to sample the isochrones maps so as to produce an estimated outlet hydrograph. We view this as a calibration problem, not least given the very poor coverage of rainfall recording devices typical in river catchments. However, if there is a downstream flood problem, it is common for there to be a river flow record, and so we focus on using the flow record to infer the isochrones maps that produce the measured flow. Each isochrone map is convolved with the observed rainfall, corrected for percentage runoff to provides a vector describing when the runoff from each (i,j) location in the model will reach the catchment outlet. This is repeated for all observed rainfalls. The question then becomes which isochrone map to use for each observed rainfall and we deal with this problem in a Monte Carlo calibration framework by randomly and then strategically sampling from all possible isochrone maps for each time step in the model. In the initial phase, we randomly sample an isochrones map for each time period to produce a hydrograph and this is repeated 200 times. We then calculate, for each time step, those isochrone maps which produce the best Nash Sutcliffe index of model efficiency for the entire flood hydrograph. In the second and subsequent phases, we repeat this process, but updating the set of isochrones maps that can be sampled as each time step, in light of the Nash Sutcliffe index results. We repeat this until we have 200 simulations all of which have a Nash Sutcliffe index >0.98. Given the dependence of our work upon calibration, we independently assess model performance with respect to internal flow field information.

Model application

Runoff percentage estimation, adjustments for baseflow and wetting up period

The focus of the spatially distributed unit hydrograph approach is upon modelling the rapid transfer of effective runoff. The effective runoff is a product of both the rainfall rate and the percentage runoff. With a discharge series inferred from the stage record, and a preliminary estimate of catchment-average rainfall, it was possible to obtain a first approximation of the estimated percentage runoff for each event being modelled through a mass balance calculation. We do this using an event-specific method, described here for the example of the 25th to 26th June 2007 event. First, we consider the total volume of water making up the flood event and the declining limb of the hydrograph, in this case between from 12 a.m. on 25th June to 12 a.m. on 29th June 2007, as compared with the rain input over the same period. For this period, the total rain volume, using the mean rainfall from the two gauges and a catchment area of 67.4 km^2 to Ropery Bridge, is *c.* 4.79×10^6 m^3 and the total discharge volume is *c.* 2.57

$\times\ 10^6$ m^3. The latter includes a volume attributable to the initial baseflow which, after correction, leaves a total of is *c.* 2.42×10^6 m^3, or a percentage runoff of about 50%. However, the calculation is complicated by the problem of how to deal with Haugh Howl and Gundale Slack (area 10.7 km^2, just under 16% of the catchment, which, according to local observations, contributed almost nothing to the June 2007 flood because much of the water was drawn into the local limestone and leaves the catchment through Costa Beck. Similarly, the sub-catchment of Levisham Beck (area 11 km^2 to Levisham Mill, also around 16% of the catchment) is partly affected by losses into the limestone, although a field visit some months after the flood indicated that the dry channels feeding into Levisham Beck had probably experience overland flow during the event.

To deal with these effects, we make two assumptions. First, for Haugh Howl and Gundale Slack we assume a small and constant baseflow of 0.4 cumecs and remove these catchments from contributing rainfall to the mass balance calculation. Second, we retain Levisham Beck, but give this a different weighting in the mass balance calculation. Thus, and for instance, after Haugh Howl and Gundale Slack are removed from the analyses, the mass balance can be achieved with a runoff coefficient of 25% set for Levisham Beck and 65% for the remaining 45.7 km^2 of Pickering Beck. Given the uncertainties in this mass balance calculation associated with the rainfall interpolation and to a lesser extent the flow gauge, we take these runoff coefficients as important calibration parameters.

We introduce one further modification. The calculations of runoff percentage are based upon the entire event. However, it is logical to expect that the runoff percentage varies as a function of the rainfall rate within the event. Thus, we introduce a weak non-linearity into runoff percentage such that it increases weakly with rainfall rate:

$$P_{eff} = A_{mb}(aP_{mb}+bP_{mb}^2) + A_{lb}(cP_{lb}+dP_{lb}^2)$$

[12]

where P_{eff} is the precipitation that becomes runoff, *mb* is the main beck, *lb* is Levisham Beck and a, b, c and d are constants that meet the criterion set by the mass balance calculation. Given that there are multiple ways in which the observed P_{eff}, as well as the possibility of error in P_{eff} itself, we treat the problem as a calibration and uncertainty issue, except that we set 0 > c > a > 1 and 0 > d > b > 1. In each case, the first term in [12] is applied to rainfall over the main Beck and the second term to rainfall over Levisham Beck, both for the calculation of the equilibrium time maps, and when the time maps are sampled to simulate the hydrograph.

Finally, we also have to provide the model with a fixed baseflow value, which on the basis of analysis, we set at 0.4 m^{3}s^{-1}.

Digital topographic data

The DEM used in these calculations is of 20 m resolution, and formed by resampling from the Ordnance Survey's source 5 m 'NEXTMAP' of Great Britain data series.

Estimates of hydraulic geometry

As noted above, a major challenge for testing multiple, diffuse land management interventions is knowledge of the spatial patterns of river geometry especially given the fact that channel width and depth will effect the ease with which the river connects with its floodplain and hence the magnitude of flow at which water switches from moving within-channel to across the floodplain. We base the hydraulic geometry estimation on the assumption that the perennial channel estimated for flows with return periods of *c.* 2 years corresponds with the bankfull discharge which is likely to be a formative flow in channel geometry terms. We then apply the discharges estimated for each cell in the perennial network to the empirical relations of the functional form derived by Leopold and Maddock (1953). Firstly, for the channel widths, we use the equation:

$$w = 1.09 Q^{0.5}$$

[13]

and then, for the channel depths (bank heights), we use:

$$d = 0.528 Q^{0.344}$$

[14]

where *w* is the width of the perennial channel and *d* its depth. The values for the exponents and coefficients in [13] and [14] are estimated, and set so as to achieve realistic values (compared with values from direct observation) for both depth and width across the whole catchment. In many cases, the predictions of *w* from [13] are smaller in magnitude than the cell width and in such cases it is the channel width rather than the cell width that is used in channel calculations, with any residual cell width distributed to equally to floodplains assumed to exist either side if the channel.

We also need to specify a threshold between channel and hillslope cells. We set this as a unit discharge of 0.003 m^2s^{-1}.

Flow resistance

Application of [1] with a Manning formulation requires cell specific estimates of Manning's *n* values. We based these on the division between hillslopes and the perennial channel network. For simplicity, we set fixed values of *n* following Chow (1958). These are 0.060 for hillslopes corresponding to an open woodland or mixed low scrub and grassland land cover type; and 0.035 for for channels corresponding to a largely unobstructed channel with. Again, we take flow resistance parameters as ones that need exploring using calibration and uncertainty analysis.

The model has the following parameters: (1) the unit discharge that defines the channel network; (2) the diffusion exponents for both hillslope and spill flows; (3) the parameters in the hydraulic geometry relationships; (4) the Manning's *n* values for both hillslopes and channels; (5) the slope coefficient, k_{bk}, used to calculate bank height elevation in the spill flow procedure; (6) parameters associated with estimation of the runoff percentage; and 7) the fixed baseflow contribution. Each of these has an impact on any equilibrium isochrone map.

Wednesday, 3 February 2010

Some background to the study; my role and the wider context

As this blog may *potentially* reach a slightly wider audience I thought it appropriate to explain in more detail my study for those that are not aware of it:

Context

The town of Uckfield, Sussex experiences regular flooding, with the flood event in 2000 being particular large. In the subsequent flood report;

(http://www.wealden.gov.uk/Planning_and_building_control/Development_Control/Uckfield%20Appeals/WD-2006-2173/Water%20%28Drainage%20and%20Flood%20Risk%29/Appendix%20W6/Appendix%20W6%20-%20Extract%20from%20BBV%20Report%20on%20Sussex%20Ouse%20Flooding.pdf)

it was stated the rainfall in a 16 hour period of 11/12th October in the Uck catchment was estimated to be a 1 in 150 year event.

Further info on 2000 flood;
http://www.geography.org.uk/resources/flooding/Uckfield

Following this event, a flood wall was built to reduce flood risk for 30 properties, however this wall is expected to be designed for a 10-year event; http://www.environment-agency.gov.uk/news/112405.aspx

My project comes at a time when there is much less money available for hard engineering approaches to flood protection such as large flood walls. There is also the realisation that such flood protection measures can have the effect of increasing flood risk downstream. In addition to this, in the event of flood wall failure, flooding can be even worse.

Therefore if it were possible to reduce flooding through the implementation of smaller-scale, diffuse, flood attenuation measures throughout the catchment this could potentially be very desirable.

For this study such measures will take the form of catchment riparian intervention measures (CRIMs). These CRIMs will most likely consist of a debris dam and riparian vegetation, with the aim of essentially slowing down water during high flow periods.

The idea behind the CRIMs is increasing the roughness of the channel and floodplain. Increasing channel roughness has the effect of reducing channel conveyance, causing small-scale local flooding. By increasing water storage in upstream areas of the catchment, the flood peak downsteam can potentially be reduced.

The hydrological model to be used is Overflow. The Overflow model is a reduced complexity model. The thinking behind use of such a model is that physically-based models, for example SWAT, require a large number of *parameters* to represent physical properties of a catchment.

There is an uncertainty associated with each parameter - therefore such models may potentially be more uncertain than simpler models. A reduced complexity model also has the benefit of allowing relatively quick simulations to be carried out allowing quicker evaluation of interventions in the catchment.

My role in this study follows previous (and continuing) work with regards to the

development of the model in Pickering and Uckfield, and also to the 'Knowledge Controversies' project:

http://knowledge-controversies.ouce.ox.ac.uk/

To summarise my role;

The aims of my masters research are:

1.To model the effects of CRIMs, placed throughout the catchment, on the flood peak downstream at Uckfield.

2. To evaluate the performance of a suitable reduced complexity model for assessing the impacts of small scale riparian woodland interventions

3. To develop an intervention strategy with the aim to reduce downstream flood risk, taking into account feasibility (e.g. biodiversity objectives)

Ed

Thursday, 4 February 2010

The Modelling Process

To all those interested:

The modelling process involved in the case of Uckfield, and in fact any similar study, is a long one with several important steps before any potential results can be achieved and analysed. It is also important that any results are viewed in the context of model uncertainty.

Therefore by updating you all on my progress, hopefully you will be able to understand and follow the steps that I take in the modelling process, as well as my masters study in general.

I am currently in the process of familiarising myself with the Overflow model. This involes gaining and developing a general understanding of how the model works through running basic instructions and looking at what output the model *can* provide. This learning stage is very important before I can look at the model more in-depth.

In addition to learning to use this model, as part of my masters degree, I am also developing a greater understanding of the more broad issues relating to the Uckfield case, particularly in terms of flood attenuation.

As allways, feel free to e-mail me with any questions you may have

Thanks, Ed

Wednesday, 21 April 2010

Sensitivity analysis

Since my last message I have completed a number of steps in the modelling process.

I have been carrying out model sensitivity analysis for Overflow. Basically this process allows me to identify how the model behaves in terms of how important each variable or parameter is to the model behaviour. So far this process has been relatively exploratory.

The model contains a number of parameters such as;
• Channel, floodplain and catchment roughness values – set as Manning's n values. Roughness affects conveyance
• Rain time maps
• Rainfall input
• Channel depth and width equations.

Each of these parameters has a default value. For example the channel network has a default Manning's n value of 0.035. (For reference a Catchment Riparian Intervention Measure (CRIM), consisting of a debris dam and buffer strip, is likely to be given Manning's n values of around 0.16 and 0.14 for the floodplain and channel respectively.)

My sensitivity analysis so far has involved varying the values of each key parameter one-at-a-time (OAT), whilst keeping the values of the other parameters fixed. A model simulation is run and the results recorded. Each simulation takes just under 10 minutes at the moment. The effect of varying each parameter on the model output (discharge) can then be analysed. The simulated discharge is seen to vary to a relatively high degree as a result of varying time maps and Manning's n values; however it's important to note that the parameters were varied over a large range.

The next step involves running simulations where every key parameter is varied at the same time, with values selected randomly. The results will show how the influence of each parameter relies on the interactions of the model parameters.

The ultimate aim of the above process is to narrow the range of potential values

each parameter can take on, to identify and quantify the uncertainty in the model and its parameters.

Secondly I have run simulations where a CRIM is added to a single reach (234 separate reaches have been identified in the catchment). This is done by changing the Manning's n values of the reach to 0.16 for the floodplain and 0.14 for the channel. 234 simulations have to been run, with a CRIM added to a different reach each time. Whilst the sensitivity analysis is being carried out I will be able to have a first look at which locations it would be beneficial to add a CRIM, in terms of a reduction is peak flood discharge.

Again please feel free to email me with any questions you have at: edward.byers@durham.ac.uk. I hope to update the blog more frequently in order to allow readers a more detailed and better understanding of the development of my study.

Thanks, Ed

Sensitivity analysis - preliminary results

As discussed in the previous update, I aimed to carry out 2000 model runs to look at how the output (river discharge) of the model varied as model variables or parameters (such as channel roughness) were varied randomly.

The greatest difficulty with this has been just making sure that everything is set up correctly for my model runs. Sometimes this has involved quite a bit of trial and error - often a lot of model errors - to get everything right. As I can automate all my simulations it would be very annoying to find after 2000 simulations I'd made a msitake. However the simulations have now been carried out (with the help of Stuart letting me use his computer as well as mine).

I have used a number of different objective functions to analyse the accuracy of model predictions of the flood hydrograph. These basically attempt to quantify the goodness of fit of my observed (2000 flood event) and simulated hydrographs. Amongst these was the Nash-Sutcliffe model efficency (NSME), which allows measurement of the variation between the observed and the simulated hydrograph.

However Nash-Sutcliffe values were very poor for nearly all of the simulations. As were results showing the error in predicted flood peak. The low values were quite discouraging as it suggests that, at least when varying parameter values, the model is a poor respresentation of the observed flood hydrograph.

However there are several potential positives to take from the simulations;
- Firstly it is now even more clear that the model is very sensitive to rainfall rate applied. This stands to reason that a very small or very (very!) large rainfall rate is not likely to produce a flood hydrograph similar to that observed in 2000. - On reflection this is good in that it would be expected that the flood hydrograph would change quite considerably under different rainfall rates.

- Secondly the NSME statistic can give misleading results if they are not looked at closely.
For example it is biased towards the highest flows, therefore a model can be given a low NSME value even if most of the flood hydrograph is correctly predicted.
Also errors in the timing of flood peak can affect the results from using the statistic.

For example it is possible to produce a pretty good qualititative simulation of the observed hydrograph of the 2000 event using a set rainfall rate. From simply looking at this we can see that the timing of the peaks is slightly out - this can greatly affect NSME values. If the timing error if corrected for, very high NSME values can be achieved - indicating a good fit.

Therefore we believe the poor results are far from suggesting the model is not useful and it highlights the importance of not just analysing results but looking at how they are analysed.

As the model is very sensitive to rainfall rate only a small range of rainfall rate is likely to produce a good simulation of the flood hydrograph, therefore when I ran 2000 simulations very few combinations of variables produced 'good' results.

However after some extra thought usefull information can be found from the simulations. Trends in parameters values can be seen and will be looked at more closely in time. A future forward step is likely to be calibrating the model using several different rain rates as the event progresses. It is hoped this may offer up more accurate results and allow better investigation of the model parameters.

On the plus side it is now possible to run much faster simulations, using the computer power of several computers so results can be obtained much sooner.

Tomorrow I shall update you on results from my screening simulations, which are quite interesting.

Ed

Screening simulations - the effects of CRIMs; preliminary results

Screening simulations

These simulations involved increasing the channel and floodplain roughness along one reach at a time to simulate the adding of a CRIM (debris dam and floodplain vegetation) and looking at the impact this has on river discharge just upstream of Uckfield.

-NOTE- I will add some images showing some of my results in the next update, which I'll add after this.

Results have been produced for all rain time maps (1mm/day - 200mm/day). A potential problem I have is in deciding on an appropriate time map to use, as discussed in my previous update. It was mentioned that goodness-of-fit statistics can be misleading. Therefore I decided to look at the effect of CRIMs where time maps 30, 36, 42 and 50mm/day were applied.

- NOTE - The model may be calibrated with different time maps throughout the storm period.

My choice was based on what was felt to produce the best hydrograph when initially compared to the observed hydrgraph. As discussed previously, the hydrograph produced when using a 30mm/day time map shows an encouragingly good qualitative fit, albeit with a time lag.

Table 1. The number of reaches in the Uck catchment where, if applied to 1 individual reach, a CRIM would decrease flood peak by more than 5, 1 and 0.1 cumecs.

Time map applied	30mm			36mm			42mm			50mm		
Reduction of flood peak (cumecs)	>5	>1	>0.1	>5	>1	>0.1	>5	>1	>0.1	>5	>1	>0.1
No. Of reaches	11	26	54	11	30	63	9	28	69	9	29	73

Table 1 shows some of my initial results. It shows for example that, using the

30mm time map, there are 11 reaches which reduce the largest flood peak by over 5 cumecs individually. It can be seen that with increased rainfall rate, more reaches have a reducing effect on the main flood peak - this is not suprising as for the higher rainfall rates initial flood peak is higher.

-NOTE- It is also important to note that there are also many reaches which increase the flood peak when a CRIM is added, and many more 'neutral' sites where the effect is insignificant. In addition to this, for various reasons some of the reaches may not be suitable for CRIMs even if the model shows that increasing roughness in that area has a positive effect on flood reduction.
For example an area of floodplain may all ready be heavily vegetated - therefore floodplain roughness cannot be increased in practice.

The results are encouraging - when looking at a qualitatively good simulation of the 2000 flood hydrograph, over 50 reaches can potentially reduce the main flood peak by over 0.1 cumecs individually.

However there are other points to consider when looking at these results;

I was quite surprised at the extent of the effect of applying CRIMs to certain reaches, largely though not exclusively located along the main Uck. Four reaches reduced the flood peak by over 10 cumecs on their own. This is an extremely large reduction.
This may be due to a model artefact. - As an additional analysis I am going to run the same simulations again but this time not increase the channel rough as much;
The default channel roughness (represented as manning's roughness, n) is 0.035;
For the results discussed here, n was increased to 0.14;
This could be potentially too high so I'll run the same simulations again, increasing channel n to 0.08. This will represent a less extreme intervention and I hope results will still be positive;

Secondly so far I have only analysed my results looking at flood peak reduction. It is not necessarily helpful to reduce the flood peak if the volume of water above critical flood discharge - the amount of water spilling onto the floodplain - remains the same over a storm event. (Though it may still be beneficial in terms of timing of flood waters)

Therefore I need to look at the volume of water above critical flood discharge. This is proving to be more difficult for me to do than hoped. I basically need to figure out how to work out the area under a section of the discharge curve. This appears to be a slightly complicated proceduce and one I haven't figured out yet.

After looking at the individual effect of adding CRIMs, I will need to look at how combinations of CRIMs affect the flood peak.

Images showing my initial results to follow....

Ed

Tuesday, 18 May 2010
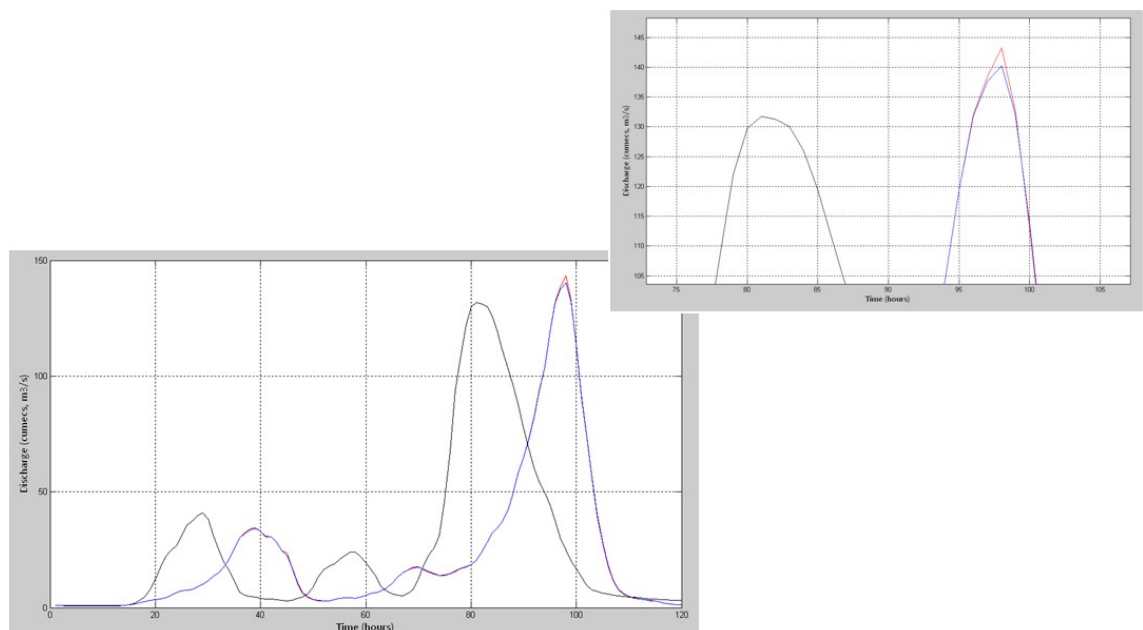
Figure 1

A figure showing;

the oberserved flood hydrograph during the 2000 flood event (black).

the simulated flood hydrograph using a 30mm/day time map with no interventions(red)

the simulated flood hydrograph using a 30mm/day time map with a CRIM added along reach 127 (blue).

The figure shows how increasing the channel and floodplain roughness at reach 127

results in a decrease in flood peak of just over 3 cumecs (m3/s)

Important to note;

The observed hydrograph is taken from the Isfield gauge downstream of Uckfield, whereas the two simulated hydrographs produce hydrographs predicted for an areas just upstream of Uckfield. This will lead to a slightly greater difference between simulated and observed hydrographs

Flood volume calculation: methods and uncertainties

In the previous update I mentioned the need to calculate the volume of water above the critical flood discharge i.e. the volume of water likely to spill onto the floodplain; a very important calculation when looking at the impact of a flood mitigation measure.

To do this, I essentially need to calculate the area of certain sections of a simulated flood hydrograph - the area under a graph. This is known as integration. The programme I am running my model in, MATLAB, allows this to be done in several different ways. However I am having problems using some of the available methods.

Therefore I am used the trapezoidal rule, which is not likely to give the most accurate estimate of the area of a graph;
http://en.wikipedia.org/wiki/Trapezoidal_rule

The following image is useful for understanding how the trapezoidal rule works
http://en.wikipedia.org/wiki/File:Trapezoidal_rule_illustration_small.svg

As it uses straight lines to approimate a curve, there are inevitably errors in area calculation - moreso than if I can use a similar but more accurate method - and therefore uncertainty in my findings. My aim is therefore to try to figure out how to use an improved method of integration. However, for the moment, the current does allow me to explore the effect of CRIMs on flood volume.

Initial results (for an uncalibrated model) on flood volume to follow soon....

Wednesday, 23 June 2010

New model and new uncertainty

Following on from my results of the GLUE uncertainty analysis (see previous updates) the decision has been made to use a calibrated version of the Overflow model, with the aim of producing flood hydrographs which more closely match the observed hydrgoraph

Nick has been working hard producing a calibrated version of the Overflow model. The key different is a different rain time map (rainfall rate) is used throughout the storm event.

The result is a much closer match between the observed and simulated hydrograph at Isfield.

However there are are few issues with the new model;

The key issue is that when a hydrograph is simulated for the meadows area upstream of Uckfield, the largest flood peak now has a double peak. This is not expected and is slightly problomatic; the simulated peak discharge upstream of Uckfield now occurs only very slightly before the peak discharge at Isfield downstream, when perhaps a slightly bigger lag would be expected. If the peak were smoother, this would most likely bring the peak discharge just upstream of Uckfield forward a couple of hours.
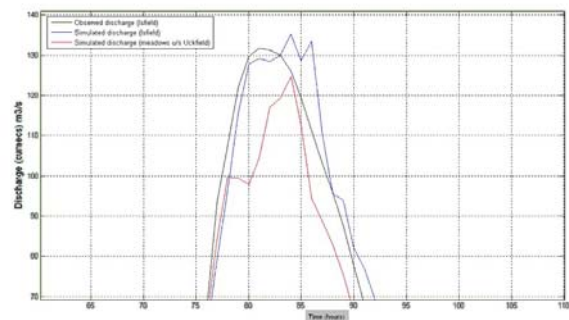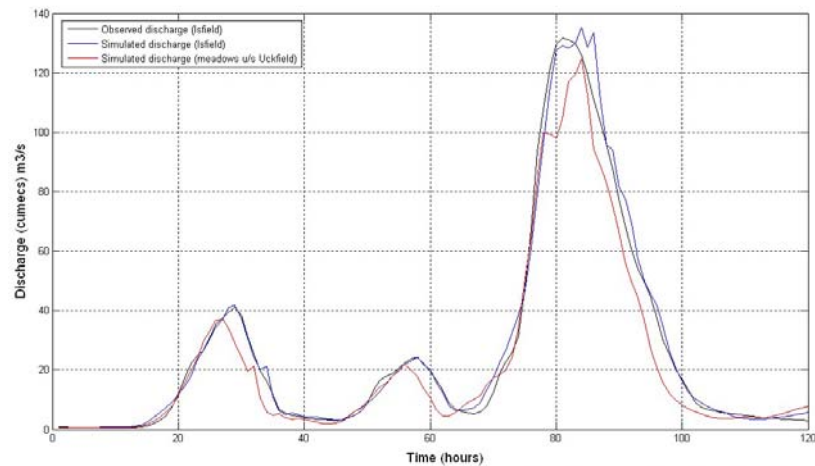
On the positive side, the peak discharge is much more realistic.

As seems to be the way with modelling, as one aspect gets better, this can create a whole new set of problems. Just like a more comlex model can bring with it just as much uncertainty and a simple model.

Ill discuss the issue of the troublesome flood peak with Stuart Lane and I'm hoping that it won't be too much of a problem. The simulated hydrograph is now certainty much a closer fit to the previous uncalibrated model. Im looking forward to (hopefully) getting some final results I can properly work as time is running short in terms of my role in this study - I think we're all hopeful of some interesting results.

Whilst slightly frustrating to work on the previous model and then have to move on to a slightly different version, my previous work has allowed me to explore the behaviour of the model and get a better understanding of the uncertainties.

I have been now working on getting results of the screening runs (see previous

updates) with the calibrated model, looking at the effects of increasing channel and floodplain roughness one reach at a time to represent the adding of a CRIM. Initial results to come…

Background to my project

subsequent posts easier to follow for those not familiar with the work

Thanks, Ed

Initial screening results from new calibrated model

As discussed the simulated hydrograph produced by the calibrated model shows a much better fit with the observed hydrograph from the 2000 flood event. In a few weeks (thousands of simulations takes quite a while) I'll be able to show more results on the uncertainty associated with the new calibrated model.

For now here are the initial screening results, similar to those presented a while ago for the old model.

A key aspect is the effect of placing a CRIM at one reach is greatly reduced. No reaches individually reduce flow peak by over 4 cumecs, as opposed to around 10 (depending on the time map used) which reduced peak flow by >5 cumecs with the old model.

One explanation for this is that the simulated peak discharge is more accurate and also lower. Therefore even if the CRIMs were still having the same effect in terms of % reduction of the initial flow peak, the reduction would be less.

Reduction of peak flow (cumecs)	>0	>1	>2	>3
Number of reaches	127	13	6	3

Importantly, from initial work with combinations of reaches, it appears that in combination the reaches have less of a reducing effect on peak flow than the sum of their parts. For example, as a simplification, two CRIM sites which on their own reduce simulated peak flow by 3 cumecs each may in combination only reduce peak flow by around 4 cumecs.

These results will be discussed in more depth soon

The effects of CRIMs applied in combination throughout the Uck catchment - uncertainty analysis to follow

As discussed previously, from the screening runs there are 127 reaches where increasing channel and floodplain roughness to simulate the adding on a Catchment Riparian Intervention Measure (CRIM) decreased downstream peak flow. It was decided that the 100 reaches with the greatest individual impact would be explored in combination.

Brief method:

Essentially for looking at CRIMs in combination I ranked the 100 reaches in order of how effective increasing channel and floodplain roughness (to simulate a CRIM e.g. debris dam and riparian vegetation planting) of that single reach in question, is on reducing downstream peak flow. So, for example the best reach reduces peak flow by ~3.5 cumecs when roughness is increased in just that reach.

A CRIM was simulated along the reach with the largest individual effect. Then a CRIM was also added to the reach with the second largest effect on downstream peak flow - a CRIM was therefore simulated in both of these reaches. If simulating a CRIM in these 2 reaches reduced downstream peak flow by more than simulating a CRIM in one reach both were retained in combination. I then simulated a CRIM in the third reach and so on. Each time a CRIM was simulated the *cumulative* effect on downstream peak flow was recorded. If simulating a CRIM in a new reach did not increase the positive impact (cumulative peak flow reduction was reduced) this reach was rejected and excluded from future combinations.

The results can be seen in the table accompanying this blog. Please give feedback on the quality of the table.

Issues

You can see from the table that the title 'reach applied (no.)' is highlighted yellow. These numbers are used in the model OVERFLOW to identify each reach and change, amongst other characteristics, roughness values. However they will have no meaning to those not using the model. Producing a figure with each reach numbered is not especially practical considering there are 234 reaches. This creates

a bit of a problem for me in communicating the results, especially in terms of where I'm simulating an intervention.

There is also somewhat of a challenge in explaining the methods I have used; the process is likely to be very confusing to others. Hopefully the table will help you see the process I went through.

To think about/uncertainty:

As previously discussed, these results must be viewed with an appreciation of the uncertainty associated with the model and its inputs.

For looking at the combination of CRIMs I have ranked reaches primarily order of effect on *peak flow*. Whilst a consideration was made of reaches with a positive impact on the flood volume above approximate channel capacity this was not the focus. There may be reaches where increasing roughness reduces excess flood volume by a large amount, whilst having a slightly negative effect on peak flow; I will try and look at such reaches in some form.

The results presented here are for one combination of interventions. A different combination could suggest a different pattern of effects and different key reaches to focus on - this would reduce uncertainty of results/recommendations.

Is simulated roughness higher than might be expected from CRIMs in reality? I hope to get results from simulating the effects of increasing channel roughness by a smaller amount.

Again feedback is much appreciated, especially regarding any problems understanding the method or results, or issues with the presentation. I would like the blog to be as easy as possible to follow so results and the uncertainty can be understood.

Table 1: Results from exploration of effects of simulating CRIMs in combination on downstream peak flow (just upstream of Uckfield; based on 2000 flood event). Initial peak flow simulated for the 2000 event (no interventions) was 124.68 cumecs (2 d. p.). The 'individual effect on peak flow' is the effect on downstream peak flow of increasing roughness in that single reach. The 'effect in combination' is the simulated peak flow downstream as a result of the number of CRIMs added (shown in the final column).

Test no.	Reach applied (no.)	Individual effect on peak flow	* Effect in combination	Cumulative reduction		No. reaches with CRIMs in combination
		Cumecs (m3/s)				
1	202	3.857	120.826	3.857		1
2	219	3.838	120.992	3.691	excluded	
3	212	3.000	120.595	4.088		2
4	175	2.879	119.304	5.379		3
5	167	2.605	118.051	6.632		4
6	158	2.005	118.321	6.362	excluded	
7	209	1.703	118.135	6.548	excluded	
8	230	1.475	117.104	7.579		5
9	218	1.458	117.328	7.355	excluded	
10	197	1.299	117.469	7.214	excluded	
11	226	1.242	116.951	7.732		6
12	157	1.122	116.914	7.769		7
13	204	1.039	116.368	8.315		8
14	222	0.955	115.935	8.748		9
15	138	0.894	116.561	8.122	excluded	
16	203	0.833	115.505	9.178		10
17	216	0.826	115.417	9.266		11
18	45	0.787	115.358	9.325		12
19	156	0.784	115.268	9.415		13
20	137	0.765	115.196	9.487		14
21	223	0.712	115.767	8.916	excluded	
22	225	0.690	115.050	9.633		15
23	136	0.687	114.810	9.873		16
24	14	0.678	114.723	9.960		17
25	131	0.675	114.646	10.037		18
26	133	0.622	114.510	10.173		19
27	128	0.616	114.313	10.370		20
28	7	0.600	114.291	10.392		21
29	189	0.528	114.264	10.419		22
30	210	0.518	114.610	10.073	excluded	
31	124	0.506	114.193	10.490		23
32	65	0.499	114.042	10.641		24
33	123	0.497	114.090	10.593	excluded	
34	8	0.488	113.862	10.821		25
35	37	0.465	113.761	10.922		26
36	200	0.465	113.686	10.997		27
37	10	0.453	113.508	11.175		28
38	127	0.431	113.606	11.077	excluded	
39	82	0.415	113.439	11.244		29
40	145	0.413	113.475	11.208	excluded	
41	193	0.402	113.419	11.264		30
42	93	0.376	113.667	11.016	excluded	
43	220	0.362	113.460	11.223	excluded	
44	181	0.358	113.362	11.301		31
45	227	0.341	113.016	11.667		32
46	232	0.317	113.015	11.668		33
47	62	0.308	113.578	11.105	excluded	
48	229	0.304	113.093	11.590	excluded	
49	206	0.272	112.881	11.802		34
50	213	0.231	112.785	11.898		35
51	5	0.226	112.748	11.935		36
52	198	0.217	112.875	11.808	excluded	
53	152	0.212	112.855	11.828	excluded	
54	130	0.204	112.707	11.975		37
55	12	0.194	112.738	11.945	excluded	
56	155	0.193	112.693	11.990		38
57	67	0.187	112.716	11.967	excluded	
58	161	0.186	112.492	12.191		39
59	177	0.154	112.640	12.043	excluded	
60	194	0.149	112.407	12.276		40
61	134	0.147	112.436	12.247	excluded	
62	144	0.143	112.492	12.191	excluded	
63	33	0.137	112.453	12.230	excluded	
64	147	0.136	112.446	12.237	excluded	
65	224	0.132	112.412	12.271	excluded	
66	221	0.130	112.439	12.243	excluded	
67	121	0.128	112.445	12.238	excluded	
68	46	0.122	112.483	12.200	excluded	
69	3	0.118	112.334	12.349		41
70	180	0.114	112.334	12.349		42
71	151	0.113	112.460	12.223	excluded	
72	1	0.102	112.325	12.357		43
73	40	0.096	112.288	12.395		44
74	2	0.093	112.292	12.391	excluded	
75	71	0.089	112.264	12.419		45
76	43	0.083	112.251	12.432		46
77	207	0.075	112.286	12.397	excluded	
78	192	0.071	112.244	12.439		47
79	142	0.066	112.266	12.417	excluded	
80	26	0.065	112.248	12.435	excluded	
81	4	0.063	112.244	12.439	excluded	
82	51	0.058	112.245	12.438	excluded	
83	63	0.058	112.232	12.451		48
84	77	0.056	112.321	12.362	excluded	
85	68	0.053	112.211	12.472		49

86	30	0.052	112.224	12.459	excluded	
87	21	0.052	112.253	12.430	excluded	
88	55	0.050	112.243	12.440	excluded	
89	13	0.048	112.188	12.495		50
90	22	0.045	112.209	12.474	excluded	
91	76	0.040	112.199	12.484	excluded	
92	73	0.039	112.188	12.495		51
93	86	0.038	112.209	12.474	excluded	
94	168	0.036	112.223	12.460	excluded	
95	143	0.034	112.233	12.450	excluded	
96	99	0.031	112.178	12.504		52
97	97	0.030	112.222	12.461	excluded	
98	23	0.029	112.218	12.465	excluded	
99	187	0.027	112.224	12.459	excluded	
100	102	0.025	112.233	12.450	excluded	

CRIM uncertainty analysis

The results of investigation into combinations of Catchment Riparian Intervention Measures (CRIMs) have been previously presented. The figure below shows the location of the CRIMs throughout the Uck catchment. Those in red have a positive effect in terms of peak flow reduction. Those in yellow have a negative effect *in combination*!

Uncertainty analysis was carried out. The 52 positive sites (see previous post and results table) were the focus of this analysis. Essentially the roughness of the channel and floodplain along these reaches was varied in order to show how different levels of roughness effect the peak flow at Uckfield during the (simulated) 2000 flood event.
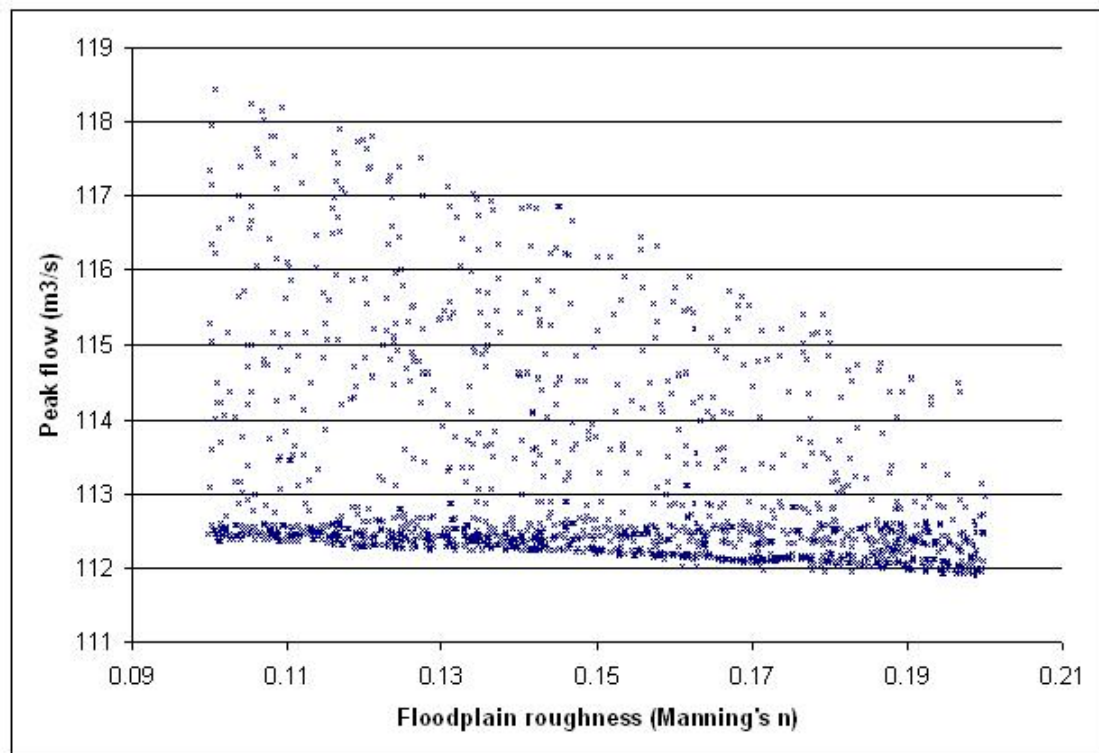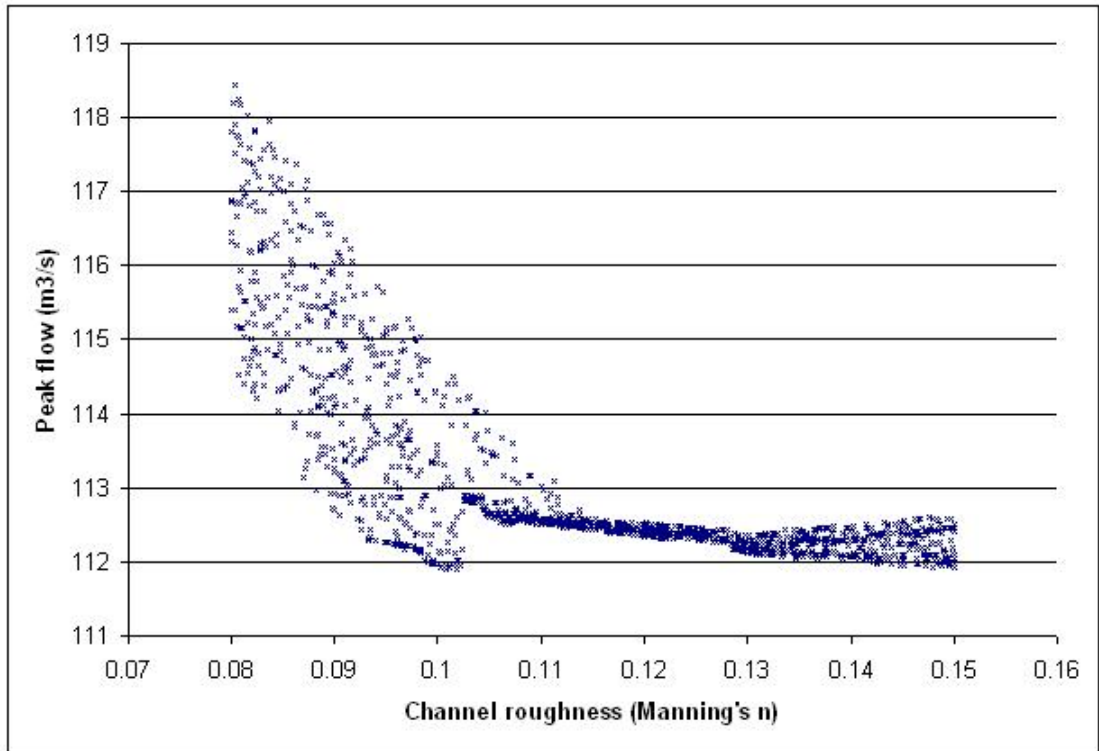
Figure 2. Each data point represents 1 model simulation where floodplain and channel roughness was randomly selected along the 52 reaches previously identified

The key finding from the CRIM Uncertainty Analysis was that similarly fine results in terms of peak flow reduction at Uckfield can be achieved when channel Manning's n is ~0.10, as

opposed to the default value for a CRIM of 0.14. This suggests a lower level of channel blockage is required for equally positive results.

HOWEVER, IMPORTANTLY, if channel n is only increased to ~0.10, floodplain roughness MUST be increased to a high level (Manning's n > ~0.16) in order to achieve the best results in relation to downstream peak flow.

Similarly, floodplain roughness can be much lower than 0.16, and providing channel n is high (> ~0.14), similarly fine results can be achieved.

it is important to note that this uncertainty analysis is only carried out for the 52 reaches identified from previous work, and will need to be repeated if different combinations of reach are selected.

Appendix C – SA results table

APPENDIX Table D. The results produced adding CRIMs throughout the catchment in combination. (Chapter 8)

Test no.	Reach applied (no.)	Individual effect on peak flow	Effect in combination	Cumulative reduction		No. reaches with CRIMs in combination
		Cumecs (m^{3}s^{-1})				
1	202	3.857	120.826	3.857		1
2	219	3.838	**120.992**	**3.691**	excluded	
3	212	3.000	120.595	4.088		2
4	175	2.879	119.304	5.379		3
5	167	2.605	118.051	6.632		4
6	158	2.005	**118.321**	**6.362**	excluded	
7	209	1.703	**118.135**	**6.548**	excluded	
8	230	1.475	117.104	7.579		5
9	218	1.458	**117.328**	**7.355**	excluded	
10	197	1.399	**117.469**	**7.214**	excluded	
11	226	1.242	116.951	7.732		6
12	157	1.122	116.914	7.769		7
13	204	1.039	116.368	8.315		8
14	222	0.955	115.935	8.748		9
15	138	0.894	**116.561**	**8.122**	excluded	
16	203	0.833	115.505	9.178		10
17	216	0.826	115.417	9.266		11
18	45	0.787	115.358	9.325		12
19	156	0.784	115.268	9.415		13
20	137	0.765	115.196	9.487		14
21	223	0.712	**115.767**	**8.916**	excluded	
22	225	0.690	115.050	9.633		15
23	136	0.687	114.810	9.873		16
24	14	0.678	114.723	9.960		17
25	131	0.675	114.646	10.037		18
26	133	0.622	114.510	10.173		19
27	125	0.615	114.313	10.370		20
28	7	0.600	114.291	10.392		21
29	189	0.528	114.264	10.419		22
30	210	0.518	**114.610**	**10.073**	excluded	
31	124	0.506	114.193	10.490		23
32	65	0.499	114.042	10.641		24

Test no.	Reach applied (no.)	Individual effect on peak flow	Effect in combination	Cumulative reduction		No. reaches with CRIMs in combination
33	123	0.497	**114.090**	**10.593**	excluded	
34	8	0.488	113.862	10.821		25
35	37	0.465	113.761	10.922		26
36	200	0.465	113.686	10.997		27
37	10	0.453	113.508	11.175		28
38	127	0.431	**113.606**	**11.077**	excluded	
39	82	0.415	113.439	11.244		29
40	145	0.413	**113.475**	**11.208**	excluded	
41	193	0.402	113.419	11.264		30
42	93	0.376	**113.667**	**11.016**	excluded	
43	220	0.362	**113.460**	**11.223**	excluded	
44	181	0.358	113.382	11.301		31
45	227	0.341	113.016	11.667		32
46	232	0.317	113.015	11.668		33
47	62	0.308	**113.578**	**11.105**	excluded	
48	229	0.304	**113.093**	**11.590**	excluded	
49	206	0.272	112.881	11.802		34
50	213	0.231	112.785	11.898		35
51	5	0.226	112.748	11.935		36
52	198	0.217	**112.875**	**11.808**	excluded	
53	152	0.212	**112.855**	**11.828**	excluded	
54	130	0.204	112.707	11.975		37
55	12	0.194	**112.738**	**11.945**	excluded	
56	155	0.193	112.693	11.990		38
57	67	0.187	**112.716**	**11.967**	excluded	
58	161	0.186	112.492	12.191		39
59	177	0.154	**112.640**	**12.043**	excluded	
60	194	0.149	112.407	12.276		40
61	134	0.147	**112.436**	**12.247**	excluded	
62	144	0.143	**112.492**	**12.191**	excluded	
63	33	0.137	**112.453**	**12.230**	excluded	
64	147	0.136	**112.446**	**12.237**	excluded	
65	224	0.132	**112.412**	**12.271**	excluded	
66	221	0.130	**112.439**	**12.243**	excluded	
67	121	0.128	**112.445**	**12.238**	excluded	
68	46	0.122	**112.483**	**12.200**	excluded	

Test no.	Reach applied (no.)	Individual effect on peak flow	Effect in combination	Cumulative reduction		No. reaches with CRIMs in combination
69	3	0.118	112.334	12.349		41
70	180	0.114	112.334	12.349		42
71	151	0.113	**112.460**	**12.223**	excluded	
72	1	0.102	112.325	12.357		43
73	40	0.096	112.288	12.395		44
74	2	0.093	**112.292**	**12.391**	excluded	
75	71	0.089	112.264	12.419		45
76	43	**0.083**	112.251	12.432		46
77	207	0.075	**112.286**	**12.397**	excluded	
78	192	**0.071**	112.244	12.439		47
79	142	**0.066**	**112.266**	**12.417**	excluded	
80	26	**0.065**	**112.248**	**12.435**	excluded	
81	4	**0.063**	**112.244**	**12.439**	excluded	
82	51	**0.058**	**112.245**	**12.438**	excluded	
83	63	0.058	112.232	12.451		48
84	77	0.056	**112.321**	**12.362**	excluded	
85	68	**0.053**	112.211	12.472		49
86	30	**0.052**	**112.224**	**12.459**	excluded	
87	21	0.052	**112.253**	**12.430**	excluded	
88	55	**0.050**	**112.243**	**12.440**	excluded	
89	13	**0.048**	112.188	12.495		50
90	22	**0.045**	**112.209**	**12.474**	excluded	
91	76	**0.040**	**112.199**	**12.484**	excluded	
92	73	**0.039**	112.188	12.495		51
93	86	**0.038**	**112.209**	**12.474**	excluded	
94	168	**0.036**	**112.223**	**12.460**	excluded	
95	143	**0.034**	**112.233**	**12.450**	excluded	
96	99	**0.031**	**112.178**	12.504		52
97	97	**0.030**	**112.222**	**12.461**	excluded	
98	23	0.029	**112.218**	**12.465**	excluded	
99	187	**0.027**	**112.224**	**12.459**	excluded	
100	102	**0.025**	**112.233**	**12.450**	excluded	

APPENDIX figure E. The results from table A, excluding results from rejected reaches.

Test no.	Reach applied	Individual effect	Effect in combination	Cumulative reduction
		Cumecs (m^3s^{-1})		
1	202	3.857	120.826	3.857
3	212	3.000	120.595	4.088
4	175	2.879	119.304	5.379
5	167	2.605	118.051	6.632
8	230	1.475	117.104	7.579
11	226	1.242	116.951	7.732
12	157	1.122	116.914	7.769
13	204	1.039	116.368	8.315
14	222	0.955	115.935	8.748
16	203	0.833	115.505	9.178
17	216	0.826	115.417	9.266
18	45	0.787	115.358	9.325
19	156	0.784	115.268	9.415
20	137	0.765	115.196	9.487
22	225	0.690	115.050	9.633
23	136	0.687	114.810	9.873
24	14	0.678	114.723	9.960
25	131	0.675	114.646	10.037
26	133	0.622	114.510	10.173
27	125	0.615	114.313	10.370
28	7	0.600	114.291	10.392
29	189	0.528	114.264	10.419
31	124	0.506	114.193	10.490
32	65	0.499	114.042	10.641
34	8	0.488	113.862	10.821
35	37	0.465	113.761	10.922
36	200	0.465	113.686	10.997
37	10	0.453	113.508	11.175
39	82	0.415	113.439	11.244
41	193	0.402	113.419	11.264
44	181	0.358	113.382	11.301
45	227	0.341	113.016	11.667
46	232	0.317	113.015	11.668

Test no.	Reach applied	Individual effect	Effect in combination	Cumulative reduction
49	206	0.272	112.881	11.802
50	213	0.231	112.785	11.898
51	5	0.226	112.748	11.935
54	130	0.204	112.707	11.975
56	155	0.193	112.693	11.990
58	161	0.186	112.492	12.191
60	194	0.149	112.407	12.276
69	3	0.118	112.334	12.349
70	180	0.114	112.334	12.349
72	1	0.102	112.325	12.357
73	40	0.096	112.288	12.395
75	71	0.089	112.264	12.419
76	43	0.083	112.251	12.432
78	192	0.071	112.244	12.439
83	63	0.058	112.232	12.451
85	68	0.053	112.211	12.472
89	13	0.048	112.188	12.495
92	73	0.039	112.188	12.495
96	99	0.031	112.178	12.504